

AD-A032 183

WASHINGTON UNIV SEATTLE OCEAN ENGINEERING RESEARCH LAB F/G 13/2  
FLOATING BREAKWATER FIELD ASSESSMENT PROGRAM, FRIDAY HARBOR, WA--ETC(U)  
SEP 76 B H ADEE, E P RICHEY, D R CHRISTENSEN DACW72-74-C-0012  
CERC-TP-76-17 NL

UNCLASSIFIED

1 OF 3

AD  
A032183



AD A032183

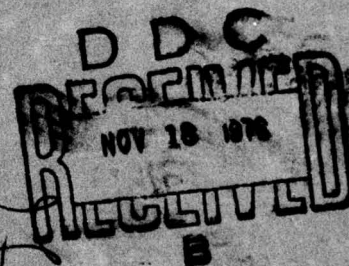
TP 76-17

**Floating Breakwater  
Field Assessment Program,  
Friday Harbor, Washington**

by

B.H. Adeo, E.P. Richey, and D.R. Christensen

**TECHNICAL PAPER NO. 76-17  
OCTOBER 1976**



Approved for public release;  
distribution unlimited.

Prepared for  
**U.S. ARMY, CORPS OF ENGINEERS  
COASTAL ENGINEERING  
RESEARCH CENTER**

Kingman Building  
Fort Belvoir, Va. 22060



Reprint or republication of any of this material shall give appropriate credit to the U.S. Army Coastal Engineering Research Center.

Limited free distribution within the United States of single copies of this publication has been made by this Center. Additional copies are available from:

*National Technical Information Service  
ATTN: Operations Division  
5285 Port Royal Road  
Springfield, Virginia 22151*

Contents of this report are not to be used for advertising, publication, or promotional purposes. Citation of trade names does not constitute an official endorsement or approval of the use of such commercial products.

The findings in this report are not to be construed as an official Department of the Army position unless so designated by other authorized documents.

ACQUISITION for	
NTIS	White Section <input checked="" type="checkbox"/>
DDG	Buff Section <input type="checkbox"/>
UNANNOUNCED	<input type="checkbox"/>
JUSTIFICATION	
BY	
DISTRIBUTION/AVAILABILITY CODES	
Dist.	AVAIL. AND/OR SPECIAL
A	

UNCLASSIFIED

SECURITY CLASSIFICATION OF THIS PAGE (When Data Entered)

REPORT DOCUMENTATION PAGE		READ INSTRUCTIONS BEFORE COMPLETING FORM
1. REPORT NUMBER TP 76-17	2. GOVT ACCESSION NO.	3. RECIPIENT'S CATALOG NUMBER (9)
4. TITLE (and Subtitle) FLOATING BREAKWATER FIELD ASSESSMENT PROGRAM, FRIDAY HARBOR, WASHINGTON		5. TYPE OF REPORT & PERIOD COVERED Technical Paper
6. AUTHOR(s) Bruce Adey Eugene P. Richey Detald R. Christensen		7. PERFORMING ORG. REPORT NUMBER
8. PERFORMING ORGANIZATION NAME AND ADDRESS Ocean Engineering Research Laboratory University of Washington Seattle, Washington 98105 409931		9. CONTRACT OR GRANT NUMBER(s) DACW72-74-C-0012 NEW
10. CONTROLLING OFFICE NAME AND ADDRESS Department of the Army Coastal Engineering Research Center (CERRE-OC) Kingman Building, Fort Belvoir, Virginia 22060		11. PROGRAM ELEMENT, PROJECT, TASK AREA & WORK UNIT NUMBERS F31538
12. MONITORING AGENCY NAME & ADDRESS (if different from Controlling Office)		13. REPORT DATE September 1976
14. SECURITY CLASS. (of this report) UNCLASSIFIED		15. NUMBER OF PAGES 224
16. DISTRIBUTION STATEMENT (of this Report) Approved for public release; distribution unlimited.		17. DECLASSIFICATION/DOWNGRADING SCHEDULE
18. DISTRIBUTION STATEMENT (of the abstract entered in Block 20, if different from Report) (18) CEREC (19) TP-76-17		
19. SUPPLEMENTARY NOTES		
20. KEY WORDS (Continue on reverse side if necessary and identify by block number) Breakwaters Wave reflection Floating breakwaters Wave attenuation Waves Friday Harbor, Washington Wave transmission		
21. ABSTRACT (Continue on reverse side if necessary and identify by block number) A theoretical model for predicting the dynamic behavior of a floating breakwater is presented along with a report on a field experiment designed to provide basic data for verifying the model. Additional data were taken from the literature and from auxiliary laboratory experiments. The dynamic behavior characteristics investigated were: (A) Total transmitted and reflected waves and their components; (B) wave forces on the breakwater; (C) motions of the breakwater; and (D) forces on the mooring lines. The		

DD FORM 1 JAN 73 1473 EDITION OF 1 NOV 65 IS OBSOLETE

UNCLASSIFIED

SECURITY CLASSIFICATION OF THIS PAGE (When Data Entered)

409931

4

JB



UNCLASSIFIED

SECURITY CLASSIFICATION OF THIS PAGE(When Data Entered)

prediction model was developed from two-dimensional, linearized solutions of the hydrodynamical equations formulated in terms of a boundary value problem for the velocity potential. Some nonlinear effects are considered. Results for the predicted transmission coefficients were in good agreement with laboratory and field data, and they showed how the influence of fixed-body transmission, and of sway, heave, and roll motions on the transmission coefficient changed with increasing values of the parameter, beam (width) to wavelength ratio. The shape of the curves predicting the mooring line forces as a function of the beam (width) to wavelength ratio (or of wave frequency) followed those for the measured responses, but predicted magnitudes did not agree closely with measured values.

↳ The floating breakwater at Friday Harbor, Washington, was used as the field experimental platform; it was instrumented to record the incident and transmitted waves, mooring line forces, and the acceleration components of sway, heave, and roll. Ninety-five 17-minute records were obtained during the period 30 December 1974 to 5 May 1975. Statistical summaries of all data are presented with analyses of selected transmitted waves, transmission coefficients, and acceleration components. The summaries and analyses constitute a performance report of a particular floating breakwater as well as an input to the development of the theoretical model.



## PREFACE

This report is published to provide coastal engineers with a basic analytical procedure in the evaluation of certain floating breakwater types as structures for protecting particular sites against wind waves. The work was carried out under the coastal construction program of the U.S. Army Coastal Engineering Research Center (CERC).

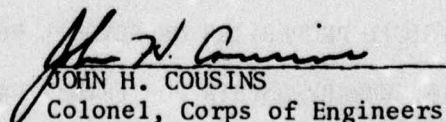
This report was prepared by Dr. Bruce H. Adee, Assistant Professor of Mechanical Engineering, Mr. Derald R. Christensen, Research Engineer, and Dr. Eugene P. Richey, Professor of Civil Engineering, of the Ocean Engineering Research Laboratory, University of Washington, Seattle, Washington, under CERC Contract No. DACW72-74-C-0012.

Special appreciation is extended to the port of Friday Harbor, Washington, for the use of the floating breakwater for the field assessment part of the study. Mr. Robert Hovey, Port Engineer, and Mr. Jack Fairweather, Port Superintendent, provided generous assistance with the numerous logistics problems in the installation and maintenance of the measuring equipment. The sensor monitoring and recording package was adapted from a design developed in a contemporary project sponsored by the University of Washington Sea Grant Program for monitoring two other floating breakwaters of a different type. Data from these two sites were used for comparative purposes in the analyses of the Friday Harbor breakwater.

Dr. D. Lee Harris, Chief, Oceanography Branch, was the CERC contract monitor for the report under the general supervision of Mr. R.P. Savage, Chief, Research Division.

Comments on this publication are invited.

Approved for publication in accordance with Public Law 166, 79th Congress, approved 31 July 1945, as supplemented by Public Law 172, 88th Congress, approved 7 November 1963.

  
JOHN H. COUSINS  
Colonel, Corps of Engineers  
Commander and Director

# CONTENTS

	Page
CONVERSION FACTORS, U.S. CUSTOMARY TO METRIC (SI) . . . . .	7
SYMBOLS AND DEFINITIONS . . . . .	8
I INTRODUCTION. . . . .	9
II THEORETICAL ANALYSIS. . . . .	12
1. Linear Theoretical Model. . . . .	13
2. Nonlinear Theoretical Model . . . . .	19
3. Results . . . . .	22
III FIELD DATA. . . . .	49
1. Layout. . . . .	49
2. Instrumentation . . . . .	49
3. Wind Data . . . . .	49
4. Waves . . . . .	49
5. Cable Forces. . . . .	53
6. Motion Package. . . . .	53
7. Data Acquisition System . . . . .	53
8. Data Processing and Analysis. . . . .	54
IV COMPARISON OF THEORY WITH FIELD DATA FOR FRIDAY HARBOR BREAKWATER. . . . .	64
V CONCLUSIONS . . . . .	71
LITERATURE CITED. . . . .	72
APPENDIX	
A HYDROSTATIC RESTORING FORCES AND SPRING CONSTANTS . . . . .	74
B MOORING ANALYSIS. . . . .	79
C LINEAR HYDRODYNAMIC COEFFICIENTS. . . . .	104
D FLOATING BREAKWATER ANALYSIS. . . . .	107
E DERIVATION OF PRESSURE TO SECOND ORDER FOR TWO PROGRESSIVE WAVES AT DIFFERENT FREQUENCIES. . . . .	148
F PHYSICAL PROPERTIES OF SEVERAL FLOATING BREAKWATERS . . . . .	156
G DATA SUMMARY SHEETS FOR FRIDAY HARBOR FLOATING BREAKWATER. . . . .	160
H INCIDENT AND TRANSMITTED WAVE SPECTRAL PLOTS. . . . .	180



## CONTENTS

### APPENDIX-Continued

	Page
I     LOW-FREQUENCY SPECTRAL ANALYSIS OF FORCE DATA . . . . .	192
J     HIGH-FREQUENCY SPECTRAL ANALYSIS OF FORCE AND MOTION DATA . . . . .	200
K     WAVE MEASUREMENT. . . . .	218

### TABLE

Summary of anchor cable force statistics. . . . .	61
---	----

### FIGURES

1 Aerial view of Friday Harbor breakwater . . . . .	11
2 A two-dimensional floating breakwater . . . . .	14
3 Linear system representative of a floating breakwater . . . . .	20
4 Filtered low-frequency seaward mooring line force, Tenakee, Alaska. . . . .	21
5 Transmission coefficient for proposed Oak Harbor breakwater . . . . .	24
6 Transmission coefficient for a rectangular breakwater . . . . .	26
7 Transmission coefficient for a rectangular breakwater restricted to sway motion only . . . . .	27
8 Transmission coefficient for a rectangular breakwater restricted to heave motion only. . . . .	29
9 Transmission coefficient for a rectangular breakwater . . . . .	30
10 Transmission coefficient for Alaska-type breakwater model . . . . .	31
11 Transmission coefficient for rigidly fixed Alaska-type breakwater model . . . . .	33
12 Transmission coefficient for Alaska-type breakwater, Tenakee, Alaska. . . . .	34
13 Theoretically predicted transmission coefficient, Friday Harbor breakwater. . . . .	36



# CONTENTS

## FIGURES-Continued

	Page
14 Theoretically predicted sway motion response, Friday Harbor breakwater . . . . .	38
15 Theoretically predicted heave motion response, Friday Harbor breakwater . . . . .	39
16 Theoretically predicted roll motion response, Friday Harbor breakwater . . . . .	40
17 Seaward mooring line force for proposed Oak Harbor breakwater . . . . .	42
18 Seaward mooring line mooring-force coefficient, Tenakee, Alaska . . . . .	44
19 Recorded time series, Tenakee, Alaska . . . . .	45
20 Theoretically predicted long-period sway response of Alaska-type breakwater, Tenakee, Alaska . . . . .	46
21 Theoretically predicted seaward mooring line mooring-force coefficient, Friday Harbor breakwater. . . . .	47
22 Theoretically predicted long-period sway response, Friday Harbor breakwater. . . . .	48
23 General location map. . . . .	50
24 Field experiment site location map. . . . .	51
25 Instrumentation location plan, Friday Harbor breakwater . . . . .	52
26 Instrumentation and recording package layout. . . . .	55
27 Average transmission curves for Friday Harbor breakwater. . . . .	59
28 Transmission coefficient for Friday Harbor breakwater . . . . .	65
29 Sway acceleration response for Friday Harbor breakwater . . . . .	66
30 Heave acceleration response for Friday Harbor breakwater. . . . .	67
31 Roll acceleration response for Friday Harbor breakwater . . . . .	68
32 Seaward mooring line mooring-force coefficient, Friday Harbor breakwater . . . . .	70

# **CONVERSION FACTORS, U. S. CUSTOMARY TO METRIC (SI) UNITS OF MEASUREMENT**

U.S. customary units of measurement used in this report can be converted to metric (SI) units as follows:

Multiply	by	To obtain
inches	25.4	millimeters
	2.54	centimeters
square inches	6.452	square centimeters
cubic inches	16.39	cubic centimeters
feet	30.48	centimeters
	0.3048	meters
square feet	0.0929	square meters
cubic feet	0.0283	cubic meters
yards	0.9144	meters
square yards	0.836	square meters
cubic yards	0.7646	cubic meters
miles	1.6093	kilometers
square miles	259.0	hectares
acres	0.4047	hectares
foot-pounds	1.3558	newton meters
ounces	28.35	grams
pounds	453.6	grams
	0.4536	kilograms
ton, long	1.0160	metric tons
ton, short	0.9072	metric tons
degrees (angle)	0.1745	radians
Fahrenheit degrees	5/9	Celsius degrees or Kelvins <sup>1</sup>

<sup>1</sup>To obtain Celsius (C) temperature readings from Fahrenheit (F) readings, use formula:  $C = (5/9)(F - 32)$ .  
To obtain Kelvin (K) readings, use formula:  $K = (5/9)(F - 32) + 273.15$ .



# SYMBOLS AND DEFINITIONS

$A_1, A_2$	Amplitudes of two incident waves
$a_i$	Amplitude of sway, heave, or roll motion for $i = 1, 2, 3$
$B$	Characteristic beam of breakwater
$C_0$	Body contour
$C_T$	Transmission coefficient
$F_j(t)$	Sway, heave, or roll exciting forces or moment for $j = 1, 2, 3$
$KH_{ij}$	Hydrostatic restoring-force coefficient for force in the $j$ th direction due to motion in the $i$ th direction
$KM_{ij}$	Similar to $KH_{ij}$ but due to the mooring system
$k_1, k_2$	Wave numbers of two incident waves
$L$	Incident wavelength
$m_{ij}$	Mass or moment of inertial when $i = j$ , 0 when $i \neq j$
$\vec{n}$	Unit interior normal to body surface
$P(x, y, t)$	Pressure
$\vec{r}$	Vector from center of gravity to a point on the body surface
$\alpha_i, \dot{\alpha}_i, \ddot{\alpha}_i$	Sway, heave, or roll motion; speed or acceleration
$\epsilon$	Phase angle
$\delta_1, \delta_2$	Phase angles for two incident waves
$\eta(x, t)$	Free-surface elevation
$\eta_I(x, t)$	Wave surface elevation for incident wave
$\eta_T(x, t)$	Wave surface elevation for transmitted wave
$\lambda_{ij}$	Damping coefficient for force in the $j$ th direction related to velocity in the $i$ th direction
$\mu_{ij}$	Added-mass or inertial-force coefficient for force in the $j$ th direction related to acceleration in the $i$ th direction
$\rho$	Fluid density
$\phi$	Velocity potential
$\omega$	Frequency
$\omega_1, \omega_2$	Frequencies for two incident waves



FLOATING BREAKWATER FIELD ASSESSMENT PROGRAM,  
FRIDAY HARBOR, WASHINGTON

by  
B.H. Adee, E.P. Richey,  
and D.R. Christensen

I. INTRODUCTION

Floating structures for use in the attenuation of water waves were introduced by Joly (1905). Little was done with the concept until the Bombardon floating breakwater was deployed to form a harbor during the Normandy invasion of World War II. The use of mobile harbors for potential military applications provided the incentive for extensive work during the postwar years. Representative articles from this period include those by Minikin (1948) who discussed floating breakwaters in general terms, Carr (1951) who used basic mechanics to predict transmission characteristics, and the review of the performance of the Bombardon by Lochner, Faber, and Penny (1948). In 1957, the Naval Civil Engineering Laboratory, Port Hueneme, California, began a concerted exploration of the existing knowledge of transportable units that could serve as breakwaters or piers. Results of the study are summarized in Naval Civil Engineering Laboratory (1961), which was an invaluable state-of-the-art assessment with particular emphasis on military uses under the rather severe site criteria of an incident wave with a 15-foot height, 13-second period, minimum water depth of 40 feet, inshore transmitted wave height of 4 feet, and tidal range of 12 feet. A sequel to the earlier study (Naval Civil Engineering Laboratory, 1971) surveyed concepts for "transportable" breakwaters, including over 60 in the "floating" category. Although no breakwater system was disclosed which would meet the stringent military site criteria and transportability requirement, these state-of-the-art reviews sparked renewed interest in the floating breakwater for nonmilitary applications. A review of developments in floating breakwaters was summarized by Richey and Nece (1974); Seymour (1974) introduced a new and innovative concept for wave attenuation using a system of tethered floats which may have application over a wide range of wave conditions.

Continually increasing pleasure boat ownership has nearly exhausted the available supply of moorage space in many areas. The need for additional moorage space in conjunction with escalating construction costs and more stringent environmental restrictions require careful scrutiny of alternatives to the traditional fixed breakwater and excavation techniques employed in marina construction. Productive time in weather-dependent, waterborne activities such as construction, logging, and cargo handling could be increased if protective floating, transportable breakwaters were used. Other uses in the control of shoreline erosion and in the emerging mariculture industry may also be found.

The information on the performance of floating breakwaters, i.e., their wave attenuating characteristics, mooring line forces, and motions, is contained primarily in reports of laboratory scale model tests with monochromatic incident waves; the few exceptions are the early analytical work by Carr (1951) and the occasional piece of information from a full-scale test like that performed by Harris (1974). There is a need for a fundamental analytical procedure to predict the performance characteristics of floating breakwaters with arbitrary cross section when exposed to a given incident wave. This procedure could be used to systematically compare performance information available in the literature, to examine new design proposals, and either eliminate or reduce and systematize auxiliary experimental studies.

The development of the predictive procedure was the primary thrust of the project with the concomitant field assessment of a full-scale floating breakwater in operation at Friday Harbor, Washington (Fig. 1). The analytical model developed from the two-dimensional, linearized solutions of the hydrodynamical equations formulated in terms of a boundary value problem for the velocity potential. The model was refined progressively by comparisons with results already reported in the literature, by auxiliary laboratory tests, and by the results from the Friday Harbor field program, where measurements of incident and transmitted waves, mooring line forces, and acceleration in sway, heave, and roll were measured over a 6-month period.

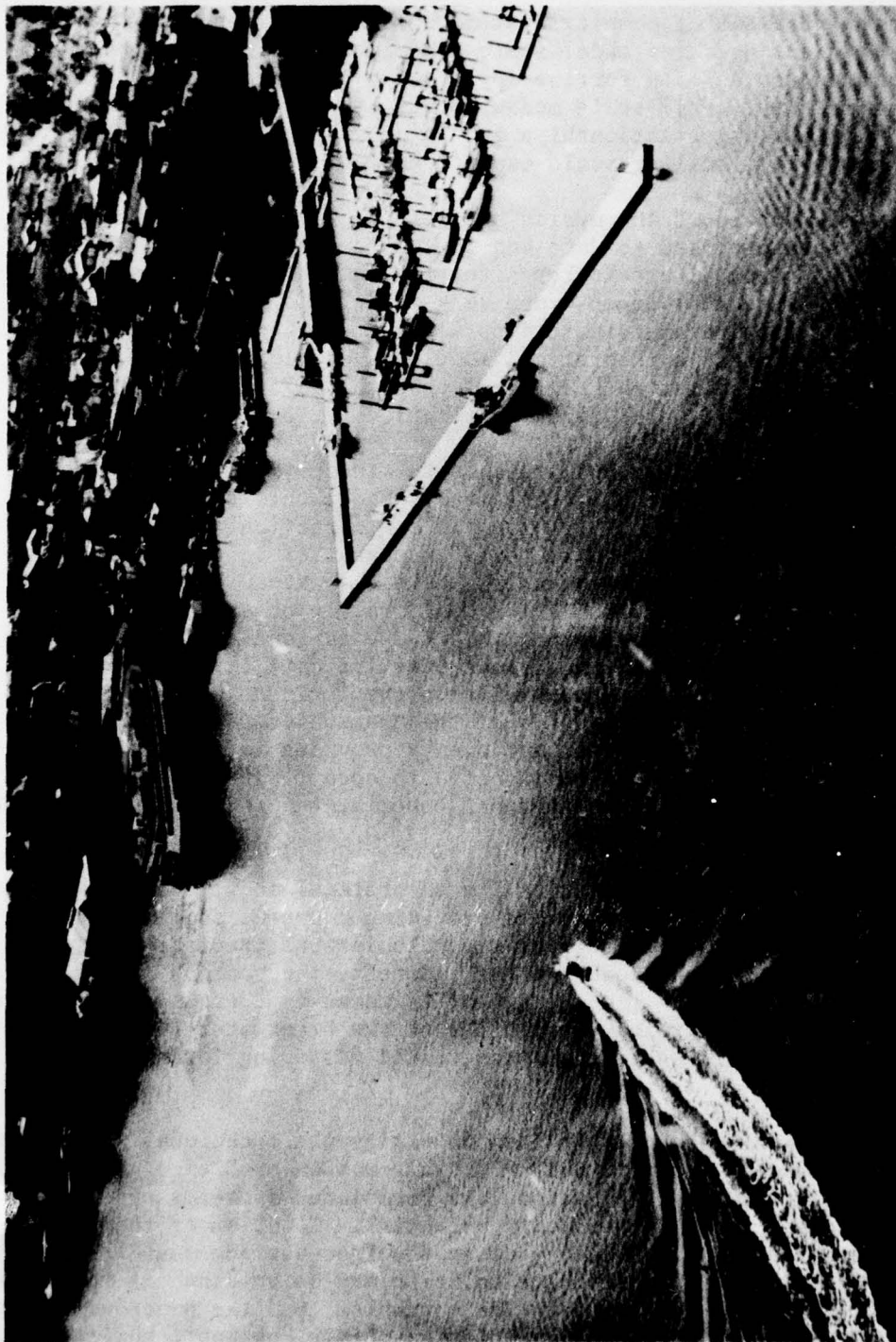


Figure 1. Aerial view of Friday Harbor breakwater.



## II. THEORETICAL ANALYSIS

In the analysis of complex systems such as floating breakwaters, there is a great need for model-scale experiments to predict their performance and provide data for the application of rational engineering design principles. Full-scale measurements are also extremely valuable in verifying scaling relationships and in providing confidence that the data obtained from smaller scale experiments are reasonable.

When one considers the myriad possible breakwater configurations which have been proposed to date and the different conditions which prevail at each potential breakwater site, the number of required model tests and the attendant expense are very large. To avoid this expense and also to permit parametric studies aimed at obtaining optimum breakwater configurations, a theoretical model was developed. The goal was to theoretically predict the performance which could be measured in laboratory studies or at prototype installations.

The initial restriction imposed on the theoretical model was to consider only two-dimensional conditions. Under this restriction the breakwater is assumed to be very long in one direction with long-crested waves approaching so that their crests are parallel to the long axis of the breakwater. At most breakwaters where the wave climate results from wind-generated waves, this condition would rarely be approached. However, experiments performed using a boat wake to generate incident waves on the beam and at an angle to a breakwater indicate larger breakwater motions and larger transmitted waves when the incident wave crests approach parallel to the long axis of the breakwater (Stramandi, 1975). As a design tool, a two-dimensional theory provides information on the worst conditions which might be expected to occur. In addition, the extensive two-dimensional wave-channel experiments provide the data needed to test the theoretical model.

Throughout the development of the theoretical model, every attempt was made to orient the model toward providing a useful tool applicable to realistic problems. To perform the calculations the user need only know the incident wave frequencies of interest, the contour of the breakwater cross section (catamaran- or trimaran-type cross sections are permitted), and the physical properties of the breakwater (these include mass, mass moment of inertia, and the static restoring-force coefficients).

The approach used here has been to employ the techniques which naval architects have developed to deal with ship motion problems. Mathematically, the hydrodynamic equations are formulated in terms of a boundary value problem for the velocity potential. Solution of this complete problem is presently impossible because the free-surface boundary condition is nonlinear. An approximate solution may be obtained if restrictions are imposed on the boundary value problem, and the procedure of linearization is applied. The restrictions limit the applicability of

the solution to cases of small incident wave amplitude and small motion response of the breakwater.

When using the linearized theory which is presented here, one must be well aware of the limits of applicability which are imposed on the results in order to permit the formulation of a tractable mathematical problem. Care must also be exercised because these restrictions may exclude phenomena which occur in nature from appearing in the mathematical analysis. For instance, field observations clearly demonstrate the occurrence of mooring line force oscillations at periods greater than those which could be attributed directly to wind-generated wave excitation. Using a linearized approach, these long-period oscillations would not appear in the analysis. A theoretical model which includes nonlinear behavior of the system is required if these long-period oscillations are to be included.

A possible nonlinear mechanism for the transfer of wave energy to lower frequencies has been postulated and is presented to supplement the linear analysis.

#### 1. Linear Theoretical Model.

The problems involved in theoretically predicting the performance of a two-dimensional floating breakwater are illustrated in Figure 2. Here an incident wave approaches the breakwater on the beam. A part of the energy contained in the incident wave is reflected, part passes beneath the breakwater, and some is lost through dissipation. Another part of the incident wave energy excites the motions of the breakwater. These motions are restrained by the mooring system. The oscillating breakwater in turn generates waves which travel away from the breakwater in the directions of the reflected and transmitted waves. The total transmitted wave is the sum of the component which passes beneath the breakwater and the components generated by the breakwater motions. The total reflected wave is composed similarly.

In completing the calculations, the information which is of most interest to the designer includes:

- (a) Total transmitted and reflected waves including their components.
- (b) Wave forces on the breakwater.
- (c) Motions of the breakwater.
- (d) Forces on the mooring lines.

For the two-dimensional breakwater, definitions for the motions are shown in Figure 2. Sway is defined as the oscillation perpendicular to the long axis, or along the x-coordinate axis. Heave is the vertical



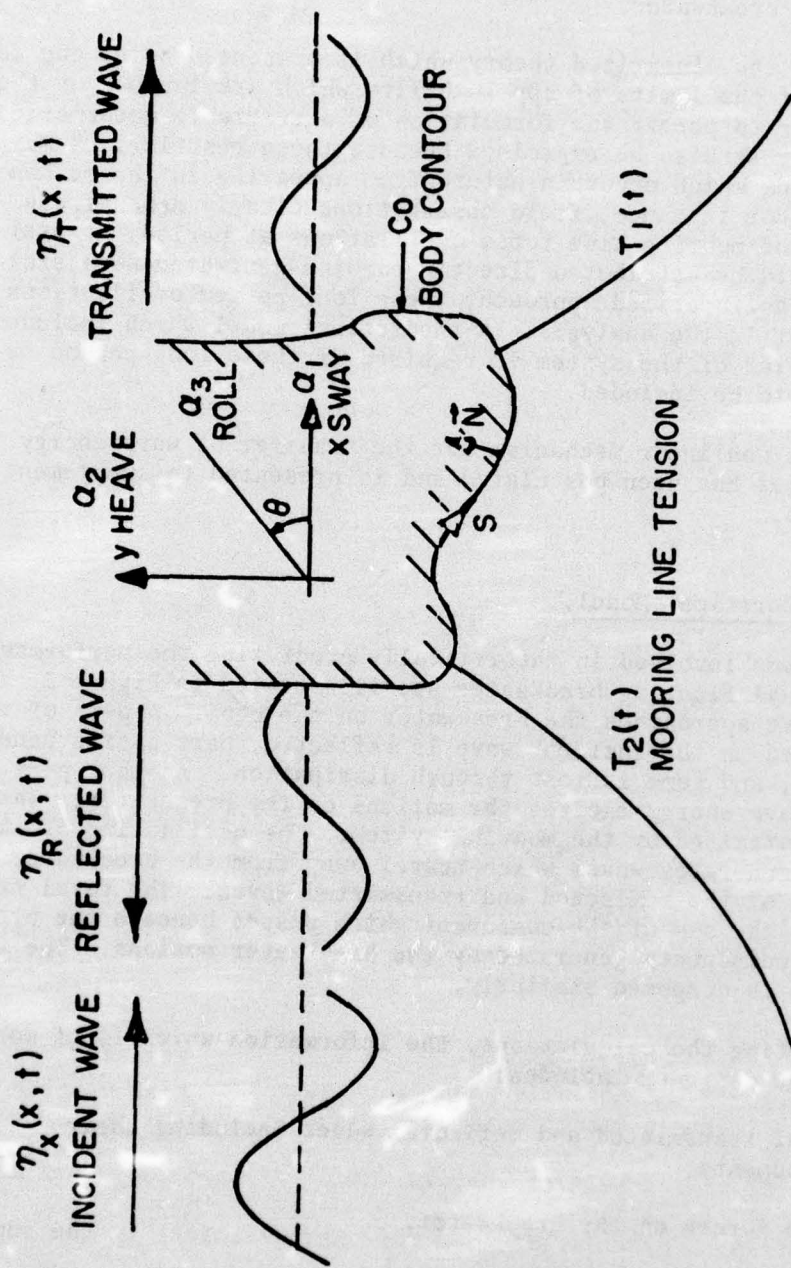


Figure 2. A two-dimensional floating breakwater.

motion of the breakwater along the y-coordinate axis, and roll is the rotation about the long axis or the z-coordinate direction.

As long as the problem is linear, computing the performance of a floating breakwater may be separated into three parts:

- (a) Formulate equations of motion.

Calculate hydrostatic forces and moments.

Evaluate hydrodynamic coefficients in equations of motion.

Compute exciting forces on breakwater.

Solve for the motions and motion-generated waves.

Compute forces in the mooring lines.

- (b) Solve for the waves diffracted by a rigidly restrained breakwater.

- (c) Sum components to obtain total reflected and total transmitted waves.

When combined, these parts of the calculation provide complete performance data for a two-dimensional breakwater.

a. Breakwater Motions. In deriving the equations of motion, Newton's law is used.

$$m_{ij} \ddot{\alpha}_i = \Sigma \text{ forces}; \quad (1)$$

here:

$\alpha_i$  = motion of the breakwater in sway, heave, and roll for  $i = 1, 2, 3$ , respectively. The dot above indicates differentiation with respect to time.

$m_{ij}$  = mass or mass moment of inertia when  $i = j$  and zero when  $i \neq j$ .

Expanding this equation to include the various forces in the summation yields:

$$\begin{aligned} m_{ij} \ddot{\alpha}_i &= F_j \text{ (inertial)} + F_j \text{ (wave damping)} \\ &+ F_j \text{ (friction)} + F_j \text{ (hydrostatic)} + F_j \text{ (mooring)} \\ &+ F_j \text{ (wave exciting)} \end{aligned}$$



The inertial force (or added-mass force) arises when the breakwater accelerates, which also accelerates the fluid around it. The motion-generated waves are moving away from the breakwater and result in the wave-damping term. A term representing the forces due to viscosity is included, but these forces are neglected in the analysis. Experience in ship motion analysis (Salvesen, 1970) has shown this to be acceptable for all motions but roll, where damping may make a more significant contribution than for sway and heave motions. At present, the main reason for neglecting the frictional forces is that they lead to nonlinear terms in the equations of motion, which make their solution far more complex. Hydrostatic forces arise because of changes in the displaced volume of the breakwater when it moves. In this analysis the mooring forces are modeled as simple springs with their contribution to the damping and inertial forces considered small in comparison to similar terms resulting from the breakwater motion. The wave exciting force results from the incident waves striking the breakwater.

If we neglect the nonlinear terms and assume that the fluid is inviscid, then the equations of motion describing the coupled sway, heave, and roll motions of the breakwater are of the form:

$$\sum_{i=1}^3 \{ (m_{ij} + \mu_{ij}) \ddot{\alpha}_i + \lambda_{ij} \dot{\alpha}_i + (KH_{ij} + KM_{ij}) \alpha_i \} = F_j(t) \quad (2)$$

for  $j = 1, 2, 3$ .

The symbols are defined as follows:

$\mu_{ij}$  = added-mass coefficient with the  $\mu_{ij} \ddot{\alpha}_i$  representing the added-mass force or moment in the  $j$ th direction due to acceleration in the  $i$ th direction.

$\lambda_{ij}$  = damping-force coefficient relating damping force or moment in the  $j$ th direction to velocity in the  $i$ th direction.

$KH_{ij}$  = hydrostatic spring constant relating the restoring force or moment in the  $j$ th direction to displacement in the  $i$ th direction.

$KM_{ij}$  = similar to  $KH_{ij}$  but due to the mooring system.

$F_j$  = exciting force or moment in the  $j$ th direction.

In order to solve these equations, the physical mass and moment of inertia, added mass and damping coefficients, static spring constants, and the exciting forces must all be known. Mass and moment of inertia are computed directly from the specifications of the breakwater section. The  $KH_{ij}$  are derived directly from hydrostatic considerations in Appendix A, while approximate values for  $KM_{ij}$  are obtained by using a discretized approximation for the mooring line as described in Appendix B. Potential

theory and the principle of linear superposition permit derivations for the hydrodynamic coefficients and forcing function  $\mu_{ij}$ ,  $\lambda_{ij}$  and  $F_j(t)$ .

Steady-state solutions of the form:

$$\alpha_i(t) = a_i \sin(\omega t + \delta_i) \text{ for } i = 1, 2, 3 \quad (3)$$

are assumed. Substitution of the assumed solution (eq. 3) into the equations of motion (eq. 2) yields a set of linear algebraic equations which may be solved for the unknown amplitudes and phase angles  $a_i$  and  $\delta_i$ . Transfer functions,  $H_i$ , are then defined by the  $a_i$  and  $\delta_i$  since the incident waves are assumed to be sinusoidal.

b. Hydrodynamic Coefficients and Waves. Potential theory is employed in computing the reflected and transmitted waves, hydrodynamic coefficients and the exciting forces. Under the assumptions of small incident waves, small breakwater motions and an inviscid fluid, the velocity potentials may be found and the problem subdivided using the principle of linear superposition. The total velocity potential:

$$\phi_{\text{total}} = \phi_{\text{incident}} + \phi_{\text{diffracted}} + \phi_{\text{motion}}^{(i)} \text{ for } i = 1, 2, 3 \quad (4)$$

is the sum of the incident wave potential, the diffracted wave potential and the potential resulting from forced sway, heave, and roll motions.

The incident wave potential is well known and may be expressed directly. Obtaining the diffracted wave and breakwater motion potentials requires the solution of boundary value problems. These problems and their solutions are described in Appendix C. Appendix D provides the computer program used to calculate breakwater performance.

When the velocity potentials have been obtained, the free-surface elevation at any position is found using the linearized free-surface boundary condition:

$$\eta(x, t) = -\frac{1}{g} \phi_t(x, 0, t). \quad (5)$$

Here:

$\eta(x, t)$  = free-surface elevation measured from stillwater level ( $y = 0$ ),

$g$  = acceleration of gravity,

$\phi_t(x, 0, t)$  = derivative of the velocity potential with respect to time evaluated at  $y = 0$ .



$$\eta_{\text{total}}(x,t) = -\frac{1}{g} \{ \phi_t \text{ incident}(x,0,t) + \phi_t \text{ diffracted}(x,0,t) + \phi_t^{(i)} \text{ motion}(x,0,t) \}. \quad (6)$$

The fluctuating component of pressure in the fluid and on the breakwater hull surface may be computed using Bernoulli's equation:

$$P(x,y,t) = -\rho \phi_t(x,y,t). \quad (7)$$

By computing pressures on the hull surface and integrating these around the contour, the forces on the breakwater may be computed. The force per unit length acting on the breakwater is then:

$$F(t) = \int_{C_0} P \vec{n} ds. \quad (8)$$

In this case,

$F(t)$  = force on the breakwater,

$\vec{n}$  = unit interior normal vector on the hull surface,

$C_0$  = contour of breakwater cross section.

The rolling moment is:

$$M(t) = \int_{C_0} P \vec{r} \times \vec{n} ds, \quad (9)$$

where,

$\vec{r}$  = the vector from the center of gravity to a point on the surface.

To compute the exciting forces on the breakwater in linear theory, the pressure due to the incident and diffracted waves is integrated over the hull surface. These forces and moments become:

$$\begin{aligned} F_1(t) &= \left\{ -\rho \int_{C_0} [\phi_t \text{ incident}(s,t) + \phi_t \text{ diffracted}(s,t)] \vec{n} ds \right\} \cdot \vec{i}, \\ F_2(t) &= \left\{ -\rho \int_{C_0} [\phi_t \text{ incident}(s,t) + \phi_t \text{ diffracted}(s,t)] \vec{n} ds \right\} \cdot \vec{j}, \\ F_3(t) &= \left\{ -\rho \int_{C_0} [\phi_t \text{ incident}(s,t) + \phi_t \text{ diffracted}(s,t)] \vec{r} \times \vec{n} ds \right\} \cdot \vec{k}. \end{aligned} \quad (10)$$

Hydrodynamic coefficients are found using the potential resulting from forced oscillation of the breakwater. In this case the pressure

integrated over the surface has a component in phase with acceleration and a component in phase with velocity. The component in phase with acceleration is normally referred to as the added mass, while the component in phase with velocity is the damping.

The hydrodynamic coefficients shown in this section are derived in greater detail in Appendix C.

c. Mooring Forces. At the time the spring constants for the mooring lines are computed, mooring force coefficients are also calculated. These are:

$$\frac{\Delta F}{\Delta \alpha_i} = \text{change in mooring line force per unit displacement in sway, heave, or roll when } i = 1, 2, \text{ or } 3, \text{ respectively.}$$

The forces in the mooring lines may then be computed once the motions have been found.

$$\text{Mooring Force} = \sum_{i=1}^3 \left( \frac{\Delta F}{\Delta \alpha_i} \right) \alpha_i(t)$$

The description of the linear system is now complete. The block diagram in Figure 3 shows the relationships among the calculations which are required.

## 2. Nonlinear Theoretical Model.

Measurements taken at the Tenakee, Alaska, floating breakwater before this research program was begun indicated the presence of a long-period oscillatory motion of the breakwater. These long-period motions were manifested most clearly in the measured mooring line forces. Looking at these, one can visually observe an oscillation with a period of about 60 seconds superimposed over the expected shorter period oscillations. Figure 4 shows the results of a spectral analysis of the seaward mooring line data after a low-pass filter has been applied (the technique for performing the spectral analysis is given in Section III of this report).

The linear theoretical model permits the system to respond only at the frequency of the incident wave. In order to explain the presence of these long-period oscillations, nonlinearities must be included in the analysis. To perform a mathematically complete analysis including all nonlinear effects is beyond the present state of the art. However, in the case of the floating breakwater, one can show that if two incident waves are considered and second-order terms are retained, then an exciting force is present at the difference between the frequencies of the incident waves. The complete derivation in Appendix E shows that the nonlinear pressure may be expressed as:



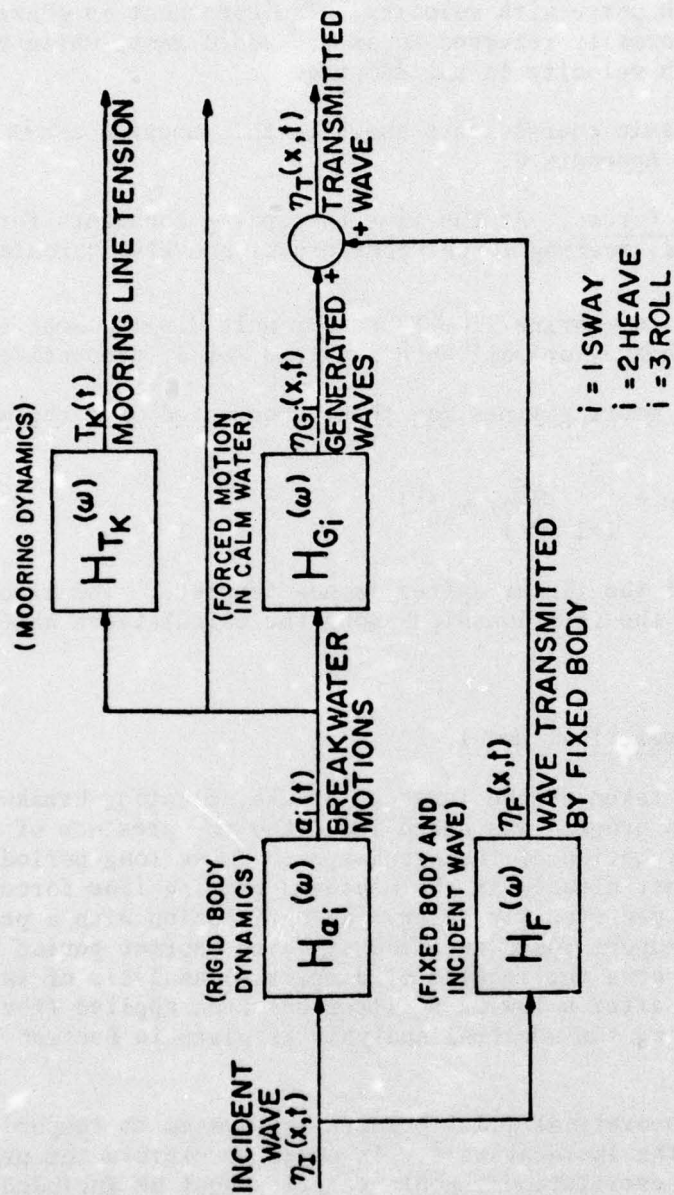


Figure 3. Linear system representative of a floating breakwater.

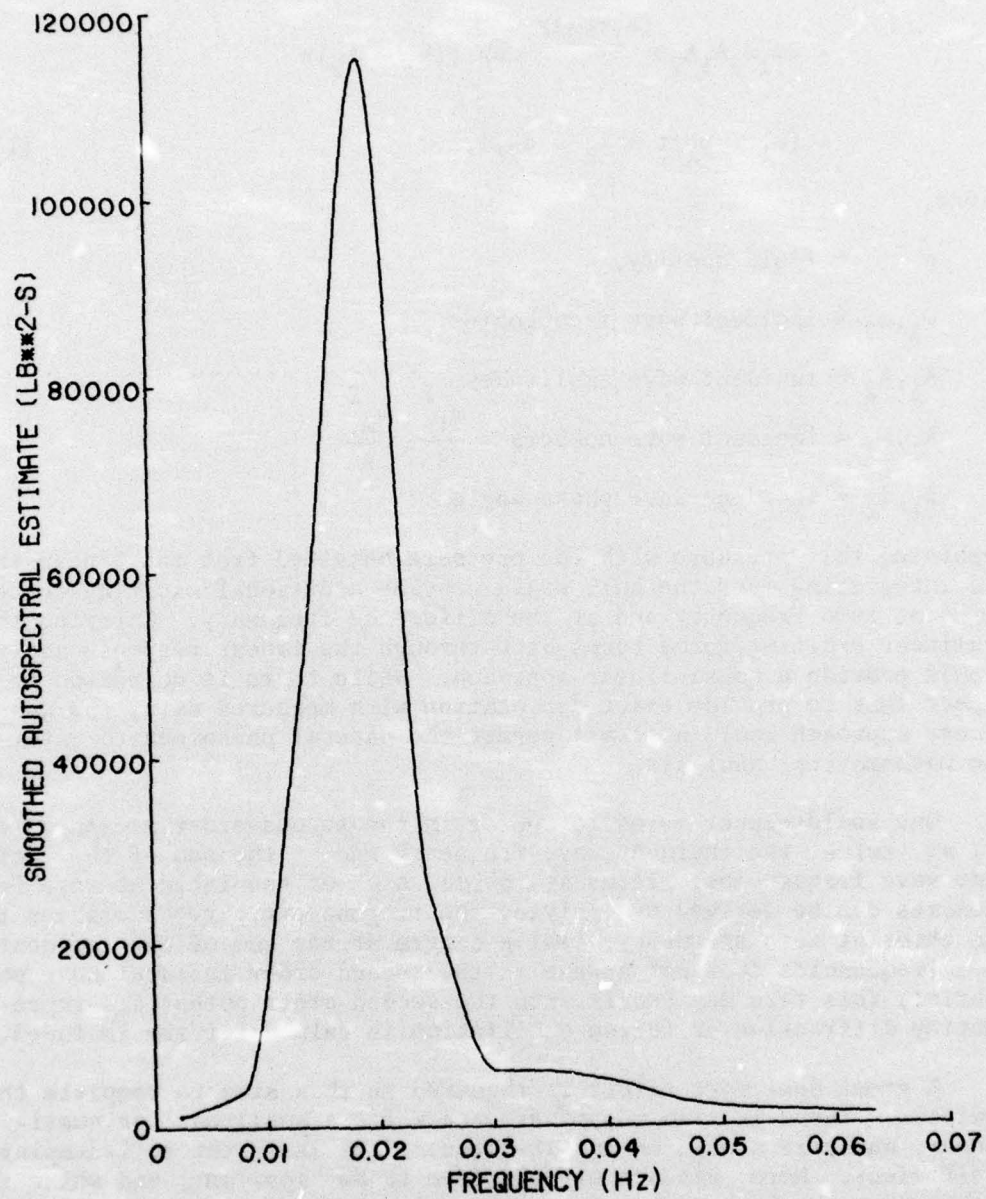


Figure 4. Filtered low-frequency seaward mooring line force, Tenakee, Alaska (record TK7-23).



$$\begin{aligned}
P(t) = & - \frac{\rho}{2} \{ \omega_1^2 A_1^2 e^{2k_1 t} + \omega_2^2 A_2^2 e^{2k_2 y} \\
& - 2\omega_1 \omega_2 A_1 A_2 e^{(k_1 + k_2)y} \cos [(k_1 - k_2)x \\
& - (\omega_1 - \omega_2)t + \delta_1 - \delta_2] \},
\end{aligned}
\tag{11}$$

where,

$\rho$  = fluid density,

$\omega_1, \omega_2$  = incident wave frequencies,

$A_1, A_2$  = incident wave amplitudes,

$k_1, k_2$  = incident wave numbers =  $\frac{\omega_1}{g}, \frac{\omega_2}{g}$ ,

$\delta_1, \delta_2$  = incident wave phase angles.

Combining this pressure with the pressure obtained from the linear theory and integrating over the hull would provide additional exciting-force terms at zero frequency and at the difference frequency. Carrying the nonlinear exciting-force terms back through the linear response analysis should provide a quasi-linear approach. While there is no reason to expect this to provide exact correlation with measured data, the quasi-linear approach would at least permit the natural phenomena to enter into the mathematical analysis.

One would expect terms to appear in the second-order pressure (eq. 11) at twice the incident wave frequency and at the sum of the incident wave frequencies. Terms at twice each of the incident wave frequencies can be derived by applying the trigonometric relationships to the terms at zero frequency. While a term at the sum of the incident wave frequencies does not appear in the second-order incident wave potential, this term may result when the second-order potentials representing diffraction or forced oscillation in calm water are included.

A great deal more effort is required in this area to complete the analysis. There is also one other area where a nonlinear, or quasi-linear, analysis should be investigated. This is in the roll-damping coefficient. Here, viscous effects seem to be important, and while the problem has not been dealt with within the present study, investigators have included a term proportional to velocity squared in the equation for roll motion.

### 3. Results.

The computer program given in Appendix D has been developed to

calculate the values of hydrodynamic coefficients, breakwater motions, and the wave field. Input variables include:

- (a) The body contour,  $C_0$ , represented by a series of points on the contour.
- (b) The physical properties of the body: mass, mass moment of inertia, and position of the center of gravity.
- (c) The mooring system spring constants.
- (d) The hydrostatic restoring spring constants.
- (e) The incident wave frequency,  $\omega$ .

In this program the exciting forces and moments appearing in the equations of motion and the fixed-body parts of the transmitted and reflected waves are found by computing the forces, moments, and waves which result when a rigidly fixed body is struck by a sinusoidal incident wave of frequency  $\omega$ . Motions are found by computing the steady-state solution to the three equations of motion. The hydrodynamic coefficients and the waves generated by the body motions are found by computing the forces, moments, and waves which result when the body is forced to oscillate in stillwater in pure sway, pure heave, or pure roll.

The physical properties used in the performance calculations for the various breakwaters are collected in Appendix F.

a. Wave Transmission. To assess the performance of a floating breakwater, one quantity which is commonly used is the transmission coefficient. This is simply the transmitted wave amplitude divided by the incident wave amplitude,  $|\eta_T(x,t)|/|\eta_I(x,t)|$  for monochromatic incident waves.

(1) Proposed Oak Harbor Breakwater. At one time the Corps of Engineers was considering a marina and floating breakwater at Oak Harbor, Washington. Model experiments were carried out by Davidson (1971) to determine transmission characteristics and mooring forces. The breakwater itself had a catamaran-type cross section. A comparison between the theoretically predicted and experimentally measured transmission coefficient is shown in Figure 5. This figure as well as the others plotted in this section and Section IV were drawn using a CALCOMP plotter. The plotting program uses a parabolic fit to determine additional points between the given data. Varying numbers of data points were used to describe each curve depending on its behavior. Data points were closely spaced in regions where the theoretical predictions indicated large changes in curvature. Wavelength is calculated in all the figures using the relationship between wavelength and period for waves in deep water.

In this case, the results compare reasonably well except for the



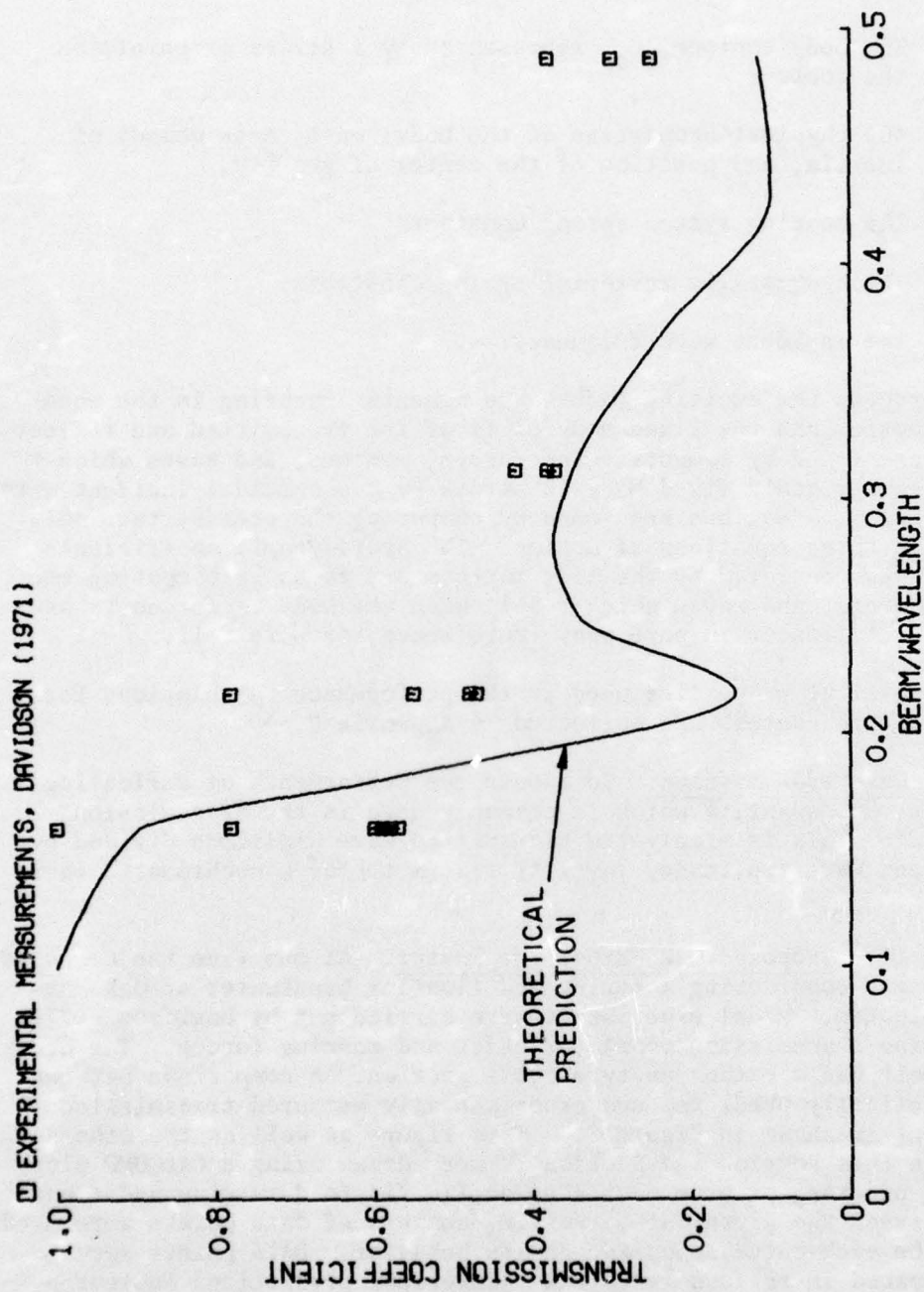


Figure 5. Transmission coefficient for proposed Oak Harbor breakwater.

predicted dip in transmission just above a B/L (beam/wavelength) of 0.2. There is also some difference at higher B/L ratios.

The theory predicts that the part of the transmitted wave which would result where the body is rigidly fixed is almost 1 for a B/L less than 0.1 and drops rapidly at higher B/L ratios to the point where it is of little consequence beyond 0.2. Waves generated by the breakwater motions play an increasing role for B/L ratios above 0.15. Heave motion is the major contributor to the transmitted wave in the very narrow band of B/L between 0.15 and 0.18 with a predicted heave resonance at a B/L of about 0.18. The dip occurs because the waves generated by heave and sway motions are almost 180° out of phase and cancel each other out. At B/L ratios above 0.25, sway motion assumes an increasingly dominant role. Roll motions are small throughout and generate only very small waves.

(2) Rectangular Breakwater. A breakwater of rectangular cross section with the same beam and draft as the proposed Oak Harbor breakwater was tested at the University of Washington by Nece and Richey (1972). Results for the water depth of 29.5 feet are shown in Figure 6.

Again the agreement is reasonable. Further experiments with this model have confirmed the existence of the trough at a B/L of 0.2. However, this phenomenon can be observed only for very small wave heights. For practical purposes, the dip may be smoothed over considerably. The major discrepancy is at the high B/L ratios where the theory shows considerably greater transmission than is actually measured in the model tests. Since the transmitted wave is almost totally a result of sway motion, the problem must lie in the wave predicted by this motion.

Over the entire range of wavelengths of interest, the predicted results follow the pattern previously discussed for the proposed Oak Harbor breakwater. The transmitted wave is almost completely a result of fixed-body transmission followed by regions of heave resonance, heave and sway cancellation, and finally, sway wave generation as the B/L increases.

It is interesting to note that there is very little difference between the open-well breakwater and the closed rectangle of the same overall dimensions.

(3) Rectangular Breakwater Tested by Sutko and Haden. In some recent experiments Sutko and Haden (1974) have examined the effect that restricting breakwater motions has on the transmission coefficient. They used a rectangular breakwater model with a beam-to-draft ratio of 1.5. Plexiglas end assemblies were used to restrict the breakwater motions.

Figure 7 shows the transmission coefficient when the breakwater is restricted to sway motions only. Here, the transmitted wave contains a component resulting from the fixed-body transmission and a component



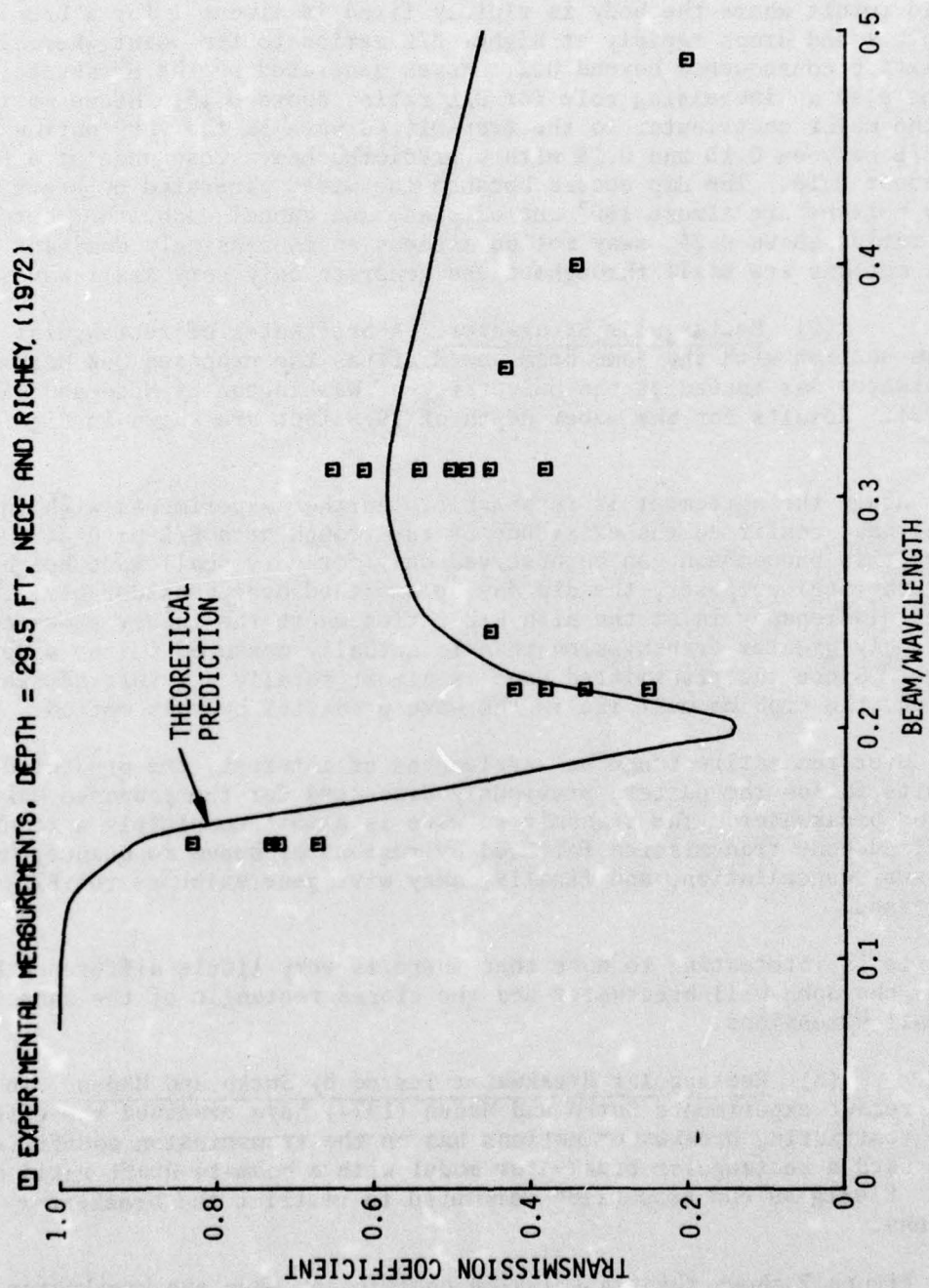


Figure 6. Transmission coefficient for a rectangular breakwater.

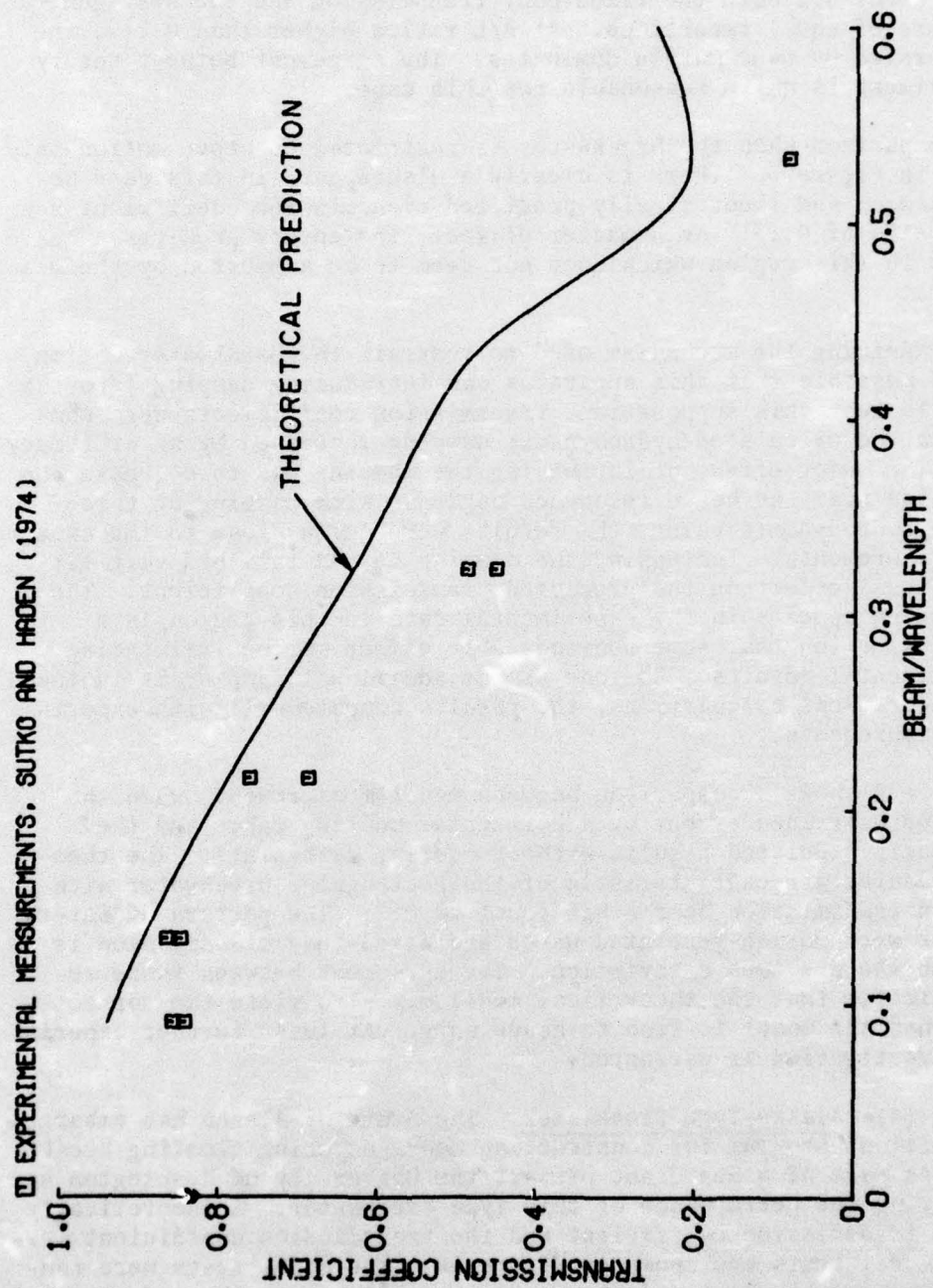


Figure 7. Transmission coefficient for a rectangular breakwater restricted to sway motion only.



resulting from the wave generated by the sway motion. At very low B/L ratios the fixed-body transmission is the more important component. At a B/L of about 0.1 both the fixed-body transmission and the sway-generated wave are of equal importance. At B/L ratios higher than 0.215, the wave generated by sway motion dominates. The agreement between theory and experiment is quite reasonable for this case.

A comparison when the breakwater is restricted to heave motion only is shown in Figure 8. There is clearly a discrepancy in this case between measured and theoretically predicted transmission coefficient near the B/L ratio of 0.13. As a matter of fact, the theory predicts a heave resonance in this region which does not seem to be supported by the measured data.

In examining the mechanism used to restrain the breakwater motion, it seemed possible that this apparatus was introducing damping into the system. To test this supposition, transmission coefficients were computed with the calculated hydrodynamic damping increased by an arbitrary amount. The major effect of increasing the damping was to decrease the transmission near the heave resonance region. With damping at three times the hydrodynamic value, the results were quite close to the experimental measurements. Increasing the damping beyond this had very little additional effect on the predicted transmission coefficient. The scatter which appears in the experimental data in this region is a further indication that some nonrepeatable effect may be influencing the experimental results. So long as the additional damping is included in the theoretical calculations, the results compare well with experimental measurements.

Figure 9 shows a comparison between model measurements when the model is unrestrained except by a horizontal mooring cable and the theoretically predicted results without mooring restraints. The theoretical results are characteristic of the rectangular breakwater with the dip in transmission near a B/L equal to 0.2. The pattern of interactions between motion-generated waves and fixed-body transmission is similar to the previous description. The agreement between these results indicates that the theoretical model may also yield the correct results when the model is free to heave only. At least further experimental investigation is warranted.

(4) Alaska-Type Breakwater. The State of Alaska has embarked on an ambitious program for constructing moorages using floating breakwaters. As part of a Sea Grant project the University of Washington has been studying the performance of this type breakwater. A theoretically predicted transmission coefficient and the transmission coefficient measured in model tests are shown in Figure 10. The model tests were conducted using very small incident waves (wave heights on the order of 0.2 to 0.3 feet at prototype scale). Results for larger wave slopes were not included in the figure but do show the same trends with lower values of transmission coefficient. Theoretical predictions without added damping and with double the hydrodynamic damping are shown in Figure 10.

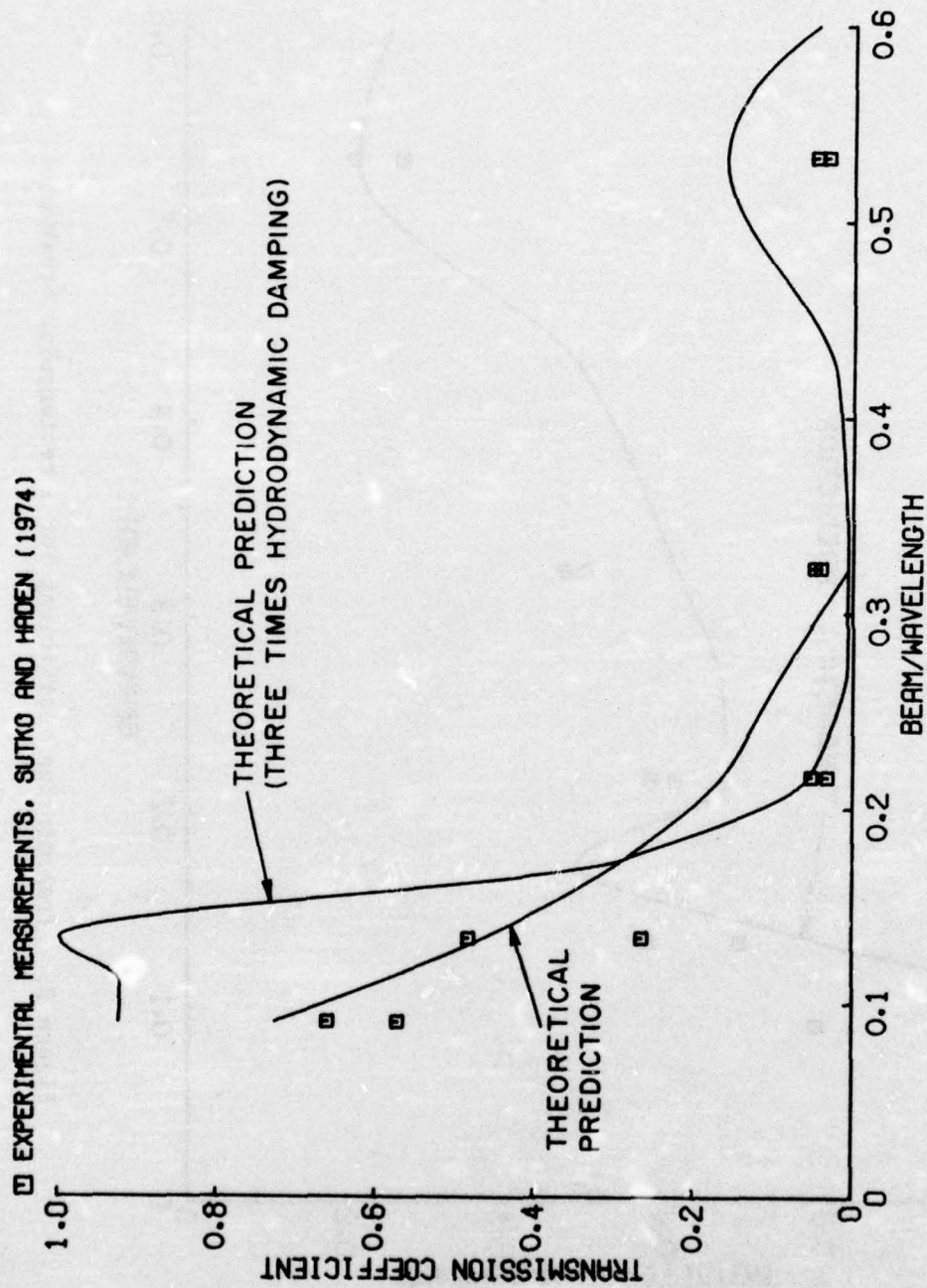


Figure 8. Transmission coefficient for a rectangular breakwater restricted to heave motion only.



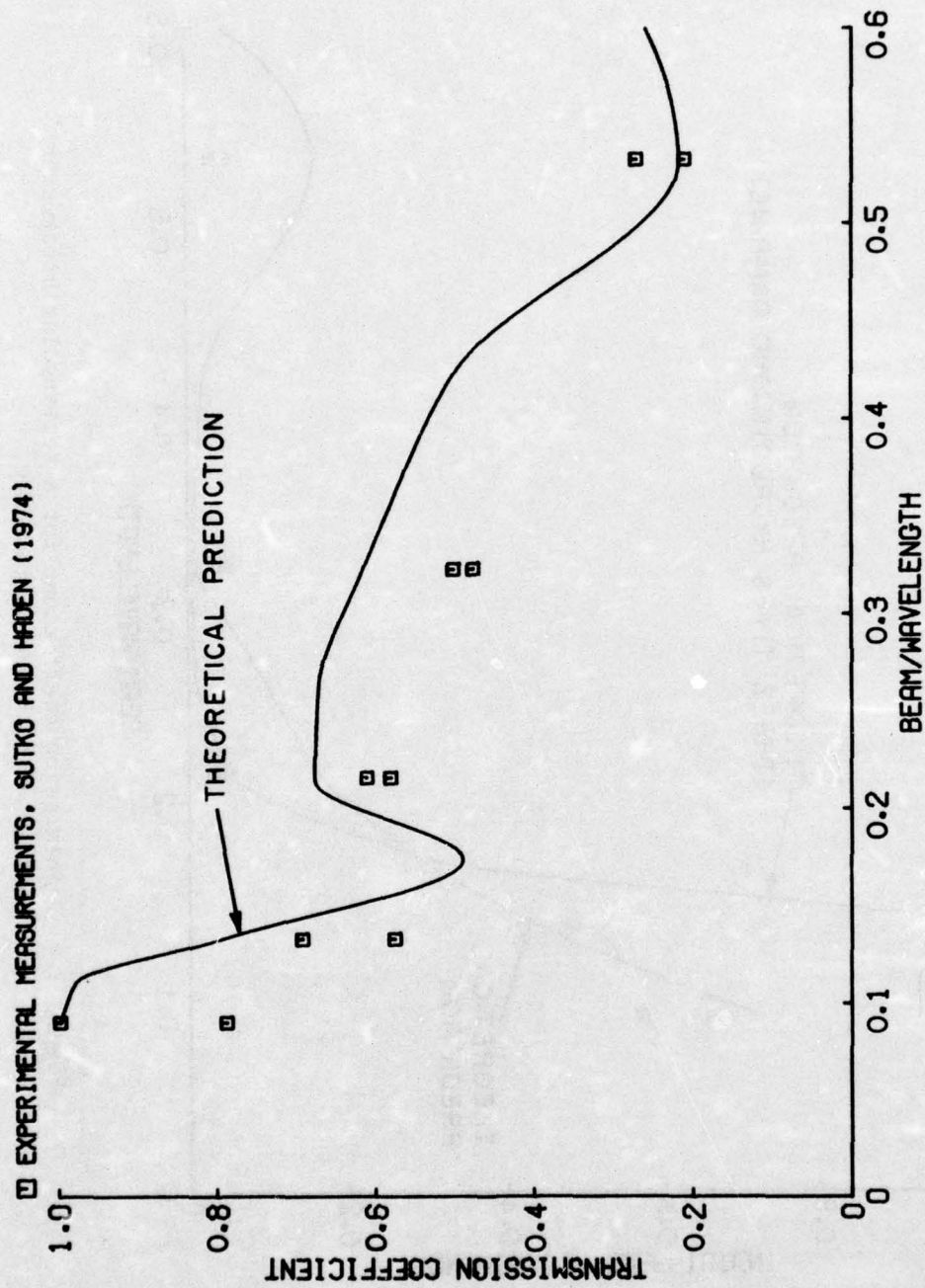


Figure 9. Transmission coefficient for a rectangular breakwater.

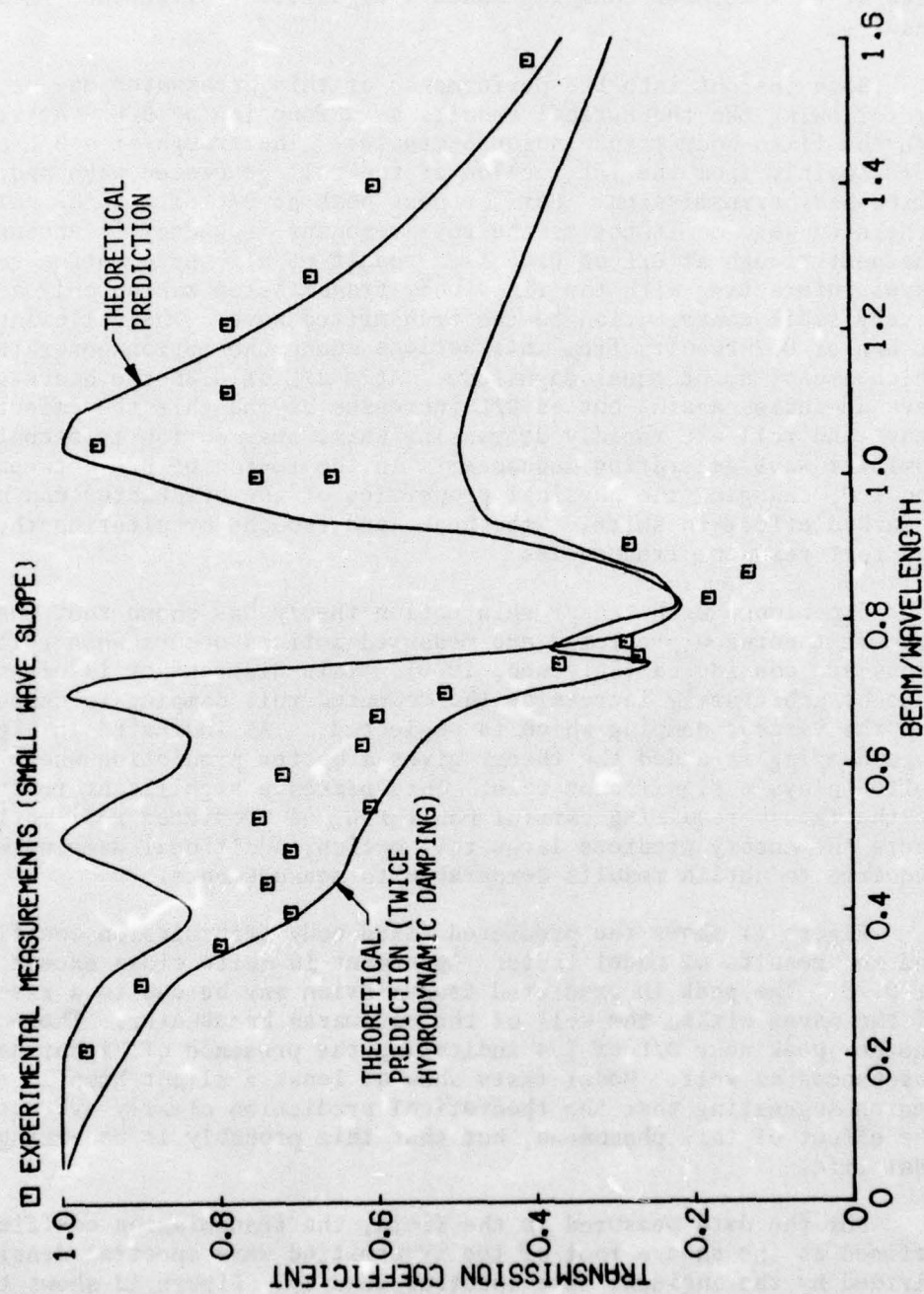


Figure 10. Transmission coefficient for Alaska-type breakwater model.



Clearly the increased damping makes a significant difference in the results.

Some insight into the performance of this breakwater may be gained by following the theoretical results as a function of  $B/L$ . At very low  $B/L$  the fixed-body transmission dominates. The trough at a  $B/L$  of 0.4 comes mainly from the interaction of the roll-generated wave and the fixed-body transmission. For the next peak at  $B/L$  of 0.5 the roll-generated wave dominates as the roll resonant frequency is encountered. The next trough at  $B/L$  of 0.65 is a result of all three motion-generated waves interacting with the fixed-body transmission making only a relatively small contribution to the transmitted wave. The following peak at  $B/L$  of 0.7 results from interactions among the motion-generated waves which are of about equal magnitude. At a  $B/L$  of 0.86 the heave-generated wave dominates again, but as  $B/L$  increases beyond this the effect of heave and roll are rapidly decreasing while sway motion is becoming the dominant wave-generating mechanism. In the region of  $B/L$  between 0.4 and 1.0, changing the physical properties of the breakwater can have a marked effect in shifting the peaks and troughs by altering the heave and roll resonant frequencies.

Experience with linear ship motion theory has shown that the worst agreement between predicted and measured motions occurs when rolling motions are considered (Salvesen, 1970). This discrepancy is often overcome by arbitrarily increasing the computed roll damping to compensate for the viscous damping which is neglected. As indicated in Figure 10, when damping is added the theory gives a better prediction where roll motion plays a significant role. This places a significant restriction on the theory requiring careful monitoring of predicted roll motion. Where the theory predicts large roll motion, additional damping will be required to obtain results comparable to measurements.

Figure 11 shows the predicted fixed-body transmission coefficient and the results of model tests. Agreement is quite close except at  $B/L$  of 0.78. The peak in predicted transmission may be due to a resonance of the waves within the well of the catamaran breakwater. There is another peak near  $B/L$  of 1.4 indicating the presence of higher harmonic resonances as well. Model tests show at least a slight hump in this region suggesting that the theoretical prediction clearly overestimates the effect of this phenomena, but that this probably is occurring in real life.

For the data measured in the field, the transmission coefficient is defined as the square root of the transmitted wave spectral density divided by the incident wave spectral density. Figure 12 shows the transmission coefficient derived from the data obtained at the Tenakee, Alaska breakwater. The theoretically predicted transmission coefficient with the computed hydrodynamic damping doubled is also shown for comparison. Details of the technique used in the spectral analysis of the field data may be found in Section III.

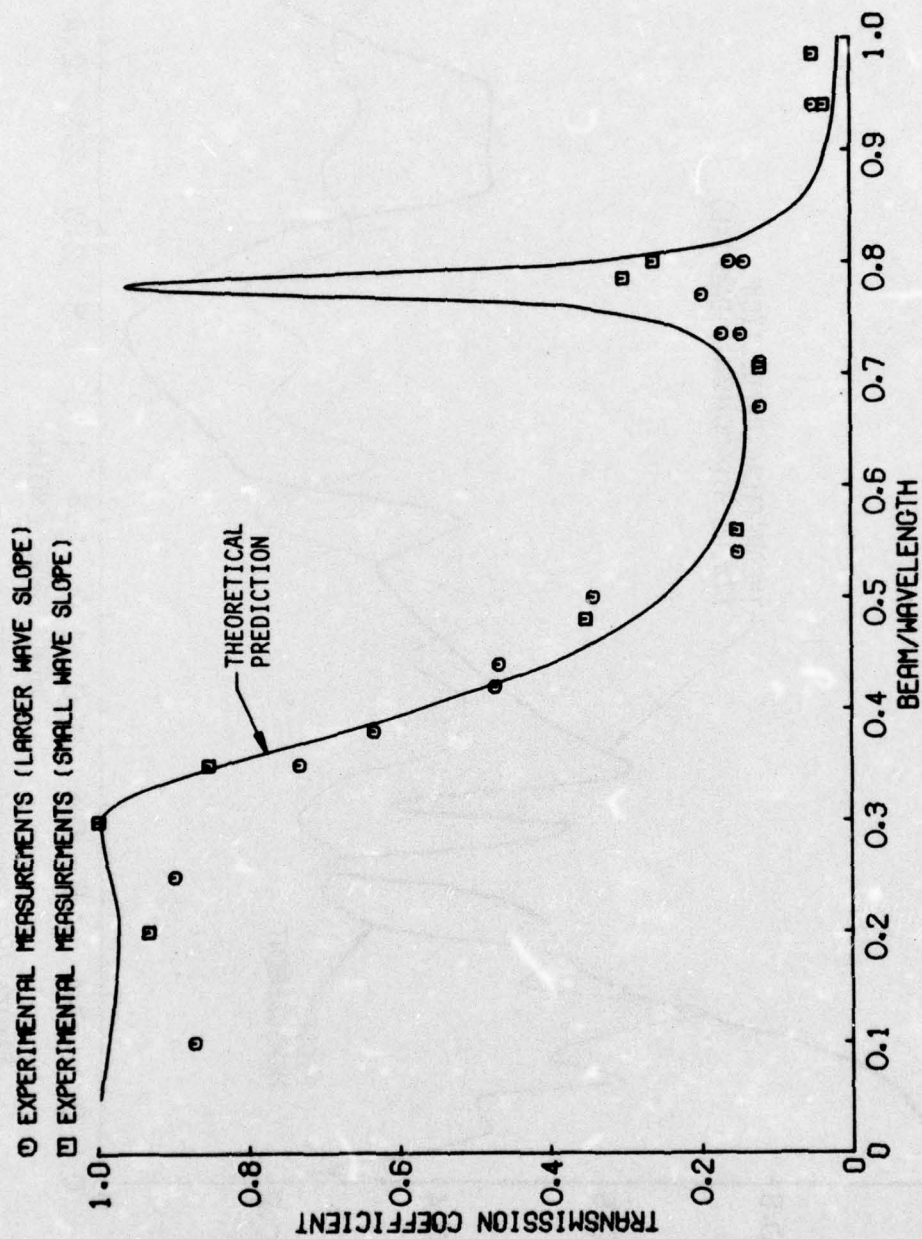


Figure 11. Transmission coefficient for a rigidly fixed Alaska-type breakwater model.



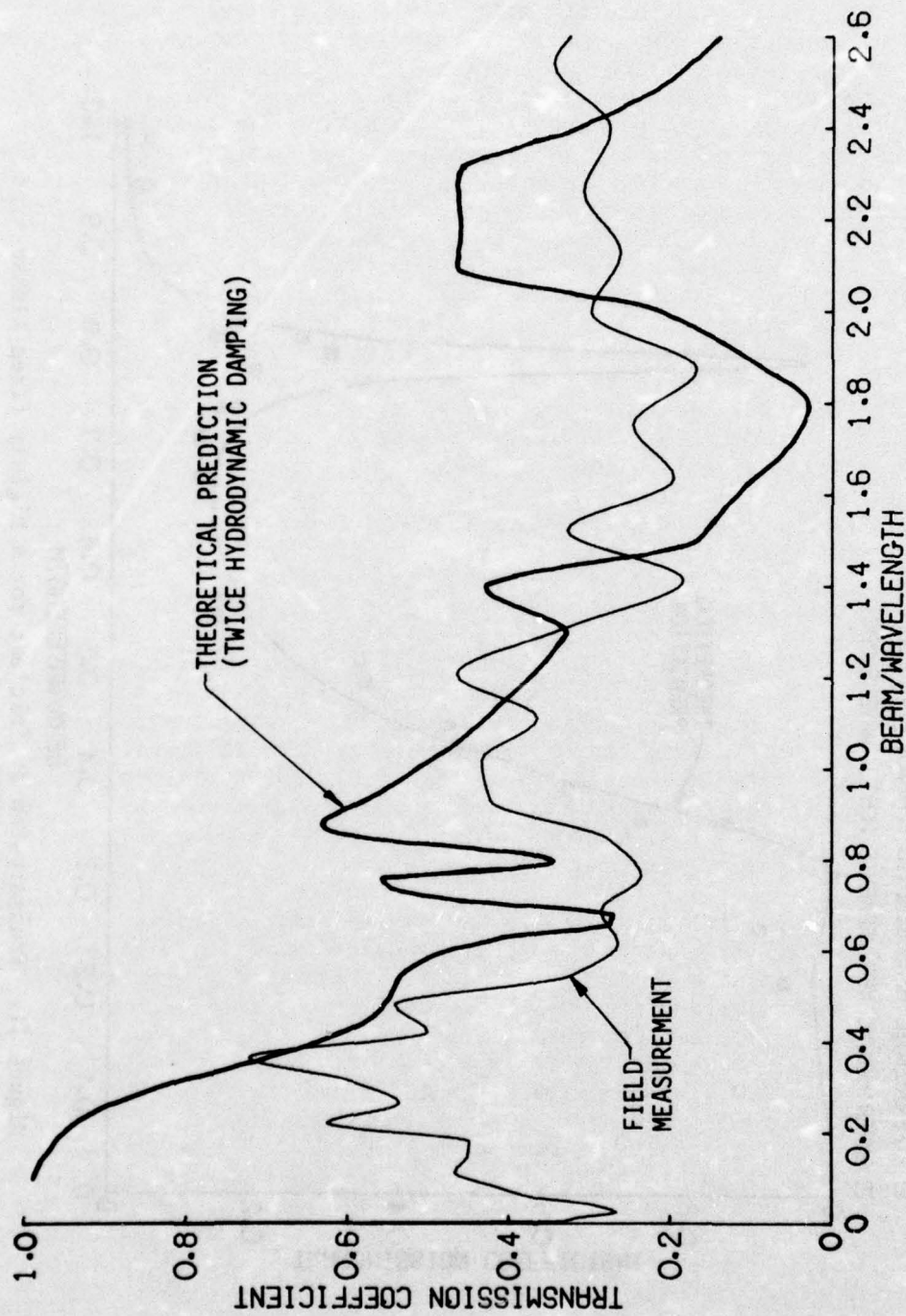


Figure 12. Transmission coefficient for Alaska-type breakwater, Tenakee, Alaska (record TK7-23).

It should be noted that the model for the Alaska-type breakwater was not built to the correct scale to represent the prototype. Further investigation of the physical properties of the prototype after the model tests were complete revealed that it was heavier than originally predicted. The physical properties used in making the theoretical calculations are correct for all the comparisons made in this report. However, care must be exercised in comparing the model test results and the field measurements directly. The physical properties for all the breakwaters discussed in this section are in Appendix F.

The first trough in the transmission coefficient curve results because the wave generated by roll tends to cancel the fixed-body transmission. The sway-generated wave is small but cancels a little bit of the heave-generated wave. The total transmitted wave is then almost in phase with the heave-generated wave at a slightly reduced amplitude. Complex interactions among the components of the transmitted wave continue to result in oscillations of the transmission coefficient up through a  $B/L$  of 0.9. At values of  $B/L$  above this, the transmitted wave is primarily a result of sway motion except for the peak at  $B/L$  equal to 1.4 which results from an increase in the fixed-body transmission. Considering the complexity of the breakwater response, the agreement should be considered to be reasonably good.

(5) Friday Harbor Breakwater. The computed transmission coefficient for the Friday Harbor breakwater is shown in Figure 13. As in the case of the Alaska breakwater calculations, the computations of wave-damping coefficients have been arbitrarily doubled to reduce the excessive calculated motions in the region of resonant motions. In this figure the spacing of data points varies. More points are used to specify the curve in regions of rapid change so that the plotted result accurately represents the theoretical prediction.

In Figure 13, the first trough in transmission coefficient at about  $B/L = 0.5$  results from heave- and roll-generated waves canceling the fixed-body wave transmission. This transmission coefficient is well below the transmission coefficient which would be obtained with the breakwater rigidly restrained and only fixed-body transmission waves passing through. As  $B/L$  increases, there is a peak at about 0.7. At this point the heave-generated wave has almost vanished, and the fixed-body transmission is also small. The larger transmission coefficient is primarily the result of a roll-generated wave with a smaller component resulting from sway motion. The next trough at a  $B/L$  of 0.9 occurs as the heave motion-generated wave increases and cancels the roll and sway motion-generated components. The fixed-body transmission is very small at  $B/L$  of 0.9. As  $B/L$  increases beyond 0.9 the transmitted wave is almost totally the result of sway motion of the breakwater.

At larger  $B/L$  ratios there are several oscillations in the



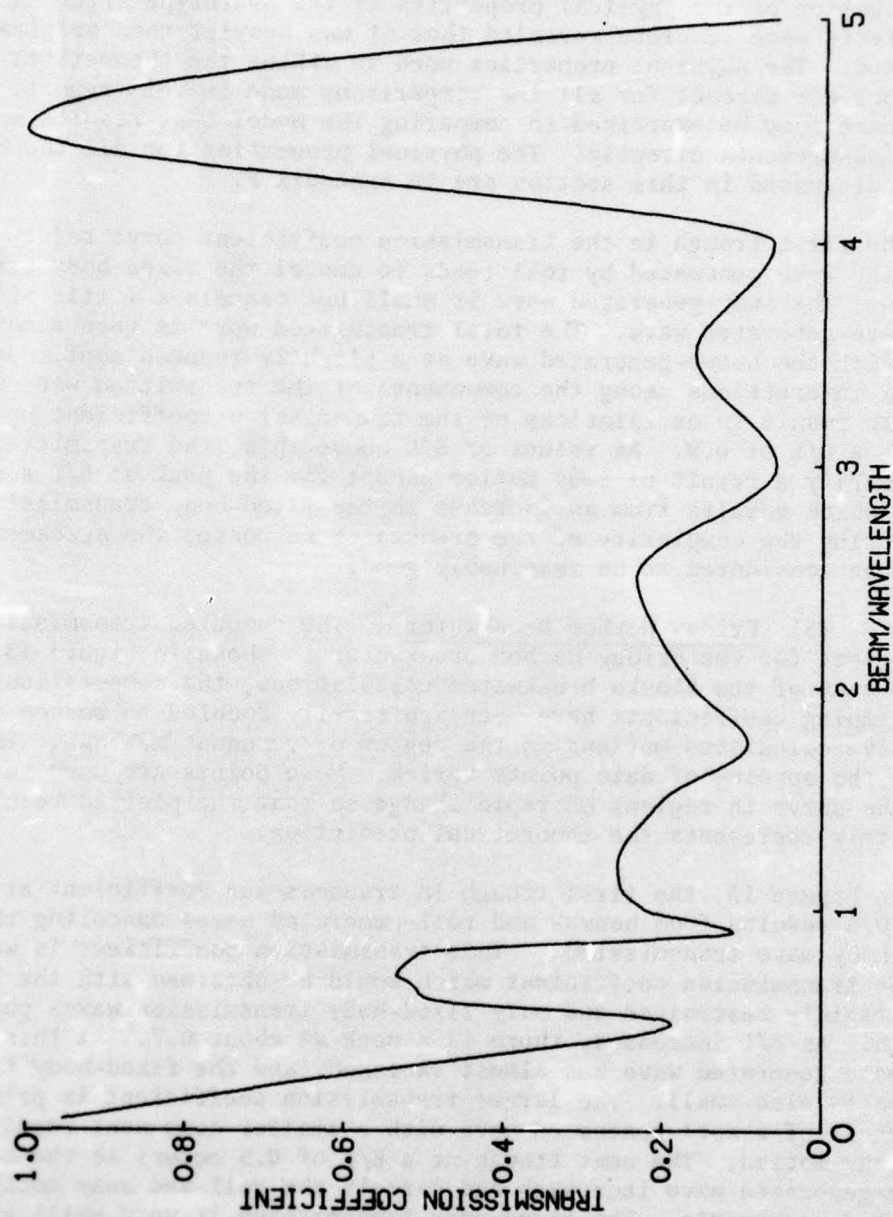


Figure 13. Theoretically predicted (twice hydrodynamic damping) transmission coefficient, Friday Harbor breakwater.

transmission coefficient curve. In this region one must be careful of the analysis because there are certain "irregular frequencies" or "John" frequencies where the approach adopted here breaks down mathematically (John, 1950). These are described with reference to the integral equation technique by Frank (1967). It is extremely difficult to predict where the first of these irregular frequencies will occur when the breakwater cross section is as complicated as the Friday Harbor breakwater. If this cross section were rectangular with the same exterior dimensions as the Friday Harbor breakwater, then the first irregular frequency would occur at  $B/L \approx 1.7$ . In practice, one may watch for this mathematical phenomenon by checking the determinant of the matrix inverted to solve the system of equations. In fact, this does decrease in the region of  $B/L$  of 1.7 but does not indicate a singular matrix for the calculation in this region of  $B/L$ . Since this is beyond the frequency range of primary interest, it is best to simply view the results at  $B/L$  greater than 1.7 with extreme caution. The oscillations in the transmission coefficient in this region of  $B/L$  are probably the result of these irregular frequencies.

b. Breakwater Motions. In the wave channel experiments performed to date, there has been no attempt to compute the breakwater motions. While the transmission coefficient is the primary measure of breakwater performance, the motions may be very important to the designer, particularly if boats are to be tied to the breakwater. For the theoretical analysis, this is a critical intermediate step where extensive experimental measurements used for comparison would be invaluable.

Friday Harbor Breakwater. The theoretically predicted motions of the Friday Harbor breakwater are shown in Figures 14, 15, and 16. The motion response is almost the same as one would expect from an uncoupled spring, mass, dashpot linear system. The only unusual behavior is the null response in heave at  $B/L$  of about 0.75. This null occurs at a point where there is a phase shift in the "added-mass" force, a phenomenon which has been observed in experiments with catamaran-type cross sections (Lee, Jones, and Bedel, 1971), and is a result of resonant wave conditions within the open well of the catamaran.

c. Mooring Line Forces. In recent years a great deal of effort has been expended in understanding and predicting mooring line performance, particularly for moored ships and drilling rigs (e.g., American Society of Civil Engineers, 1971). While many of these analysis techniques could be applied to the moorings of floating breakwaters, this has not been done to date. There are also very few model-scale experiments in which mooring forces have been measured and only a few cases where good field data are available.

Two techniques for calculating the spring constants for mooring lines have been used. At first the catenary equations were applied to find the change in force per unit displacement. While this approach leads to a fairly simple algorithm for the calculation, there are a few problems. In several cases spring constants were needed when the mooring



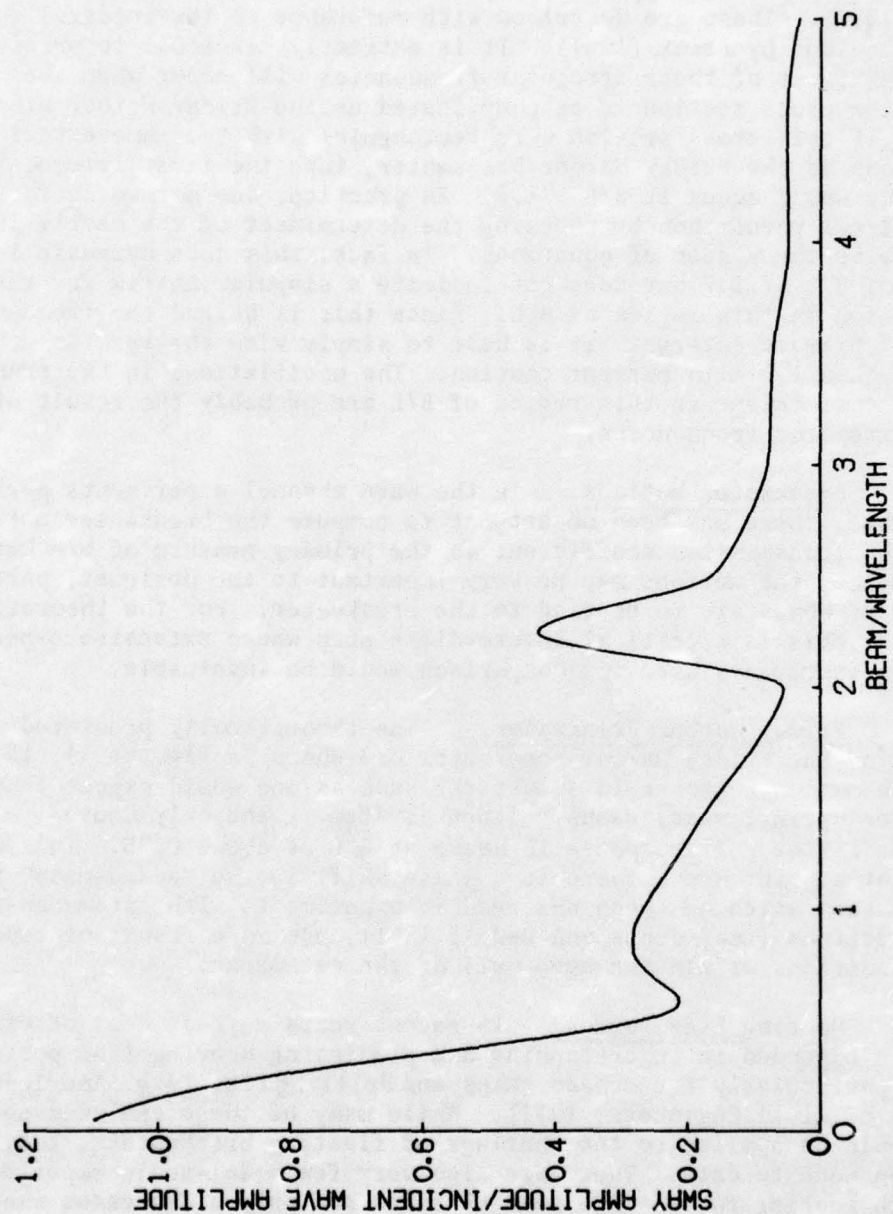


Figure 14. Theoretically predicted (twice hydrodynamic damping) sway motion response, Friday Harbor breakwater.

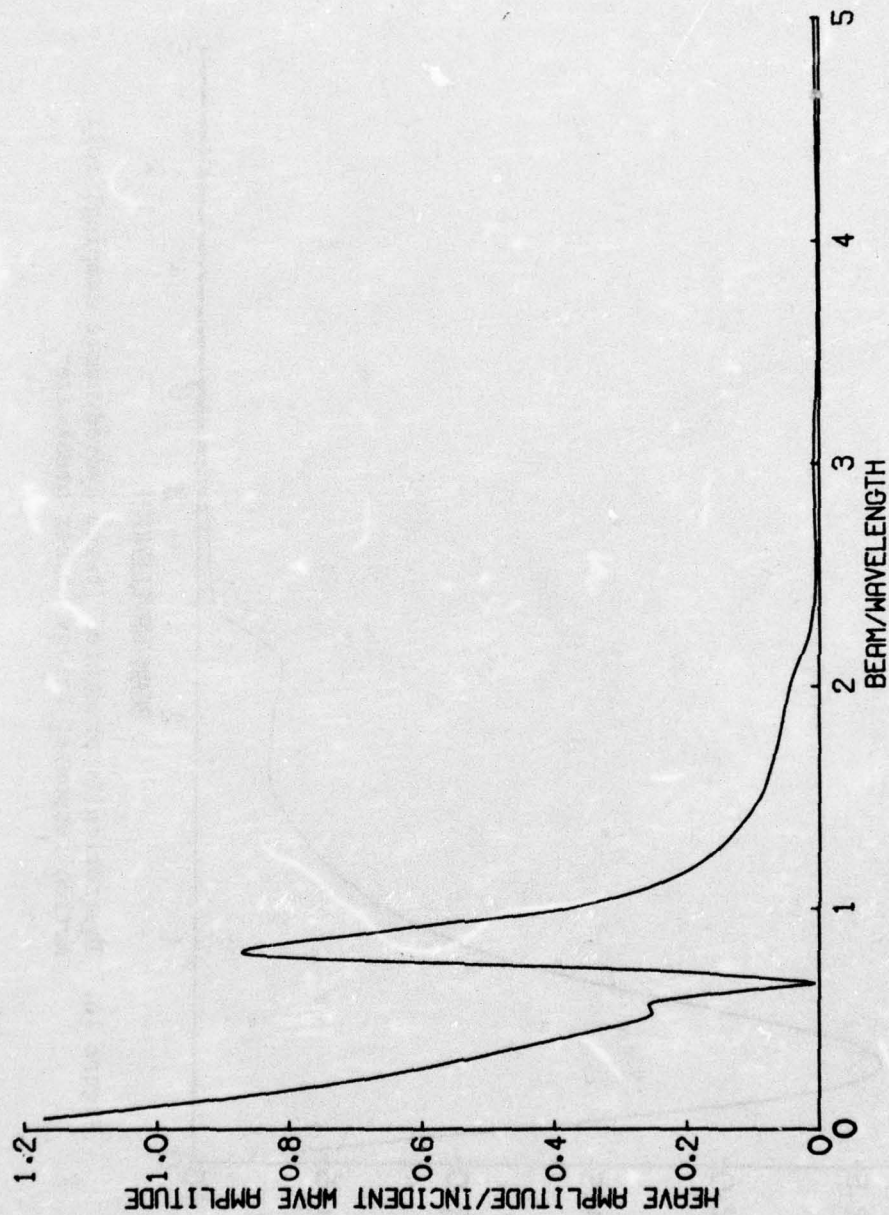


Figure 15. Theoretically predicted (twice hydrodynamic damping) heave motion response, Friday Harbor breakwater.



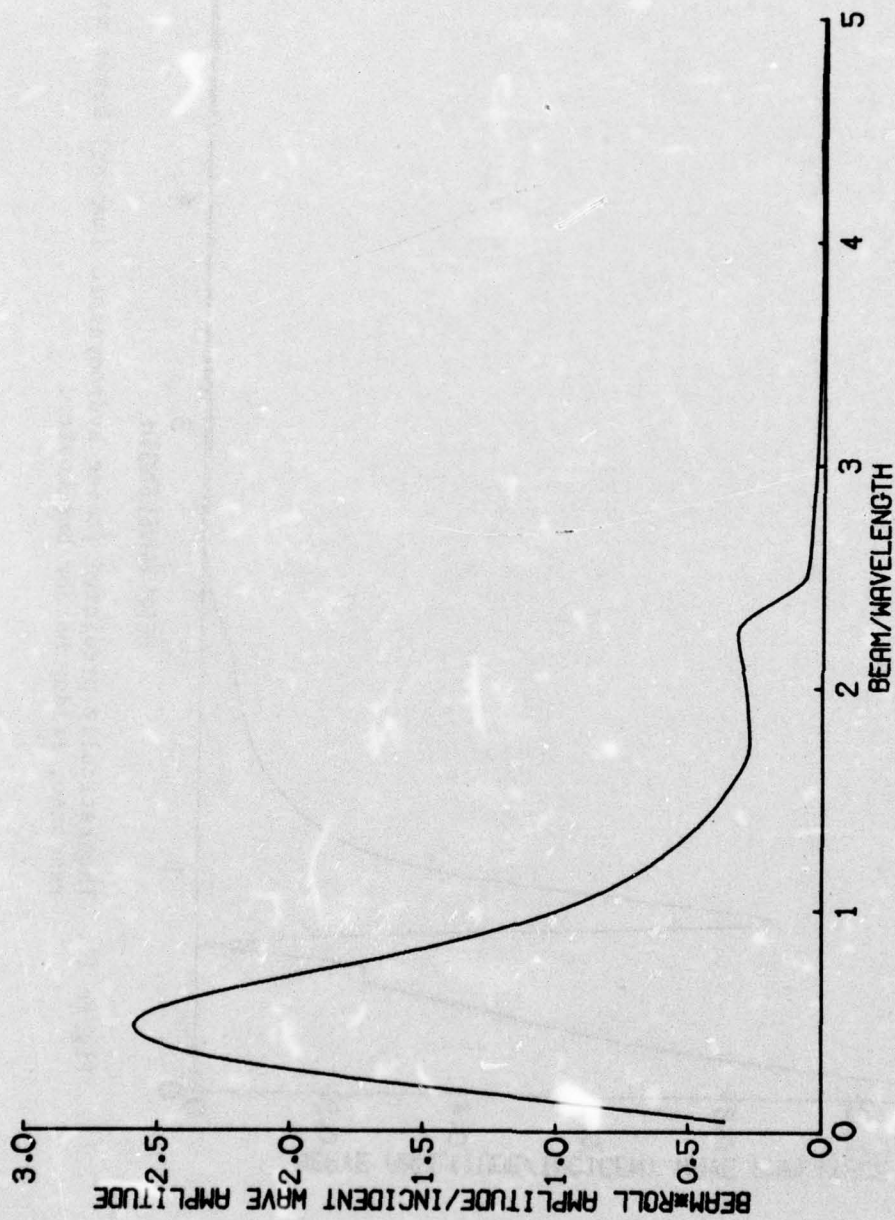


Figure 16. Theoretically predicted (twice hydrodynamic damping) roll motion response, Friday Harbor breakwater.

line was too taut to allow it to become tangent to the bottom at the anchor. If this condition occurs, or as it is approached, the catenary equations no longer apply. For many full-scale installations, a combination chain and synthetic line anchor cable is used. This combination anchor cable presents problems in attempting to use the catenary equations.

Comparisons between the mooring line forces calculated using the catenary equations to predict spring constants showed poor agreement with measured results (Adee, 1975). While the general trends were reproduced, an increase in the predicted spring constants of about a factor of 4 would have been required to bring the theoretical prediction into agreement with the measured results.

To overcome the problems encountered in using the catenary equations, a system based on discretization of the mooring line and static equilibrium was developed. This method is described in Appendix B.

(1) Proposed Oak Harbor Breakwater. One of the few model tests in which mooring line forces were measured was performed by Davidson (1971) for the floating breakwater proposed for Oak Harbor, Washington. The model configuration with properties scaled to the prototype is included in Appendix F. The shape of this breakwater is basically an inverted bathtub with foam flotation.

Applying the theory to predict the mooring line force in the seaward anchor line at a water depth of 29.5 feet, one obtains the results shown in Figure 17. The mooring-force coefficient is defined as the amplitude of the force oscillation divided by incident wave amplitude times the weight per unit length of the breakwater. In this figure, the large range of the experimental results is directly related to incident wave amplitude. The smaller incident wave amplitudes generally produce lower measured mooring line forces per unit amplitude except at the beam to wavelength ratio of 0.49. Since the linear theory is mathematically correct only in the limit as wave amplitude tends to zero, one would expect the best correlation between theoretically predicted and measured results for small amplitude incident waves. The results shown in Figure 17 are consistent with this expectation. However, the very large difference in mooring line forces as incident wave amplitude increases indicates a highly nonlinear response.

A potential explanation for the nonlinear response observed in these experiments results from the condition of the mooring lines at the 29.5-foot water depth used for the model tests. Under these conditions, the mooring lines no longer maintain a catenary shape. When the initial tension in the mooring lines is increased to this level, they respond with very large changes in mooring line force for very small displacements of the breakwater. Consequently, small deviations in the planned positioning of the anchors will lead to large changes in forces in the mooring line. This condition clearly should be avoided in prototype installations where very large mooring line forces are to be avoided.



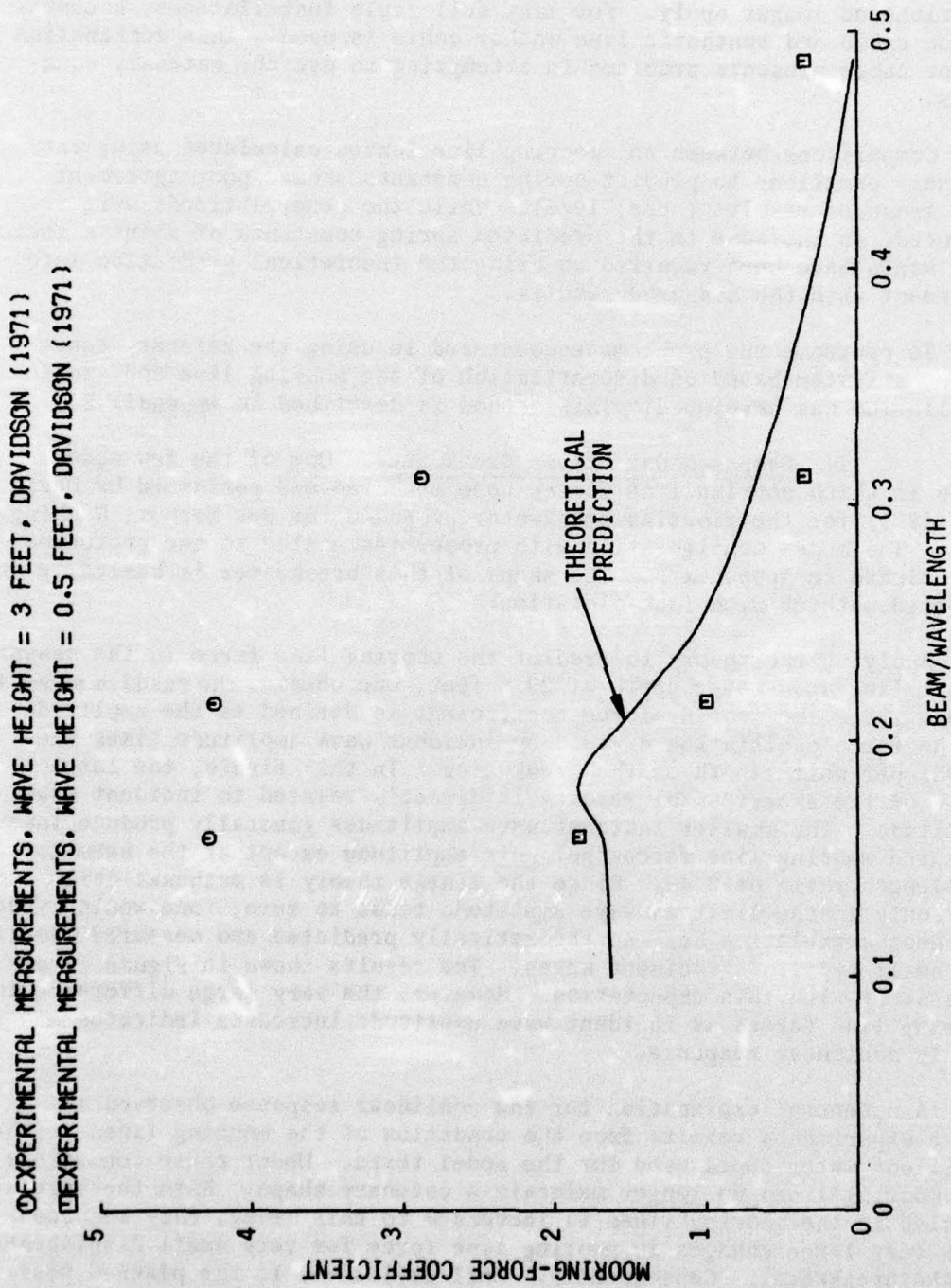


Figure 17. Seaward mooring line force for proposed Oak Harbor breakwater.

A second possible explanation of the nonlinearity results when the "drift force" on the breakwater is considered. If one carries the hydrodynamic analysis to second order, there are terms at zero frequency which yield a force on the breakwater in the direction in which the incident waves are traveling. This force has the same effect as increasing the initial tension in the mooring line and is proportional to wave amplitude squared. Increasing the initial tension tends to increase the spring constants of the mooring lines leading to larger oscillating forces as well.

(2) Alaska-Type Breakwater. Mooring-force coefficients theoretically predicted and measured for the Tenakee, Alaska, breakwater are shown in Figure 18. For the field data the mooring-force coefficient is obtained by taking the square root of the mooring-force spectral density divided by the incident wave spectral density and then dividing by the weight per unit length of the breakwater. Again, as with the Oak Harbor model experiments, there is good agreement, especially in predicting the peak in the curve near B/L of 0.65.

One important aspect of the mooring line problem which should not be overlooked is a comparison between the model-scale results and the field measurements. For the Alaska-type breakwater, all the measured results indicate the amplitude of oscillation in mooring line force is in the order of hundreds of pounds, not thousands of pounds, as was predicted for the Oak Harbor breakwater in the model-scale tests.

When the mooring line tension data recorded at Tenakee are plotted as a function of time as in Figure 19, one observes that there clearly are oscillations associated with the incident waves. However, there are also low-frequency oscillations which are of greater magnitude. A complete explanation of the origin of these low-frequency forces has not been developed. However, one possible explanation is that these forces are a result of breakwater oscillation at the sway resonant frequency. Since the spring constant for sway motion is very small, one would expect a long natural period. Theoretically predicted sway motion response for the breakwater is plotted in Figure 20. Predicted natural periods are 64, 37, and 29 seconds for tidal conditions of mean lower low water (MLLW), +10 and +20 feet, respectively. By applying a high-pass filter to the field data, one obtains the spectrum of force oscillation shown in Figure 4. Here, a peak is at a period of about 53 seconds (tide height = +7 feet). The predicted sway natural frequency is at 45 seconds when the tide height is +7 feet, which indicates that this explanation is plausible.

(3) Friday Harbor Breakwater. The predicted performance of a seaward mooring line on the Friday Harbor breakwater is shown in Figure 21 for a tide height of +5.33 feet. The Friday Harbor mooring lines are different than those at the other breakwaters. They are composed of a section of chain attached to the breakwater, followed by a length of nylon rope and, finally, another section of chains at the bottom. This particular tidal condition was chosen because it is the condition during record FH 7-8 used later for comparison.



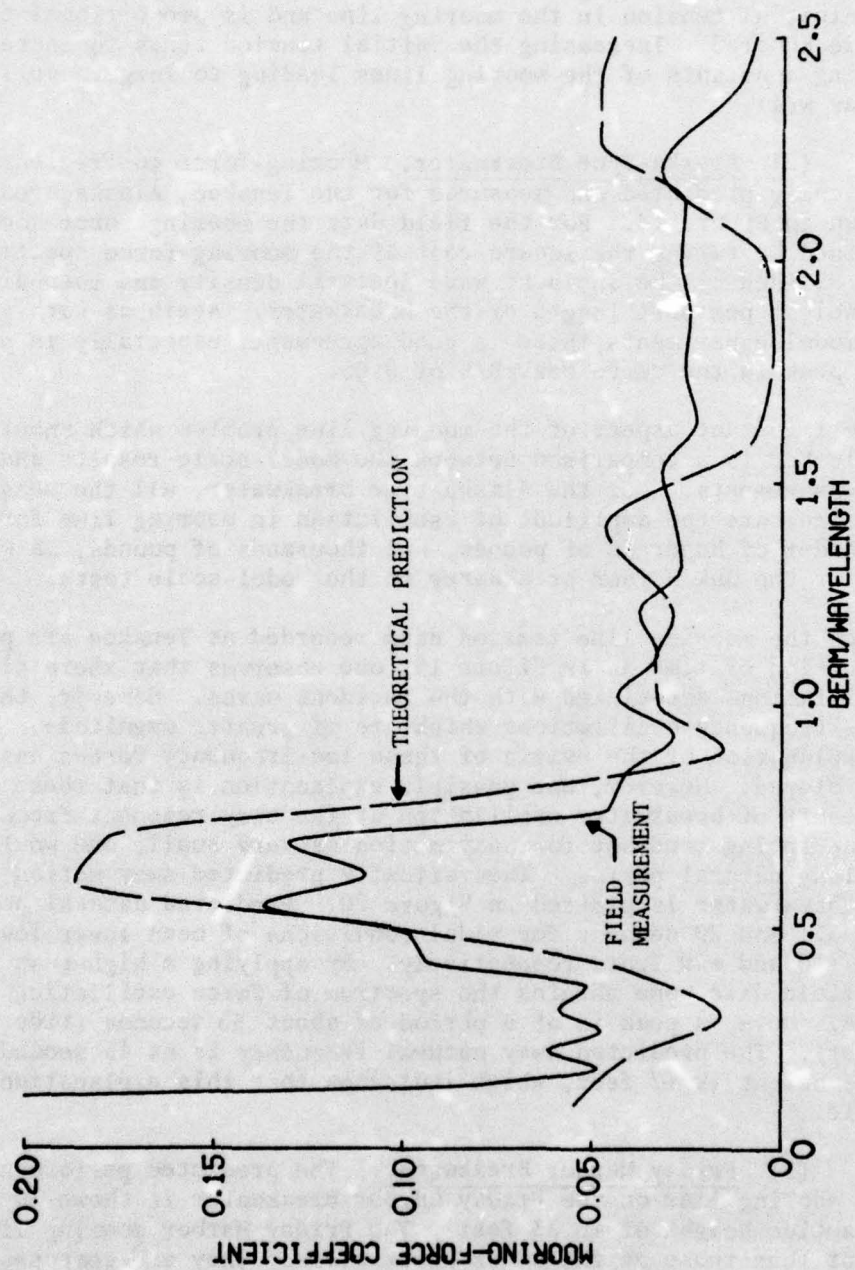


Figure 18. Seaward mooring line mooring-force coefficient, Tenakee, Alaska (record TK7-23).

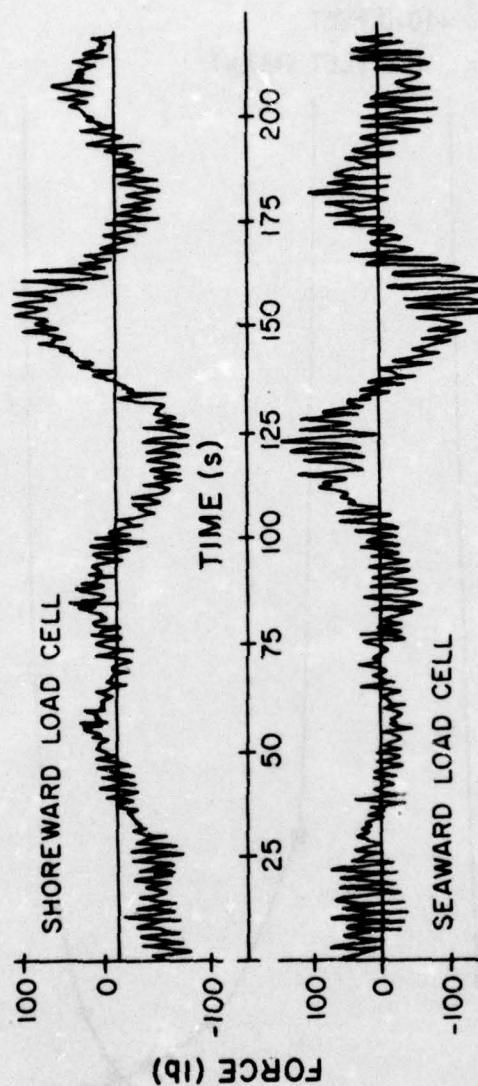


Figure 19. Recorded time series, Tenakee, Alaska  
(record TK7-23).



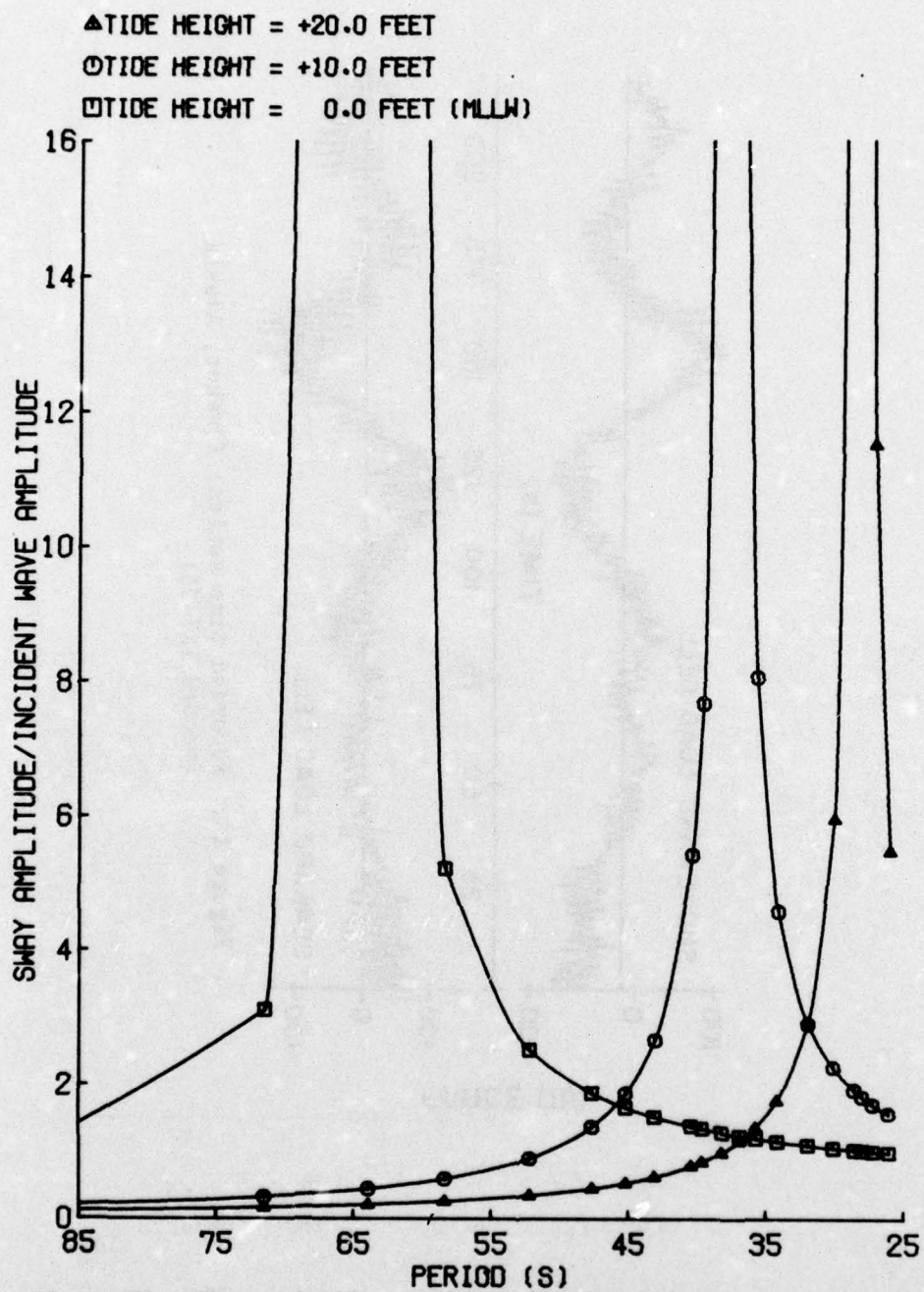


Figure 20. Theoretically predicted long-period sway response of Alaska-type breakwater, Tenakee, Alaska.

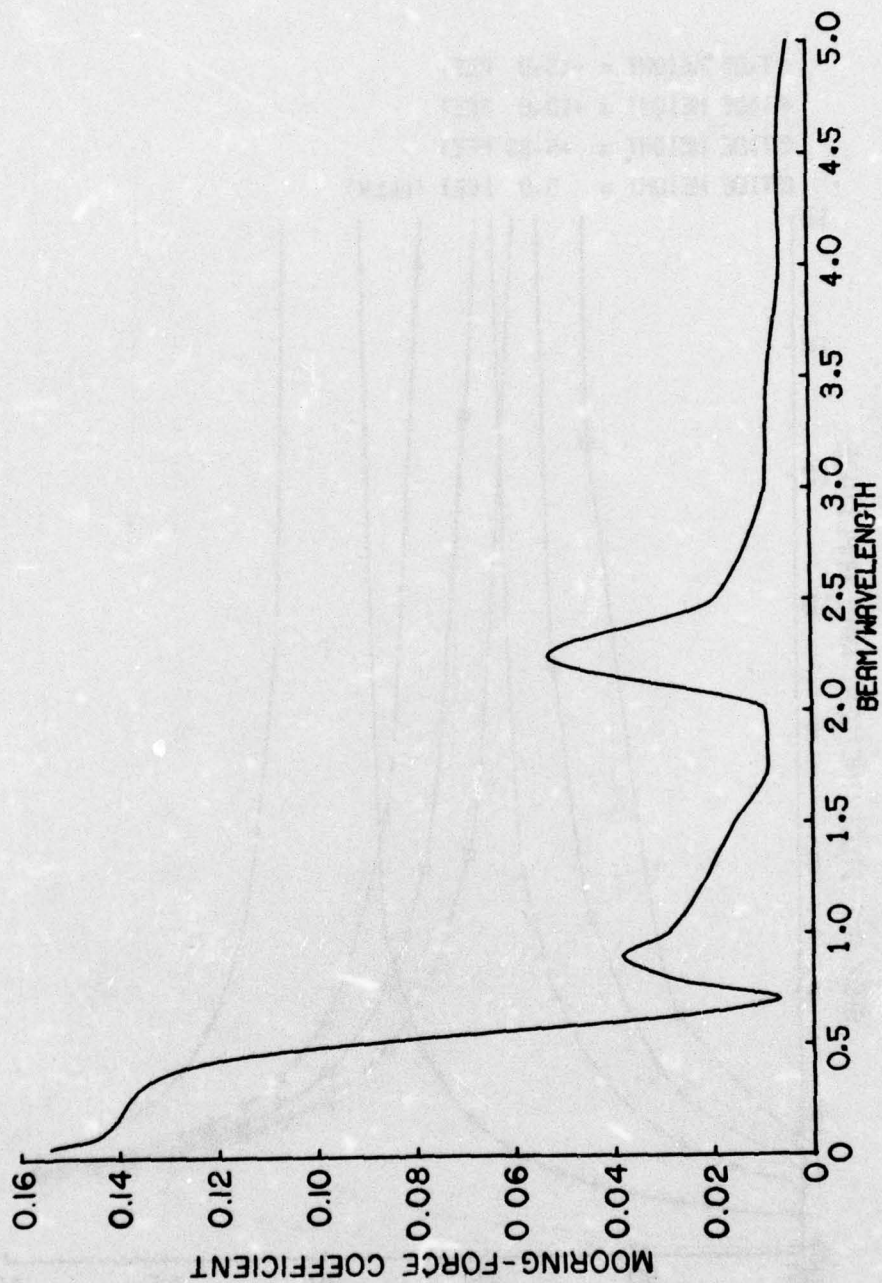


Figure 21. Theoretically predicted seaward mooring line mooring-force coefficient, Friday Harbor breakwater.



Low-frequency predicted sway motion and resonance are shown in Figure 22 for MLLW, +5.33 feet, +10 feet, and +15 feet tide heights.

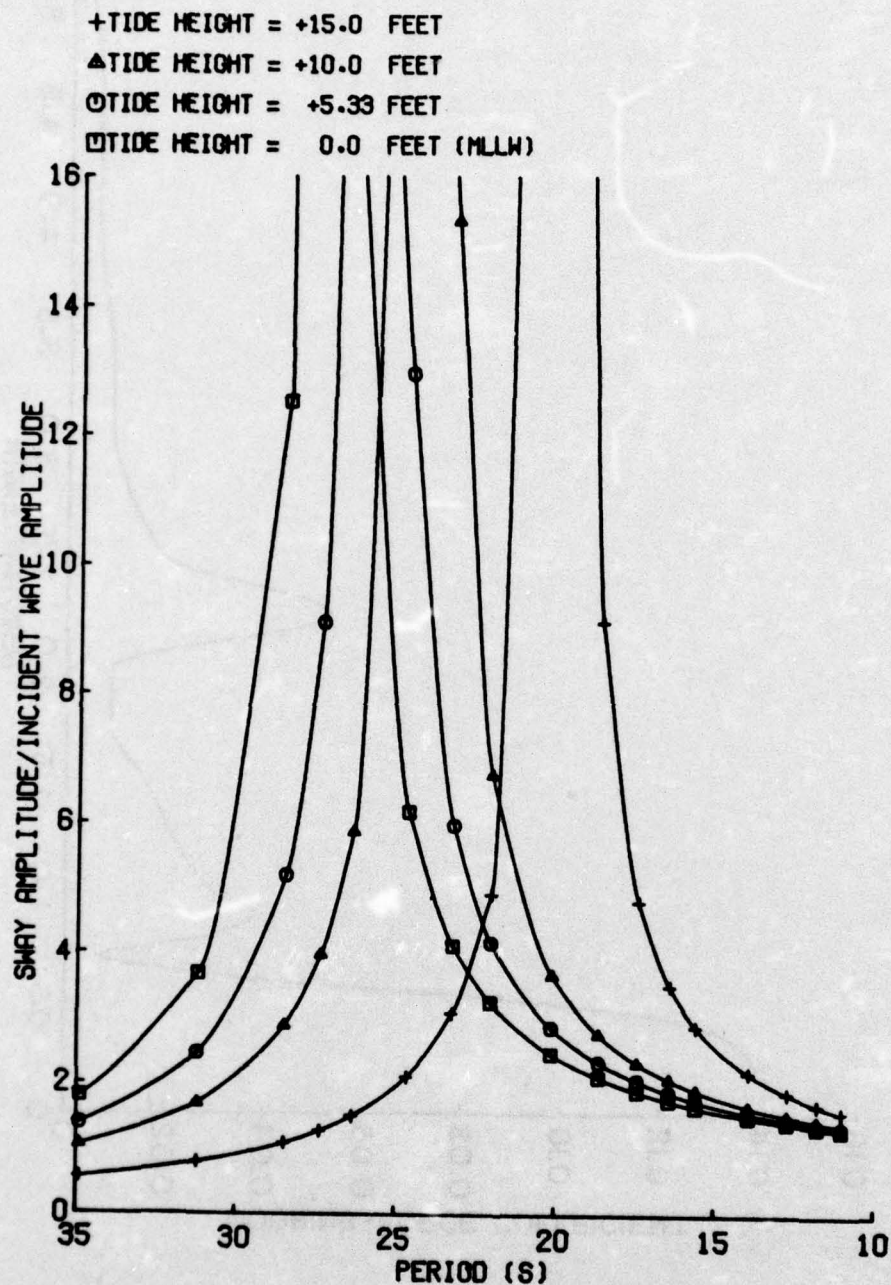


Figure 22. Theoretically predicted long-period sway response, Friday Harbor breakwater.

### III. FIELD DATA

#### 1. Layout.

The site of the floating breakwater instrumented in this study is located at Friday Harbor, Washington, on San Juan Island, just east of Victoria, British Columbia (Fig. 23). The breakwater is 25 feet wide, 904 feet long, anchored in approximately 40 feet of water, and was installed in October 1972. The structure is made of Polyolefin flotation tanks linked together by a matrix of large wooden timbers. It is laid out in an expanded L-shape, the inside angle being  $115^\circ$ , with the shorter leg (227 ft.) directed toward shore and the longer leg (627 ft.) toward magnetic north. The site itself is protected on three sides by San Juan and Brown Islands off the harbor entrance. This leaves an 0.25-mile-wide channel into the harbor with a northeasterly fetch of about 1.7 nautical miles. Southeasterly winds can also generate waves of importance parallel to the shorter leg where the fetch is about 1 nautical mile.

#### 2. Instrumentation.

The shorter leg was instrumented in this study for two reasons: (a) the most frequent winds are out of the southeast, and (b) barges were to be tied to the longer leg during the winter months for added protection. However, the wave gages are positioned to give the proper incident and transmitted wave data for all relative wind directions (Figs. 24 and 25).

Four types of time-dependent data which are basic to describing the response of the breakwater were collected: (a) wind velocity and direction; (b) wave heights at key locations; (c) anchor cable forces; and (d) directional acceleration and angular motions of the breakwater. The locations of the measuring sensors are shown on Figure 25. Signals from the sensors were carried by underwater cable to the recording system which was located in a small building mounted near the center of the short leg.

#### 3. Wind Data.

Windspeed and direction were measured by Weather Measure Corporation's W121 sensor. Some additional circuitry was required to record the windspeed, and the sensor was recalibrated to this circuit. The sensor was mounted on the breakwater at the intersection of the two legs at 20 feet above the water surface.

#### 4. Waves.

Wave characteristics were measured at four locations with the second



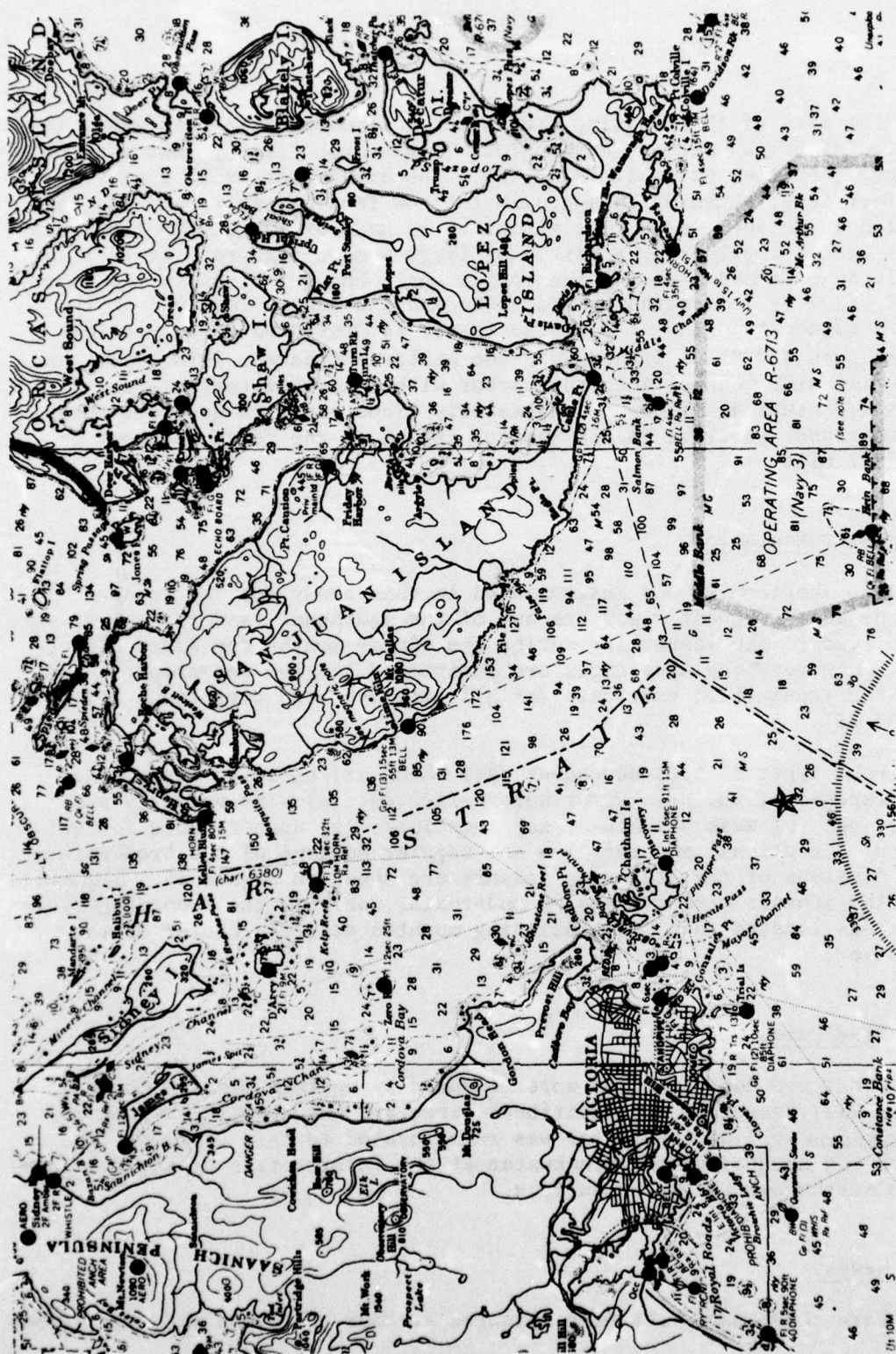


Figure 23. General Location Map

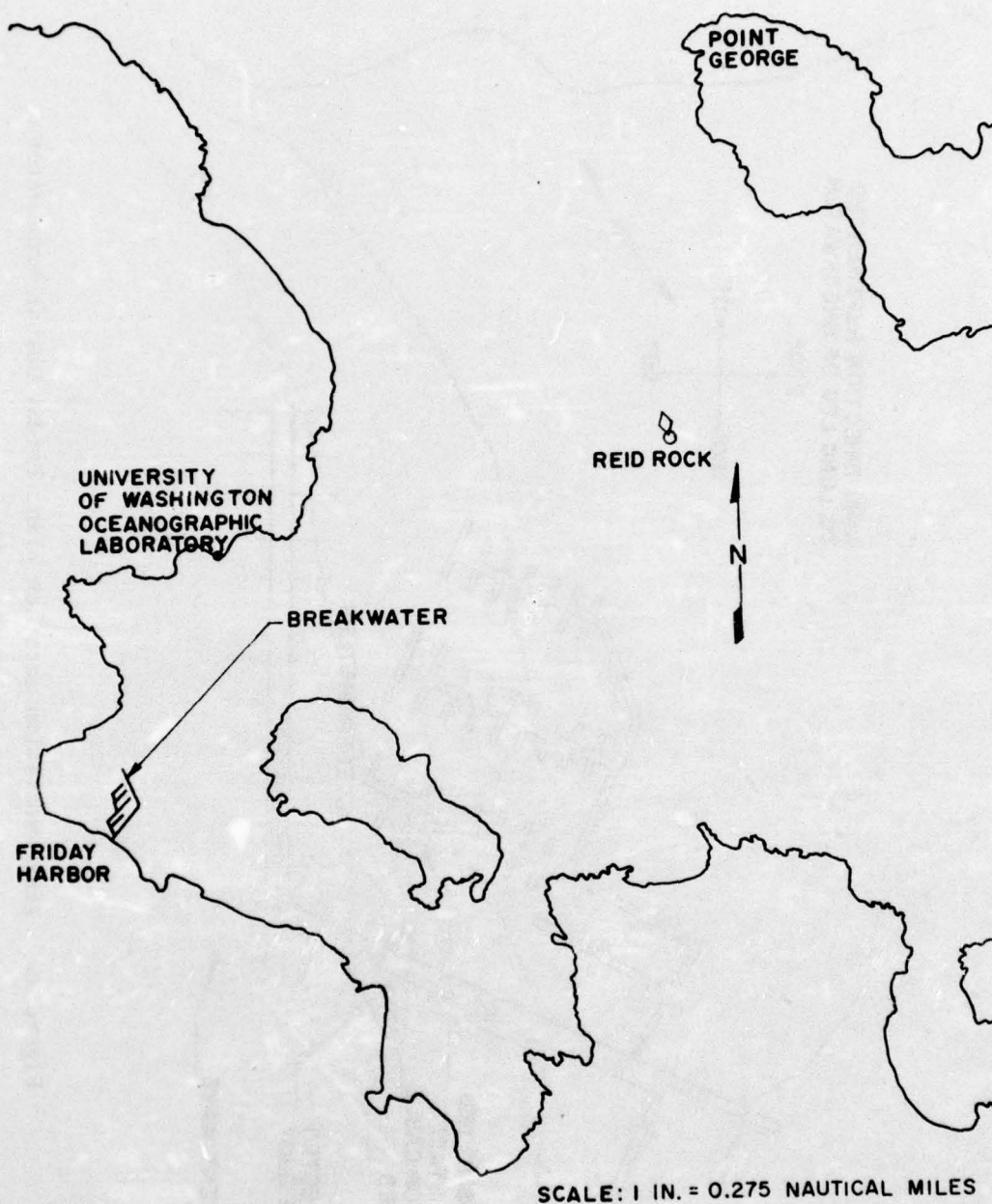


Figure 24. Field experiment site location map.



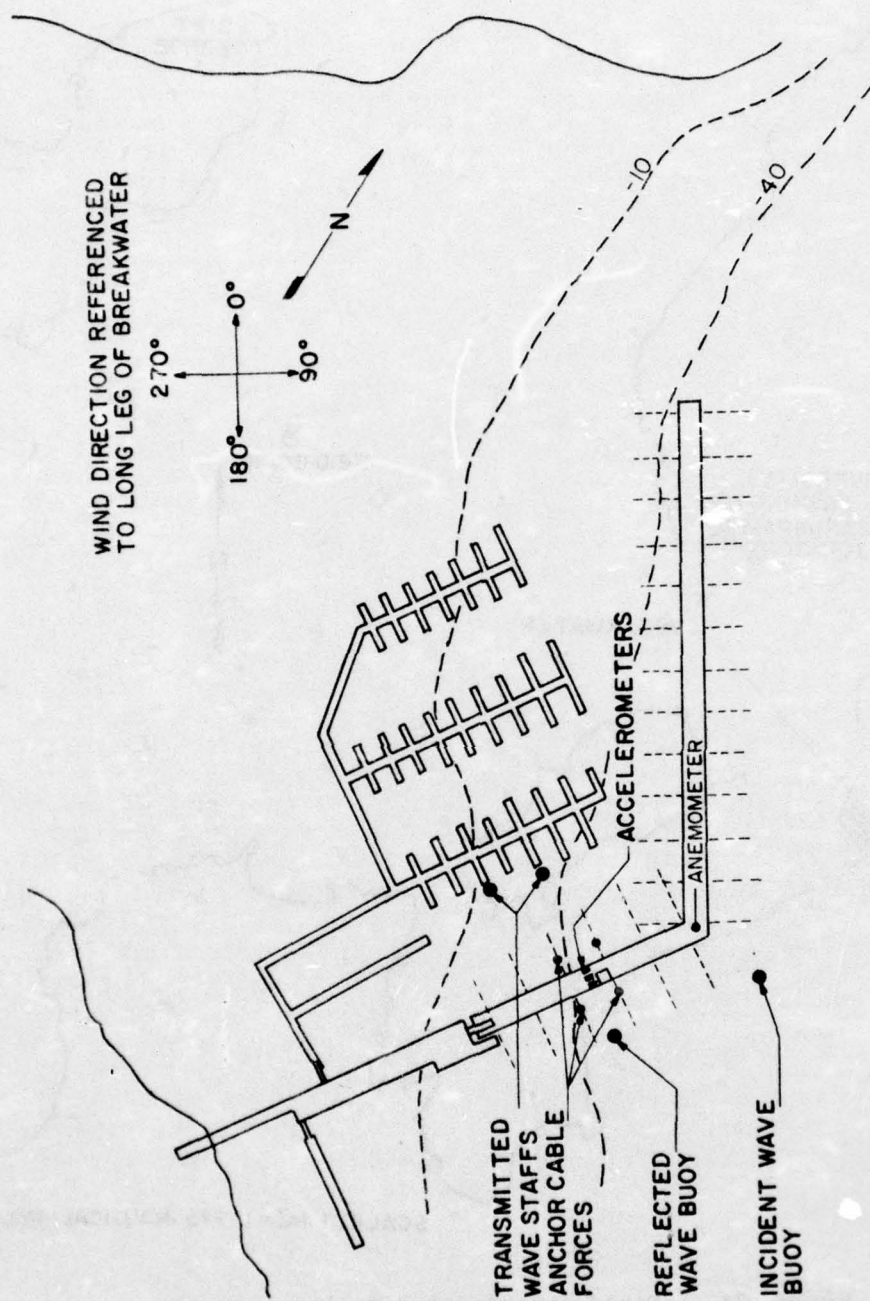


Figure 25. Instrumentation location plan, Friday Harbor breakwater.

transmitted gage being used as a backup. Two spar buoys instrumented to measure wave elevation were located outboard of the breakwater and positioned so that one measured the incident wave field, and the other measured the incident plus reflected wave field. Two stationary gages were attached to pilings behind the breakwater to measure transmitted wave height. All four gages were of the resistance type. The spar buoys were used outside the breakwater to help reduce navigation hazards and because of the costs and logistics of placing stationary piling at these locations.

The buoys were made of two sections of PVC pipe, the lower section being 6 inches in diameter and 15 feet long, and the upper section of 3-inch diameter and 12 feet in length with the upper 8 feet wound with a resistance wire. Four feet were exposed above the water surface, and a 2.5-foot-diameter disc was attached to the bottom to damp vertical motions. The natural periods in heave and roll, respectively, are 18 and 14 seconds, well above the anticipated maximum wave period of about 4 seconds. See Appendix J for a complete description of the wave staff and buoy designs.

#### 5. Cable Forces.

Anchor cable forces were measured using a bonded strain gage-type load cell that was placed in the anchor chains beneath the water surface. These cells and the associated electronics were designed and built for this project. They have an overall system accuracy of 0.75 percent of the designed or rated total load cell capacity over a temperature range of 10° Celsius (design load 12,500 pounds). These load cells employ a four-arm wheatstone bridge circuit which has two strain gages in each leg of the bridge and are self-temperature compensating. The units are O-ring sealed and wired directly to the bridge amplifier circuitry mounted in the recording package.

#### 6. Motion Package.

Breakwater accelerations were measured using three Kistler servo-accelerometers (Model 303T). One accelerometer, oriented horizontally, was mounted at the center of the breakwater to measure the sway acceleration. The other two were oriented vertically and mounted at opposite outboard edges of the breakwater to measure the vertical accelerations. The heave acceleration was obtained by taking the average of the signals from the two outboard accelerometers; the roll acceleration was obtained by taking the difference of these two signals and dividing by the distance between them. The accelerometer locations are indicated in Figure 25.

#### 7. Data Acquisition System.

The data recording and electronic package was built around the Sea



Data Corporation's Series 610 four-track incremental digital cassette tape recorder. The complete package, which included all the electronic circuitry for the individual transducers plus the tape recorder, was housed in a watertight, 6-inch-diameter PVC cylinder 5 feet in length. The system was designed to be operated manually or in a completely automated mode, thus requiring only periodic tape changes (Fig. 26).

In its automatic mode, the system was activated when the windspeed reached or exceeded a preset value and stayed there for at least 1 minute. At this point, a single 17-minute sample of all the inputs was taken. Each 68 minutes following this, another 17-minute sample was recorded if the wind was still above its preset value; if not, the system was shutdown until the windspeed increased. Each 17-minute record consisted of 2,048 samples, taken at 0.5-second intervals, of all 13 channels plus a clock channel. Twenty-five of these records could be recorded on a single cassette tape.

#### 8. Data Processing and Analysis.

The initial step in the data handling was to transfer the data from the individual cassettes to seven-track magnetic tape by means of the Sea Data reader. These tapes were then converted to a computer compatible format on the University of Washington's CDC 6400 computer. The histograms for all records plus the basic statistics, i.e., the minimum, maximum, mean values and standard deviations as well as the transmission coefficients based on these standard deviations, were then computed and tabulated (App. G). A digital filter, with a cutoff frequency of 0.05 hertz (Gold and Radar, 1969) was applied to the transmitted wave data prior to these tabulations to remove tidal drift. The transmission coefficients given in these summary sheets are a ratio of the standard deviations for the transmitted and the incident wave gages.

In the initial conversion, the data were checked for reader errors. These points were smoothed using a linear interpolation between the preceding and the following good data points. Following this, the data were checked for extreme values. Data points departing from the mean by more than five standard deviations were smoothed in the same manner as were the reader errors. In no case did the number of errors warrant elimination of a complete record (greater than six bad points). Record FH 11-1, however, had bad data for channels 3, 4, 5, 7, and 8. This record was run manually while calibrations were being made, and the affected channels were not connected properly at this time. The final edited data were then stored on magnetic tape.

The autospectra for all the wave data for all records were computed with a more complete analysis of the force and acceleration data applied to the more desirable events.

Digital filtering techniques were used prior to spectral analysis on all the wave and force data. The procedures used follow those given

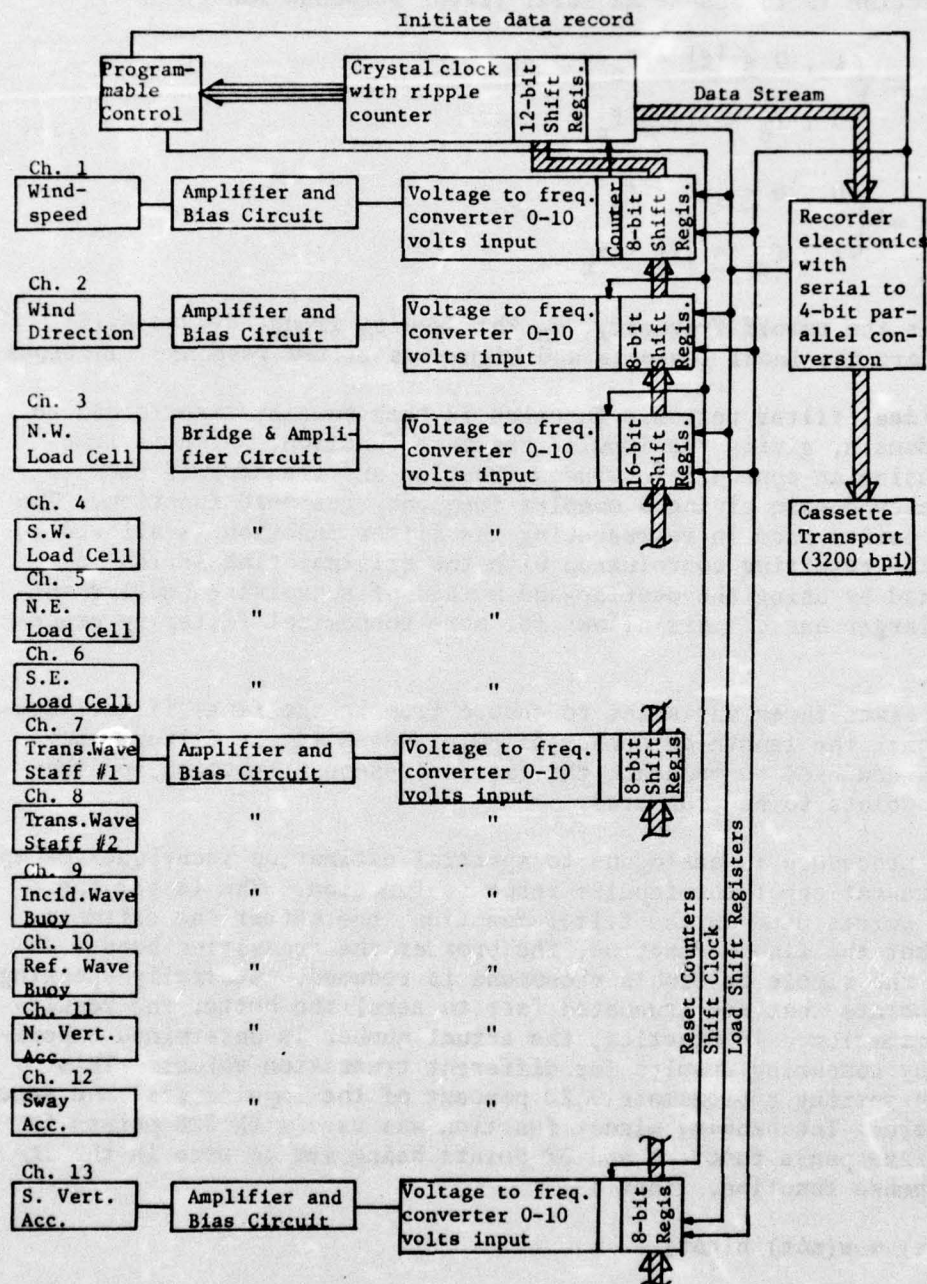


Figure 26. Instrumentation and recording package layout.



by Gold and Radar (1969). The first step in the development of this filter function is to assume an ideal filter response function.

$$F_l(f) = \begin{cases} 1, & 0 \leq |f| \leq f_c \\ 0, & f_c < |f| \leq f_n \end{cases} \quad (12)$$

$$F_h(f) = \begin{cases} 0, & 0 \leq |f| < f_c \\ 1, & f_c \leq |f| \leq f_n \end{cases}$$

where  $f_c$  is the cutoff frequency,  $f_n$  the Nyquist frequency, and  $F_l(f)$  and  $F_h(f)$  are the ideal low-pass and high-pass filter response functions.

The ideal filter response function is then Fourier-transformed to the time domain, giving the impulse response function, which is truncated by using an appropriate window function and transformed back to the frequency domain giving a complex frequency response function. The number of points used in representing the filter function is allowed to vary and the resulting convolution with the original time series is accomplished by using the overlap-add method of convolving smaller series with larger ones. This allows for more economical filtering procedures.

This gives three variables to choose from in the final filter function design: the length or number of points used in the filter, the type of window used to truncate the impulse response function, and the number of points to be truncated.

This procedure is analogous to spectral estimation techniques except for the truncation of the impulse response function. The larger the number of points used in the filter function, the better the estimate. The smoother the window function, the broader the transition band. In addition, the ripple or Gibb's phenomena is reduced. Generally speaking, the more points that are truncated (set to zero) the better the resulting approximation. In practice, the actual number is determined experimentally by comparing results for different truncation values. This results in setting approximately 20 percent of the impulse response function to zero. The hanning window function was used with 128 points in the filter response function and 38 points being set to zero in the impulse response function. That is:

$$h(n\Delta t) = w(n\Delta t) h(n\Delta t)$$

and

$$w(n\Delta t) = \begin{cases} \frac{1}{2} (1 + \cos \pi \frac{n-1}{45}), & 1 \leq n \leq 45 \\ 0, & 45 < n < 83 \\ \frac{1}{2} (1 - \cos \pi \frac{128-n}{45}), & 83 \leq n \leq 128, \end{cases} \quad (13)$$

where  $h(n\Delta t)$  is the impulse response function and  $w(n\Delta t)$  is the hanning window function. The final filter response function is defined as:

$$F(f_n) = \sum_n \beta(n\Delta t) e^{-j2\pi f_n \Delta t},$$

where  $j = \sqrt{-1}$  and  $\Delta t$  is the constant time interval between samples.

The transition band or the frequency increment traversed by the cutoff of the filter function can be approximated by:

$$\lambda = \frac{10}{128} = 0.078$$

and the maximum stopband attenuation for the hanning window is 55 decibels. These values can only be achieved through proper filter design. The actual values for the filters used are  $\lambda = 0.08$  and a maximum attenuation of greater than 55 decibels. The ripples in the passband for each filter used were below 0.01 percent. These values could be improved on by increasing the number of points used for the filter response function estimate. Also the stopband attenuation could be improved, at the expense of a wider transition band for a given size filter function by using the Blackman window function. However, the accuracy of the filter response functions used exceeds that of the measurements and is sufficient for this application.

After initial processing and prior to all spectral calculations a tapered cosine data window was applied to the first and last 10 percent of the data to reduce spillover of spectral energy to adjacent frequency points. For data stretching from  $n = 1$  to  $n = N$ , the formulas for the data window are:

$$w(n\Delta t) = \begin{cases} \frac{1}{2} (1 - \cos \pi \frac{n-1}{0.1N}) & \text{for } 1 \leq n \leq 0.1N \\ 1 & \text{for } 0.1N < n < 0.9N \\ \frac{1}{2} (1 - \cos \pi \frac{N-n}{0.1N}) & \text{for } 0.9N \leq n \leq N. \end{cases} \quad (14)$$

The data were then transformed directly using fast Fourier transformation procedures and smoothed by averaging adjacent raw spectral components. Initial sampling was performed at 0.5-second intervals with 2,048 samples per record, and 20 adjacent points averaged together in the autospectral calculations to get the final smoothed spectral estimates. This gives a frequency resolution of 0.0195 hertz with 40 degrees of freedom per spectral estimate.

All of the wave data was high-pass filtered, using the filtering techniques previously outlined with a cutoff frequency of 0.05 hertz. This was done to remove the tidal influence on the transmitted wave staffs and to eliminate any possible buoy motion in the incident wave records. Also the anchor cable force data were separated into a low-and



high frequency signal using the same filtering procedures. For the high-frequency case this was done to remove the influence of the large low-frequency spikes in the spectra. A high-pass filter with a cutoff frequency of 0.1 hertz was used.

For a closer look at the low-frequency information in the anchor cable force data, a new time series was generated from the original record by sampling every eighth data point. To reduce aliasing of the higher frequency energy in the original signal, each record was low-pass filtered prior to this sampling using the filtering techniques previously outlined with a cutoff frequency of 0.2 hertz. The sampling of every eighth point of the original time series gives a sampling interval of 4 seconds, a Nyquist frequency of 0.125 hertz and a record length of 256 points or 1,024 seconds. Five raw spectral points were averaged together to give the final smoothed spectral estimates. This results in a frequency resolution of 0.0049 hertz with 10 degrees of freedom per spectral estimate.

A total of 95 records was recorded at the site from 1330 hours on 30 December to 3 May 1975. There were no known equipment failures or breakdowns except for one of the load cells going off scale at low tide on the first tape (FH 7, NW load cell channel 3). A complete summary of these events is given in Appendix G. Also, Figure 25 gives the relative locations of the individual transducers.

The wind direction in all cases is referred to the long leg, which has a north-south compass bearing (magnetic declination in this area is  $23^\circ$  east). There are two wind-direction windows of interest. For the long leg, the directions are approximately  $50^\circ$  to  $95^\circ$ ; for the short leg,  $130^\circ$  to  $160^\circ$  (Figs. 24 and 25).

Two storm events were chosen for presentation and further analysis. These events cover records FH 7-6 through FH 7-12 and FH 11-8 through FH 11-14 (Apps. G and H). They were chosen because of their directions relative to the short and long legs, respectively, and because of their duration and magnitude. Both events lasted for over 7 hours with maximum windspeeds in excess of 35 miles per hour, with all the mean wind direction within or close to the desired wind-direction windows. Appendix H gives the pertinent wave spectra and transmission curves for the above two events.

The average overall response or transmission curves for the events within each wind-direction window and for all the recorded data, are given in Figure 27. These plots were obtained by averaging the square root of the ratio of the transmitted to the incident wave spectras for the records indicated for each curve. Therefore, they have the same frequency resolution of 0.0195 hertz.

A puzzling feature in all the transmission response curves calculated from field data is the rise at lower frequency to a value near one and then dropping off again. This can partially be attributed to a lack of

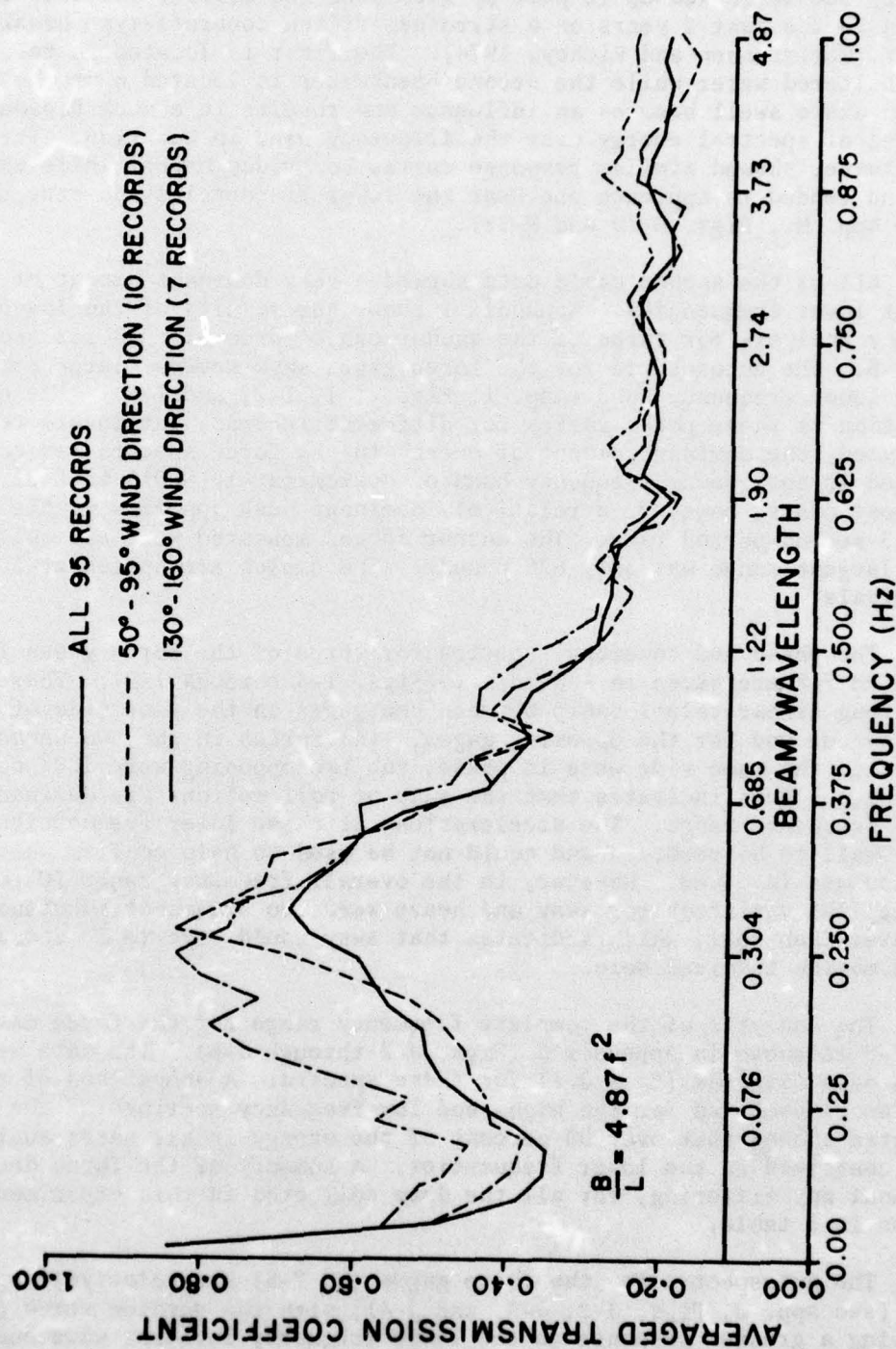


Figure 27. Average transmission curves for Friday Harbor breakwater.



energy in the incident wave spectra at lower frequencies. This possibility can be backed up in part by data from two similar projects undertaken in the past 2 years on a styrofoam-filled concrete-type breakwater (Christensen and Richey, 1974). The first is located in relatively sheltered water while the second breakwater is located near the open ocean where swell becomes an influence and results in a much broader spread of spectral energy over the frequency band in question. The first breakwater showed similar response curves to Friday Harbor while the second tended to approach one near the lower frequencies and stay there (see App. H., Figs. H-10 and H-11).

All of the anchor cable data showed a very dominant amount of energy at lower frequencies. Appendix I shows the results of the low-frequency analysis for three of the anchor cable force signals for record FH 7-8. The autospectra for the force gages show several large peaks in this lower frequency band (App. I, Figs. I-1, I-2, and I-3). The exact location of these peaks varies for different records, but in all records analyzed, the dominant amount of energy in the force spectra was contained in this lower frequency band of approximately 0.015 to 0.05 hertz. In most cases, however, a relatively dominant peak appeared in the 56- to 63-second-period range. The anchor forces measured were all quite low; the largest range was only 628 pounds. The cables are spaced at 50-foot intervals.

The phase and coherency spectra for three of the force gages for record FH 7-8 are given in Appendix I (Figs. I-4 through I-7). They show a strong linear relationship between the gages on the same side of the breakwater and for the opposing gages. The forces in the two anchor lines on the same side were in phase; the two opposing were 180° out of phase. This indicates that the sway or roll motions are dominant in this frequency range. The accelerations at these lower frequencies were too small to be recorded and could not be used to help confirm which motion was involved. However, in the overall frequency range (0 to 1.0 hertz) the variances for sway and heave were two orders of magnitude greater than roll, which indicates that sway would have to be the dominant motion involved here.

The analysis of the complete frequency range for the force data for FH 7-8 is shown in Appendix J (Figs. J-2 through J-8). The data were high-pass filtered ( $f_c = 0.1$ ) for these spectra. A comparison of the variances computed for the high- and low-frequency sections of the force spectra showed that over 90 percent of the energy in all cases analyzed was contained in the lower frequencies. A summary of the force data, without any filtering, for all the data collected in this experiment is given in a table.

The autospectra for the force gages (FH 7-8) are relatively spread out (see App. J, Figs. J-2, J-3, and J-4), with the outside force gages showing a greater response to the lower frequency incident wave energy than the inside gages. However, the outside and the opposing gages show relatively high coherency, with the outside gages being in phase and the

Table. Summary of anchor cable force statistics.  
Standard deviations (pounds) Maximum values (pounds) Variations, max. to min. (pounds)

	NW	SW	NE	SE	NW	SW	NE	SE	NW	SW	NE	SE
FH7 - 1	9.155	9.811	7.016	6.077	39.086	30.896	31.920	17.545	60.000	64.000	48.000	36.340
FH7 - 2	24.025	51.877	14.026	30.339	57.895	161.549	42.344	96.340	136.000	272.000	80.000	176.960
FH7 - 3	16.689	65.078	13.839	38.205	75.380	325.976	66.357	193.091	88.000	500.000	120.000	278.080
FH7 - 4	.000	89.072	14.051	55.777	75.580	445.255	43.045	278.098	88.000	628.000	84.000	390.280
FH7 - 5	2.037	97.282	16.930	61.033	15.646	333.143	47.802	221.935	16.000	560.000	108.000	350.760
FH7 - 6	18.688	50.922	11.194	27.338	40.508	196.487	23.366	90.272	76.000	222.000	60.000	137.460
FH7 - 7	10.657	82.997	14.872	46.791	51.649	259.791	50.953	162.782	56.000	472.000	100.000	274.920
FH7 - 8	1.003	86.332	13.652	48.214	7.844	291.235	37.668	173.786	8.000	496.000	80.000	290.720
FH7 - 9	1.128	80.256	12.471	47.411	7.793	362.348	34.456	197.821	8.000	540.000	68.000	304.940
FH7 - 10	5.188	131.594	19.011	82.184	26.359	397.524	48.775	283.358	28.000	636.000	96.000	410.800
FH7 - 11	20.866	86.769	15.340	52.033	88.545	305.942	43.058	195.538	108.000	520.000	88.000	306.520
FH7 - 12	34.384	62.609	19.570	38.895	72.790	306.050	41.584	191.549	172.000	424.000	128.000	282.260
FH7 - 13	20.978	39.646	14.441	26.267	46.319	199.034	39.261	136.431	148.000	304.000	100.000	257.540
FH7 - 14	21.201	40.827	12.234	24.107	66.110	173.650	37.349	116.288	144.000	260.000	88.000	172.220
FH7 - 15	24.710	54.314	14.292	31.875	108.727	195.614	57.304	109.471	176.000	344.000	96.000	188.020
FH7 - 16	6.604	82.334	15.615	49.404	33.703	328.021	44.489	193.378	36.000	514.000	92.000	300.200
FH7 - 17	.000	71.200	9.815	36.055	33.703	224.199	38.805	118.011	36.000	372.000	64.000	192.760
FH7 - 18	.000	47.441	7.594	21.849	33.703	162.227	20.866	93.127	36.000	280.000	48.000	137.460
FH7 - 19	21.840	41.588	14.847	20.752	54.065	157.809	35.505	78.933	104.000	340.000	104.000	145.360
FH7 - 20	2.534	16.865	20.600	11.112	23.655	216.094	98.244	69.665	24.000	232.000	116.000	105.880
FH8 - 1	23.966	10.425	16.246	10.748	24.963	49.370	80.237	8.724	132.000	64.000	96.000	58.460
FH8 - 2	24.306	66.479	9.749	31.996	55.198	300.522	24.714	154.788	132.000	420.000	52.000	211.720
FH8 - 3	19.813	99.339	11.028	53.237	50.892	322.562	29.327	172.246	108.000	524.000	60.000	267.020
FH8 - 4	22.521	141.836	13.626	76.751	48.645	680.252	26.833	382.881	120.000	860.000	72.000	477.160
FH8 - 5	17.970	67.053	8.112	32.591	44.309	223.880	20.041	119.896	100.000	348.000	44.000	175.380
FH9 - 1	18.110	50.773	9.177	27.526	67.313	231.713	33.520	121.875	124.000	336.000	68.000	164.320
FH9 - 2	13.179	23.756	10.432	15.784	51.008	187.160	28.923	99.722	124.000	292.000	60.000	153.260
FH9 - 3	14.533	36.725	8.396	19.000	36.082	72.692	35.365	47.053	76.000	136.000	64.000	88.480
FH9 - 4	19.735	50.283	7.926	23.144	36.982	132.153	25.851	81.354	88.000	216.000	56.000	121.660
FH9 - 5	17.808	45.376	7.724	22.556	55.144	142.958	18.757	70.823	112.000	284.000	40.000	116.920
FH9 - 6	21.681	51.506	10.536	27.655	54.692	173.777	28.025	91.162	124.000	292.000	56.000	150.100
FH9 - 7	19.174	38.606	10.916	20.378	45.004	99.019	29.555	52.121	96.000	188.000	60.000	101.120
FH9 - 8	19.020	40.774	13.595	25.726	45.430	141.364	32.545	92.043	108.000	224.000	76.000	150.100
FH9 - 9	13.796	30.255	8.942	17.901	38.755	111.779	26.357	73.252	80.000	180.000	60.000	112.180
FH9 - 10	16.768	42.001	10.086	24.075	57.927	142.372	29.720	82.378	108.000	236.000	60.000	135.880
FH9 - 11	21.662	56.483	9.820	32.725	55.551	198.810	27.283	105.899	120.000	340.000	52.000	176.960
FH9 - 12	18.393	73.711	8.438	38.399	61.469	242.349	20.758	129.546	124.000	436.000	52.000	214.880
FH9 - 13	16.287	62.127	7.077	29.598	41.474	222.018	16.948	119.112	96.000	336.000	44.000	173.800
FH9 - 14	17.753	76.333	8.323	38.727	41.791	292.927	23.927	142.024	108.000	436.000	52.000	232.280
FH9 - 15	26.975	68.463	11.023	33.762	65.956	212.446	22.988	114.642	124.000	332.000	52.000	176.960
FH9 - 16	18.338	31.378	16.039	21.074	38.091	98.716	35.680	64.331	96.000	144.000	80.000	107.440
FH9 - 17	20.233	38.920	16.823	25.271	49.889	121.439	43.842	76.554	112.000	200.000	96.000	129.560
FH9 - 18	21.148	55.706	11.080	32.035	47.555	240.434	27.454	148.562	136.000	340.000	64.000	282.240
FH9 - 19	21.472	50.908	8.997	26.494	62.454	164.064	26.247	94.187	120.000	288.000	48.000	156.420
FH9 - 20	16.001	33.948	6.131	14.763	40.317	130.442	14.502	61.505	100.000	200.000	36.000	88.480
FH9 - 21	14.684	32.971	6.941	15.069	39.140	92.387	21.002	37.499	84.000	176.000	40.000	69.520



Table. Summary of anchor cable force statistics (continued).

Standard deviations				Maximum values				Variations, max. to min.				
(pounds)				(pounds)				(pounds)				
NW	SW	NE	SE	NW	SW	NE	SE	NW	SW	NE	SE	
FM9-22	14,200	32,860	8,144	17,977	43,288	109,508	22,458	57,980	88,000	220,000	48,000	116,600
FM9-23	24,902	62,139	14,784	36,615	59,439	237,321	45,548	150,064	146,000	384,000	92,000	230,680
FM9-24	21,917	54,967	13,017	32,035	56,463	222,087	32,201	136,193	144,000	356,000	76,000	200,660
FM9-25	18,545	46,342	10,659	27,186	61,652	135,638	36,108	80,267	108,000	268,000	64,000	151,680
FM10-1	3,957	5,271	3,182	3,632	10,237	10,746	9,290	9,131	34,166	30,532	24,757	26,861
FM10-2	24,742	50,725	15,561	22,265	94,834	168,742	67,476	73,974	186,000	280,000	115,555	124,820
FM10-3	21,037	61,374	11,987	36,717	52,322	197,755	54,176	129,148	120,000	404,000	88,000	279,660
FM10-4	27,303	76,380	11,272	42,955	93,124	389,259	43,285	208,183	200,000	560,000	84,000	292,300
FM10-5	22,494	65,805	13,598	37,841	56,107	202,384	37,065	123,866	124,000	360,000	74,000	212,000
FM11-1	22,328	56,817	7,509	28,550	48,012	189,991	17,951	109,744	108,000	304,000	62,000	160,000
FM11-2	24,406	53,350	14,372	33,448	63,307	182,538	46,743	122,528	142,000	294,000	86,000	190,000
FM11-3	22,882	59,094	10,775	32,883	58,274	271,120	28,511	134,525	150,000	404,000	60,000	202,000
FM11-4	24,054	63,906	8,467	30,352	54,022	246,449	27,250	117,612	122,000	386,000	56,000	186,000
FM11-5	23,151	66,432	8,436	29,896	69,535	201,553	21,213	82,841	134,000	366,000	44,000	146,000
FM11-6	28,009	68,262	13,612	37,728	63,996	254,244	33,133	124,014	164,000	396,000	74,000	196,000
FM11-7	34,270	93,910	16,206	53,663	75,529	333,183	40,172	205,989	176,000	526,000	86,000	304,000
FM11-8	28,525	77,068	14,429	48,228	76,095	254,254	45,259	156,353	162,000	430,000	84,000	262,000
FM11-9	30,270	77,342	17,305	48,061	79,208	236,058	53,389	147,266	168,000	424,000	96,000	282,000
FM11-10	35,451	87,205	20,977	53,710	114,203	290,567	72,657	187,479	228,000	490,000	136,000	310,000
FM11-11	34,954	68,446	22,771	44,982	109,038	235,470	80,708	163,276	214,000	430,000	148,000	282,000
FM11-12	39,062	84,688	22,362	50,437	110,991	309,132	59,975	153,687	232,000	522,000	118,000	274,000
FM11-13	13,971	21,354	9,562	11,443	62,201	99,147	44,326	48,563	102,000	148,000	64,000	72,000
FM12-1	9,098	19,909	5,368	11,137	21,490	64,595	14,199	34,845	46,000	108,000	30,000	56,000
FM12-2	18,660	35,685	10,805	22,129	40,248	138,962	34,395	85,847	106,000	208,000	74,000	128,000
FM12-3	22,653	43,195	14,695	26,162	58,226	178,015	45,467	103,876	142,000	296,000	94,000	170,000
FM12-4	19,137	39,018	11,795	23,009	50,916	153,139	31,666	87,406	126,000	248,000	68,000	146,000
FM12-5	14,011	26,324	7,753	15,326	46,851	107,505	27,827	55,024	100,000	180,000	50,000	100,000
FM12-6	19,667	36,519	11,697	22,201	50,547	150,864	35,346	98,391	128,000	236,000	82,000	158,000
FM12-7	26,255	53,094	14,696	32,887	72,426	196,275	40,011	129,161	156,000	326,000	94,000	204,000
FM12-8	23,462	44,167	13,576	29,269	49,645	143,406	32,260	100,631	122,000	226,000	72,000	154,000
FM12-9	36,376	77,993	19,146	45,590	100,799	296,819	54,695	170,487	224,000	472,000	114,000	262,000
FM12-10	29,763	83,770	17,150	48,104	95,243	256,215	57,197	145,447	196,000	504,000	164,000	278,000
FM12-11	25,076	69,811	12,488	41,639	67,139	250,153	38,582	168,483	150,000	440,000	78,000	276,000
FM12-12	24,012	66,572	9,373	36,446	55,361	183,384	20,981	102,581	120,000	308,000	50,000	166,000
FM12-13	21,781	54,227	7,195	24,182	58,399	184,949	21,444	85,238	124,000	294,000	44,000	140,000
FM12-14	40,126	51,751	39,879	20,837	136,208	110,201	139,250	49,158	216,000	268,000	206,000	108,000
FM12-15	51,112	54,756	26,527	16,088	233,839	218,919	109,241	80,787	346,000	356,000	165,000	124,000
FM12-16	22,067	52,260	11,290	26,120	49,497	161,298	29,337	83,695	110,000	258,000	66,000	136,000
FM12-17	19,434	47,133	9,794	23,689	43,586	186,820	25,805	82,684	112,000	278,000	56,000	132,000
FM12-18	28,223	74,717	9,644	29,630	107,602	340,358	31,808	133,561	208,945	474,000	70,000	200,000
FM13-1	25,606	73,194	10,994	30,246	57,596	307,876	24,964	132,105	134,000	444,000	62,000	182,000
FM13-2	30,135	78,112	13,818	37,252	79,236	289,342	36,656	134,101	170,000	458,000	76,000	212,000
FM13-3	35,103	96,943	17,090	53,806	71,049	306,891	41,425	139,855	166,000	478,000	92,000	296,000
FM13-4	24,136	47,125	12,540	27,668	76,648	186,446	36,807	107,207	158,000	310,000	78,000	176,000
FM13-5	24,260	40,460	13,459	24,938	56,828	142,378	36,660	77,077	124,000	240,000	72,000	140,000
FM13-6	40,252	111,057	17,216	58,518	91,917	346,205	48,480	198,638	210,000	578,000	98,000	316,000
FM13-7	38,769	114,883	16,219	61,259	83,843	460,616	42,063	207,324	198,000	684,000	86,000	338,000

outside leading the inside gage by approximately  $180^\circ$  over the frequency range of 0.25 to 0.37 hertz. This indicates that the forces are relatively uninfluenced by waves above approximately 0.37 hertz. This frequency range is also where the transmission curves rise to near unity. This agrees with the low-frequency analysis and suggests that the response is similar over the complete frequency range below 0.37 hertz.

The acceleration force, autospectral and cross-spectral analysis results, are also given in Appendix J for the higher frequency range for record FH 7-8. No dominant features were observed in the motion spectra. Their peak values and spread of energy with frequency appear to follow the general character of the incident wave spectra in all records analyzed. This implies that any natural frequencies in each of the motions is outside the range of significant incident wave energy. The cross-spectral analysis shows a high coherency and zero phase shift between the heave and roll accelerations. In both the sway and roll, and the sway and heave accelerations, the sway acceleration leads by approximately  $180^\circ$  over the range of significant incident wave energy and then tapers to near-zero phase shift at higher frequencies. Also, the coherency is high enough over the incident wave energy band to imply near linearity between all three motions.

These conclusions are based on positive sway being outward from the short leg (south), heave positive up, and the positive roll to be clockwise around a positive axis pointing westerly toward shore.



#### IV. COMPARISON OF THEORY WITH FIELD DATA FOR FRIDAY HARBOR BREAKWATER

Although the Friday Harbor breakwater has a very complex geometry and does not respond as a rigid body to the incident wave excitation, it is important to draw some comparisons between the theoretical prediction of performance and the field measurements. In seeking a "typical event" from the enormous quantity of data gathered, the goal was to find a case where the wind was reasonably close to being on the beam of the short leg of the breakwater.

The one striking item which emerges from the data is the similarity of all the transmission coefficients examined. These curves seem identical no matter what the wind direction. This was not expected because there were barges tied to the breakwater along the entire long leg, while there were none along the shorter leg. A further investigation of the reasons for the similarity is certainly warranted.

The record selected for comparison with the theory was FH 7-8. Figure G-3 in Appendix G shows the incident and transmitted wave spectra and transmission coefficient. This record is also listed in the statistical summaries of Appendix F. The spectral analysis using a high-pass filter was performed as described in Section III.

A comparison of the theoretically predicted and measured transmission coefficient is shown in Figure 28. So long as the calculated hydrodynamic damping is doubled in the theoretical analysis, the results are quite good. As described in Section II, the peak in the transmission curve at a frequency of 0.95 hertz probably results from the "irregular frequency" phenomenon which occurs in this mathematical formulation.

Comparisons of sway, heave, and roll acceleration predictions with measurements are shown in Figures 29, 30, and 31, respectively. Here, the acceleration response has been nondimensionalized by multiplying by the beam or beam squared, as appropriate, and dividing by the acceleration of gravity times the incident wave amplitude.

In the case of sway acceleration, the theory overpredicts the values throughout the entire frequency range. The peak at 0.5 hertz appears in the correct location, but the measured values would need to be doubled to bring the curves into better agreement.

For heave acceleration the curves appear to be in closer agreement, at least above the frequency of 0.4 hertz. Below 0.4 hertz there seems to be little correlation.

Roll acceleration seems to show the worst agreement of all. Here again, the predicted accelerations are considerably higher than the measured values.

There are several possible explanations for the discrepancy between predicted and measured accelerations. In the field, even if the wind

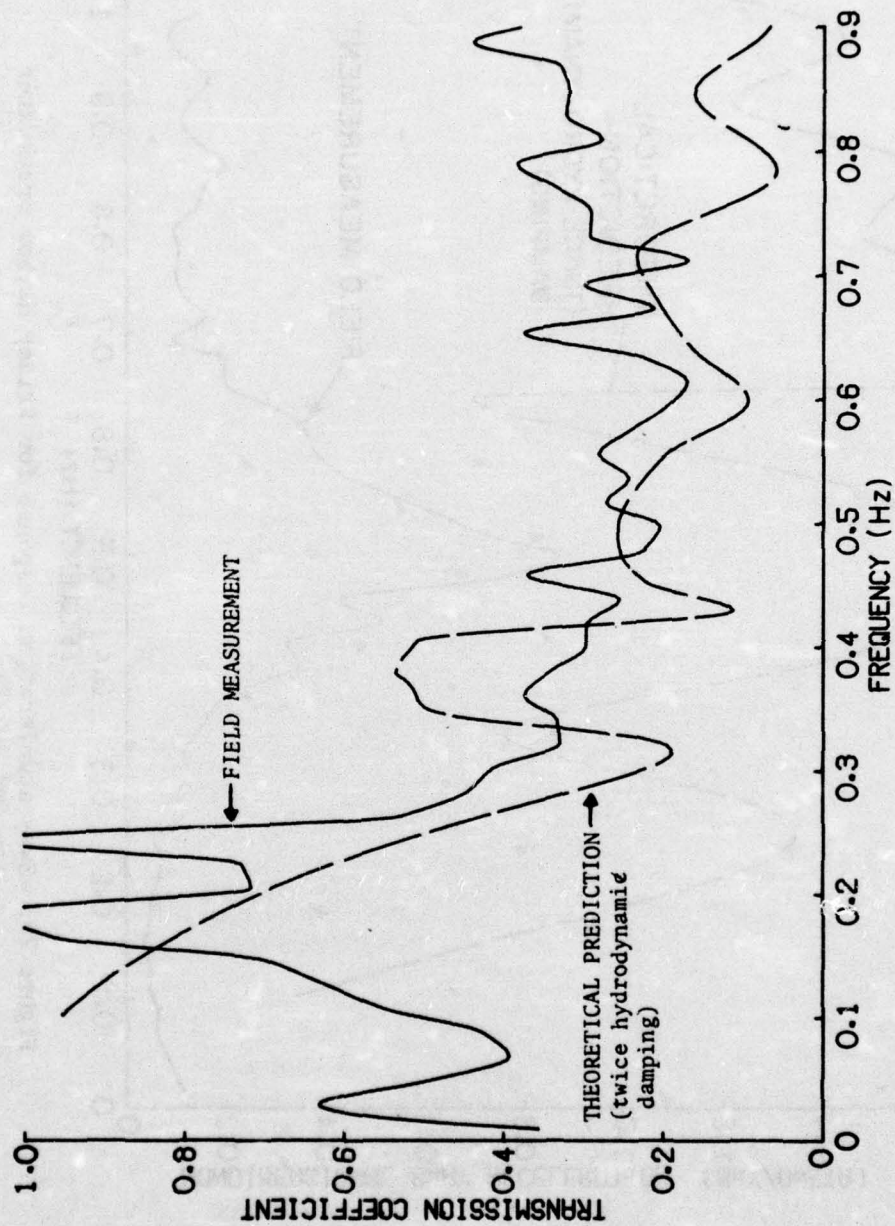


Figure 28. Transmission coefficient for Friday Harbor breakwater (record FH7-8).



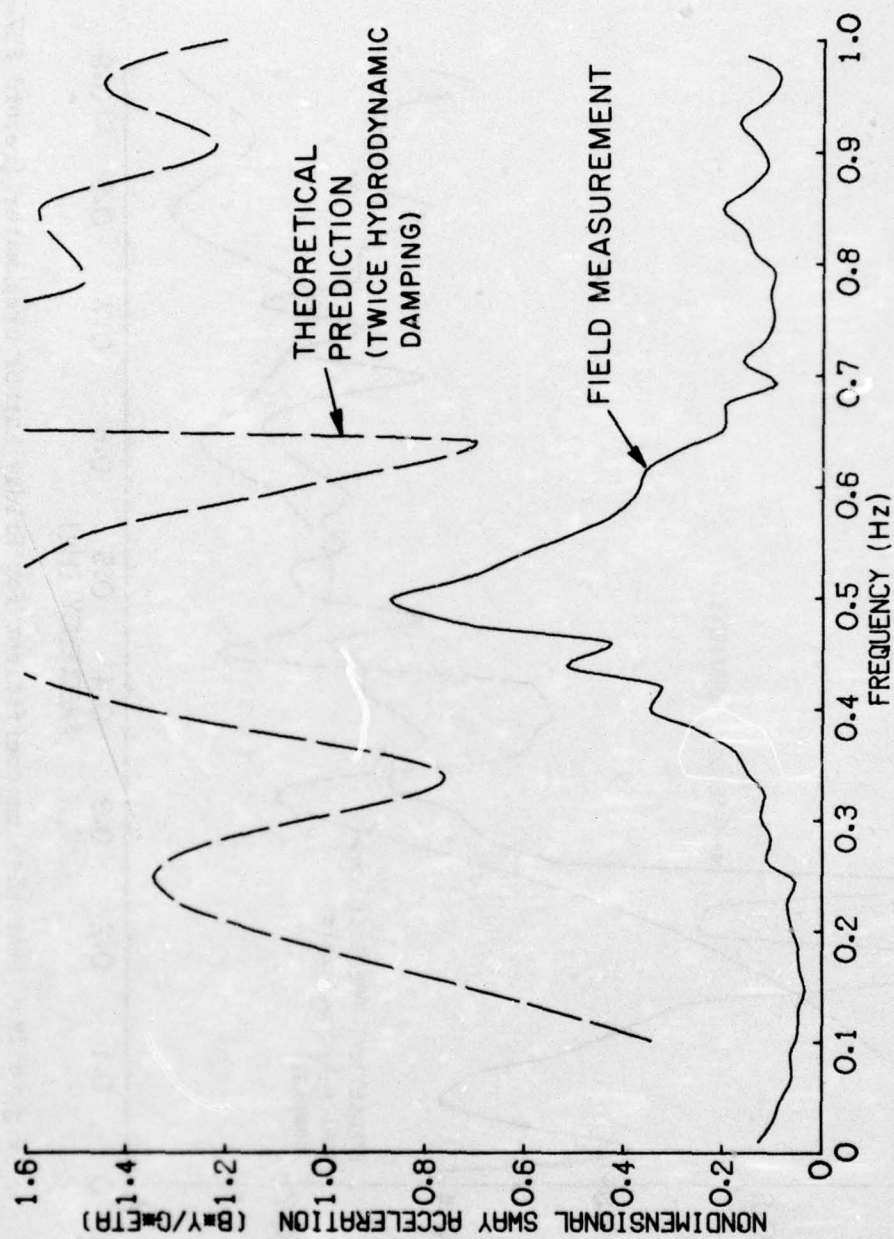


Figure 29. Sway acceleration response for Friday Harbor breakwater (record FH7-8).

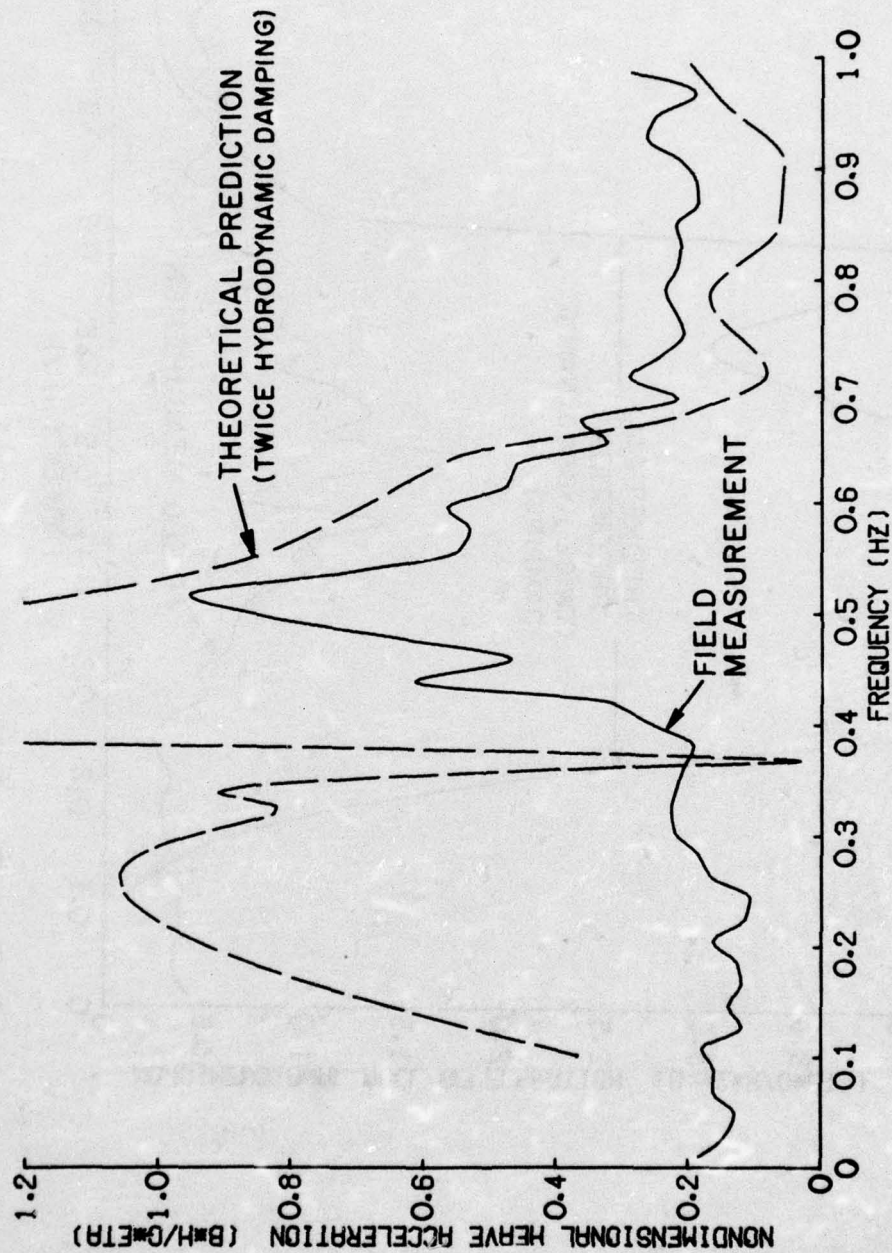


Figure 30. Heave acceleration response for Friday Harbor breakwater (record FH7-8).



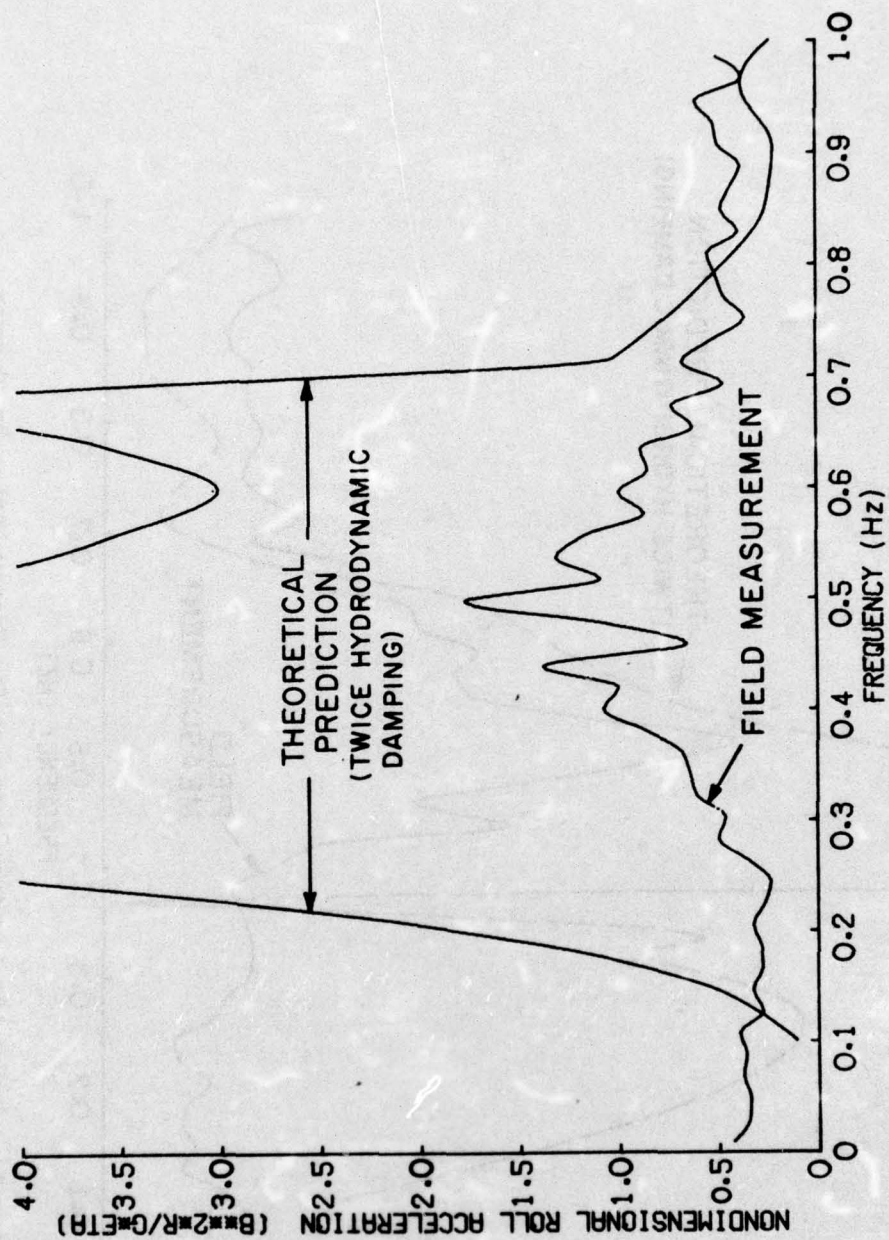


Figure 31. Roll acceleration response for Friday Harbor breakwater (record FH7-8).

were blowing directly on the beam of the breakwater, one would not find the condition of long-crested waves impinging directly on the beam of the breakwater. As a result, the breakwater is not excited uniformly along its entire length. Therefore, the breakwater itself provides restraint against motions which are excited in a local area. The construction of this particular breakwater is also quite flexible, which allows for considerable internal damping of the wave-excited motions. The barges tied to the long leg also serve to restrain the motion and provide additional damping.

There is a strong need, in this case, to provide laboratory data on the breakwater motions, which could be further correlated with the theory and the measured motions.

If one looks at the measured accelerations by themselves, a considerable resemblance in all three degrees of freedom appears. Further, if these accelerations are viewed along with the incident wave spectrum, considerable similarity appears again, suggesting that further investigation of the measurement scheme would also be welcome.

The final comparison to be made is between the theoretically predicted and measured mooring-force coefficient. The theoretical prediction and measured data for the seaward mooring line is shown in Figure 32. The correlation appears to be quite good in this case.

In looking at the time series of force on the mooring lines and the windspeed, one can observe a definite correlation between the wind gusts and increases in the mooring force. This is probably a result of the large barges tied to the structure which act almost as sails. If this is the case, the increase in tension caused by the mean wind on the barges needs to be accounted for. No attempt has been made to do this.

The most common method of presenting the spectral data obtained in the field uses a frequency scale rather than the nondimensional beam/wavelength scale used in Section II. In this section the comparisons are made using a frequency scale. For the Friday Harbor breakwater (beam = 25 feet) the conversion is:

$$\frac{B}{L} = \frac{2\pi B f^2}{g} = 4.87 f^2$$

assuming deepwater waves.



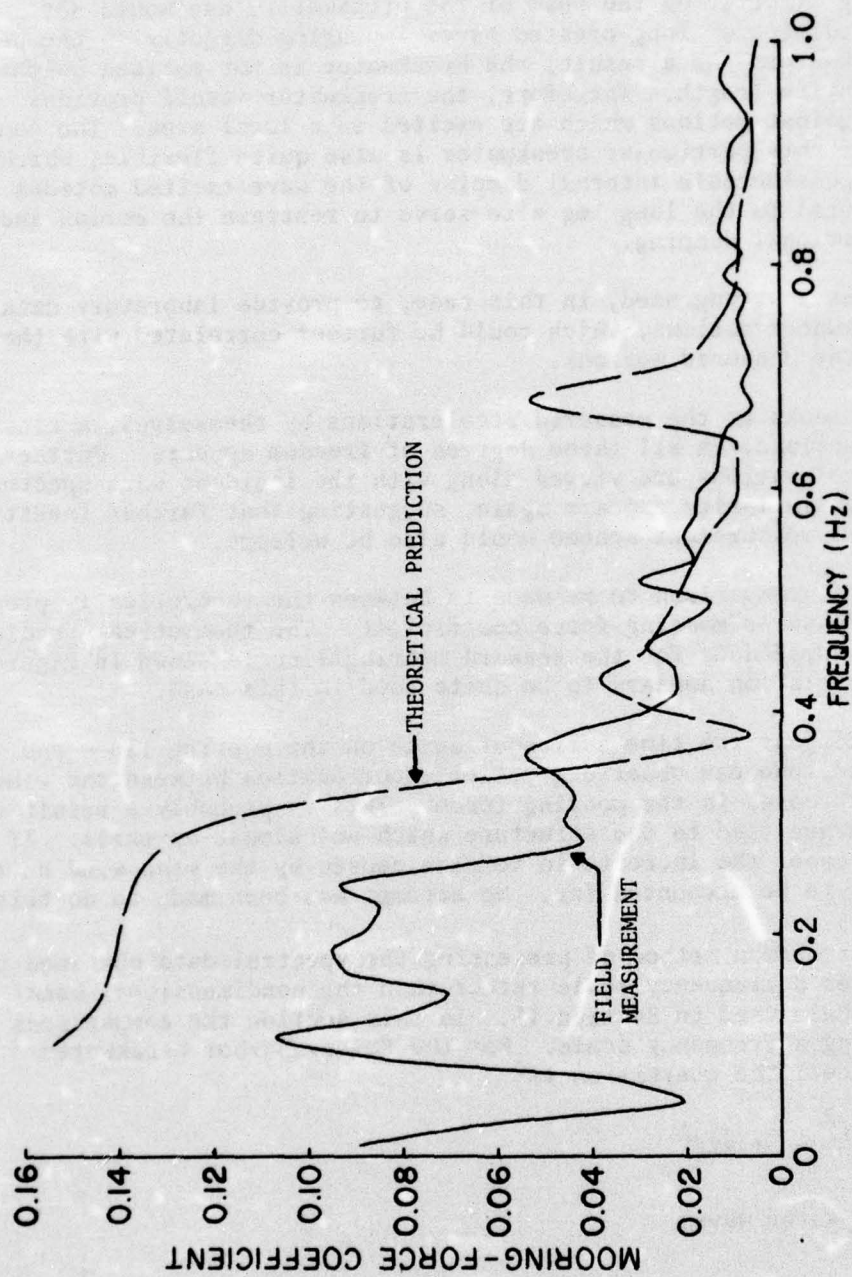


Figure 32. Seaward mooring line mooring-force coefficient, Friday Harbor breakwater (record FH7-8).

## V. CONCLUSIONS

Results for the predicted transmission coefficients were in good agreement with laboratory and field data, and they showed how the influence of fixed-body transmission, and of sway, heave, and roll motions on the transmission coefficient changed with increasing values of the beam to wavelength ratio.

The curves predicting the mooring line forces as a function of the beam to wavelength ratio (or of incident wave frequency) followed those for the measured responses. Care must be exercised in the analysis of mooring line forces because there is strong evidence of nonlinear behavior.

An extreme storm event did not occur during the sampling season at Friday Harbor, nor during two winter sampling periods on the Alaskan breakwaters; however, the anchor forces measured were about an order of magnitude less than anticipated.

The barges tied to the long leg of the breakwater did not noticeably affect the transmission coefficients above a frequency of about 0.3 hertz, since the curves for all incident directions were approximately coincident above that mean frequency. Below the frequency of 0.3 hertz, it appears that the barges may have reduced the transmitted energy somewhat.

The extension of the theoretical model to include second-order terms showed the presence of additional exciting-force terms at zero frequency and at the difference frequency of the incident waves. Additional work on the basic theoretical model is needed to incorporate these terms into the calculations for mooring forces. The most appropriate means of verifying the role of the second-order terms may be in a model basin, where breakwaters of simple cross section and incident wave spectra having only two or three components could be employed under controlled conditions.



#### LITERATURE CITED

- ADEE, B.H., "Analysis of Floating Breakwater Mooring Forces," *Ocean Engineering Mechanics*, American Society of Mechanical Engineers, New York, 1975.
- AMERICAN SOCIETY OF CIVIL ENGINEERS, "Berthing and Mooring Ships," *Proceedings of a Nato Advanced Study Institute*, Lisbon, Portugal, July 1965.
- CARR, J.H., "Mobile Breakwaters," *Proceedings of the Second Conference on Coastal Engineering*, Nov. 1951, pp. 281-295.
- CHRISTENSEN, D.R., and RICHEY, E.P., "Prototype Performance Characteristics of a Floating Breakwater," Marine Technical Report Series Number 24, 1974 Floating Breakwater Conference Papers, University of Rhode Island, Kingston, R.I., Apr. 1974.
- DAVIDSON, D.D., "Wave Transmission and Mooring Force Tests of Floating Breakwater, Oak Harbor, Washington," Technical Report H-71-3, U.S. Army Engineer Waterways Experiment Station, Vicksburg, Miss., Apr. 1971.
- FRANK, W., "Oscillations of Cylinders in or Below the Free Surface of Deep Fluids," Report 2375, Naval Ship Research and Development Center, Bethesda, Md., Oct. 1967.
- GOLD, B., and RADAR, C.M., *Digital Processing of Signals*, McGraw-Hill, New York, 1969.
- HARRIS, A.J., "The Harris Floating Breakwater," Marine Technical Report Series Number 24, 1974 Floating Breakwater Conference Papers, University of Rhode Island, Kingston, R.I., Apr. 1974.
- JOHN, F., "On the Motion of Floating Bodies," *Communications on Pure and Applied Mathematics*, Vol. 3, 1950.
- LEE, C.M., JONES, H., and BEDEL, J.W., "Added Mass and Damping Coefficients of Heaving Twin Cylinders in a Free Surface," Report 3695, Naval Ship Research and Development Center, Bethesda, Md., Aug. 1971.
- LOCHNER, R., FABER, O., and PENNY, W., "The Bombardon Floating Breakwater," *The Civil Engineer in War*, The Institution of Civil Engineers, Vol. 2, London, 1948, p. 256.
- MINIKIN, R.R., "Floating and Foundationless Breakwaters," *Engineering*, Dec., 1948, pp. 557-579.
- NECE, R.E., and RICHEY, E.P., "Wave Transmission Tests on Floating Breakwater for Oak Harbor, Washington," Technical Report No. 32, University of Washington, Charles W. Harris Hydraulics Laboratory, Seattle, Wash., Apr. 1972.

SALVESEN, N., TUCK, E., and FALTINSEN, O., "Ship Motions and Sea Loads," *Transactions of the Society of Naval Architects and Marine Engineers*, Vol. 78, 1970, pp. 250-257.

STRAMANDI, N., "Transmission Response of Floating Breakwaters to Ship Waves," Masters Thesis, University of Washington, Seattle, Wash., 1975.

SUTKO, A.A., and HADEN, E.L., "The Effect of Surge, Heave and Pitch on the Performance of a Floating Breakwater," Marine Technical Report Series Number 24, 1974 Floating Breakwater Conference Papers, University of Rhode Island, Kwnngston, R.I., Apr. 1974.

NAVAL CIVIL ENGINEERING LABORATORY, "Mobile Piers and Breakwaters - An Exploratory Study of Existing Concepts," Technical Report 127, Port Hueneme, Calif., Apr. 1961.

NAVAL CIVIL ENGINEERING LABORATORY, "Transportable Breakwaters - A Survey of Concepts," Technical Report R-727, Port Hueneme, Calif., May 1971.



## APPENDIX A

### HYDROSTATIC RESTORING FORCES AND SPRING CONSTANTS

Hydrostatic restoring forces and spring constants are computed for the two-dimensional analysis under the following assumptions:

- (a) The body rotates about the origin of the coordinate system and all forces and moments are computed about that point.
- (b) The body has vertical sides in the region of its waterplane.
- (c) All motions are small.

#### 1. Sway Motion.

In the horizontal plane the body is in neutral equilibrium. Therefore, there are no hydrostatic restoring forces and

$$KH_{11} = KH_{12} = KH_{13} = 0. \quad (A-1)$$

#### 2. Heave Motion.

Vertical displacement of the body results in a change in the buoyant volume of the body and consequently a change in the buoyant force on the body. Since this force must be perpendicular to the waterline, there is no change in the horizontal force as a result of vertical displacement and

$$KH_{21} = 0. \quad (A-2)$$

If one considers a small vertical displacement,  $\delta y$ , there is a resulting change in volume:

$$\delta V = -\delta y A_w \quad (\text{for } \delta y + \text{upwards}).$$

Here,  $A_w$  is the waterplane area. The vertical force then is:

$$F = KH_{22}\delta y = -\rho g A_w \delta y,$$

or

$$KH_{22} = \rho g A_w = \rho g [x_b - x_a]. \quad (A-3)$$

In this equation  $x_a$  and  $x_b$  denote the sides of the body as shown in the Figure in this appendix. Since the vertical force may be regarded as acting at the centroid of the waterplane area,  $x_c$ , the moment may be expressed.

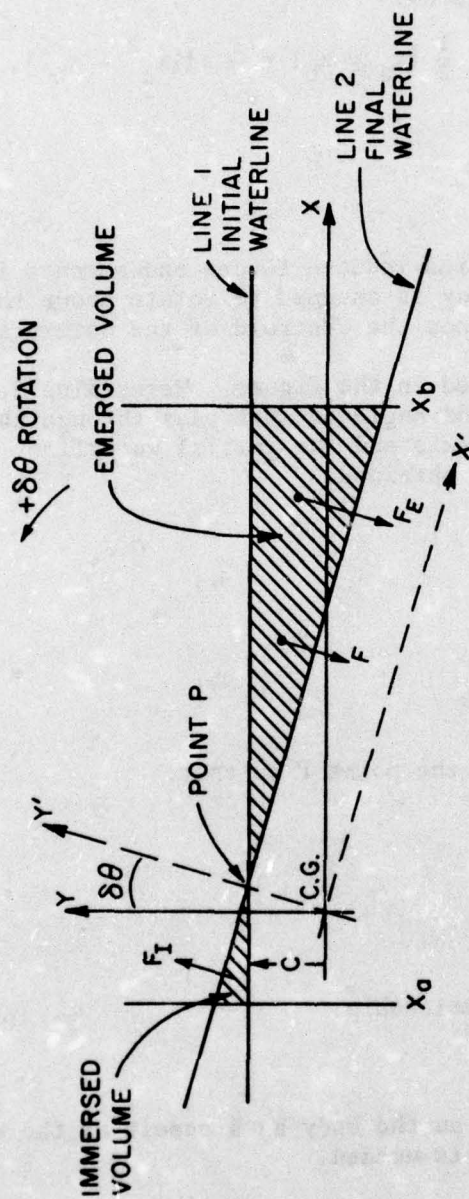


Figure. A-1 Schematic of floating breakwater near the waterplane.



$$M = K_{23} \delta y = - \rho g A_w x_c \delta y.$$

Substituting for  $x_c$  and  $A_w$  yields:

$$KH_{23} = - \rho g A_w x_c = - \rho g A_w \frac{1}{2} [x_a + x_b] = \frac{1}{2} \rho g [x_a^2 - x_b^2]. \quad (A-4)$$

### 3. Roll Motion.

The analysis of roll motion-induced forces and moments is complicated by the fact that the body is assumed to rotate about the origin of the coordinate system and not the centroid of the waterplane.

The problem is illustrated in the figure. Here, line 2, the waterline after rotation through an angle  $\delta\theta$  must pass through the intersection of the  $y'$  coordinate axis and the initial waterline. Equations for lines 1 and 2 may then be obtained.

$$\text{Line 1: } y = c.$$

$$\text{Line 2: } y = mx + b.$$

The slope of line 2 is:

$$m = \frac{\Delta y}{\Delta x} = - \tan \delta\theta.$$

Line 2 must also pass through the point P so that:

$$x_p = + c \tan \delta\theta$$

and

$$y_p = c.$$

These equations yield the relationship:

$$b = c(1 + \tan^2 \delta\theta).$$

To find the force acting on the body as a result of the rotation, the net lost or gained volume is needed.

$$\begin{aligned} \delta V &= \int_{x_a}^{x_b} (mx + b - c) dx \\ &= \int_{x_a}^{x_b} [(-x \tan \delta\theta + c(1 + \tan^2 \delta\theta) - c)] dx \end{aligned}$$

$$= -\frac{1}{2} [x_b^2 - x_a^2] \tan \delta\theta + c[x_b - x_a] \tan^2 \delta\theta.$$

By applying the "small angle" approximation and neglecting terms of the order of  $\delta\theta^2$ . Then,

$$\delta V \approx \frac{1}{2} [x_a^2 - x_b^2] \delta\theta$$

and the force is:

$$F \approx \frac{1}{2} \rho g [x_a^2 - x_b^2] \delta\theta.$$

The x and y components of the force are:

$$F_x = F \cos \delta\theta \approx \frac{1}{2} \rho g [x_a^2 - x_b^2] \delta\theta \cos \delta\theta$$

and

$$F_y = F \sin \delta\theta \approx \frac{1}{2} \rho g [x_a^2 - x_b^2] \delta\theta \sin \delta\theta.$$

Again applying the small angle approximation one finds:

$$F_x \approx \frac{1}{2} \rho g [x_a^2 - x_b^2] \delta\theta$$

and

$$F_y \approx 0.$$

The hydrostatic spring constants coupling roll to sway and heave are then:

$$KH_{31} = 0 \quad (A-5)$$

and

$$KH_{32} = \frac{1}{2} \rho g [x_a^2 - x_b^2]. \quad (A-6)$$

To obtain the moment induced by roll motion compute:

$$\text{Moment of Gained Volume} = -\left(\frac{1}{2} x_a^2 \tan \delta\theta\right) \left(\frac{2}{3} x_a\right) \approx \frac{1}{3} x_a^3 \delta\theta,$$

$$\text{Moment of Lost Volume} \approx \frac{1}{3} x_b^3 \delta\theta$$

and

$$\text{Moment of Original Volume} = W y_b \delta\theta.$$

In this formula,

$$W = \text{weight per unit length}$$



and

$y_b$  = distance the center of buoyancy is below the center of gravity.

The total moment then is:

$$M = \frac{\rho g}{3} (x_b^3 - x_a^3) \delta\theta + W y_b \delta\theta,$$

and the spring constant becomes:

$$KH_{33} = \frac{\rho g}{3} (x_b^3 - x_a^3) + W y_b. \quad (A-7)$$

Expressed in traditional naval architecture terminology, this reduces to:

$$KH_{33} = WGM, \quad (A-8)$$

where

GM = metacentric height.

#### 4. Collected Results.

$$KH_{11} = KH_{12} = KH_{13} = KH_{21} = KH_{31} = 0$$

$$KH_{22} = \rho g [x_b - x_a]$$

$$KH_{23} = KH_{32} = \frac{1}{2} \rho g [x_a^2 - x_b^2] \quad (A-9)$$

$$KH_{33} = \frac{\rho g}{3} [x_b^3 - x_a^3] + W y_b.$$

## APPENDIX B

### MOORING ANALYSIS

#### 1. Purpose of the Program.

Computer program BRKMOOR computes the forces and moments imparted by a pair of mooring cables on a floating breakwater section. BRKMOOR also computes the changes in the mooring cable tensions and the spring-constant values for the moorings as the breakwater moves in sway, heave, or roll.

#### 2. Program Description.

Program BRKMOOR is written primarily in FORTRAN IV although FORTRAN II print statements are used.

The program consists of the main program BRKMOOR and the subroutines LINE2, CHAIN, NYLON, EQU LIB, SPRING, and LTERPS.

BRKMOOR **calculates** the forces in a mooring cable by using a discretized approximation to the cable. The cable is divided into the number of segments specified in the input data. Each segment may be of a different material or size. Each segment is in turn divided into a specified number of sections. The cable is considered to be made of these sections with the weight of each section concentrated at the node at the bottom of the section. Connecting each node is a straight but elastic section.

The main part of the program specifies 15 different angles at the attachment, ranging from nearly vertical to nearly straight to the farthest reasonable anchor position. A first guess at a top tension is made.

LINE2 then sums down the cable computing forces and coordinates of each node starting with the initial angle and initial tension. The position of the end of the cable is compared with the specified water depth at the anchor. The initial tension is adjusted and the summation repeated until the cable ends at the proper depth. Control then returns to the main program.

LINE2 calls the subroutines NYLON or CHAIN to compute the strain of the cable section of the appropriate material. If other materials are used new subroutines should be written for strain computation, along with the appropriate calling expression in LINE2.

At each angle the cable forces at the attachment and the anchor position are stored in arrays. EQU LIB then computes the breakwater equilibrium position for the specified conditions.

SPRING is called by EQU LIB. SPRING computes the change in mooring



cable tensions with breakwater displacement in sway, heave, and roll and the spring constants of the moorings on the breakwater.

LTERPS is a linear interpolation subroutine which computes the slope,  $\frac{\Delta Y}{\Delta X}$ , and the interpolated value of Y for a given X and an array of X vs. Y values. LTERPS is called by EQU LIB and SPRING.

### 3. Type of Computer and Peripherals.

BRKMOOR was written for use on the CDC 6400 computer. It uses about 40,000 words of memory. No peripherals other than the card reader and line printer are required.

### 4. Input Data.

The input to BRKMOOR is as follows:

Card #1 - Title card, Format (8A10).

80 alphanumeric characters max.

Card #2 - Breakwater geometry card, Format (5F10.0).

YCG = Vertical location of breakwater CG relative to water surface.

XCAB(1) = x coordinate of cable #1 attachment to breakwater (the CG is at X = 0 and cable #1 is defined as the cable with its anchor in the +x direction).

YCAB(1) = y coordinate of cable #1 attachment to breakwater.

XCAB(2) = x coordinate of cable #2 attachment to breakwater.

YCAB(2) = y coordinate of cable #1 attachment to breakwater.

Card #3 - Number of desired conditions Format (12).

(Also number of condition cards to follow)

Card #4 - Condition cards, Format (4F10.0).

(One card for each condition)

FEXT = Force applied to the breakwater not due to moorings in x direction (could be due to wave action, tide, wind, etc. force in pounds).

SEP = Anchor separation in horizontal direction (feet).

TENS1 = Nominal tension in cable #1 (lb.).

TENS2 = Nominal tension in cable #2 (lb.).

It should be noted that only the following condition combinations are possible:

SEP

SEP+FEXT

TENS1

TENS1+FEXT

TENS2

TENS2+FEXT

TENS1+TENS2

- Card #5 - Tide Card, Format (I1,9X,5F10.0).  
 NTIDE = Number of tide values to follow (max = 5).  
 TIDE = Tide position in feet relative to that at which the anchor depths are given.
- Card #6 - Cable #1 Parameters, Format (I2,8X,2F10.0).  
 NSEG = Number of different segments (types of cable materials) from which the cable is constructed.  
 DEPTH = Depth of water at the anchor (feet).  
 BSLOPE = Slope of bottom in region of anchor (feet/feet).
- Card #7 - Cable segment properties Format (I5,5X,2F10.0,A10,F10.0).  
 One card for each of the number of segments listed in card 6 parameter NSEG.  
 NSECT = Number of sections into which it is desired to divide the cable segment.  
 ALSEG = The length of this cable segment.  
 WPF = Weight per foot in water of the cable material in this segment.  
 MATL = Material name (as the program now stands this must be CHAIN or NYLON (Name must begin in column 31)).  
 DIAM = Diameter of the nylon rope or of the chain link in inches.
- Card #8 and #9 - Same as cards #6 and #7 only as applies to cable. #2.

Table B-1 illustrates the input cards for a test case. All the read statements for the program are in the main program along with comments and explanations of input requirements.

##### 5. Mathematical Procedures and Program Limitations.

The basic cable computations which take place in LINE2 require some explanation. As was stated previously, the weight of each cable section is considered to be concentrated at the bottom of the section. In order to find the shape of the cable, summations of forces are computed for static equilibrium at each node. At each node we know the tension in the cable section above the node as well as the angle of that section with the horizontal. Figure B-1 illustrates the cable about the  $i$ th node.

If the angle  $\phi_i$  is taken to be the angle from the horizontal, then the angle  $\phi_{i+1}$  can be computed as follows:

$$\phi_{i+1} = \tan^{-1} \left[ \frac{T_i \sin \phi_i + W_i}{T_i \cos \phi_i} \right], \quad (B-1)$$

where  $T_i$  = tension in section  $i$ ,

$W_i$  = weight of section  $i$  concentrated at node  $i$ .



TEST CASE -- MEASURED CHAIN TEST 3/11/76				
0.	1.	0.	-1.	0.
06				
0.	58.02			
	58.21			
		36.		
		42.		
	54.			
		36.	30.	
1				
01	7.167			
00030	29.33	.722	CHAIN	.25
01	7.167			
00030	29.33	.722	CHAIN	.25

Table B-1. Example input for program BRKMOOR.

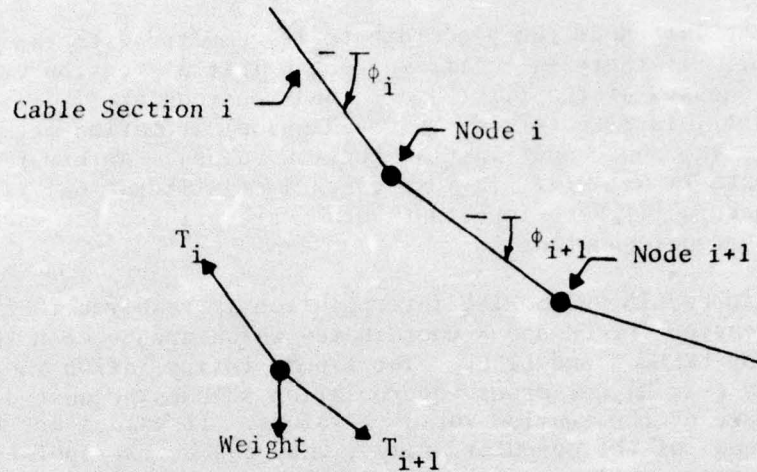


Figure B-1. Cable sections about node i and free body diagram of node i.

This new angle is then used to compute the tension in the next section:

$$T_{i+1} = \frac{T_i \cos \phi_i}{\cos \phi_{i+1}} \quad (B-2)$$

LINE2 computes the angle and tension of each **section** starting from the top. At each section the angle is compared with the slope of the bottom. When the angle  $\phi$  is parallel or more positive than the bottom then  $\phi$  is set to the slope of the bottom.

The x and y coordinates of each node are computed.

$$X_{i+1} = X_i + L_{EXT_{i+1}} \cos \phi_{i+1} \quad (B-3)$$

$$Y_{i+1} = Y_i + L_{EXT_{i+1}} \sin \phi_{i+1} \quad (B-4)$$

where  $X_i$  = x coordinate of node i

$Y_i$  = y coordinate of node i

$L_{EXT}$  = length of section when under tension.



At the last node the  $y$ -coordinate is compared with the depth of the anchor. If there is a difference the initial tension value is adjusted. Guesses at the first and second tensions are made. From then on a secant (discrete form of Newton Raphson) iteration method is used to compute the subsequent initial tension values. An error of  $0.0001 \times \text{depth}$  is allowed. In most cases 4 or 5 iterations yield the desired accuracy. Some important values are printed for each iteration to aid in troubleshooting.

Within EQUILIB and SPRING interpolation is required to find the values of tension forces and  $x$  coordinates which are between the points computed by BRKMOOR and LINE2. The linear interpolation routine LTERPS was chosen over higher-order interpolation schemes because of the asymptotic nature of the tension versus  $\lambda$  values. If values are requested beyond the ends of the computer arrays, they can be extrapolated, but a warning message will be printed by EQUILIB.

An iterative procedure is required within EQUILIB if the anchor separation condition is selected. Again the secant iteration method is used. EQUILIB prints out values at each iteration which can aid in troubleshooting but which can normally be ignored.

Subroutine CHAIN computes the strain in a chain using the basic elastic properties of a steel bar with a total area equal to the area of both parts of the links, and a factor of 6 to allow for the deformation characteristics of the links. This factor of 6 came from a finite element computation.

Subroutine NYLON computes the strain in a nylon rope using a power-function fit of the form:

$$\epsilon = AX^\beta,$$

where  $\epsilon$  = Strain,  
 $A = 0.02052$ ,  
 $\beta = 0.2237$ ,

$$X = \frac{T}{D^2},$$

$T$  = Tension (pound),  
 $D$  = Diameter of rope (inches).

This function was determined using a least-squares power-function fit of experimental data provided by Sampson Cordage Works for their 2-in-1 nylon braided rope.

An experimental verification test was conducted as a check of the program. A chain was suspended from a spring scale. Measurements were made of the length of the chain, its weight and the tension in two geometrical configurations. The program gave computed values of the tension very close to those measured.

6. Flow Chart.

Figure B-2 illustrates the flow chart of BRKMOOR and its subroutines.

7. Program Comments and Glossary of Terms.

The program listing contains many comments which aid in following the logic of the program. The important variable names are explained as well as the input requirements.

8. Run Time and Memory Size.

BRKMOOR requires about 40 seconds on the CDC 6400 to compile and compute results for one value of the tide parameter. Each additional tide value requires about 30 seconds additional time. These values are for cables divided into 50 sections each. Time should be somewhat proportional to the total number of cable sections. The number of test conditions has much less effect on time than does the tide. As stated previously, a central memory of about 40,000 octal is required.

9. Run and Card Deck Setup Procedures and Special Operation Instructions.

In order to run the FORTRAN source program deck on the University of Washington CDC 6400, the following deck is required:

BMOOR,T40.	Job card
ACCOUNT	(Account no., password)
FORTRAN.	
LGO(LC=6000)	LC = line count value; depends on how many tides and conditions are run
7/8/9	
FORTRAN DECK	
7/8/9	
DATA DECK	
6/7/8/9	

10. Sample Output Data.

Example output from program BRKMOOR is shown in Table B-2; a listing of program BRKMOOR is shown in Table B-3.



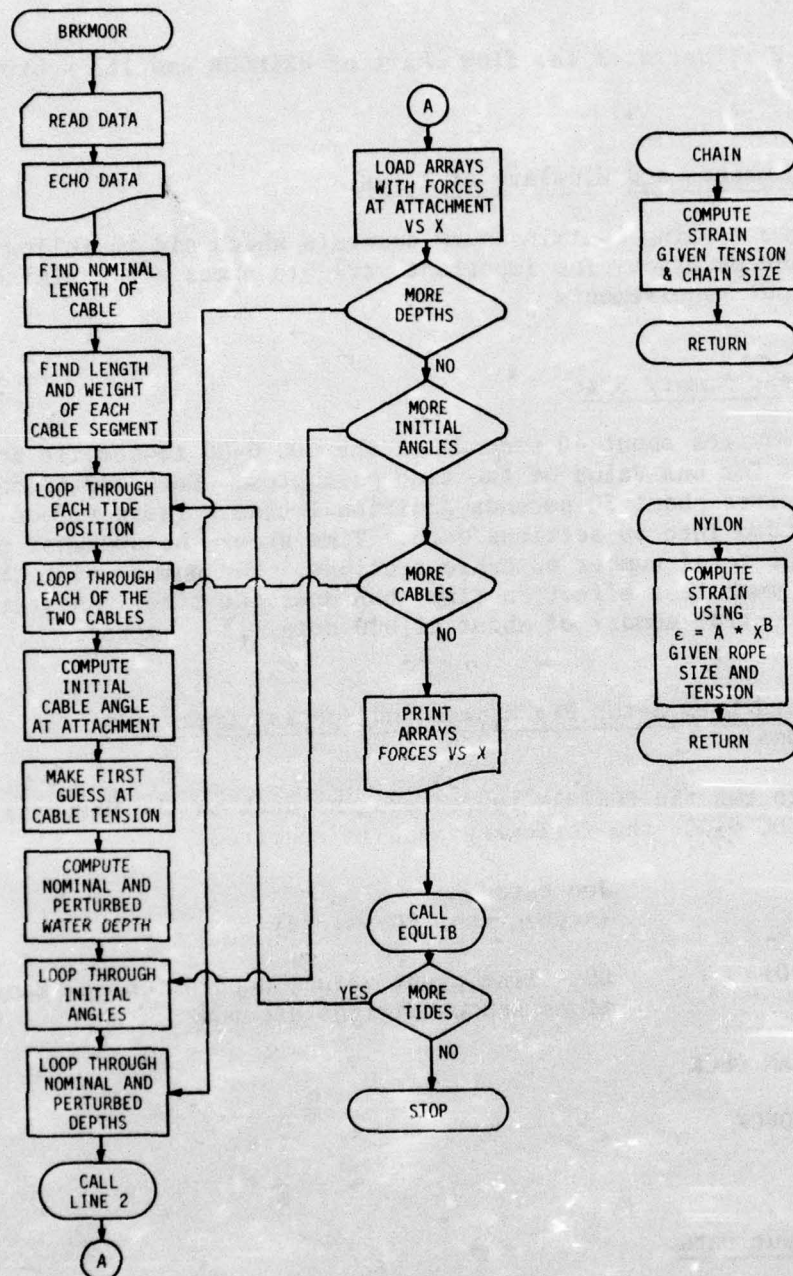


Figure B-2. Flow chart for program BRKMOOR.

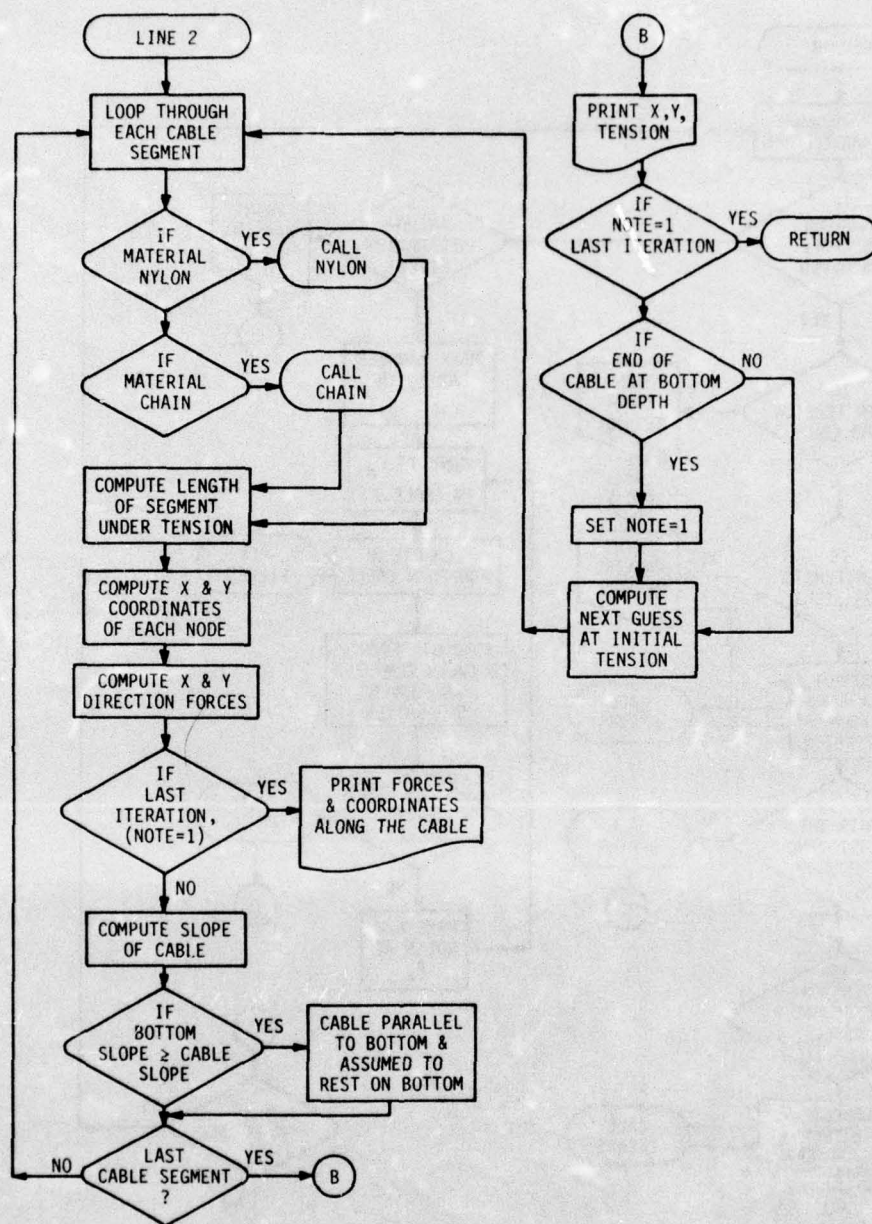


Figure B-2. Continued



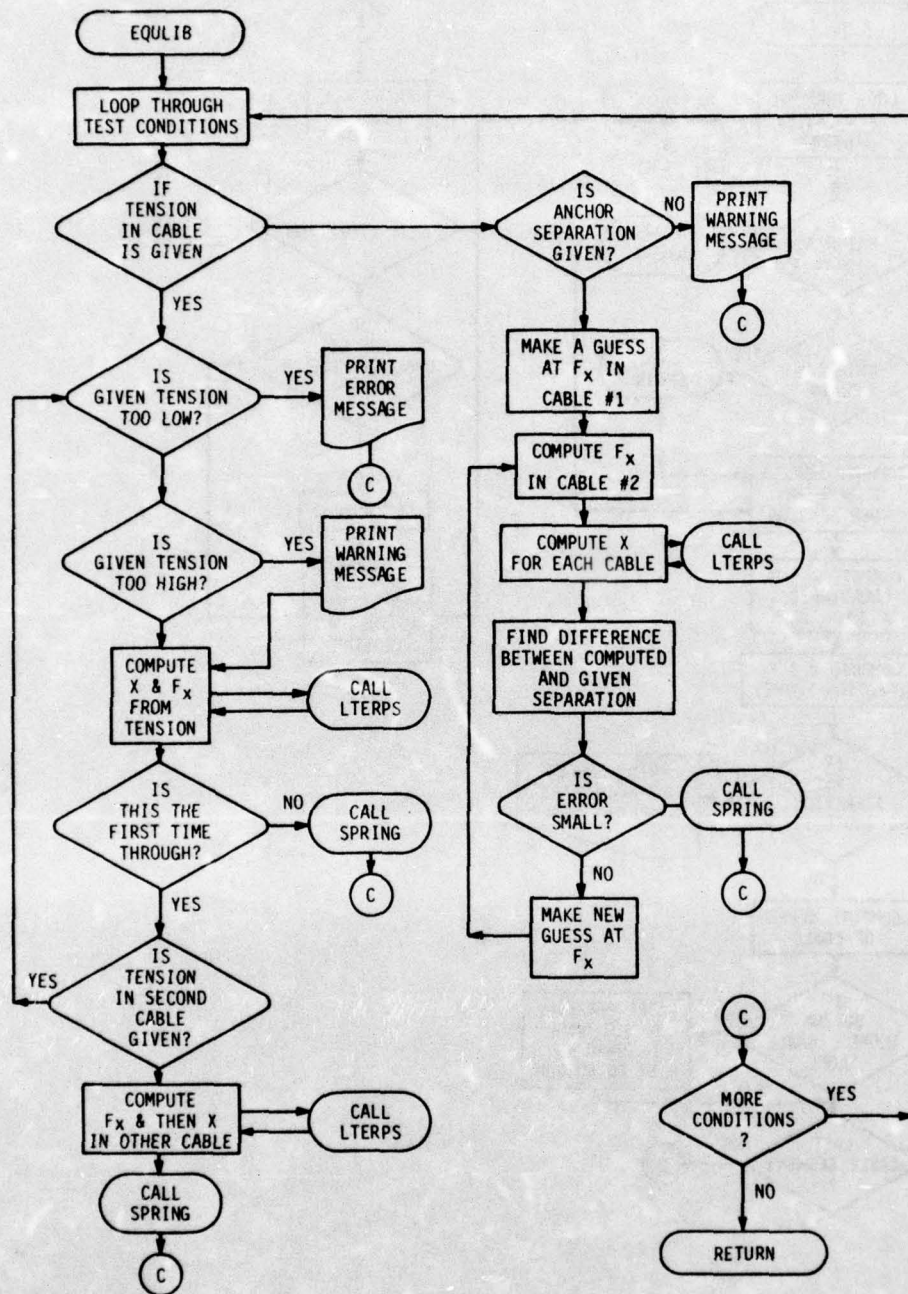


Figure B-2. Continued

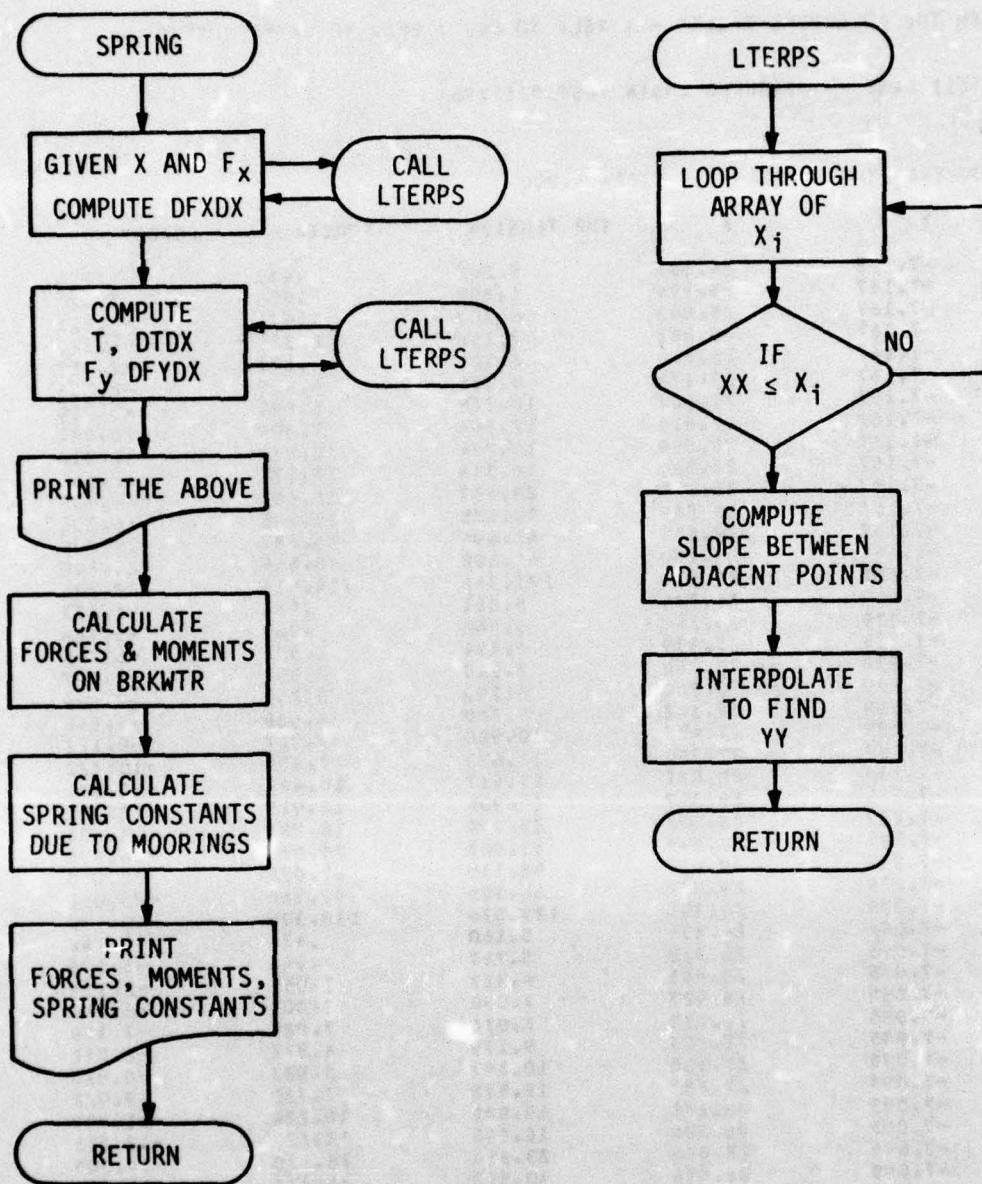


Figure B-2. Continued



IN THE FOLLOWING TABLES - X REL. TO CG, Y REL. TO WATER SURFACE

TEST CASE -- MEASURED CHAIN TEST 3/11/76

MOORING LINE NUMBER= 1 TIDE= -.000

Y	X	TOP TENSION	FORCEX	FORCEY
-7.167	24.605	5.202	.430	-5.184
-7.167	25.294	5.802	.956	-5.722
-7.167	25.893	6.407	1.574	-6.211
-7.167	26.387	7.158	2.326	-6.770
-7.167	26.804	8.101	3.257	-7.417
-7.167	27.174	9.278	4.419	-8.158
-7.167	27.507	10.776	5.899	-9.019
-7.167	27.814	12.704	7.809	-10.021
-7.167	28.099	15.254	10.338	-11.216
-7.167	28.366	18.714	13.777	-12.664
-7.167	28.619	23.557	18.601	-14.454
-7.167	28.859	30.675	25.695	-16.755
-7.167	29.089	41.694	36.687	-19.809
-7.167	29.290	61.608	56.444	-24.690
-7.167	29.410	121.346	114.814	-39.276
-7.239	24.544	5.251	.434	-5.233
-7.239	25.258	5.848	.963	-5.768
-7.239	25.839	6.494	1.595	-6.295
-7.239	26.346	7.240	2.353	-6.847
-7.239	26.769	8.190	3.292	-7.499
-7.239	27.142	9.380	4.468	-8.248
-7.239	27.477	10.900	5.967	-9.122
-7.239	27.790	12.833	7.888	-10.122
-7.239	28.077	15.417	10.449	-11.336
-7.239	28.347	18.906	13.919	-12.795
-7.239	28.602	23.805	18.797	-14.606
-7.239	28.844	31.005	25.971	-16.935
-7.239	29.077	42.115	37.058	-20.010
-7.239	29.277	62.505	57.266	-25.050
-7.239	29.395	125.036	118.305	-40.470
-7.095	24.658	5.160	.426	-5.142
-7.095	25.328	5.757	.948	-5.678
-7.095	25.945	6.327	1.555	-6.133
-7.095	26.427	7.080	2.301	-6.696
-7.095	26.839	8.016	3.223	-7.339
-7.095	27.205	9.179	4.372	-8.071
-7.095	27.536	10.657	5.833	-8.918
-7.095	27.837	12.578	7.732	-9.922
-7.095	28.122	15.085	10.224	-11.092
-7.095	28.386	18.508	13.624	-12.525
-7.095	28.636	23.314	18.410	-14.305
-7.095	28.874	30.353	25.425	-16.579
-7.095	29.102	41.256	36.302	-19.601
-7.095	29.303	60.738	55.647	-24.341
-7.095	29.426	117.875	111.530	-38.152

Table B-2. Example output from program BRKMOOR.

TEST CASE -- MEASURED CHAIN TEST 3/11/76

MOORING LINE NUMBER= 2 TIDE= -.000

Y	X	TOP TENSION	FORCEX	FORCEY
-7.167	-24.605	5.202	-.430	-5.184
-7.167	-25.294	5.802	-.956	-5.722
-7.167	-25.893	6.407	-1.574	-6.211
-7.167	-26.387	7.158	-2.326	-6.770
-7.167	-26.804	8.101	-3.257	-7.417
-7.167	-27.174	9.278	-4.419	-8.158
-7.167	-27.507	10.776	-5.899	-9.019
-7.167	-27.814	12.704	-7.809	-10.021
-7.167	-28.099	15.254	-10.338	-11.216
-7.167	-28.366	18.714	-13.777	-12.664
-7.167	-28.619	23.557	-18.601	-14.454
-7.167	-28.859	30.675	-25.695	-16.755
-7.167	-29.089	41.694	-36.687	-19.809
-7.167	-29.290	61.608	-56.444	-24.690
-7.167	-29.410	121.346	-114.814	-39.276
-7.239	-24.544	5.251	-.434	-5.233
-7.239	-25.258	5.848	-.963	-5.768
-7.239	-25.839	6.494	-1.595	-6.295
-7.239	-26.346	7.240	-2.353	-6.847
-7.239	-26.769	8.190	-3.292	-7.499
-7.239	-27.142	9.380	-4.468	-8.248
-7.239	-27.477	10.900	-5.967	-9.122
-7.239	-27.790	12.833	-7.888	-10.122
-7.239	-28.077	15.417	-10.449	-11.336
-7.239	-28.347	18.906	-13.919	-12.795
-7.239	-28.602	23.605	-18.797	-14.606
-7.239	-28.844	31.005	-25.971	-16.935
-7.239	-29.077	42.115	-37.058	-20.010
-7.239	-29.277	62.505	-57.266	-25.050
-7.239	-29.395	125.036	-118.305	-40.470
-7.095	-24.658	5.160	-.426	-5.142
-7.095	-25.328	5.757	-.948	-5.678
-7.095	-25.945	6.327	-1.555	-6.133
-7.095	-26.427	7.080	-2.301	-6.696
-7.095	-26.839	8.016	-3.223	-7.339
-7.095	-27.205	9.179	-4.372	-8.071
-7.095	-27.536	10.657	-5.833	-8.918
-7.095	-27.837	12.578	-7.732	-9.922
-7.095	-28.122	15.085	-10.224	-11.092
-7.095	-28.386	18.508	-13.626	-12.525
-7.095	-28.636	23.314	-18.410	-14.305
-7.095	-28.874	30.353	-25.425	-16.579
-7.095	-29.102	41.256	-36.302	-19.601
-7.095	-29.303	60.738	-55.647	-24.341
-7.095	-29.426	117.675	-111.530	-38.152

Table B-2. Continued



TEST CASE -- MEASURED CHAIN TEST 3/11/76

FOR THE CONDITIONS --

TIDE = -.00  
 EXTERNALLY APPLIED HORIZONTAL FORCE, FEXT = .000LB.  
 HORIZONTAL ANCHOR SEPARATION, SEP = 58.020FEET  
 NOMINAL TENSION IN CABLE 1 = -.000 LB.  
 NOMINAL TENSION IN CABLE 2 = -.000 LB.

CABLE NO.	FX	FY	X	Y	DFXDX	DFXDY	DFYDX	DFYDY	TENSION
1	32.933	-18.766	29.011	-7.167	-4.781E+01	1.328E+01	1.346E+01	-5.134E+00	3.793E+01
2	-32.933	-18.766	-29.011	-7.167	-4.781E+01	-1.328E+01	-1.346E+01	-5.134E+00	3.793E+01

CABLE NO.	DTDX	DTDY	DTDR
-----------	------	------	------

1	-4.7919E+01	1.4203E+01	1.4203E+01
2	4.7919E+01	1.4203E+01	-1.4203E+01

92

FORCES AND MOMENTS ON BREAKWATER AT EQUILIBRIUM DUE TO MOORING LINES

FS = .0000  
 FH = -37.5323  
 MF = .0000

SPRING CONSTANTS SWAY DIRECTION

KP11 = 9.56100E+01  
 KP12 = .0  
 KP13 = -2.65637E+01

SPRING CONSTANTS HEAVE DIRECTION

KP21 = .0  
 KP22 = 1.02676E+01  
 KP23 = .0

SPRING CONSTANTS ROLL DIRECTION

KP31 = -2.69150E+01  
 KP32 = .0  
 KP33 = 1.02676E+01

Table B-2. Continued

BMOORUD //////////////////////////////////////

RUNT VERSION FEB 74 B 13:04 04/09/76

```

      PROGRAM BRKMOOR(INPUT,OUTPUT,PUNCH,TAPE5=INPUT,TAPE6=OUTPUT)
C
C PROGRAM BRKMOOR COMPUTES THE FORCES AND SPRING CONSTANTS THAT A PAIR
C OF MOORING CABLES IMPART ON A FLOATING BREAKWATER SECTION
C
C*****
C INPUT
C FIRST CARD--TITLE - 80 ALPHANUMERIC CHARACTERS
C BREAKWATER GEOMETRY--
C NUMBER OF TEST CONDITIONS
C TEST CONDITIONS--ONE CARD FOR EACH SET
C TIDE CARD--NUMBER OF TIDE CONDITIONS AND THE CONDITIONS
C FOR FIRST CABLE--NUMBER OF SEGMENTS ANCHOR DEPTH AND BOTTOM SLOPE
C FOR EACH OF ABOVE CABLE SEGMENTS --CARD WITH SEGMENT PROPERTIES
C REPEAT --NUMBER OF SEGMENTS AND THEIR PROPERTIES FOR SECOND CABLE
C*****
C
3      COMMON/ONE/NSEG(2),NSECT(2,5),WSECT(2,5), MATL(2,5),DIAM(2,5),
2      ALSECT(2,5)
3      COMMON/TWO/WY(2,3),EX(2,3,20),FX(2,3,20),FY(2,3,20),TENS(2,3,20),
2      FEXT(9),SEP(9),TENS1(9),TENS2(9),NANGLE,NCOND,TITLE(8)
3      COMMON/FOUR/YCG,XCAB(2),YCAB(2),TIDE(5),ITIDE
3      DIMENSION WPF(2,5),ALSEG(2,5),          DEPTH(2),BSLOPE(2),ALNOM(2)
3      PI=3.1415926535
C***READ A TITLE CARD -- 80 CHARACTERS MAX
5      READ 3,TITLE
12     3      FORMAT(8A10)
12     PRINT 16,TITLE
20     16     FORMAT(11H1,5X,8A10///)
C***READ AND ECHO THE BREAKWATER GEOMETRY
20     2      READ 5,YCG,XCAB(1),YCAB(1),XCAB(2),YCAB(2)
C YCG=Y COORDINATE OF CG RELATIVE TO WATER SURFACE
42     5      FORMAT(5F10.0)
42     OUTPUT,YCG,XCAB(1),YCAB(1),XCAB(2),YCAB(2)
C XCAB(I)=X COORD OF CABLE I ATTACHMENT RELATIVE TO CG
C YCAB(I)=Y COORD OF CABLE I ATTACHMENT RELATIVE TO WATER SURFACE
C NOTE--CABLE NUMBER 1 IS THE CABLE WITH ITS ANCHOR IN THE +X DIRECTION
C***INPUT THE NUMBER OF DESIRED CONDITION CARDS MAX NUMBER=9
72     READ 10,NCOND
100    10     FORMAT(I2)
C***READ AND ECHO DESIRED CONDITIONS
100    DO 17 ICOND=1,NCOND
102     READ 15,FEXT(ICOND),SEP(ICOND),TENS1(ICOND),TENS2(ICOND)
121    15     FORMAT(4F10.0)
121    17     OUTPUT, FEXT(ICOND),SEP(ICOND),TENS1(ICOND),TENS2(ICOND)
C FEXT=EXTERNALLY APPLIED FORCE (HORIZONTAL DIRECTION) LB.
C SEP =ANCHOR SEPERATION IN THE X DIRECTION FT.
C TENS1=TENSION IN CABLE 1 LB.
C TENS2=TENSION IN CABLE 2 LB.
C INPUT SEP, OR TENS1 OR TENS2 OR BOTH TENS1 AND TENS2
C***READ AND ECHO TIDE CONDITIONS
C NTIDE=NUMBER OF TIDE CONDITIONS MAX=5
C TIDE=TIDE POSITION RELATIVE TO NOMINAL DEPTH MEASUREMENTS FT.
151    READ 20, NTIDE,(TIDE(I),I=1,NTIDE)
166    20     FORMAT(11,9X,5F10.0)

```

Table B-3. Listing of program BRKMOOR.



PUNT VERSION FEB 74 B 13:04 04/09/76

```

166      OUTPUT,NTIDE,TIDE
C LOOP THROUGH THE TWO CABLES
201      DO 65 I=1,2
C***INPUT THE CABLE PROPERTIES AND BOTTOM DEPTH AND SLOPE
203      READ 22,NSEG(I),DEPTH(I),BSLOPE(I)
217      22 FORMAT(I2,8X,2F10.0)
C NSEG= NUMBER OF CABLE SEGMENTS OR MATERIALS
C DEPTH= DEPTH OF THE WATER AT THE ANCHOR FT.
C BSLOPE= SLOPE OF THE BOTTOM (FT RISE/FT)
217      PRINT 25
223      25 FORMAT(///5X,*I NUMBER SECTIONS SEGMENT LENGTH WT PER FOOT*
2 4X* MATERIAL DIAMETER*/I
223      NS=NSSEG(I)
226      DO 30 J=1,NS
C***FOR EACH CABLE SEGMENT INPUT
C NSECT(I)= NUMBER OF SECTIONS INTO WHICH CABLE SEGMENT I IS DIVIDED
C ALSEG(I)=LENGTH OF CABLE SEGMENT I FT.
C WPF(I)= WEIGHT PER FOOT IN WATER OF CABLE SEGMENT J LB/FT
C MATL= MATERIAL OF CABLE SEGMENT EITHER NYLON OR CHAIN
C MUST BE LEFT JUSTIFIED IN DATA FIELD
C DIAM=DIAMETER OF ROPE OR CHAIN LINK INCHES
230      READ 40,NSECT(I,J),ALSEG(I,J),WPF(I,J),MATL(I,J),DIAM(I,J)
264      40 FORMAT(I5,5X,2F10.0,A10,F10.0)
264      30 PRINT 50,J,NSECT(I,J),ALSEG(I,J),WPF(I,J),MATL(I,J),DIAM(I,J)
326      50 FORMAT(X,I5,8X,I5,8X,F10.2,4X,F10.2,9X,A10, 5X,F6.3)
C***FIND THE NOMINAL LENGTH OF THE CABLE, LENGTH AND WEIGHT OF SECTIONS
326      ALNOM(I)=0.
331      DO 60 J=1,NS
332      ALNOM(I)=ALNOM(I)+ALSEG(I,J)
343      ALSECT(I,J)=ALSEG(I,J)/NSECT(I,J)
357      60 WSECT(I,J)=WPF(I,J)*ALSECT(I,J)
375      65 CONTINUE
377      BSLOPE(2)=-BSLOPE(2)
C***LOOP THROUGH THE TIDE POSITIONS
403      DO 400 ITIDE=1,NTIDE
C***LOOP THROUGH THE CABLES
405      DO 150 I=1,2
406      PRINT 70
411      70 FORMAT(1H1,5X*NOTE--IN THE FOLLOWING TABLES X AND Y ARE MEASURED
2RELATIVE TO THE CABLE ATTACHMENT*/I)
C D=Y DIRECTION SEPARATION BETWEEN ANCHOR AND ATTACHMENT
411      D=DEPTH(I)+TIDE(ITIDE)+YCAB(I)
C***COMPUTE INITIAL ANGLES TO BE USED
C NANGLE=NUMBER OF ANGLES USED MAX=20
421      NANGLE=15
423      PHIMIN=ASIN(D/ALNOM(I))
431      DELPHI=(PI/2.-PHIMIN)/FLOAT(NANGLE+1)
443      PHIONE=-PI/2.
C***COMPUTE A FIRST GUESS FOR THE INITIAL TENSION FOR STEEPEST ANGLE
444      ALSUM=0.
445      TZERD=0.
446      DAF=D+(ALNOM(I)-D)*BSLOPE(I)
456      NS=NSEG(I)
461      DO 90 J=1,NS
463      NSS=NSECT(I,J)
470      DO 90 K=1,NSS

```

Table B-3. Continued

AD-A032 183

WASHINGTON UNIV SEATTLE OCEAN ENGINEERING RESEARCH LAB F/G 13/2  
FLOATING BREAKWATER FIELD ASSESSMENT PROGRAM, FRIDAY HARBOR, WA--ETC(U)  
SEP 76 B H ADEE, E P RICHEY, D R CHRISTENSEN DACW72-74-C-0012  
CERC-TP-76-17 NL

UNCLASSIFIED

2 OF 3  
AD  
A032183





RUNT VERSION FEB 74 B 13:04 04/09/76

```

471      ALSUM=ALSUM+ALSECT(I,J)
477      IF(ALSUM.GT.DAF) GO TO 95
502      90  TZERO=TZERO+WSECT(I,J)
515      95  CONTINUE
C  COMPUTE THE NOMINAL AND PERTURBED DEPTHS
515      DREF=D
517      DELD=DREF/100.
521      DPLUS=DREF+DELD
522      DMINUS=DREF-DELD
C***LOOP THROUGH THE INITIAL ANGLES
524      DO 100 K=1,NANGLE
525      PRINT 97,I,K,NANGLE,TIDE(ITIDE)
541      C7  FORMAT(/X*CABLE NUMBER *I1*  INITIAL ANGLE NO. *I2*  OF *I2
2 *  TIDE = *F5.2/)
541      PHIONE=PHIONE+DELPHI
C***LOOP THROUGH THE NOMINAL DEPTH AND PERTURBED DEPTHS
543      DO 100 J=1,3
545      IPRINT=0
C*****TO SKIP THE PRINTING OF EACH CATINAPY - INSERT A GO TO 1111
546      IF(J.EQ. 1) IPRINT=1
551      1111 IF(J.EQ. 1) D=DREF
555      IF(J.EQ. 2) D=DPLUS
561      IF(J.EQ. 3) D=DMINUS
565      WY(I,J)=YCAB(I)-D
575      OUTPUT,J,K,D,YCAB(I),WY(I,J),PHIONE
627      CALL LINE2(I,PHIONE,TZERO,C,BSLOPE(I),X,Y,FORCEX,FORCEY,IPRINT)
642      EX(I,J,K)=XCAB(I)-X*(-1)**I
660      FX(I,J,K)=FORCEX*(-1)**I
674      FY(I,J,K)=FORCEY
703      TENS(I,J,K)=TZERO
C  WY(I,J)=Y COORD OF THE ANCHOR TO NO. 1 CABLE--WATER SURFACE=ORIGIN
C  EX(I,J,K)=X COORD OF ANCHOR RELATIVE TO CG OF BREAKWATER
C  TENS=TENSION AT ATTACHMENT
C  FX=FORCE AT ATTACHMENT IN X DIRECTION
C  FY=FORCE AT ATTACHMENT IN Y DIRECTION
712      100 CONTINUE
C  END OF CABLE LOOP
716      150 CONTINUE
720      PRINT 102
724      102  FORMAT(1H1,5X*IN THE FOLLOWING TABLES - X REL. TO CG, Y REL. TO WA
2TER SURFACE*/)
724      DO 160 I=1,2
726      PRINT 103,TITLE
733      103  FORMAT( 5X,8A10 )
733      PRINT 105,I,TIDE(ITIDE)
744      105  FORMAT(///5X*MOORING LINE NUMBER= *I1,*  TIDE=*F6.3//
2 10X,*Y*14X,1HX,8X,*TOP TENSION*7X*FORCEX*7X*FORCEY*/)
744      DO 120 J=1,3
746      DO 120 K=1,NANGLE
747      PRINT 110,WY(I,J),EX(I,J,K),TENS(I,J,K),FX(I,J,K),FY(I,J,K)
1013      110  FORMAT(5X,5(F11.3,4X))
1013      120 CONTINUE
1020      PRINT 125
1023      125  FORMAT(1H1)
1023      160 CONTINUE
1025      CALL EQULTB

```

Table B-3. Continued

RUNT VERSION FEB 74 B 13:04 04/09/76

	C	END OF TIDE LOOP
1026	400	CONTINUE
1031		STOP
1033		END

Table B-3. Continued



```

15      SUBROUTINE LINE2(K,PHIONE,TZERO,DEPTH,BSLOPE,X,Y,FORCEX,FORCEY,IP)
      COMMON/ONE/NSEG(12),NSECT(2,5),WSECT(2,5), MATL(2,5),DIAM(2,5),
      2 ALSECT(2,5)
      C**THE INPUT TO SUBROUTINE LINE
      C PHIONE=INITIAL ANGLE OF CABLE
      C TZERO=INITIAL GUESS OF TENSION AT TOP OF CABLE
      C**SUBROUTINE LINE COMPUTES
      C TZERO= TENSION AT CABLE TOP
      C FORCEX=FORCE IN X DIRECTION AT CABLE TOP
      C FORCEY=FORCE IN Y DIRECTION AT CABLE TOP
      C X=HORIZONTAL SEPERATION BETWEEN TOP AND BOTTOM OF CABLE
      C Y=VERTICAL SEPERATION BETWEEN TOP AND BOTTOM OF CABLE
      C**GO DOWN THE CABLE SECTION BY SECTION COMPUTE TENSION,ANGLE,
      C EXTENDED LENGTH,X AND Y COORDINATES
15      PI=3.14159
16      NITER=0
17      MNITER=25
21      NOTE=0
22      T=TZERO
23      152 NITER=NITER+1
25      IF(IP .EQ. 0) GO TO 153
27      IF(NOTE .EQ. 0) GO TO 153
31      PRINT 155
35      155 FORMAT(/5X*I      J      X      Y      TENSION      LSECT*
      2 6X,*LEXT PHI-DEGREES  FORCEY  FORCEX*/)
35      153 Y=0.
37      X=0.
43      PHI=PHIONE
44      NSS=NSEG(K)
47      158 DO 200 I=1,NSS
51      NS=NSECT(K,I)
56      DO 200 J=1,NS
57      PHIO=PHI+180./PI
61      IF(MATL(K,I) .EQ. 5HNYLON )GO TO 165
67      IF(MATL(K,I) .EQ. 5HCHAIN )GO TO 160
75      160 CALL CHAIN(DIAM(K,I),T,STRAIN)
105      GO TO 170
111      165 CALL NYLON(DIAM(K,I),T,STRAIN)
121      170 ALEXT=ALSECT(K,I)*(1.+STRAIN)
134      X=X+ALEXT*COS(PHI)
145      Y=Y+ALEXT*SIN(PHI)
152      TCOS=T*COS(PHI)
156      TSIN=T*SIN(PHI)
162      IF(IP .EQ. 0) GO TO 185
170      IF(NOTE .EQ. 0) GO TO 185
172      PRINT 180,I,J,X,Y,T,ALSECT(K,I),ALEXT,PHIO,TSIN,TCOS
231      180 FORMAT(X,2I5,8F10.3)
231      185 IF(I .EQ. NSS .AND. J .EQ. NS) GO TO 200
247      SLOPE=(TSIN+WSECT(K,I))/TCOS
257      IF(SLOPE .GE. BSLOPE) SLOPE=BSLOPE
262      PHI=ATAN(SLOPE)
266      T=TCOS/COS(PHI)
271      200 CONTINUE
302      FORCEX=TZERO*COS(PHIONE)
311      FORCEY=TZERO*SIN(PHIONE)

```

Table B-3. Continued

RUNT VERSION FEB 74 B 13:04 04/09/76

```

320      OUTPUT,NITER,Y,X,TZERO
      C***THE SECOND GUESS OF INITIAL TENSION IS COMPUTED
350      IF(NITER .GT. 1) GO TO 220
353      TZOLD=TZERO
354      TZERO=TZERO*ABS(DEPTH/Y)
365      YOLD=Y
367      T=TZERO
370      GO TO 152
      C***THE SURSEQUENT INITIAL TENSIONS ARE COMPUTED USING SECANT ITERATIO
370      220      RELER=ABS(1.+Y/DEPTH)
402      IF(NOTE .EQ. 1) GO TO 300
405      IF(NITER .GE. MNITER .OR. RELER .LE. .0001 ) NOTE=1
424      DEROLD=DEPTH*YOLD
426      DERR=DEPTH*Y
430      T=TZOLD-DEROLD*(TZERO-TZOLD)/(DERR-DFROLD)
437      IF(T .LE. 0.) T=TZERO/2.
443      YOLD=Y
445      TZOLD=TZERO
446      TZERO=T
447      GO TO 152
447      300      RETURN
450      END

```

JNT VERSION FEB 74 B 13:04 04/09/76

```

      SUBROUTINE CHAIN(D,T,STRAIN)
6      PI=3.14159
7      E=30.E6
11     AREA=D*D*PI/2.
      C C=ELONGATION FACTOR -- C=6 FOR OVAL CHAIN
14     C=6.
15     STRAIN=C*T/(AREA*E)
21     RETURN
22     END

```

UNT VERSION FEB 74 B 13:04 04/09/76

```

      SUBROUTINE NYLON(D,T,STRAIN)
6      X=T/(D*D)
10     A=.02052
12     B=.2237
13     STRAIN=A*X**B
20     RETURN
21     END

```

Table B-3. Continued



```

      SUBROUTINE EQUILB
      COMMON/TWO/XY(2,3),EX(2,3,20),FX(2,3,20),FY(2,3,20),TENS(2,3,20),
2      FEXT(9),SEP(9),TENS1(9),TENS2(9),NANGLE,NCOND,TITLE(8)
      COMMON/THREE/X(2),F(2)
      DIMENSION SEPDI(3),FO(3)
      C****EQUILB FINDS THE BREAKWATER EQUILIBRIUM POSITTON
      C***LOOP THROUGHT THE TEST CONDITIONS
      DO 100 IC=1,NCOND
4      IF(SEP(IC) .NE. 0.) GO TO 20
7      IF(TENS1(IC) .NE.0.)GO TO 10
13     IF(TENS2(IC) .NE.0.)GO TO 12
17     PRINT 155
23     155 FORMAT(/X*NO INITIAL CONDITIONS SPECIFIED*)
23     GO TO 100
      C***FOR THE CASES WHERE INITIAL TENSION IS GIVEN THE FOLLOWING IS USED
24     10 T=TENS1(IC)
27     I=1
31     J=2
32     GO TO 14
33     12 T=TENS2(IC)
36     I=2
40     J=1
41     14 OUTPUT,I,NANGLE,T
57     IF(T .GE. TENS(I,1,1)) GO TO 18
70     PRINT 16
74     GO TO 100
75     18 IF(T .GE. TENS(I,1,NANGLE)) PRINT 17
111    16 FORMAT(/5X*GIVEN TENSION CLOSE TO OP LESS THAN WEIGHT OF VERTICAL
      2 MOORING LINE*/5X*NO FURTHER EVALUATION ATTEMPTED *//)
111    17 FORMAT(/5X*GIVEN TENSION TOO GREAT FOR EVALUATION WITHOUT*
      2 *EXTRAPOLATION*/5X*USE RESULTS WITH CAUTION*//)
111    CALL LTERPS (I,1,NANGLE,TENS,EX,T,X(I),DUMMY)
123    OUTPUT,X(I),T
137    CALL LTERPS (I,1,NANGLE,TENS,FX,T,F(I),DUMMY)
151    OUTPUT,F(I)
162    IF(I .EQ. 1 .AND. TENS2(IC) .NE. 0) GO TO 12
177    IF(TENS1(IC) .NE. 0 .AND. TENS2(IC) .NE. 0) GO TO 40
214    F(J)=-F(I)-FEXT(IC)
224    OUTPUT,F(J)
234    CALL LTERPS (J,1,NANGLE,FX,EX,F(J),X(J),DUMMY)
250    OUTPUT,X(J)
      C NOTE-- F(I)=X DIRECTION FORCE ON CABLE I , X(I)=X COORD OF ANCHOR
261    GO TO 40
      C***FOR THE CASE WHERE ANCHOR SEPERATION IS GIVEN
      C MAKE A FIRST AND SECOND GUESS AT FORCE
262    20 IA=(NANGLE+1)/2
270    EPS=SEP(IC)*.0001
274    DO 30 II=1,2
275    X(1)=EX(1,1,IA)
305    F(1)=FX(1,1,IA)
315    OUTPUT,F(1),II,FEXT(IC),SEP(IC),IA
344    FO(II)=F(1)
351    F(2)=-F(1)-FEXT(IC)
361    OUTPUT,F(2)
371    CALL LTERPS (2,1,NANGLE,FX,EX,F(2),X(2),DUMMY)

```

Table B-3. Continued

RUNT VERSION FEB 74 B 13:04 04/09/76

```

405      ASEP=X(1)-X(2)
413      SEPDIF(II)=SEP(IC)-ASEP
421      OUTPUT,II,IA,X(1),X(2),F(1),F(2),SEP(IC),ASEP,SEPDIF(II)
466      IF(ABS(SEPDIF(II)) .GT. EPS) GO TO 24
476      GO TO 40
477      24  IF(SEPDIF(II) .GE. 0.) GO TO 26
503      IA=1
505      GO TO 30
505      26  IA=NANGLE
507      30  CONTINUE
C***USE SECANT INTERPOLATION FOR THE SUBSEQUENT FORCE TRIALS
511      MN=20
513      DO 34 K=1,MN
514      FO(3)=FO(1)-SEPDIF(1)*(FO(2)-FO(1))/(SEPDIF(2)-SEPDIF(1))
540      IF(FO(3) .LE. 0.) FO(3)=FO(2)/2.
552      F(1)=FO(3)
557      F(2)=-F(1)-FEXT(IC)
567      DO 32 I=1,2
570      32  CALL LTERPS (I,1,NANGLE,FX,EX,F(I),X(I),DUMMY)
605      ASEP=X(1)-X(2)
613      SEPDIF(3)=SEP(IC)-ASEP
621      OUTPUT,K,X(1),X(2),F(1),F(2),ASEP,SEPDIF(3)
657      IF(ABS(SEPDIF(3)) .LE. EPS) GO TO 3P
667      IF(K .EQ. MN) GO TO 36
672      FO(1)=FO(2)
677      FO(2)=FO(3)
704      SEPDIF(1)=SEPDIF(2)
711      SEPDIF(2)=SEPDIF(3)
716      34  CONTINUE
720      36  PRINT 37
724      37  FORMAT(/5X*MAX NUMBER OF ITERATIONS REACHED*/)
724      38  DO 39 I=1,2
726      IF(ABS(F(I)) .GT. ABS(FX(I,1,NANGLE))) PRINT 42
750      39  IF(ABS(F(I)) .LT. ABS(FX(I,1,1))) PRINT 43
775      42  FORMAT(/5X*ANCHOR SEPERATION TOO GREAT FOR EVALUATION WITHOUT EXT
2RAPOLATING--USE RESULTS WITH CAUTION*/)
775      43  FORMAT(/5X*ANCHOR SEPERATION TOO LITTLE FOR EVALUATION WITHOUT EX
2TRAPOLATION--USE RESULTS WITH CAUTION*/)
775      40  CALL SPPING(IC)
777      100 CONTINUE
1002      RETURN
1002      END

```

Table B-3. Continued



```

        SUBROUTINE SPRING(IC)
6      COMMON/TWO/WY(2,3),EX(2,3,20),FX(2,3,20),FY(2,3,20),TENS(2,3,20),
        2 FEXT(9),SEP(9),TENS1(9),TENS2(9),NANGLE,NCOND,TITLE(8)
6      COMMON/THREE/X(2),F(2)
6      COMMON/FOUR/YCG,XCAB(2),YCAB(2),TIDE(5),ITIDE
6      DIMENSION DFXDX(2),DFYDX(2),DFXDY(2),DFYDY(2),D(3),FXX(2,3),
        2 FYX(2,3),FV(2),DTDX(2),DTDY(2),DTR(2),T(2,3)
6      REAL KM11,KM12,KM13,KM21,KM22,KM23,KM31,KM32,KM33
C****SUBROUTINE SPRING COMPUTES THE BREAKWATER SPRING CONSTANTS
C***COMPUTE THE SPRING CONSTANTS FOR EACH CABLE
C HORIZONTAL FORCE AT EQUILIBRIUM=F(I) FOR CABLE I
C VERT FORCE AT EQUILIBRIUM=FV(I) FOR CABLE I
6      DO 14 I=1,2
7      DO 12 J=1,3
10     CALL LTERPS (I,J,NANGLE,EX,FX,X(I),FXX(I,J),DF)
27     IF(J.EQ. 1) DFXDX(I)=DF
35     CALL LTERPS (I,J,NANGLE,EX,TENS,X(I),T(I,J),DT)
54     IF(J.EQ. 1) DTDX(I)=DT
62     12 CALL LTERPS (I,J,NANGLE,EX,FY,X(I),FYX(I,J),D(J))
107    DTDY(I)=(T(I,3)-T(I,2))/(WY(I,2)-WY(I,3))
133    DFYDX(I)=D(1)
140    FV(I)=FYX(I,1)
147    DFYDY(I)=(FYX(I,2)-FYX(I,3))/(WY(I,2)-WY(I,3))*(-1.)
174    DFXDY(I)=(FXX(I,2)-FXX(I,3))/(WY(I,2)-WY(I,3))*(-1.)
221    14 CONTINUE
223    PRINT 16,TITLE
230    16 FORMAT(1H1,8A10)
230    PRINT 15,TIDE(ITIDE),FEXT(IC),SEP(IC),TENS1(IC),TENS2(IC)
261    15 FORMAT(///X*FOR THE CONDITIONS --*/
        1 5X*TIDE = *F5.2/
        2 5X*EXTERNALLY APPLIED HORIZONTAL FORCE, FEXT= *F10.3*L8.*/
        3 5X*HORIZONTAL ANCHOR SEPERATION, SEP= *F10.3*FEET*/
        4 5X*NOMINAL TENSION IN CABLE 1 =*F10.3* L8.*/
        5 5X*NOMINAL TENSION IN CABLE 2 =*F10.3* L8.*/
261    PRINT 18
265    18 FORMAT(/5X*CABLE NO.   FX*10X*FY*11X,1HX,11X*Y*9X*DFXDX*7X,
        2 *DFXDY*7X*DFYDX*7X*DFYDY*,5X,*TENSION*//)
265    DO 20 I=1,2
270    20 PRINT 25, I,F(I),FV(I),X(I),WY(I,1),DFXDX(I),DFYDX(I),DFXDY(I),
        2 DFYDY(I),T(I,1)
337    25 FORMAT(9X,I1,4(2X,F10.3),5(X,E11.3))
C***NOW CALCULATE FORCES AND SPRING CONSTANTS FOR THE BREAKWATER
C S=SWAY MOTION   +X DIRECTION FEET
C H=HEAVE MOTION  +Y DIRECTION
C R=ROLL MOTION   COUNTERCLOCKWISE RADIANS
C FS=FORCES CAUSING SWAY DUE TO THE MOORING LINES
C FH=FORCES CAUSING HEAVE DUE TO MOORING LINES
C EMR=MOMENTS CAUSING ROLL DUE TO MOORING LINES
C CHANGE YCAB TO BE DIST TO CG IN Y DIRECTION
337    YCAB(1)=YCAB(1)-YCG
345    YCAB(2)=YCAB(2)-YCG
352    FS=F(1)+F(2)
360    FH=FV(1)+FV(2)
365    EMR=FV(1)*XCAB(1)+FV(2)*XCAB(2)-F(1)*YCAB(1)-F(2)*YCAB(2)
C***CALCULATE CHANGE IN TENSIONS WITH BREAKWATER MOTIONS

```

Table B-3. Continued

```

413      DO 26 I=1,2
414      26  DTDY(I)=CTDY(I)*XCAB(I)-DTDY(I)*YCAB(I)
432      PRINT 27
435      27  FORMAT(/5X+CABLE NO.  DTDY*8X*DTDY*8X*DTDR//)
435      DO 28 I=1,2
440      28  PRINT 29,I,DTDY(I),DTDY(I),DTDR(I)
461      29  FORMAT(9X,I1,3(XE11.4))
      C  SPRING CONSTANTS SWAY DIRECTION
461      KM11=(DFXDX(1)+DFXDX(2))*(-1.)
471      KM12=(DFYDX(1)+DFYDX(2))*(-1.)
500      KM13=(DFYDX(1)*XCAB(1)+DFYDX(2)*XCAB(2)-DFXDX(1)*YCAB(1)-DFXDX(2)*
      2  YCAB(2))*(-1.)
      C  SPRING CONSTANTS HEAVE
530      KM21=(DFXDY(1)+DFXDY(2))*(-1.)
537      KM22=(DFYDY(1)+DFYDY(2))*(-1.)
546      KM23=(DFYDY(1)*XCAB(1)+DFYDY(2)*XCAB(2)
      2  -DFXDY(1)*YCAB(1)-DFXDY(2)*YCAB(2))*(-1.)
      C  SPRING CONSTANTS ROLL DIRECTION
576      KM31=(DFXDY(1)*XCAB(1)+DFXDY(2)*XCAB(2)-DFXDX(1)*YCAB(1)
      2  -DFXDX(2)*YCAB(2))*(-1.)
626      KM32=(DFYDY(1)*XCAB(1)+DFYDY(2)*XCAB(2)
      2  -DFYDX(1)*YCAB(1)-DFYDX(2)*YCAB(2))*(-1.)
656      KM33=(XCAB(1)**2+DFYDY(1)*XCAB(2)**2+DFYDY(2)
      2  +YCAB(1)**2+DFXDX(1)*YCAB(2)**2+DFXDX(2)
      3  -XCAB(1)*YCAB(2)*(DFYDX(1)+DFXDY(1))
      4  -XCAB(2)*YCAB(2)*(DFYDX(2)+DFXDY(2)))*(-1.)
756      PRINT 30,FS,FH,EHR
767      30  FORMAT(/5X+FORCES AND MOMENTS ON BREAKWATER AT EQUILIBRIUM DUE *
      2  *TO MOORING LINES*/10X*FS= *F12.4/10X*FH= *F12.4/10X*MR= *F12.4)
767      PRINT 32,KM11,KM12,KM13
1001      32  FORMAT(/5X+SPRING CONSTANTS SWAY DIRECTION*/10X*KM11 = *E12.5/
      2  10X*KM12 = *E12.5/10X*KM13 =*E12.5)
1001      PRINT 34,KM21,KM22,KM23
1013      34  FORMAT(/5X+SPRING CONSTANTS HEAVE DIRECTION*/10X*KM21 = *E12.5/
      2  10X*KM22 = *E12.5/10X*KM23 =*E12.5)
1013      PRINT 36,KM31,KM32,KM33
1025      36  FORMAT(/5X+SPRING CONSTANTS ROLL DIRECTION*/10X*KM31 = *E12.5/
      2  10X*KM32 = *E12.5/10X*KM33 =*E12.5//)
1025      PRINT 38
1031      38  FORMAT(1H1)
1031      RETURN
1032      END

```

Table B-3. Continued



RUNT VERSION FEB 74 B 13:04 04/09/76

```
13      SUBROUTINE LTERPS (I,J,N,X,Y,XX,YY,DYDX)
13      DIMENSION X(2,3,20),Y(2,3,20)
13      NMD=N-1
15      DO 10 K=1,NMD
16      L=K+1
20      IF(XX .EQ. X(I,J,L)) GO TO 30
27      IF(ABS(XX) .LT. ABS(X(I,J,L))) GO TO 20
55      10 CONTINUE
60      20 DYDX=(Y(I,J,L)-Y(I,J,K))/(X(I,J,L)-X(I,J,K))
111     YY=Y(I,J,K)+(XX-X(I,J,K))*DYDX
131     RETURN
132     30 IF(L .EQ. N) GO TO 20
134     M=L+1
136     DYDX=(Y(I,J,M)-Y(I,J,K))/(X(I,J,M)-X(I,J,K))
167     YY=Y(I,J,L)
176     RETURN
176     END
```

Table B-3. Continued

## APPENDIX C

### LINEAR HYDRODYNAMIC COEFFICIENTS

The linear theoretical model used in solving the floating break-water problem has been discussed extensively by Frank (1967). He developed the approach to solving the boundary value problem which has come to be known as the "Frank close-fit method". The reader is referred to the original reference for a complete presentation of the method.

In this approach, the classical linear boundary value problem requires that Laplace's equation be satisfied throughout the fluid domain:

$$\nabla^2 \phi(x, y, t) = 0 \quad \text{for } y < 0. \quad (C-1)$$

The free-surface boundary condition is applied on the undisturbed free surface:

$$\phi_{tt}(x, 0, t) + g\phi_y = 0 \quad \text{for } y = 0. \quad (C-2)$$

The body-surface boundary condition requires that no fluid flow through the body surface:

$$\nabla \phi(x, y, t) \cdot \vec{n} \Big|_{C_0} = \vec{V}_i(s) \cdot \vec{n}(s). \quad (C-3)$$

The bottom boundary condition for infinite depth is of the form:

$$\lim_{y \rightarrow -\infty} \phi_y(x, y, t) = 0. \quad (C-4)$$

In addition there is a radiation condition specifying that the waves travel away from the body.

Because the problem is assumed to be linear, the velocity potential may be decomposed and several boundary value problems considered. If this is done the total potential becomes:

$$\phi = \phi_1 + \phi_2 + \phi_3 + \phi_4 + \phi_5. \quad (C-5)$$

Here,

$\phi_1$  = potential representing pure sway motion in calm water,

$\phi_2$  = potential representing pure heave motion in calm water,

$\phi_3$  = potential representing pure roll motion in calm water,



$\phi_4$  = potential representing the waves diffracted by a fixed body,

$\phi_5$  = incident wave potential.

Another velocity potential may be defined:

$\phi_6$  = potential for total fixed-body problem,

so that

$$\phi_6 = \phi_4 + \phi_5.$$

Using this decomposition of the velocity potential, the boundary value problems may be expressed as:

$$\begin{aligned} \nabla^2 \phi_i(x, y, t) &= 0 \quad \text{for } y < 0, \\ \phi_{i,tt}(x, 0, t) + g\phi_{i,y} &= 0 \quad \text{for } y = 0, \\ \lim_{y \rightarrow -\infty} \phi_{i,y}(x, y, t) &= 0, \end{aligned} \tag{C-6}$$

and

$$\left. \nabla \phi_i \cdot \vec{n} \right|_{C_0} = \vec{V}_i(s) \cdot \vec{n}(s) \quad \text{for } i = 1, 2, 3$$

or

$$\left. \nabla \phi_i \cdot \vec{n} \right|_{C_0} = 0 \quad \text{for } i = 4, 6.$$

These boundary value problems are solved directly using the Frank method which distributes singularities over the hull surface. These singularities satisfy the radiation condition, Laplace's equation, the free-surface boundary condition and the bottom boundary condition. To satisfy the body boundary condition requires the formulation of a set of linear equations whose solution reveals the strength of each singularity distributed on the body.

Once the velocity potential is found the pressure may be found from Bernoulli's equation:

$$P(x, y, t) = -\rho \phi_t(x, y, t). \tag{C-7}$$

The force on the body surface is:

$$\vec{F} = \int_{C_0} P(s) \vec{n}(s) ds, \tag{C-8}$$

and the moment is:

$$M = \int_{C_0} P(s) [\vec{r} \times \vec{n}] ds. \quad (C-9)$$

The added-mass and damping coefficients are found by considering the cases  $i = 1, 2, 3$ . The forces and moments computed using these potentials may be separated into components in phase with acceleration and velocity. The component in phase with acceleration yields the added-mass coefficients and the component in phase with velocity yields the damping coefficients. Exciting forces and moments are computed when the case  $i = 6$  is considered.

Special Symbols for Appendix C.

$\vec{n}(s)$  = unit interior normal vector to the body surface

$s$  = indicates arc length along body contour

$C_0$  = body contour

$P(s)$  = pressure on body surface

$\vec{V}(s)$  = velocity of body surface

$\Phi$  = total velocity potential



## APPENDIX D

### FLOATING BREAKWATER ANALYSIS

#### 1. Purpose of the Program.

Computer program BRK2D performs a performance analysis for two-dimensional floating breakwaters of arbitrary cross section. This analysis includes predictions of the hydrodynamic coefficients, the dynamics and mooring line forces.

#### 2. Program Description.

Program BRK2D is written using both FORTRAN II and FORTRAN IV statements.

The program consists of the main program BRK2D and the subroutines COEFF, COMP, PHYSCL, POTOUT, DYNAMC, MORTEN, CPV, LNEQF.

The subroutines COEFF and COMP calculate the quantities needed to formulate the linear equations for the velocity potential. COMP calls on LNEQF to solve these linear simultaneous equations.

Subroutine PHYSCL calculates the physical quantities including added-mass and damping coefficients and surface elevations per unit amplitude of motion.

CPV is a subroutine which evaluates the Cauchy principal value integral in the Green function.

LNEQF is a packaged subroutine to solve simultaneous linear equations using the Gaussian reduction method.

#### 3. Type of Computer and Peripherals.

BRK2D was written for use on the CDC 6400 computer. It uses about 55000 words of memory. No peripherals other than the card reader, line printer and card punch are required.

#### 4. Input Data.

The first cards in the data deck are label cards for the output. These are shown in the example input in Table D-1 for the example and are not included here. Following these cards, the input for BRK2D is:

Card #1 - Title card, Format (8A10).  
80 alphanumeric characters.

Card #2 - Logical control card, Format (5I10,6I5).

N = Number of straight line segments used to fit the hull.

NW = Number of points on the free surface where wave height is to be computed.

NWAVEL = Number of wavelengths at which computations are  
 to be performed.  
 ISYM = 1 for symmetric section.  
 = Anything else for non-symmetric section.  
 ISKIP = 1 Do not solve equations of motion,  
 2 Do not solve potential problem (read in  
 coefficients from data),  
 = Anything else solve potential problem and equa-  
 tions of motion.  
 LC = Number of body segments which represent spaces be-  
 tween multiple hull configurations (1 to 5).  
 JC = Designates the segment number for segments repre-  
 senting spaces between multiple hulls.

Card #3 - Parameter card, Format (5F10.3,3A10).  
 AREA = Crosssectional area of immersed body.  
 B = Characteristic beam as specified by BTITLE.  
 D = Distance below free surface to origin of users  
 coordinate system (all motions are referred to that  
 point).  
 ROE = Fluid density.  
 GEE = Acceleration of gravity.  
 BTITLE = Specifies B.

Card #4 - Beam/wavelength specification, Format (10F8.5).  
 BOL = Beam/wavelength ratios for computation (up to 10  
 different ratios may be used).

Card #5 - Offset cards, Format (2F10.3).  
 There must be N+1 cards giving the offset points. In the  
 version of the program used here, N must be less than or  
 equal to 23 because of dimension statements.  
 R(1,I) = X-coordinate of offset point.  
 R(2,I) = Y-coordinate of offset point.

Card #6 - Hydrostatic spring constants, Format (9F8.3).  
 This is read in subroutine DYNAMC.  
 RKHYD (1,1) =  $KH_{11}$ .  
 RKHYD (1,2) =  $KH_{12}$ .  
 RKHYD (1,3) =  $KH_{13}$ .  
 RKHYD (2,1) =  $KH_{21}$ .  
 RKHYD (2,2) =  $KH_{22}$ .  
 RKHYD (2,3) =  $KH_{23}$ .  
 RKHYD (3,1) =  $KH_{31}$ .  
 RKHYD (3,2) =  $KH_{32}$ .  
 RKHYD (3,3) =  $KH_{33}$ .

Card #7 - Physical properties, Format (6F10.3,3F5.2,I5).  
 This is read in subroutine DYNAMC.  
 AREA = Crosssectional area.  
 B = Characteristic beam.  
 XG = X-coordinate of the center of gravity.  
 YG = Y-coordinate of the center of gravity.  
 RMASS = Mass per unit length of breakwater.  
 RINERT = Mass moment of inertia per unit length of  
 breakwater.



DAMP(1) = Added damping in sway. In the equations of motion sway damping will be  $1 + \text{DAMP}(1)$  times the computed hydrodynamic damping.

DAMP(2) = Added damping in heave.

DAMP(3) = Added damping in roll.

NPUNCH = 0, punch data cards containing computed transmission coefficient, motion response and mooring-force coefficient.

= Anything else, do not punch data cards.

Card #8 - Mooring spring constants, Format (9F8.3).

This is read in subroutine DYNAMC.

RKMOR(1,1) =  $KM_{11}$ .

RKMOR(1,2) =  $KM_{12}$ .

RKMOR(1,3) =  $KM_{13}$ .

RKMOR(2,1) =  $KM_{21}$ .

RKMOR(2,2) =  $KM_{22}$ .

RKMOR(2,3) =  $KM_{23}$ .

RKMOR(3,1) =  $KM_{31}$ .

RKMOR(3,2) =  $KM_{32}$ .

RKMOR(3,3) =  $KM_{33}$ .

Card #9 - Mooring-line response parameters, Format (6F10.2).

This card is read in subroutine MORTEN.

DELT(1,1) =  $\Delta F / \Delta \alpha_1$  for shoreward mooring line. This is the change in mooring line force per unit displacement in sway.

DELT(1,2) =  $\Delta F / \Delta \alpha_2$  for shoreward mooring line.

DELT(1,3) =  $\Delta F / \Delta \alpha_3$  for seaward mooring line.

DELT(2,1) =  $\Delta F / \Delta \alpha_1$  for seaward mooring line.

DELT(2,2) =  $\Delta F / \Delta \alpha_2$  for seaward mooring line.

DELT(2,3) =  $\Delta F / \Delta \alpha_3$  for seaward mooring line.

Note: The last 3 cards (#7, #8, and #9) provide the information needed for the dynamic analysis. If it is desirable to perform calculations varying the data, these cards may be repeated with different input data. There is a limit of 25 different sets of data. In the example data shown in Table D-1, there are 3 different conditions used.

## 5. Mathematical Procedures and Program Limitations.

The mathematics has been described in the report and Appendix C.

The main limitations are that at most 23 offset points may be used to describe the shape. This has been found to be very adequate for the configurations considered thus far. Little change in the results occurs when more than 15 points are used. Computer time increases about as the square of the number of points.

A listing of the program is given in Table D-2.

## 6. Flow Chart.

A flow chart is given in a figure of this appendix.

MU11/QM	MU12/QM
MU13/(QM*B)	MU21/QM
MU22/QM	MU23/(QM*B)
MU31/(QM*B)	MU32/(QM*B)
MU33/(QM*B*B)	LAMBDA12/QD
LAMBDA11/QD	LAMBDA21/QD
LAMBDA13/(QD*B)	LAMBDA23/(QD*B)
LAMBDA22/QD	LAMBDA32/(QD*B)
LAMBDA31/(QD*B)	
LAMBDA33/(QD*B*B)	
FX/QF	FY/QF
MZ/(QF*B)	
GEN BY SWAY/SWAY	GEN BY HEAVE/HEAVE
GEN BY ROLL/ROLL(RAD)*B	REFLECTED BY FXD BDY/ETA
INCIDENT/ETA	REFLECTED + INCIDENT/ETA
TRANS BY FXD BDY/ETA	
BEAM/WAVELENGTH	DIMENSIONAL FREQUENCY - 47
ADDED MASS QM = AREA*PDE	DAMPING QD = AREA*PTE*W
WAVE FORCES QF=AREA*PDE*ETA+W2PHASE REL TO ETA AT X=0 - DEG	
PHASE REL TO BODY MOTION - DEGWAVE FIELD - AMPLITUDE RATIO	
POSITION - X/WAVELENGTH	DIMENSIONAL POSITION - X
SWAY AMPLITUDE/ETA	HEAVE AMPLITUDE/ETA
ROLL AMPLITUDE(RAD)*B/ETA	
GEN BY RESULTANT SWAY/ETA	GEN BY RESULTANT HEAVE/ETA
GEN BY RESULTANT ROLL/ETA	TOTAL TRANSMITTED/ETA
TOTAL REFLECTED/ETA	
MOTION RESPONSE	
OAK HARBOR BREAKWATER - CORPS OF ENGINEERS TESTS	
23 0 10 0 0 1 12	17 MAY 1975
12.6 10.0 0.0 1.9905 32.2 FULL BEAM	
.1 .154290 .180 .216311 .250 .280 .312298 .371 .429 .487825	
-5.0 0.0	
-5.0 -1.25	
-5.0 -2.50	
-5.0 -3.75	
-5.0 -5.00	
-4.583 -5.00	
-4.583 -3.75	
-3.223 -3.75	
-3.223 -2.50	
-3.223 -1.25	
-4.583 -1.25	
-4.583 0.00	
4.583 0.00	
4.583 -1.25	
3.223 -1.25	
3.223 -2.50	
3.223 -3.75	
4.583 -3.75	
4.583 -5.00	
5.0 -5.00	
5.0 -3.75	
5.0 -2.50	
5.0 -1.25	
5.0 0.0	
0.0 0.0 0.0 0.0 64.5 0.0 0.0 0.0 1165.	
12.6 10.0 0.0 0.0 -2.34 25.1 621. 0. 0. 0. 1	
0. 0. 0. 0. 0. 0. 7. 0. 0. 0. 0.	
12.6 10.0 0.0 0.0 -2.34 25.1 621. 0. 0. 0. 0.	
116.8 -5.24 166.2 -5.732 10.21 -3.372 159.9 2.763 281.9	
-1376. 410.6 -1607. 1172. 280.9 1713.	
12.6 10.0 0.0 -2.34 25.1 621. 1. 1. 1.	
116.8 -5.24 166.2 -5.732 10.21 -3.372 159.9 2.063 281.9	
-1376. 410.6 -1607. 1172. 280.9 1713.	

Table D-1. Example input for program BRK2D (Oak Harbor breakwater).



BRK2DHU //

RUNT VERSION FEB 74 B 17:12 04/23/76

```

      PROGRAM BRK2D (INPUT,OUTPUT,PUNCH,TAPE5=INPUT,TAPE6=OUTPUT)
C***LATEST REVISION ***** 27 AUGUST 1975
C***PROGRAM BRK2D COMPUTES THE FIRST-ORDER RESPONSE OF AN OSCILLATING
C   CYLINDER ON OR NEAR THE FREE SURFACE OF AN IDEAL FLUID OF
C   INFINITE DEPTH
3     COMMON RI12(25,25),RK56(25,25),POT(25,25),H0W(25,25),FF(25,4),
      IFI(25,6),RI(25,25),RJ(25,25),RK(25,4),RL(25,4),
      ZRMU(3,3,10),RLAM(3,3,10),FB(3,10),DELF(3,10),HWR(25,6,10),
      DELW(25,6,10),XDL(25,10)
3     COMMON/ONE/X(25),Y(25),XA(25),YB(25),ANG(25),DEL(25),VV(25)
      1,FEIN(25),FTIN(25),RNDRM(25,3),JC(5)
3     COMMON/TWO/CC3(25),SS3(25)
3     COMMON /THREE/ N,NNW, NWAVEL, ISYM, ISKTP, NC, PIE,GAMMA,M,TK,TP
3     COMMON/THREE/ WAVEL(10),WN(10),R7L(17),TL
3     COMMON/SIX/XN(5),CN(5)
3     COMMON /SEVEN/ AREA, R, D, RDE, GEE, RTITLE(3), TITLE(4)
3     COMMON / EIGHT/ LBLMU(3,3,3), LBLAM(3,3,3), LBLFB(3,3,3), LBLHWR(7,3),
      LBL(10,3), DEG(3,10)
3     COMMON /NINE/ LBLRAR(3,3), LBLHWR(5,3), LRLR(5,3)
3     COMMON/TEN/DELT(2,3),FDR(2,10),PHAS(2,10),FDRND(2,10),PHASD(2,10)
3     REAL K
3     DATA XN/.263560319718,1.413403059107,3.59442577104/,
      1 7.095810005859,12.640800844276/
3     DATA CN/.521755610553,.398666811083,.0759424496417,
      1 .00361175467992,.00002336997739/
3     PIE=ATAN2(0.,-2.)
7     TP=2.*PIE
10    GAMMA=0.57721566
C***BEGIN READING INPUT DATA AND PRINTING EACH CHECK
12    3000 FORMAT (6A10)
C*****READ TABLES FOR PRINT OUT
12    READ 3000, ((LBLMU(I,J,L), L = 1,3), J = 1,3), I = 1,3)
36    READ 3000, ((LBLAM(I,J,L), L = 1,3), J = 1,3), I = 1,3)
63    READ 3000, ((LBLFB(J,L), L = 1,3), J = 1,3)
103   READ 3000, ((LBLHWR(J,L), L = 1,3), J = 1,7)
123   READ 3000, ((LBL(J,L), L = 1,3), J = 1,10)
143   READ 3000, ((LBLRAR(J,L), L = 1,3), J = 1,3)
163   READ 3000, ((LRLHWR(J,L), L = 1,3), J = 1,5)
203   READ 3000, (LRLR(1,L), L = 1,3)
220   READ 20, TITLE
226   20 FORMAT (8A10)
226   PRINT 30, TITLE
234   30 FORMAT (14I, 9A10//)
234   READ 50, N, NW, NWAVEL, ISYM, ISKTP, LC, JC
256   50 FORMAT (5I10, 6I5)
C     N = NUMBER OF STRAIGHT LINE SEGMENTS TO BE USED TO FIT
C     THE HULL.....NOTE. THERE MUST BE N+1 OFFSET POINTS
C     NW = NUMBER OF POINTS ON FREE SURFACE WHERE WAVE HEIGHT IS
C     TO BE COMPUTED. THIS IS IN ADDITION TO THE COMPUTATION OF
C     WAVE HEIGHT 4.0 WAVELENGTHS ON EITHER SIDE OF THE BODY
C     WHICH IS PERFORMED AUTOMATICALLY
C     NWAVEL = NUMBER OF WAVELENGTHS AT WHICH COMPUTATIONS ARE TO
C     BE PERFORMED
C     ISYM = 1 FOR SYMMETRIC SECTION
C           = ANYTHING ELSE FOR NON-SYMMETRIC SECTION

```

Table D-2. Listing of program BRK2D

RUNT VERSION FEB 74 B 17:12 04/23/76

```

C      ISKIP = 1 DO NOT SOLVE EQUATIONS OF MOTION
C      = 2 DO NOT SOLVE POTENTIAL PROBLEM (READ IN COEFFS)
C      = ANYTHING ELSE SOLVE FOR COEFFICIENTS AND DYNAMICA
C      NUMBER OF BODY SEGMENTS WHICH REPRESENT FREE SURFACE BETWEEN
C      CATAMARAN HULLS. SEGMENT NUMBERS SPECIFIED BY JC15
254      NAW = NW + 2
260      NC = N - LC
262      NW1 = 25 - N - 2
264      IF (NW .LT. 0) NW = 0
267      IF (NW .GT. NW1) NW = NW1
273      PRINT 60, N, NW, NAWEL, ISYM, ISKIP, LC, JC
315      60 FORMAT (1JX*NUMBER OF SEGMENTS =*, I4//
1          1 10X*NUMBER OF FREE-SURFACE STATIONS =*, I4//
2          2 10X*NUMBER OF WAVELENGTHS =*, I4//
3          3 10X*ISYM =*, I4// 10X*ISKIP =*, I4//
4          4 10X*NC = *, I5, *, JC = *, I5 //)
315      READ 70, AREA, B, D, ROE, GEE, (BTITLE(I), I = 1,3)
342      70 FORMAT (5F10.3, 3A10)
C      AREA = CROSSSECTIONAL AREA OF IMMERSED BODY
C      B = CHARACTERISTIC LENGTH AS SPECIFIED BY BTITLE
C      D = DISTANCE BENEATH SURFACE OF ORIGIN OF USER'S COORDINATE
C      SYSTEM (+). ALL MOTIONS REFERRED TO THAT POINT AND BODY
C      SHAPE SPECIFIED IN THAT SYSTEM
C      ROE = FLUID DENSITY
C      GEE = ACCELERATION OF GRAVITY
342      PRINT 80, AREA, B, (BTITLE(I), I = 1,3), D, ROE, GEE
367      80 FORMAT(10X*AREA = *, F10.3 //, 10X*B = *F10.3, 5X, 3A10
2          2 //10X*D = * F10.3 // 10X*FLUID DENSITY = * F10.5//
3          3 10X*ACCELERATION OF GRAVITY =*, F10.3//)
367      IF (ISKIP .EQ. 2) GO TO 303
372      READ 100, (BOL(I), I = 1, NAWEL)
406      100 FORMAT (10F8.5)
C      BOL = BEAM/WAVELENGTH RATIO FOR COMPUTATIONS
406      DO 600 I = 1, NAWEL
410      600 WAVELENGTH(I) = B/BOL(I)
C      WAVELENGTH(I) = DIMENSIONAL WAVELENGTH OF INCIDENT WAVES
417      PRINT 110, (BOL(I), I = 1, NAWEL)
433      110 FORMAT (10X*BEAM/WAVELENGTH RATIOS OF INCIDENT WAVES*// (23X10F11.5
1          1))
C*****INITIALIZE OUTPUT VARIABLES
433      DO 113 IL = 1,10
435      WNL(IL) = 0.0
437      BOL(IL) = 0.0
442      DO 114 I = 1,3
444      FB(I,IL) = 0.0
450      DELFB(I,IL) = 0.0
455      DO 114 J = 1,3
456      RMU(I, J, IL) = 0.0
465      PLAM(I, J, IL) = 0.0
474      114 CONTINUE
500      DO 112 I = 1, 25
501      XOL(I,IL) = 0.0
505      DO 112 J = 1,6
507      HWB(I,J,IL) = 0.0
516      DELW(I,J,IL) = 0.0
525      112 CONTINUE

```

Table D-2. Continued



RUNT VERSION FEB 74 B 17:12 04/23/76

```

531      113 CONTINUE
C****COMPUTE (R/WAVEL) AND NONDIMENSIONAL WAVE NO.
533      DO 115 IL = 1, N/WAVEL
534      BUL(IL) = R/WAVEL(IL)
541      115 WN(IL) = TP * R/WAVEL(IL)
C***READ IN OFFSETS OF CYLINDER
551      NUP = N + 1
553      NUPP = NUP + 2
555      NTOP = NUPP + NW - 1
557      N1 = N + 1 + NW
561      READ 130, (RI(1,I),RI(2,I),I=1,NUP)
603      130 FORMAT (2F10.5)
C      RI(1,I),RI(2,I) = DIMENSIONAL X, Y COORDINATE OF OFFSET
C      POINTS, RESPECTIVELY
633      IF (NW .LT. 1) GO TO 195
C***READ IN ADDITIONAL POINTS ON THE FREE SURFACE WHERE WAVE HEIGHTS
C      ARE TO BE COMPUTED. TWO STORAGE LOCATIONS MUST BE LEFT BLANK
C      FOR THE POSITION 4 WAVELENGTHS FROM THE BODY
606      READ 130, (RI(1,I),RI(2,I),I=NUPP,NTOP)
C      RI(1,I),RI(2,I) = COORDINATES OF POINTS ON FREE SURFACE WHERE
C      WAVE HEIGHT IS TO BE COMPUTED. THIS IS TRUE FOR I .GT. N + 3
C***NON-DIMENSIONALIZE OFFSETS
631      DO 180 I = NUPP,NTOP
633      X(I) = RI(1,I)/R
642      180 Y(I) = -1.0E-08
647      195 CONTINUE
547      DO 190 I = 1,NUP
651      XB(I) = RI(1,I)/R
653      190 YB(I) = RI(2,I)/R
C... COMPUTE MIDPOINT, ANGLE AND LENGTH OF STRAIGHT-LINE SEGMENTS.
C****AND COMPONENTS OF NORMAL TO BODY
671      JF = 0
672      DO 200 J=1,N
674      X(J)=0.5*(XB(J)+XB(J+1))
705      Y(J)=0.5*(YB(J)+YB(J+1))
717      T1=YB(J+1)-YB(J)
725      T2=XB(J+1)-XB(J)
732      ANG(J)=ATAN2(T1,T2)
740      CC3(J)=COS(ANG(J))
747      SS3(J)=SIN(ANG(J))
756      VV(J)=X(J)*CC3(J)+Y(J)*SS3(J)
772      DEL(J) = SQRT(T2**2 + T1**2)
1007      RNORM(J,1) = -SS3(J)
1015      RNORM(J,2) = CC3(J)
1023      RNORM(J,3) = VV(J)
1031      200 CONTINUE
1034      PRINT 30, TITLE
1041      PRINT 250
1045      250 FORMAT (6X*CYLINDER GEOMETRY*///10X*NONDIMENSIONAL OFFSETS*,
1      1 11X*NON-DIMENSIONAL OFFSETS*, 5X*MIDPOINTS OF SEGMENTS*//
2      6X*I*, 16X*Y*, 9X*Y*, 19X*X*, 9X*Y*, 19X*X*, 9X*Y*,
3      18X*SLOPE*, 4X*LENGTH*//
1045      PRINT 270, (I,RI(1,I),RI(2,I),XB(I),YB(I),Y(I),Y(I),ANG(I),
1      1 DEL(I),I=1,N)
1113      270 FORMAT (X, I6, 4(10X2F10.3))
1113      NL = N + 1

```

Table D-2. Continued

RUNT VERSION FEB 74 3 17:12 04/23/76

```

1115      PRINT 270, NL, RI(1,NL), RI(2,NL), YR(NL), YR(NL)
1143      PRINT 281
1147      281 FORMAT (//10X, *POSITIONS FOR WAVE HEIGHT CALCULATIONS*/)
1147      280 FORMAT (//)
1147      IF (NW .LT. 1) GO TO 290
1152      PRINT 271, (I,RI(1,I),RI(2,I),X(I),Y(I),T=NUPP,NTOP)
1204      271 FORMAT(X,16, 2(10X, 2F10.3))
1204      PRINT 280
1210      290 M = N + NW + 2
C*****TRANSFER TO COORDINATE SYSTEM IN FREE SURFACE
1213      DO 285 I = 1,N
1214      YR(I) = YR(I) - D/R
1222      285 Y(I) = Y(I) - D/R
1233      YR(NUP) = YR(NUP) - D/R
C COMPUTE FACTORS OF I AND K INDEPENDANT OF FREQUENCY
1242      CALL COEFF
1243      YSURF = -1.0E-08 * B
C... START FREQUENCY ITERATION.
1245      DO 301 IL = 1, NWAVEL
1247      K = WN(IL)
C ALL POTENTIALS INITIALIZED TO ZERO.
C*****FE(I,J) = NONDIMENSIONAL AMPLITUDE OF POTENTIAL AT POINT I DUE TO
C*****MODE J. (ASSOCIATED WITH COS(WT) ). FT(I,J) IS SIMILAR TO FE(I,J)
C*****BUT ASSOCIATED WITH SIN(WT). J = 1,2,3,4,5,6 IMPLY RESPECTIVELY
C*****SWAY, HEAVE, ROLL, DIREFRACTED, INCIDENT AND DIREFRACTED + INCIDENT
1252      DO 1 I=1,25
1253      DO 1 J = 1,6
1254      FE(I,J)=0.
1261      FI(I,J)=0.
1265      1 CONTINUE
C***ADD POINTS TO THE OFFSET ARRAY FOUR WAVELENGTHS FROM THE ORIGIN
C ON THE FREE SURFACE
1271      X(N+1) = 4.0 * WAVEL(IL)/B
1303      X(N+2) = -4.0 * WAVEL(IL)/B
1307      Y(N+1) = YSURF
1312      Y(N+2) = YSURF
C***COMPUTE INCIDENT WAVE POTENTIALS AND NORMAL VELOCITIES
1316      DO 402 I = 1,M
1317      DO404 IC = 1,5
1320      404 IF(I .EQ. JC(IC)) GO TO 402
1326      EY = EXP(K*Y(I))
1335      CKX = COS(K*X(I))
1344      SKX = SIN(K*X(I))
1353      IF(I .GT. N) GO TO 403
1356      FEIN(I) = EY*(SS3(I)*SKX + CC3(I)*CKX)
1370      FIIN(I) = -EY*(SS3(I)*CKX - CC3(I)*SKX)
1403      403 FE(I,5) = EY*CKX*(1./K)
1414      FI(I,5) = EY*SKX*(1./K)
1424      402 CONTINUE
1427      AK = K/B
1431      WRF = SQRT(GEE*AK)
1436      WF = WRF/TP
1440      WT = 1.0/WF
1441      PRINT 300, K, WRF, WF, WT, WAVEL(TL)
1460      300 FORMAT (//, * WAVE NUMBER = K =*, F9.5, 5X*CTRICULAR FREQUENCY =*,
1          F9.5, 5X*FREQUENCY =*, F9.5, 5X*PERIOD =*, F10.5,

```

Table D-2. Continued



RUNT VERSION FEB 74 8 17:12 04/23/76

```

      2      5X*WAVLENGTH =*, F10.4)
1460      TK=2.0/K
      C      FIRST-ORDER POTENTIALS ON CYLINDER ARE FIRST CALCULATED.
1462      CALL COMP(K)
      C... FIRST-ORDER PHYSICAL QUANTITIES ARE CALCULATED.
1464      CALL PHYSCL(K)
1466      301 CONTINUE
1471      1009 FORMAT (10F8.5)
1471      ISKIPI = 2
      C*****PUNCH RESULTS OF POTENTIAL SOLUTION ON CARDS
1472      PUNCH 20, TITLE
1500      PUNCH 50, N, NW, N*WAVEL, ISYM, ISKTP1, IC, JC
1522      PUNCH 70, AREA, H, D, ROE, GEE, BTITLE
1542      PUNCH 1009, (WN(IL), IL = 1,10), (RDL(TL), TL = 1,10)
1564      DO 310 I = 1,3
1566      PUNCH 1009, (FB(I,IL), IL = 1,10), (DFLB(T,IL), IL = 1,10)
1613      DO 310 J = 1,3
1615      310 PUNCH 1009, (RMU(I,J,IL), IL = 1,10), (RLAM(T,J,IL), IL = 1,10)
1652      DO 320 I = 1,NNW
1654      PUNCH 1009, (XOL(I,IL), IL = 1,10)
1673      DO 320 J = 1,6
1572      320 PUNCH 1009, (HWB(I,J,IL), IL = 1,10), (DFLW(I,J,IL), IL = 1,10)
1730      303 CONTINUE
1730      115 CONTINUE
1730      CALL DYNAMIC
1731      302 CONTINUE
1731      STOP
1733      END

```

Table D-2. Continued

```

SUBROUTINE DYNAMIC
2   COMMON R112(25,25),RK56(25,25),POT(25,25),HOW(25,25),FF(25,6),
1FI(25,6),RI(25,25),RJ(25,25),RK(25,4),RL(25,4),
2RMU(3,3,10),RLAM(3,3,10),FB(3,10),DELF(3,10),HWR(25,6,10),
3 DELW(25,6,10),XOL(25,10)
2   COMMON/ONE/X(25),Y(25),XB(25),YB(25),ANG(25),DEL(25),VV(25)
1,FEIN(25),FIIN(25),RNDRM(25,3),JC(5)
2   COMMON/TWO/N,NNW,NWAVEL,ISYM,ISKIP,NC,PIE,GAMMA,M,TK,TP
2   COMMON/THREE/WAVEL(10),WN(10),BOL(TL)
2   COMMON/FOUR/RAR(3,10),DELR(3,10),HWR(25,3,10),DELWR(25,3,10),
2 HWT(25,10),DELWT(25,10),RKHYD(3,3),RKMDR(3,3),RKT9(3,3),
3 XG,YG,RMASS,RINERT,DAMP(3)
2   COMMON/SEVEN/AREA,B,D,ROE,GEE,RTITLE(3),TITLE(R)
2   COMMON/TEN/DELT(2,3),FOR(2,10),PHAS(2,10),FORND(2,10),PHASD(2,10)
2   DIMENSION A(6,6),C(6),ERASE(6)
2   IF (ISKIP.NE.2) GO TO 100
C*****READ POTENTIAL COEFS IF ISKIP = 2
5   READ 1009,(WN(IL),IL = 1,10),(BOL(TL),TL = 1,10)
27  1009 FORMAT(10F8.3)
27  DO 110 I = 1,3
31  READ 1009,(FB(I,IL),IL = 1,10),(DELF(I,IL),IL = 1,10)
56  DO 110 J = 1,3
60  110 READ 1009,(RMU(I,J,IL),IL = 1,10),(RLAM(I,J,IL),IL = 1,10)
115 DO 120 I = 1,NNW
117 READ 1009,(XOL(I,IL),IL = 1,10)
133 DO 120 J = 1,6
135 120 READ 1009,(HWR(I,J,IL),IL = 1,10),(DELW(I,J,IL),IL = 1,10)
173 100 CONTINUE
C*****OUTPUT POTENTIAL COEFS
173 CALL POTOUT
174 IF (ISKIP.EQ.1) GO TO 140
C*****READ DIMENSIONAL HYDROSTATIC SPRING CONSTANTS
177 READ 1008,((RKHYD(I,J),J=1,3),I=1,3)
C*****START LOOPING THROUGH DIFFERENT DYNAMIC CONFIGURATIONS
217 DO 140 K1 = 1,50
221 READ 1010,AREA,B,XG,YG,RMASS,RINERT,DAMP(1),DAMP(2),DAMP(3),
1 NPUNCH
253 1010 FORMAT(6F10.3,3F5.2,15)
253 IF (EOF,5) 121,122
256 121 STOP
260 122 CONTINUE
262 DO 5 K2 = 1,3
5 IF (DAMP(K2).EQ.-C.O) DAMP(K2) = 0.0
C XG,YG = COORDINATES OF THE CENTER OF GRAVITY OF THE BODY
C .....NOTE. MOMENTS AND MOMENTS OF INERTIA ARE COMPUTED
C ABOUT THE CENTER OF GRAVITY
C DAMP ADDS CORRECTION FOR VISCOUS OR NONLINEAR DAMPING
C*****READ DIMENSIONAL MOORING SPRING CONSTANTS
272 READ 1008,((RKMDR(I,J),J=1,3),I=1,3)
312 1008 FORMAT(9F6.3)
C*****NONDIMENSIONALIZE SPRING CONSTANTS,MASS,MOMENT OF INERTIA
C*****AND CG COORDINATES
312 Q = AREA*ROE*GEE/R
316 DO 130 I = 1,3
317 DO 130 J = 1,3

```

Table D-2. Continued



RUNT VERSION FEB 74 8 17:12 04/23/76

```

320      IF(RKMOR(I,J) .EQ. -0.0) RKMOR(I,J) = 0.0
331      RKT8(I,J) = (RKHYD(I,J) + RKMOR(I,J))/0
346      130 IF(I.EQ. 3 .OR. J.EQ. 3) RKT8(I,J) = RKT8(I,J)/B
372      RKT8(3,3) = RKT8(3,3)/B
402      RMASB = RMAS/(AREA*POF)
406      RINERB = RINERT/(AREA*ROE*B*B)
412      XGB = XG/B
413      YGB = YG/B
C*****START WAVELENGTH LOOP
415      DO 150 IL = 1,10
416      IF (IL .GT. NWAVEL) GO TO 160
C*****SET VALUES IN NONDIMENSIONALIZED ALGEBRAIC EQUATIONS OF MOTION
421      A(1,1) = RKT8(1,1) - WN(IL) * (RMASB + RMU(1,1,IL))
445      A(2,2) = RKT8(2,2) - WN(IL) * (RMASB + RMU(2,2,IL))
471      A(3,3) = RKT8(3,3) - YGB*RMASB - WN(IL) * (RINERB + RMU(3,3,IL) +
1 (XGB**2 + YGB**2) * RMASB)
531      A(1,2) = RKT8(1,2) - WN(IL) * RMU(1,2,IL)
552      A(1,3) = RKT8(1,3) - WN(IL) * (RMU(1,3,IL) - YGB*RMASB)
576      A(2,3) = RKT8(2,3) - WN(IL) * (RMU(2,3,IL) + XGB*RMASB)
623      A(2,1) = A(1,2)
633      A(3,1) = A(1,3)
643      A(3,2) = A(2,3)
652      DO 20 I = 1,3
654      DO 10 J = 1,3
655      A(I+3, J+3) = A(I,J)
666      A(I,J+3) = RLAM(I,J,IL)*SORT(WN(IL))
C ADD CORRECTION FOR VISCOUS DAMPING
705      IF (I .EQ. J) A(I,J+3) = (1.0 + DAMP(I))*A(I,J+3)
723      10 A(I+3,J) = - A(I,J+3)
736      C(I) = FB(I,IL) * SIN(DELF8(I,IL))
753      20 C(I+3) = FB(I,IL) * COS(DELF8(I,IL))
771      SCALE = 1.
773      NN = 6
C*****SOLVE ALGEBRAIC EQS OF MOTION. B(1), B(2), B(3) = AMPLITUDES
C*****OF COS(WT), B(4), B(5), B(6) = AMPLITUDES OF SIN(WT) FOR SWAY, HEA
C*****AND ROLL AT CENTER FO USERS COORDINATE SYSTEM.
774      LL = LNEQF(6,NN,1,A,C,SCALE,ERASE)
1005      DO 30 I = 1,3
C*****AMPLITUDE AND PHASE OF RESPONSE
1006      RAR(I,IL) = SORT(C(I)**2 + C(I+3)**2)
1032      30 DELR(I,IL) = ATAN2(C(I),C(I+3))
1047      DO 40 I = 1, NNW
1050      AW = 0.
1051      BW = 0.
1052      90 DO 50 J = 1,3
C*****RESULTANT WAVE AMPLITUDE AND PHASE FOR SWAY, HEAVE ROLL.
1054      HWR(I,J,IL) = HWB(I,J,IL) * RAR(J,IL)
1072      DELWR(I,J,IL) = DELW(I,J,IL) + DELR(J,IL)
1111      AW = AW + HWR(I,J,IL) * SIN(DELWR(I,J,IL))
1132      50 BW = BW + HWR(I,J,IL) * COS(DELWR(I,J,IL))
1155      IF(XOL(I,IL).LT. 0.) GO TO 70
C*****TOTAL REFLECTED WAVE (VECTOR ADDITION)
1163      AW = AW + HWB(I,6,IL) * SIN(DELW(I,6,IL))
1204      BW = BW + HWB(I,6,IL) * COS(DELW(I,6,IL))
1225      GO TO 45
C*****TOTAL TRANSMITTED WAVE(VECTOR ADDITION)

```

Table D-2. Continued

RUNT VERSION FEB 74 B 17:12 04/23/75

```

1225 76 AW = AW + HWB(I,4,IL) * SIN(DELW(I,4,TL))
1246 RW = RW + HWB(I,4,IL) * COS(DELW(I,4,TL))
1267 45 HWT(I,IL)=SQRT(AW**2 + RW**2)
1307 DELWT(I,IL)=ATAN2(AW,RW)
1317 40 CONTINUE
1321 GO TO 150
C*****SET OUTPUTS FOR IL .GT. NMAVEL
1322 160 DO 170 I = 1,3
1324 RAR(I,IL) = 0.0
1330 170 DELR(I,IL) = 0.0
1337 DO 180 I = 1,25
1340 HWT(I,IL) = 0.0
1344 DELWT(I,IL) = 0.0
1351 DO 180 J = 1,3
1352 HWR(I,J,IL) = 0.0
1361 180 DELWR(I,J,IL) = 0.0
1374 150 CONTINUE
C***** OUT PUT DYNAMIC RESULTS
1376 CALL DYNOUT
1377 NMOR = 0
1400 DO 139 IP = 1,3
1402 DO 139 IQ = 1,3
1403 IF (RKMR(IP,IQ) .EQ. 0.0) GO TO 139
1410 NMOR = NMOR + 1
1412 139 CONTINUE
1416 IF (NMOR .NE. 0) CALL MORTEN
1421 IF (NPUNCH .NE. 0) GO TO 140
1423 PUNCH 2000
1427 2000 FORMAT (*1111111111*)
1427 PUNCH 2005, (RQL(IQ),HWT(1,IQ),RAR(1,TO),RAR(2,IQ),RAR(3,TO),
1 IO = 1,10)
1466 2005 FORMAT (SF10.4)
1466 PUNCH 2000
1472 PUNCH 2010, (RQL(IQ),FJRND(1,IQ),FJRND(2,TO),IO=1,10)
1517 2010 FORMAT (F10.4,2E20.4)
1517 140 CONTINUE
1521 RETURN
1522 END

```

Table D-2. Continued



RUNT VERSION FEB 74 8 17:12 04/23/76

```

      SUBROUTINE MORTEN
C***SUBROUTINE MORTEN COMPUTES FORCES IN THE MOORING LINES
2   COMMON/FOUR/RAR(3,10),DELR(3,10),HWR(25,3,10),DELWR(25,3,10),
      2 HWT(25,10),DELWT(25,10),RKHYD(3,3),RKMDR(3,3),RKTB(3,3),
      3 XG, YG, RMASS, RINERT, DAMP(3)
2   COMMON /SEVEN/ AREA, B, D, ROE, GFE, RTITLE(3), TITLE(8)
2   COMMON/TEN/DELT(2,3),FOR(2,10),PHAS(2,10),FORND(2,10),PHASD(2,10)
2   READ 10, ((DELT(I,J),J=1,3),I=1,2)
22  10 FORMAT (6F10.2)
C   DELT(1,I),I=1,3 = CHANGE IN FORCE IN SHOREWARD MOORING LINE
C   PER UNIT DISPLACEMENT IN SWAY, HEAVE AND ROLL
C   DELT(2,I),I=1,3 = CHANGE IN FORCE IN SEAWARD MOORING LINE
C   PER UNIT DISPLACEMENT IN SWAY, HEAVE AND ROLL
22  CAB = 1.0/(ROE*GEE*AREA)
26  CONS = 180.0/ACOS(-1.0)
32  DO 100 J = 1,2
34  PRINT 20
37  20 FORMAT (///20X*MOORING LINE MODEL RESULTS*/)
37  IF (J.EQ. 1) PRINT 18
45  IF (J.EQ. 2) PRINT 19
53  18 FORMAT (30X*SHOREWARD MOORING LINE*/)
53  19 FORMAT (30X*SEAWARD MOORING LINE*/)
53  PRINT 30, (DELT(J,K),K=1,3)
70  30 FORMAT (* CHANGE IN FORCE PER UNIT DISPLACEMENT IN SWAY, HEAVE*
      1 * AND ROLL, RESPECTIVELY **, 3F10.4//)
C***COMPUTE FORCES IN MOORING LINES AND PHASE
70  DO 50 I = 1,10
72  AA = RAR(1,I)*DELT(J,1)
103 AB = RAR(2,I)*DELT(J,2)
114 AC = RAR(3,I)*DELT(J,3)/B
126 TS = AA*SIN(DELR(1,I)) + AB*SIN(DELR(2,I)) + AC*SIN(DELR(3,I))
154 TC = AA*COS(DELR(1,I)) + AB*COS(DELR(2,I)) + AC*COS(DELR(3,I))
203 FOR(J,I) = SQRT(TS*TS + TC*TC)
215 PHAS(J,I) = ATAN2(TC,TS)
225 FORND(J,I) = CAB*FOR(J,I)
236 PHASD(J,I) = CONS*PHAS(J,I)
246 50 CONTINUE
C***PRINT RESULTS
250 PRINT 80, (FOR(J,I),I=1,10),(PHASD(J,I),I=1,10),
      1 (FORND(J,I),I=1,10)
306 80 FORMAT (3X*MOORING LINE RESPONSE*/5X*FORCE AMPLITUDE/ETA*, 11X,
      1 10E10.3/5X*PHASE REL TO ETA AT X=0 - DEG *, 10F10.4//
      2 5X30HFORCE AMPLITUDE/ROE*G*AREA*ETA, 10F10.3)
306 100 CONTINUE
310 RETURN
311 END

```

Table D-2. Continued

RUNT VERSION FEB 74 9 17:12 04/23/76

```

      SUBROUTINE COEFF
      THIS SUBROUTINE CALCULATES THE PARTS OF I(T,J) AND K(I,J)
      WHICH ARE INDEPENDENT OF FREQUENCY NUMBER K.
2      C
      COMMON RI12(25,25),RK56(25,25), POT(25,25), HOW(25,25),FE(25,6),
      IFI(25,6), RI(25,25), RJ(25,25), RK(25,4), RL(25,4),
      2RMU(3,3,10), RLAN(3,3,10), FB(3,10), DELFB(3,10), HWR(25,6,10),
      3 DELW(25,6,10), XOL(25,10)
      2      COMMON/ONE/X(25),Y(25),XB(25),YB(25),ANG(25),DEL(25),VV(25)
      1,FEIN(25), FIIN(25), RNORM(25,3), JC(5)
      2      COMMON /TWO/ N,NNW, NWAVEL, ISYM, TSKIP, NC, PIE,GAMMA,M,TK,TP
      2      COMMON/ONE2/CC3(25),SS3(25)
      2      N2 = N/2
      6      DO 1 I = 1,M
      10      IF(I .GT. N) GO TO 7
      13      IF(ISYM .EQ. 1 .AND. I .GT. N2) GO TO 7
      26      X11 = X(I) - XB(1)
      34      Y11=Y(I)-YB(1)
      41      X21 = X11 + XB(1)
      45      Y21=Y(I)+YB(1)
      53      PP1=ALOG(X11**2+Y11**2)
      66      PQ1=ALOG(X11**2+Y21**2)
      101      TP1=ATAN2(Y11,X11)
      105      TQ1=ATAN2(Y21,X11)
      111      DO 1 J = 1,N
      112      X12=X(I)-XB(J+1)
      120      Y12=Y(I)-YB(J+1)
      124      Y22=Y(I)+YB(J+1)
      131      PP2=ALOG(X12**2+Y12**2)
      144      PQ2=ALOG(X12**2+Y22**2)
      157      TP2=ATAN2(Y12,X12)
      163      TQ2=ATAN2(Y22,X12)
      C      CORRECTION FOR DISCONTINUITY IN ATAN2 AT PIE
      167      IF(X11 .GT. 0. .OR. X12 .GT. 0.) GO TO 6
      201      IF(TP2 .GT. 0. .AND. TP1 .LT. 0.) TP1 = TP1 + TP
      214      IF(TP2 .LT. 0. .AND. TP1 .GT. 0.) TP1 = TP1 - TP
      227      C3 = CC3(J)
      232      S3=SS3(J)
      235      A1=PIE
      237      IF(I-J)2,3,2
      241      2 A1=TP1-TP2
      243      3 A2=TQ2-TQ1
      245      A5=C3*(-XB(J+1)+XB(J)-X12*0.5*PP2+X11*0.5*PP1
      1+Y12*TP2-Y11*TP1)+S3*(YB(J)-YB(J+1)-X12*TP2
      1-Y12*0.5*PP2+X11*TP1+Y11*0.5*PP1)
      307      A6=C3*(-XB(J+1)+XB(J)-X12*0.5*PQ2+X11*0.5*PQ1
      1+Y22*TQ2-Y21*TQ1)-S3*(-YB(J)+YB(J+1)-X12*TQ2
      1-Y22*0.5*PQ2+X11*TQ1+Y21*0.5*PQ1)
      351      4 X11=X12
      353      Y11=Y12
      354      Y21=Y22
      356      PP1=PP2
      357      PQ1=PQ2
      361      TP1=TP2
      362      TQ1=TQ2
      364      RI12(I,J) = A1 - A2

```

Table D-2. Continued



COEFF

RUNT VERSION FEB 74 8 15:19 03/18/76

```
372      RK56(1,J) = A3 - A6
377      G3 TO 1
400      7 00 200 L = 1,N
402      RI12(1,L) = 0.0
407      200 RK56(1,L) = 0.0
416      1 CONTINUE
423      RETURN
424      END
```

Table D-2. Continued

```

SUBROUTINE COMP(K)
C THIS SUBROUTINE COMPUTES THE COEFFICIENTS DEPENDENT ON K
C AND CALLS ON LNEQF TO SOLVE THE SIMULTANEOUS EQUATIONS
C FOR THE VELOCITY POTENTIALS FE(I,J) AND FI(I,J), FOR FE2
6 COMMON R112(25,25),RK56(25,25),POT(25,25),HOW(25,25),FE(25,6),
1FI(25,6),R1(25,25),RJ(25,25),RK(25,4),RL(25,4),
2RMU(3,3,10),RLAM(3,3,10),FB(3,10),DELEFA(3,10),HWR(25,6,10),
3 DELW(25,6,10),XOL(25,10)
6 COMMON/ONE/X(25),Y(25),XB(25),YB(25),ANG(25),DFL(25),VV(25)
1,FEIN(25),FIIN(25),PNORM(25,3),JC(5)
6 COMMON/ONE2/CC3(25),SS3(25)
6 COMMON /TWO/ N,NNW, NWAVEL, ISYM, TSKIP, NC, PIE, GAMMA, M, TK, TP
6 DIMENSION A(50,50),B(50,4),ERASE(57)
6 REAL K
6 N2 = N/2
12 DO 1 I=1,M
13 DO 6 I2= 1,4
14 RK(I,I2) = 0.0
21 6 RL(I,I2) = 0.0
27 DO 4 IC = 1,5
31 4 IF ( I .EQ. JC(IC) ) GO TO 1
37 IF(ISYM .NE. 1) GO TO 8
42 IF(I .GT. N2 .AND. I .LE. N) GO TO 9
55 8 X11 = X(I) - XB(1)
63 X21 = X11 + XB(1)
66 Y21=Y(I)+YB(1)
74 PQ1=ALOG(X11**2+Y21**2)
107 TQ1=ATAN2(Y21,X11)
113 CALL CPV(X11,Y21,E21,C11,S11,A911,A1011,K)
124 C21=C11
126 S21=S11
127 A921=A911
131 A1021=A1011
132 DO 7 J=1,N
135 X12=X(I)-XB(J+1)
143 Y22=Y(I)+YB(J+1)
147 PQ2=ALOG(X12**2+Y22**2)
163 TQ2=ATAN2(Y22,X12)
167 S3=SS3(J)
172 C3=CC3(J)
175 CALL CPV(X12,Y22,E22,C12,S12,A912,A1012,K)
206 DO 13 IC = 1,5
211 13 IF(J .EQ. JC(IC)) GO TO 41
217 A3=A1011-A1012
221 A4=E21*S11-E22*S12
225 A7=S3*(0.5*(PQ1-PQ2)+A912-A911)+C3*(TQ1-TQ2+A1011-A1012)
243 A8=E21*SIN(K*X11-ANG(J))-E22*SIN(K*X12-ANG(J))
266 5 RI(I,J) = 2. * A3 + R112(I,J)
300 IF (I .NE. J) GO TO 3
303 RI(I,J) = RI(I,J) - TP
314 3 RJ(I,J) = -TP*A4
322 POT(I,J) = TK*A7 + RK56(I,J)
334 HOW(I,J) = -TK*PIE*A8
342 DO 10 L = 1,3
344 RK(I,L) = RK(I,L) + POT(I,J) * RNTRN(J,L)

```

Table D-2. Continued



RUNT VERSION FEB 74 B 17:12 04/23/75

```

365 10 RL(I,L) = RL(I,L) + HOW(I,J) * RNOQM(J,L)
410 RK(I,4) = RK(I,4) - FEIN(J)*POT(I,J) + FITN(J)*HOW(I,J)
435 RL(I,4) = RL(I,4) - FEIN(J)*HOW(I,J) - FITN(J)*POT(I,J)
463 41 IF(J=N)2,7,7
466 2 X11=X12
470 Y21=Y22
471 P01=P02
473 T01=T02
474 A911=A912
476 A1011=A1012
477 C11=C12
501 S11=S12
502 E21=E22
504 7 CONTINUE
507 GO TO 1
507 9 IS = N - 1 + 1
512 DO 12 L = 1,3
513 RK(I,L) = RK(IS,L) + (-1.0)**L
527 12 RL(I,L) = RL(IS,L)*(-1.0)**L
545 DO 11 J = 1,N
546 DO 16 IC = 1,5
547 16 IF (J.EQ. JC(IC)) GO TO 11
555 JS = N - J + 1
560 RI(I,J) = RI(IS,JS)
570 RJ(I,J) = RJ(IS,JS)
601 RK(I,4) = RK(I,4) - FEIN(J)*POT(IS,JS) + FITN(J)*HOW(IS,JS)
627 RL(I,4) = RL(I,4) - FEIN(J)*HOW(IS,JS) - FITN(J)*POT(IS,JS)
655 11 CONTINUE
660 1 CONTINUE
663 I2 = 0
664 32 DO 22 I=1,N
666 DO 14 IC = 1,5
667 14 IF(I.EQ. JC(IC)) GO TO 22
675 I2 = I2 + 1
677 II = I2 + NC
701 DO 31 L = 1,4
702 B(I2,L) = RK(I,L)
712 31 B(II,L) = RL(I,L)
725 J2 = 0
726 DO 22 J=1,N
730 DO 15 IC = 1,5
731 15 IF (J.EQ. JC(IC)) GO TO 22
737 J2 = J2 + 1
741 JN = J2 + NC
743 A(I2,J2) = RI(I,J)
754 A(I2,JN) = - RJ(I,J)
765 A(II,J2) = RJ(I,J)
776 A(II,JN) = RI(I,J)
1007 22 CONTINUE
1014 SCALE=1.
1015 NN = 2*NC
1017 LL=LNEOF(50,NN,4,A,9,SCALE,ERASE)
1030 PRINT 27,SCALE
1035 27 FORMAT(//,5X,*DETERMINANT= *,1PE12.4)
1035 I2 = 0
1035 DO 26 I = 1,N

```

Table D-2. Continued

RUNT VERSION FEB 74 B 17:12 04/23/76

```

1041      DO 17 IC = 1,5
1042      17 IF(I.EQ. JC(IC)) GO TO 26
1050      I2 = I2 + 1
1052      II = I2 + NC
1054      DO 35 L = 1,4
1055      FE(I,L) = B(I2,L)
1065      35 FI(I,L) = B(II,L)
1100      26 CONTINUE
1103      29 RETURN
1104      END

```

Table D-2. Continued



```

SUBROUTINE PHYSCL(K)
6      COMMON RI(25,25),RK56(25,25), POT(25,25), HDW(25,25),FE(25,6),
      IFI(25,6), RI(25,25), RJ(25,25), RK(25,4), RL(25,4),
      2RMU(3,3,10), RLAM(3,3,10), FB(3,10), DELF(3,10), HWB(25,6,10),
      3 DELW(25,6,10), XOL(25,10)
6      COMMON/ONE/X(25),Y(25),XB(25),YB(25),ANG(25),DEL(25),VV(25)
      1,FEIN(25), FIIN(25), RNORM(25,3), JC(5)
6      COMMON /TWO/ N,NNW, NWAVEL, ISYM, ISKT0, NC, PIE,GAMMA,M,TK,TP
6      COMMON/THREE/ WAVEL(10), WN(10), BOL(10),TL
6      COMMON /SEVEN/ AREA, B, D, ROE, GEE, RTITLE(3), TITLE(8)
6      REAL K
6      DO 3 I = 1,N
C*****MODE 6 = INCIDENT + DIFRACTED POTENTIALS
7      FE(I,6) = FE(I,4) + FE(I,5)
23      3      FI(I,6) = FI(I,4) + FI(I,5)
42      FACM = (8**2)/AREA
47      FACL = FACM*SORT(K)
53      FACP = FACM * K
55      DO 1 L = 1,3
56      DO1 M1 = 1,6
57      RA = 0.0
60      RM = 0.0
61      IF(M1 .EQ. 4) GO TO 1
63      IF(M1 .EQ. 5) GO TO 1
C*****INTIGRATE PRESSURE COMPONENTS OVER BODY
66      DO 5 I = 1,N
70      RM = RM + FE(I,M1) * RNORM(I,L) * DEL(I)
104      5      RA = RA + FI(I,M1) * RNORM(I,L) * DEL(I)
123      IF(M1 .GT. 4) GO TO 8
C*****ADDED MASS AND DAMPING IN DIRECTION L DUE TO MOTION M1 AT
C*****WAVELENGTH IL.
126      RMU(L,M1, IL) = RM*FACM
136      RLAM(L,M1, IL) = RA*FACL
145      GO TO 1
C*****WAVE FORCE AMPLITUDE AND PHASE IN DIRECTION M1 DUE TO
C*****INCIDENT WAVE AT WAVELENGTH IL
146      8      FB(L, IL) = SQRT(RM**2 + RA**2) * FACP
166      DELFB(L,IL) = ATAN2(-RA,RM)
200      1      CONTINUE
205      IW = N + 1
207      IMAX = N + NNW
211      DO 30 I = IW,IMAX
213      DO 6 L = 1,4
C*****COMPUTE POTENTIAL AT FREE SURFACE POINTS USING GREENS THEOREM
214      DO 4 J = 1, N
215      DO 10 IC = 1,5
216      10      IF(J .EQ. JC(IC)) GO TO 4
224      FE(I,L) = FE(I,L) + FE(J,L)*RI(I,J) -FI(J,L)*RJ(I,J)
255      FI(I,L) = FI(I,L) + FE(J,L)*RJ(I,J) +FI(J,L)*RI(I,J)
306      4      CONTINUE
311      FE(I,L) = (FE(I,L) - RK(I,L))/TP
326      6      FI(I,L) = (FI(I,L) - RL(I,L))/TP
C*****MODE 6 = INCIDENT + DIFRACTED POTENTIALS
344      FE(I,6) = FE(I,4) + FE(I,5)
361      FI(I,6) = FI(I,4) + FI(I,5)

```

Table D-2. Continued

RUNT VERSION FEB 74 B 17:12 04/23/76

```
375      II = I - N
C*****NON DIMENTIONALIZE FREE SURFACE POSITION WITH WAVELENGTH
377      XOL(II,IL) = X(I) * B/ WAVELENGTH
410      DO 2 M1 = 1,6
C*****WAVE AMPLITUDE AND PHASE AT POINT II DUE TO MODE M1 AT WAVELENGTH
412      HWB(II,M1,IL) = SORT(FE(I,M1)**2 + FI(I,M1)**2) * K
443      2      DELW(II,M1,IL) = ATAN2(-FI(I,M1), FE(I,M1))
470      30      CONTINUE
472      7      RETURN
473      END
```

Table D-2. Continued



```

SUBROUTINE PUTOUT
2   COMMON RI(25,25),RK5(25,25), POT(25,25), HQW(25,25),FE(25,6),
1FI(25,6), RI(25,25), RJ(25,25), RK(25,4), RL(25,4),
2RMU(3,3,10), RLM(3,3,10), FB(3,10), DELF(3,10), HWB(25,6,10),
3 DELW(25,6,10), XDL(25,10)
2   COMMON /TWO/ N,NNW, NWAVEL, ISYM, ISKT, NC, PIE,GAMMA,M,TK,TP
2   COMMON/THREE/ WAVEL(10), WN(10), BDL(10),IL
2   COMMON /SEVEN/ AREA, B, D, ROE, GFE, RTITLE(3), TITLE(3)
2   COMMON / EIGHT/LBLMU(3,3,3), LBLAM(3,3,3), L9LFB(3,3),L9LHWA(7,3),
1LBL(10,3), DEG(3,10)
2   1001 FORMAT(/3X, 3A10, / (5X, 3A10, 10F10.4))
2   1002 FORMAT (/3X, 3A10, / (5X, 3A10, 10F10.4 /5X, 3A10, 10F10.4/))
2   1003 FORMAT( 5X, 3A10, 10F10.4 / 5X, 3A10, 10F10.4 /)
2   1004 FORMAT( /3X, 3A10, 2X, 10F10.4/ 3X, 3A10, 2X, 10F10.4)
2   PRINT 2000, RTITLE
10  2000 FORMAT (1H1, 20X, *NONDIMENSIONAL POTENTIAL COEFFICIENTS* /// 25X
1 * W = SQRT(G/B), W2 = G/B* / 25X*B = *, 3A10 /
1 25X*G = ACCELERATION OF GRAVITY*/
1 25X*ROE = MASS DENSITY OF FLUID*/
225X *ETA = INCIDENT WAVE AMPLITUDE */25X,*WAVEL = INCIDENT OR GENE
3RATED WAVE LENGTH*/)
10  DO 9 IL = 1,10
12  9 DEG(1,IL) = SQRT((GEE*BDL(IL)) / (TP*B))
32  PRINT 1004,(LBL(1,K),K = 1,3), (BDL(IL), IL = 1,10),
1 (LBL(2,K), K = 1,3), (DEG(1,IL), IL = 1,10)
77  PRINT 1001, (LBL(3,K),K= 1,3), ((L9LMU(I,J,K),K= 1,3),
1(RMU(I,J,IL), IL = 1,10), J = 1,3), I = 1,3)
150 PRINT 1001, (LBL(4,K),K = 1,3), ((L9LAM(I,J,K),K = 1,3),
1(RLAM(I,J,IL), IL= 1,10), J = 1,3), I = 1,3)
221 DO 1 I = 1,3
223 DO 1 IL = 1,10
224 1 DEG(1,IL) = 57.298 * DELFB(I,IL)
241 PRINT 1002, (LBL(5,K), K = 1,3), ((L9LFB(I,K),K= 1,3),
1(FB(I,IL),IL = 1,10), (LBL(5,K), K = 1,3), (DEG(1,IL),IL=1,10)
2, I = 1,3)
324 DO 2 I = 1,NNW
326 DO 8 IL = 1,10
327 DEG(1,IL) = 0.0
334 IF(IL .GT. NWAVEL ) GO TO 8
337 DEG(1,IL) = XDL(I,IL)*8/BDL(IL)
353 8 CONTINUE
355 PRINT 1002, (LBL(8,K), K = 1,3), (L9L(9,K), K = 1,3),
1 (XDL(I,IL), IL = 1,10), (L9L(10,K), K=1,3 ), (DEG(1,IL),IL=1,10)
436 DO 3 J = 1,3
440 DO 3 IL = 1,10
441 3 DEG(J,IL) = 57.298 * DELW(I,J,IL)
460 PRINT 1003, ((L9LHWA(J,K), K = 1,3), (HWA(I,J,IL), IL = 1,10),
1 (LBL(7,K), K = 1,3), (DEG(J,IL), IL = 1,10), J = 1,3)
534 IF (XDL(I,1) .LT. 0.) GO TO 4
542 DO 5 IL = 1,10
544 5 DEG(1,IL) = 57.298 * DELW(I,6,IL)
561 PRINT 1003, (L9LHWA(7,K), K=1,3), (HWA(I,6,IL), IL = 1,10),
1 (LBL(6,K),K=1,3), (DEG(1,IL), IL = 1,10)
632 GO TO 2
633 4 DO 7 J = 1,3

```

Table D-2. Continued

RUNT VERSION FEB 74 B 17:12 04/23/74

```
635      DO 7 IL = 1,10
636      7      DEG(J,IL) = 57.298 * DELW(I,J+3, IL)
655      PRINT 1003,((LBLHMB(J,K), K = 1,3), (HWRIT(J,IL), IL = 1,10),
        1(LBL(6,K), K=1,3), (DEG(J-3,IL), IL = 1,10), J= 4.6)
732      2      CONTINUE
735      RETURN
735      END
```

Table D-2. Continued



```

      FUNCTION LNEOF(M,N,N1,A,B,DTRMNT,Z)
C.. SOLVES SIMULTANEOUS LINEAR EQUATIONS BY GAUSSIAN REDUCTION.
C.. FORTRAN IV EQUIVALENT OF LNEQS.

12      REAL A(M,M),B(M,M),Z(M),DTRMNT,RMAX,RNEXT,W,DIV
12      NM1=N-1
14      DO 40 J=1,NM1
15      J1=J+1
C.. FIND ELEMENT OF COL J, ROWS J-N, WHICH HAS MAX ABSOLUTE VALUE.
17      LMAX=J
20      RMAX=ABS(A(J,J))
34      DO 8 K=J1,N
35      RNEXT=ABS(A(K,J))
52      IF (RMAX .GE. RNEXT) GO TO 8
55      RMAX=RNEXT
57      LMAX=K
60      CONTINUE
63      IF (LMAX .NE. J) GO TO 10
C.. MAX ELEMENT IN COLUMN IS ON DIAGONAL
65      IF (A(J,J)) 20,94,20
C.. MAX ELEMENT IS NOT ON DIAGONAL. EXCHANGE ROWS J AND LMAX.
73      DO 12 L=J,N
75      W=A(J,L)
102     A(J,L)=A(LMAX,L)
113     A(LMAX,L)=W
124     DO 14 L=1,N1
125     W=B(J,L)
132     B(J,L)=B(LMAX,L)
143     B(LMAX,L)=W
154     DTRMNT = -DTRMNT
C.. ZERO COLUMN J BELOW THE DIAGONAL.
155     Z(J)=1./A(J,J)
165     DO 30 K=J1,N
167     IF (A(K,J)) 22,30,22
175     W=-Z(J)*A(K,J)
205     DO 24 L=J1,N
207     A(K,L)=W*A(J,L)+A(K,L)
230     DO 26 L=1,N1
231     B(K,L)=W*B(J,L)+B(K,L)
252     30 CONTINUE
255     40 CONTINUE
257     IF (A(N,N)) 42,94,42
265     42 Z(N)=1./A(N,N)
C.. OBTAIN SOLUTION BY BACK SUBSTITUTION.
275     DO 50 L=1,N1
277     B(N,L)=Z(N)+B(N,L)
315     DO 60 K=1,NM1
316     J=N-K
317     J1=J+1
321     DO 58 L=1,N1
322     W=0.
323     DO 56 I=J1,N
325     W=A(J,I)*B(I,L)+W
342     B(J,L)=(B(J,L)-W)/Z(J)
362     60 CONTINUE

```

LNEOF

Table D-2. Continued

RUNT VERSION FEB 74 8 17:12 04/23/75

```
C.. EVALUATE DETERMINANT.
364 IF (DTRMNT) 70,74,70
366 70 DO 72 J=1,N
370 72 DTRMNT=DTRMNT*A(J,J)
377 74 LNEOF=1
401 RETURN

C.. SINGULAR MATRIX, SET ERROR FLAG.
401 94 LNEOF = 2
403 DTRMNT=0.
404 RETURN
405 END
```

Table D-2. Continued



```

SUBROUTINE CPV(X,Y,E,C1,S1,A9,A10,K)
C ....CAUCHY PRINCIPAL VALUE INTEGRAL.
COMMON /TWO/ N,NNW, NWAVEL, ISYM, TSKIP, NC, PIE,GAMMA,M,TK,TP
COMMON/SIX/XN(5),CN(5)
REAL K
IF (Y .GE. 0.0) Y = -1.0E-08
TT=ATAN2(Y,X)
TH=PIE/2.+TT
C.....FOR NEGATIVE X,CORRECTION TO RANGE OF ATAN2.
IF(X.LT.0.)TH=TH+TP
32 AA=K*Y
34 E=EXP(AA)
43 BB=K*X
45 C1=COS(BB)
54 S1=SIN(BB)
63 R=K*SURT(X**2+Y**2)
102 SUM1=0.
103 SUM2=0.
104 IF(R.GE.10.)GO TO 13
107 SUM11=0.
110 SUM22=0.
111 FAC=1.0
113 SUM1C=1.
114 SUM2C=1.
115 SDLTH=0.
116 CDLTH=0.
117 ASSIGN 3 TO LDC
120 IF(X.EQ.0.)ASSIGN 8 TO LDC
122 RL=1.0
124 DO 1 L=1,100
125 DL=L
126 FAC=FAC*DL
130 RL=R*RL
132 DLFAC=FAC*DL
133 DLTH=DL*TH
135 A1=RL/DLFAC
137 IF(ABS(CDLTH).LE.1.E-07)GO TO 2
151 SUM1C=ABS(A1/SUM1)
157 IF(SUM1C.LE.1.E-05)GO TO 7
165 2 CDLTH=COS(DLTH)
171 SUM11=A1*CDLTH
172 SUM1=SUM1+SUM11
174 7 GO TO LDC,(3,R)
203 8 SUM2C=0.
204 GO TO 5
205 3 IF(ABS(SDLTH).LE.1.E-07)GO TO 4
217 SUM2C=ABS(A1/SUM2)
225 IF(SUM2C.LE.1.E-05)GO TO 5
233 4 SDLTH=SIN(DLTH)
237 SUM22=A1*SDLTH
240 SUM2=SUM2+SUM22
242 5 IF(SUM1C.LE.1.E-05.AND.SUM2C.LE.1.E-05)GO TO 6
261 1 CONTINUE
263 6 C=GAMMA+ALOG(R)+SUM1
C.....DISCONTINUITY OF 2PIE IF X NEGATIVE IN ET FUNCTION.

```

Table D-2. Continued

RUNT VERSION FEB 74 B 17:12 04/23/76

```
271      IF(X.LT.O.)TH=TH-TP
300      S=TH+SUM2
302      A9=E*(C1*C+S1*S)
306      A10=E*(-C1*S+S1*C)
313      GO TO 9
C... LAGUERRE QUADRATURE-FIVE POINT.
314      13 DO 14 I=1,5
316          A=XN(I)+AA
321          TERM=CN(I)/(A*A+BB*BB)
330          SUM1=TERM*A+SUM1
333      14 SUM2=TERM+SUM2
337          F=1.
340          IF(X.LT.O.)F=-1.
343          A9=F*PIE*S1*E-SUM1
347          A10=-F*PIE*C1*E+BB*SUM2
353      9 RETURN
354      END
```

Table D-2. Continued



```

SUBROUTINE DYNOUT
COMMON RI(25,25),RK56(25,25), POT(25,25), HOW(25,25),FF(25,6),
1FI(25,6), RI(25,25), RJ(25,25), RK(25,4), PL(25,4),
2RMU(3,3,10), RLAM(3,3,10), FB(3,10), DFLFR(3,10), HWB(25,6,10),
3 DELW(25,6,10), XOL(25,10)
COMMON /TWO/ N,NN4, NWAVEL, ISYM, ISKIP, NC, PIE,GAMMA,M,TK,TP
COMMON /THREE/ WAVEL(10), WN(10), BOL(10),TL
COMMON /FOUR/ RAR(3,10), DELR(3,10), HWR(25,3,10), DELW(25,3,10),
2 HWT(25,10),DELWT(25,10),RKHYD(3,3), RKMOR(3,3), RKT8(3,3),
3 XG, YG, RMAS, RINERT, DAMP(3)
COMMON /SEVEN/ AREA, B, D, RDE, GEE, BTITLE(3), TITLE(P)
COMMON /NINE/ LBLRAR(3,3), LBLHWR(5,3), LRL(5,3)
COMMON / EIGHT/ LBLMU(3,3,3), LBLAM(3,3,3), LBLFB(3,3), LBLHWR(7,3),
1LBL(10,3), DEG(3,10)
2 1001 FORMAT(/3X, 3A10, / (5X, 3A10, 10F10.4))
2 1002 FORMAT (/3X, 3A10, / (5X, 3A10, 10F10.4 /5X, 3A10, 10F10.4//)
2 1003 FORMAT( 5X, 3A10, 10F10.4 / 5X, 3A10, 10F10.4 //)
2 1004 FORMAT( /3X, 3A10, 2X, 10F10.4/ 3X, 3A10, 2X, 10F10.4)
2 PRINT 2000, AREA, B, XG, YG, RMAS, RINERT,DAMP(1),DAMP(2),DAMP(3)
33 2000 FORMAT(14I, 20X'DYNAMIC MODEL RESULTS'// * AREA=F10.3,5X*R=F10.3,
1 5X *XG=F10.3,5X*YG=F10.3,5X*RMAS=F10.3,5X*INERTIA=F10.3//
3* ADDITIONAL DAMPING ADDED- IN SWAY=F6.2* LAMDA11 IN HEAVF-
3*F6.2* LAMDA22 IN ROLL=F6.2* LAMDA33* //)
33 PRINT 2001,((RKHYD(I,J),J=1,3),I=1,3), ((RKMOR(I,J), J=1,3),I=1,3)
67 2001 FORMAT(* SPRING CONSTANTS K11 K12 K13 K21
1 K22 K23 K31 K32 K33*/
2* HYDROSTATIC*7X,9F10.3 / * MOORING*11X,9F10.3//)
67 DO 9 IL = 1,10
71 9 DEG(1,IL) = SQRT((GEE*BOL(IL)) / (TP*B))
111 PRINT 1004,(LBL(1,K),K = 1,3), (BOL(IL), IL = 1,10),
1 (LBL(2,K), K = 1,3), (DEG(1,IL), IL = 1,10)
156 DO 1 I = 1,3
160 DO 1 IL = 1,10
161 1 DEG(1,IL) = 57.298 * DELR(I,IL)
176 PRINT 1002,(LRL(1,K), K = 1,3),((LBLRAR(I,K), K = 1,3),
1 (RAK(I,IL), IL = 1,10), (LBL(6,K),K = 1,3), (DEG(1,IL),IL=1,10), I
2 = 1,3)
261 DO 2 I = 1,NNW
263 DO 8 IL = 1,10
264 8 DEG(1,IL) =XOL(I,IL)*B/BOL(IL)
301 PRINT 1002, (LBL(3,K), K = 1,3), (LRL(9,K), K = 1,3),
1 (XOL(I,IL), IL = 1,10), (LBL(10,K), K=1,3 ), (DEG(1,IL),IL=1,10)
362 DO 3 J = 1,3
364 DO 3 IL = 1,10
365 3 DEG(J,IL) = 57.298 *DELWR(I,J,IL)
404 PRINT 1003, ((LBLHWR(J,K), K = 1,3), (HWR(I,J,IL), IL = 1,10),
1 (LBL(6,K), K = 1,3), (DEG(J,IL), IL = 1,10), J = 1,3)
460 IF (XOL(I,1) .LT. 0.) GO TO 4
466 DO 5 IL = 1,10
470 DEG(2,IL) = 57.298 * DELWT(I,IL)
501 5 DEG(1,IL) = 57.298 * DELW(I,6,IL)
516 PRINT 1003, (LBLHWR(7,K), K=1,3), (HWR(I,6,IL), IL = 1,10),
1 (LBL(6,K),K=1,3), (DEG(1,IL), IL = 1,10)
567 PRINT 1003, (LBLHWR(4,K),K=1,3), (HWT(I,IL),IL = 1,10),
1 (LBL(6,K), K = 1,3), (DEG(2,IL), IL = 1,10)

```

Table D-2. Continued

DYNOUT

RUNT VERSION FEB 74 B 17:12 04/23/76

```
637      GJ TO 2
640      4      DO 7 IL = 1,17
642          DEG(1,IL) = 57.298 * DELW(I,4,IL)
655      7      DEG(2,IL) = 57.298 * DELWT(I,IL)
670          PRINT 1003, (LBLHWP(4,K),K = 1,3), (HWP(I,4,IL),IL = 1,10),
          1(LBL(6,K), K = 1,3), (DEG(1,IL), IL = 1,17), (LBLHWP(5,K),K=1,3),
          2(HWT(I,IL), IL = 1,10), (LBL(6,K),K = 1,3), (DFG(2,IL),IL=1,10)
1005      2      CONTINUE
1010          RETURN
1010          END
```

Table D-2. Continued



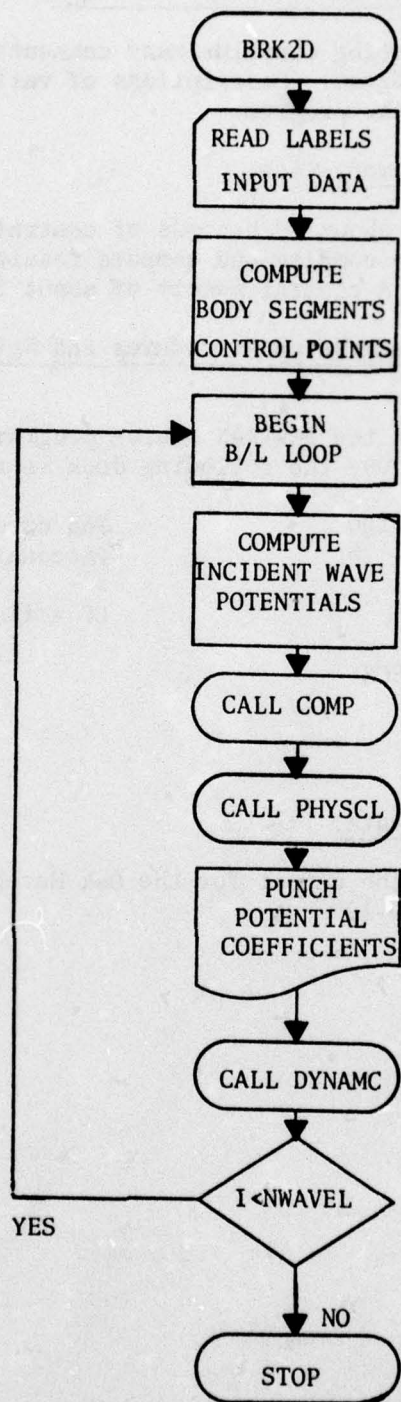


Figure. Flow chart for program BRK2D.

7. Program Comments and Glossary of Terms.

The program listing contains many comments which aid in following the logic of the program. Descriptions of variables also appear where they are read into the program.

8. Run Time and Memory Size.

BRK2D requires about 70 seconds of central processor time on the CDC 6400 computer to compile and compute results for 10 different beam wavelength ratios. A central memory of about 55,000 octal is required.

9. Run and Card Deck Setup Procedures and Special Operation Instructions.

In order to run the FORTRAN source program deck on the University of Washington CDC 6400, the following deck is required:

BRK2D,CM55000,T100.

ACCOUNT

FORTRAN

LGO(LC=6000)

7/8/9

FORTRAN DECK

7/8/9

DATA DECK

6/7/8/9

**Job card**

(Account No., password)

LC = line count value

10. Sample Output Data.

Table D-3 is the output for the Oak Harbor breakwater. The input is given in Table D-1.



17 MAY 1975

OAK HARBOR BREAKWATER - 2000 OF ENGINEERS TESTS

NUMBER OF SEGMENTS = 23  
 NUMBER OF FREE-SURFACE STATIONS = 0  
 NUMBER OF WAVELENGTHS = 13  
 IS/M = 0  
 TSKIP = 0  
 NC = 14C = 12 -0 -0 -0 -0  
 AREA = 12.600  
 B = 10.000 FULL BEAM  
 D = .000  
 FLUID DENSITY = 1.99350  
 ACCELERATION OF GRAVITY = 32.200  
 BEAM/WAVELENGTH RATIO OF INCIDENT WAVES  
 .10000 .15979 .18999 .21681 .25000 .28000 .31221 .37100 .42200 .46733

Table D-3. Example output for program BRK2D (Oak Harbor breakwater)

17 MAY 1975

## CYLINDER GEOMETRY

I	DIMENSIONAL OFFSETS		NON-DIMENSIONAL OFFSETS		WFOPOINTS OF SEGMENTS		SLICE	LENGTH
	X	Y	X	Y	X	Y		
1	-5.000	-0.00	-5.00	-0.00	-5.00	-1.003	-1.571	.125
2	-5.000	-1.250	-5.00	-1.25	-5.00	-1.25	-1.571	.125
3	-5.000	-2.500	-5.00	-2.50	-5.00	-1.500	-1.571	.125
4	-5.000	-3.750	-5.00	-3.75	-5.00	-1.750	-1.571	.125
5	-5.000	-5.000	-5.00	-5.00	-5.00	-2.000	-1.571	.125
6	-4.583	-5.000	-4.58	-5.00	-4.58	-1.750	-1.571	.125
7	-4.583	-3.750	-4.58	-3.75	-4.58	-1.500	-1.571	.125
8	-4.583	-2.500	-4.58	-2.50	-4.58	-1.250	-1.571	.125
9	-4.583	-1.250	-4.58	-1.25	-4.58	-1.000	-1.571	.125
10	-4.583	0.000	-4.58	0.00	-4.58	-0.750	-1.571	.125
11	-4.583	1.250	-4.58	1.25	-4.58	-0.500	-1.571	.125
12	-4.583	2.500	-4.58	2.50	-4.58	-0.250	-1.571	.125
13	-4.583	3.750	-4.58	3.75	-4.58	0.000	-1.571	.125
14	-4.583	5.000	-4.58	5.00	-4.58	0.250	-1.571	.125
15	-4.583	6.250	-4.58	6.25	-4.58	0.500	-1.571	.125
16	-4.583	7.500	-4.58	7.50	-4.58	0.750	-1.571	.125
17	-4.583	8.750	-4.58	8.75	-4.58	1.000	-1.571	.125
18	-4.583	10.000	-4.58	10.00	-4.58	1.250	-1.571	.125
19	-4.583	11.250	-4.58	11.25	-4.58	1.500	-1.571	.125
20	-4.583	12.500	-4.58	12.50	-4.58	1.750	-1.571	.125
21	-4.583	13.750	-4.58	13.75	-4.58	2.000	-1.571	.125
22	-4.583	15.000	-4.58	15.00	-4.58	2.250	-1.571	.125
23	-4.583	16.250	-4.58	16.25	-4.58	2.500	-1.571	.125
24	-4.583	17.500	-4.58	17.50	-4.58	2.750	-1.571	.125

## POSITIONS FOR WAVE HEIGHT CALCULATIONS

WAVE NUMBER = K	K	CIRCULAR FREQUENCY	FREQUENCY	PERIOD	WAVELENGTH
DETERMINANT =	37.1372E+14				
WAVE NUMBER = K	1.60085	CIRCULAR FREQUENCY = 1.79530	FREQUENCY = .27571	PERIOD = 3.60000	WAVELENGTH = 52.7756
DETERMINANT =	19.6121E+14				
WAVE NUMBER = K	1.14077	CIRCULAR FREQUENCY = 1.97831	FREQUENCY = .30772	PERIOD = 3.24920	WAVELENGTH = 55.5556
DETERMINANT =	45.2450E+14				
WAVE NUMBER = K	1.36226	CIRCULAR FREQUENCY = 2.06430	FREQUENCY = .33833	PERIOD = 3.00000	WAVELENGTH = 40.1231
DETERMINANT =	15.0907E+14				

Table D-3. Continued



WAVE NUMBER = K = 1.57083	CIRCULAR FREQUENCY = 2.24899	FREQUENCY = .35794	PERIOD = 2.79378	WAVELENGTH = 46.0700
DETERMINANT = 30.5359E+15				
WAVE NUMBER = K = 1.75929	CIRCULAR FREQUENCY = 2.34011	FREQUENCY = .378*1	PERIOD = 2.63557	WAVELENGTH = 35.7143
DETERMINANT = 45.3555E+15				
WAVE NUMBER = K = 1.96166	CIRCULAR FREQUENCY = 2.51327	FREQUENCY = .49006	PERIOD = 2.50000	WAVELENGTH = 32.0209
DETERMINANT = 54.6151E+15				
WAVE NUMBER = K = 2.33106	CIRCULAR FREQUENCY = 2.73971	FREQUENCY = .43604	PERIOD = 2.29337	WAVELENGTH = 26.4542
DETERMINANT = 32.0082E+15				
WAVE NUMBER = K = 2.69549	CIRCULAR FREQUENCY = 2.94409	FREQUENCY = .44989	PERIOD = 2.13272	WAVELENGTH = 23.3100
DETERMINANT = 12.9867E+14				
WAVE NUMBER = K = 3.02659	CIRCULAR FREQUENCY = 3.14153	FREQUENCY = .50000	PERIOD = 2.00000	WAVELENGTH = 20.4902
DETERMINANT = 19.1494E+16				

Table D-3. Continued

# NONDIMENSIONAL POTENTIAL COEFFICIENTS

W = SQR(TIG/8), W2 = G/R  
 0 = FULL BEAM  
 G = ACCELERATION OF GRAVITY  
 RDE = MASS DENSITY OF FLUID  
 ETA = INCIDENT WAVE AMPLITUDE  
 WAVELENGTH = INCIDENT OR GENERATED WAVE LENGTH

SEMIWAVELENGTH DIMENSIONAL FREQUENCY - W2

ADDED MASS ON = AREA\*DE

MU11/ON	7.3703	5.9455	5.4755	4.9561	4.8450	5.0204	5.5805	9.7645	-53.1777	-4.7753
MU12/ON	1.0000	1.5933	1.8000	2.1844	2.5000	2.6000	3.1222	3.7140	4.2900	4.8786
MU13/ON	1.2335	2.2857	3.3037	4.3333	5.3579	6.3768	7.4000	8.4360	9.4689	10.5000
MU21/ON	1.5889	4.458	7.118	9.6000	12.123	14.685	17.297	20.000	22.754	25.557
MU22/ON	1.5889	4.458	7.118	9.6000	12.123	14.685	17.297	20.000	22.754	25.557
MU23/ON	1.5889	4.458	7.118	9.6000	12.123	14.685	17.297	20.000	22.754	25.557
MU31/ON	1.2948	8.883	17.920	26.880	35.768	44.580	53.328	62.000	70.614	79.185
MU32/ON	1.0000	1.5933	1.8000	2.1844	2.5000	2.6000	3.1222	3.7140	4.2900	4.8786
MU33/ON	1.2335	2.2857	3.3037	4.3333	5.3579	6.3768	7.4000	8.4360	9.4689	10.5000

DAMPING QD = AREA\*QDEW

LAMDA11/QD	2.0190	3.7933	4.0284	4.0548	3.9270	3.6660	3.2821	1.9813	39.5124	5.3165
LAMDA12/QD	0.0000	0.0000	0.0000	0.0000	0.0000	0.0000	0.0000	0.0000	0.0000	0.0000
LAMDA13/QD	0.0000	0.0000	0.0000	0.0000	0.0000	0.0000	0.0000	0.0000	0.0000	0.0000
LAMDA21/QD	0.0000	0.0000	0.0000	0.0000	0.0000	0.0000	0.0000	0.0000	0.0000	0.0000
LAMDA22/QD	0.0000	0.0000	0.0000	0.0000	0.0000	0.0000	0.0000	0.0000	0.0000	0.0000
LAMDA23/QD	0.0000	0.0000	0.0000	0.0000	0.0000	0.0000	0.0000	0.0000	0.0000	0.0000
LAMDA31/QD	0.0000	0.0000	0.0000	0.0000	0.0000	0.0000	0.0000	0.0000	0.0000	0.0000
LAMDA32/QD	0.0000	0.0000	0.0000	0.0000	0.0000	0.0000	0.0000	0.0000	0.0000	0.0000
LAMDA33/QD	0.0000	0.0000	0.0000	0.0000	0.0000	0.0000	0.0000	0.0000	0.0000	0.0000

WAVE FORCES OF AREA\*QDETA\*W2

FX/OF	4.4250	5.4143	5.4209	5.2373	4.9783	4.7161	4.4149	3.6704	5.9774	4.2984
PHASE REL TO ETA AT X=0 - DEG	72.8793	60.4041	59.8750	59.1117	59.6297	62.2586	66.0442	75.1616	86.5835	92.4458
FY/OF	1.2106	3.1793	2.4019	1.5443	1.1456	0.9150	0.7381	0.5198	0.3661	0.2555
PHASE REL TO ETA AT X=0 - DEG	159.0771	80.0067	69.6023	53.9553	57.9583	59.5246	62.4599	66.8752	72.1007	79.8790
FZ/OF	0.7530	0.4555	0.3536	0.3325	0.3063	0.2838	0.2622	0.2478	0.2332	0.2179
PHASE REL TO ETA AT X=0 - DEG	72.5953	60.0131	57.9513	56.6140	57.6501	59.7044	62.9679	68.9328	73.0317	79.4742

WAVE FIELD - AMPLITUDE RATIOS

POSITION - X/WAVELENGTH	4.0000	4.0000	4.0000	4.0000	4.0000	4.0000	4.0000	4.0000	4.0000	4.0000
DIMENSIONAL POSITION - X	251.1143	222.2222	184.4925	160.0000	142.8571	128.8167	107.8167	93.2401	81.9966	72.4350
GEN BY SWAY/SHAY	3.497	5.497	7.684	9.972	12.0247	14.043	16.043	18.043	20.043	22.043
PHASE REL TO BODY MOTION - DEG	162.8661	150.7748	148.7587	147.8852	146.8450	145.6560	144.3595	142.9626	141.4734	139.8954
GEN BY HEAVE/SHAY	0.020	0.3818	1.258	2.400	3.880	5.680	7.880	10.480	13.580	17.180
PHASE REL TO BODY MOTION - DEG	79.2908	-3.982	-10.5930	-29.7700	-50.2551	-72.1615	-95.4664	-120.6664	-158.6664	-210.6664

Table D-3. Continued



GEN BY ROLL/ROLL(RAD)98	.0607	.1215	.1389	.1644	.1935	.1988	.2144	.2494	.0121	.2227
PHASE REL TO BODY MOTION - DEG	162.6661	150.7288	149.7288	147.8893	146.2451	151.6562	155.0697	162.2624	-175.4425	-175.9366
TRANS BY FWD BODY/ETA	.0870	.4397	.1626	.0349	.0426	.0448	.0429	.0386	.1027	.0399
PHASE REL TO ETA AT X=0 - DEG	-26.3043	-111.9988	-124.4312	-63.8978	-22.2265	-16.4142	-17.2571	-31.5647	53.6327	-4.5102
WAVE FIELD - AMPLITUDE RATIOS										
POSITION - X/DAVELENGTH										
DIMENSIONAL POSITION - X	-4.0000	-4.0000	-4.0000	-4.0600	-4.0000	-4.0000	-4.0000	-4.0000	-4.0000	-4.0000
PHASE REL TO BODY MOTION - DEG	-400.0000	-251.1143	-227.2222	-184.4925	-160.0000	-142.8571	-128.1197	-107.8157	-93.2401	-81.9956
GEN BY SWAY/SWAY	.3497	.4403	.7688	.8910	.9729	1.0247	1.0543	.9431	4.4957	1.8978
PHASE REL TO BODY MOTION - DEG	-17.1409	-29.2782	-31.2483	-32.1121	-30.7620	-28.3509	-24.9373	-17.7444	4.3736	4.0706
GEN BY HEAVE/HEAVE	.0029	.3938	.3258	.2490	.2120	.1886	.1688	.1399	.1154	.0919
PHASE REL TO BODY MOTION - DEG	79.2408	-4.9987	-19.5930	-29.7700	-30.2351	-28.1115	-24.3664	-16.4913	-7.2745	2.7097
GEN BY ROLL/ROLL(RAD)98	.0607	.1215	.1389	.1644	.1935	.1988	.2144	.2494	.0121	.2227
PHASE REL TO BODY MOTION - DEG	-17.1409	-29.2782	-31.2482	-32.1121	-30.7619	-28.3507	-24.9373	-17.7445	4.3644	4.0701
REFLECTED BY FWD BODY/ETA	.1130	.8163	.9230	.9491	.9329	.9543	.9551	.9546	.9576	.9582
PHASE REL TO ETA AT X=0 - DEG	63.7635	149.0779	129.1787	117.3206	116.2930	122.8550	129.8806	145.6856	170.5965	-174.8329
INCIDENT/ETA	1.0000	1.0000	1.0000	1.0000	1.0000	1.0000	1.0000	1.0000	1.0000	1.0000
PHASE REL TO ETA AT X=0 - DEG	-0.0000	-0.0000	-0.0000	-0.0000	-0.0000	-0.0000	-0.0000	-0.0000	-0.0000	-0.0000
REFLECTED + INCIDENT/ETA	1.0000	2.0000	2.0000	2.0000	2.0000	2.0000	2.0000	2.0000	2.0000	2.0000
PHASE REL TO ETA AT X=0 - DEG	0.0000	0.0000	0.0000	0.0000	0.0000	0.0000	0.0000	0.0000	0.0000	0.0000

Table D-3. Continued

DYNAMIC MODEL RESULTS

ARE--	12.000	8-	10.000	KG-	.000	YC-	-2.340	MASS-	25.100	INERTIA-	621.000
ADDITIONAL DAMPING ADDED-	IN SWAY-	.00 LAMDA11	IN HEAVE-	.00 LAMDA22	IN ROLL-	.00 LAMDA33					
SPRING CONSTANTS											
HYDROSTATIC	K11	K12	K13	K21	K22	K23	K31	K32	K33		
MOORING	.000	.000	.000	.000	.000	.000	.000	.000	.000	.000	.000
	.000	.000	.000	.000	.000	.000	.000	.000	.000	.000	.000
BEAM/HAWELENGTH											
DIMENSIONAL FREQUENCY - MZ	.1000	.1993	.1800	.2164	.2500	.2800	.3122	.3713	.4290	.4878	.5000
	.2264	.3957	.3037	.3333	.3579	.3788	.4000	.4360	.4684	.4878	.5000
MOTION RESPONSE											
SWAY AMPLITUDE/ETA	.7219	.5490	.5957	.5043	.4229	.3499	.2722	.1327	.0011	.1391	.1391
PHASE REL TO ETA AT X=0 - DEG	-90.2310	-90.4540	-90.5725	-90.7877	-90.9813	-91.1565	-91.3291	-91.5435	-91.8394	-91.8394	-91.8394
HEAVE AMPLITUDE/ETA	1.4444	2.1755	2.3789	1.3931	.7474	.4732	.3122	.1638	.0931	.0538	.0538
PHASE REL TO ETA AT X=0 - DEG	-2.2345	-27.1538	-5.9867	-9.8504	-11.5778	-11.5778	-11.5778	-10.8787	-10.0261	-8.8526	-8.8526
ROLL AMPLITUDE/RAD/ETA	.4747	.2050	.2613	.3337	.3871	.4308	.4746	.5503	.6670	.7232	.7232
PHASE REL TO ETA AT X=0 - DEG	-90.0905	-90.8493	-90.5892	-91.0865	-91.3080	-91.5136	-91.7496	-92.2407	-91.6298	-93.9513	-93.9513
WAVE FIELD - AMPLITUDE RATIOS											
POSITION - X/HAWELENGTH	4.0000	4.0000	4.0000	4.0000	4.0000	4.0000	4.0000	4.0000	4.0000	4.0000	4.0000
DIMENSIONAL POSITION - X	400.0000	251.1143	222.2222	184.4925	160.0000	142.8571	128.1197	107.8167	93.2401	81.9966	81.9966
GEN BY RESULTANT SWAY/ETA	.2524	.4419	.4379	.4498	.4115	.3586	.2870	.1251	.0049	.2826	.2826
PHASE REL TO ETA AT X=0 - DEG	72.6350	60.2548	56.1863	57.1075	58.2637	60.4993	63.7403	70.7171	-211.2665	-90.2659	-90.2659
GEN BY RESULTANT HEAVE/ETA	.1341	.8349	.7750	.3456	.1585	.0892	.0527	.0229	.0107	.0049	.0049
PHASE REL TO ETA AT X=0 - DEG	77.0563	-27.7620	-74.5637	-129.5904	-142.8529	-143.3619	-139.0781	-125.2726	-107.5406	-86.1198	-86.1198
GEN BY RESULTANT ROLL/ETA	.0258	.0249	.0363	.0549	.0710	.0856	.1018	.1373	.0091	.1611	.1611
PHASE REL TO ETA AT X=0 - DEG	72.7756	59.4795	57.8696	56.7989	57.9371	60.1376	63.3201	70.0217	-267.0723	-269.8881	-269.8881
TRANS BY FWD BODY/ETA	.9870	.4382	.1626	.0349	.0476	.0448	.0429	.0386	.1027	.3399	.3399
PHASE REL TO ETA AT X=0 - DEG	-26.3043	-111.8084	-124.4512	-63.6078	-22.2265	-16.4142	-17.2571	-31.5947	93.4327	-4.6132	-4.6132
TOTAL TRANSMITTED/ETA	.9995	.9965	.9946	.9938	.9920	.9910	.9900	.9890	.9880	.9870	.9860
PHASE REL TO ETA AT X=0 - DEG	-2.1888	-25.8277	-50.8773	51.0059	60.7136	59.2666	60.3027	62.6952	57.1880	-70.7104	-70.7104
WAVE FIELD - AMPLITUDE RATIOS											
POSITION - X/HAWELENGTH	4.0000	4.0000	4.0000	4.0000	4.0000	4.0000	4.0000	4.0000	4.0000	4.0000	4.0000
DIMENSIONAL POSITION - X	400.0000	251.1143	222.2222	184.4925	160.0000	142.8571	128.1197	107.8167	93.2401	81.9966	81.9966
GEN BY RESULTANT SWAY/ETA	.2524	.4419	.4379	.4498	.4115	.3586	.2870	.1251	.0049	.2826	.2826
PHASE REL TO ETA AT X=0 - DEG	72.6350	60.2548	56.1863	57.1075	58.2637	60.4993	63.7403	70.7171	-211.2665	-90.2659	-90.2659
GEN BY RESULTANT HEAVE/ETA	.1341	.8349	.7750	.3456	.1585	.0892	.0527	.0229	.0107	.0049	.0049
PHASE REL TO ETA AT X=0 - DEG	77.0563	-27.7620	-74.5637	-129.5904	-142.8529	-143.3619	-139.0781	-125.2726	-107.5406	-86.1198	-86.1198
GEN BY RESULTANT ROLL/ETA	.0258	.0249	.0363	.0549	.0710	.0856	.1018	.1373	.0091	.1611	.1611
PHASE REL TO ETA AT X=0 - DEG	72.7756	59.4795	57.8696	56.7989	57.9371	60.1376	63.3201	70.0217	-267.0723	-269.8881	-269.8881
TRANS BY FWD BODY/ETA	.9870	.4382	.1626	.0349	.0476	.0448	.0429	.0386	.1027	.3399	.3399
PHASE REL TO ETA AT X=0 - DEG	-26.3043	-111.8084	-124.4512	-63.6078	-22.2265	-16.4142	-17.2571	-31.5947	93.4327	-4.6132	-4.6132
TOTAL TRANSMITTED/ETA	.9995	.9965	.9946	.9938	.9920	.9910	.9900	.9890	.9880	.9870	.9860
PHASE REL TO ETA AT X=0 - DEG	-2.1888	-25.8277	-50.8773	51.0059	60.7136	59.2666	60.3027	62.6952	57.1880	-70.7104	-70.7104

Table D-3. Continued



PHASE REL TO ETA AT X=0 - DEG	-107.2314	-120.1374	-122.1374	-123.2092	-122.0699	-119.8693	-116.6869	-109.9853	-87.0653	-59.9911
REFLECTED BY FND BOV/ETA	.1190	.8143	.9230	.9491	.9529	.9543	.9551	.9546	.9576	.9582
PHASE REL TO ETA AT X=0 - DEG	63.7635	149.0775	124.1707	117.3206	116.2920	122.8550	124.6806	145.6835	173.5986	-174.5329
TOTAL REFLECTED/ETA	.C310	.4211	.7647	.9427	.9963	.8839	.8951	.9306	.9531	.9524
PHASE REL TO ETA AT X=0 - DEG	-92.2593	-117.2714	-144.7676	170.6416	158.1971	155.8747	157.0076	162.9862	171.8175	179.3934

Table D-3. Continued

# DYNAMIC MODEL RESULTS

AREA	12.600	8	10.000	KG	.000	YG	-2.340	MASS	25.100	INERTIA	621.000
ADDITIONAL DAMPING ADDED-	IN SWAY-	.00	LAMDA11	IN HEAVE-	.00	LAMDA22	IN ROLL-	.00	LAMDA33		
SPRING CONSTANTS											
HYDROSTATIC	K11	K12	K13	K21	K22	K23	K31	K32	K33		
MUONING	118.900	-5.240	166.200	-5.732	10.210	-3.372	170.900	.300	1165.600		
								2.063	281.800		
WAVE FIELD - AMPLITUDE RATIOS											
POSITION - X/NAVELENGTH											
DIMENSIONAL POSITION - X											
GEN BY RESULTANT SWAY/ETA											
PHASE REL TO ETA AT X=0 - DEG											
GEN BY RESULTANT HEAVE/ETA											
PHASE REL TO ETA AT X=0 - DEG											
GEN BY RESULTANT ROLL/ETA											
PHASE REL TO ETA AT X=0 - DEG											
TRANS BY FID BOY/ETA											
PHASE REL TO ETA AT X=0 - DEG											
TOTAL TRANSMITTED/ETA											
PHASE REL TO ETA AT X=0 - DEG											
MOTION RESPONSE											
SWAY AMPLITUDE/ETA											
PHASE REL TO ETA AT X=0 - DEG											
HEAVE AMPLITUDE/ETA											
PHASE REL TO ETA AT X=0 - DEG											
ROLL AMPLITUDE/RAD/ETA											
PHASE REL TO ETA AT X=0 - DEG											
WAVE FIELD - AMPLITUDE RATIOS											
POSITION - X/NAVELENGTH											
DIMENSIONAL POSITION - X											
GEN BY RESULTANT SWAY/ETA											
PHASE REL TO ETA AT X=0 - DEG											
GEN BY RESULTANT HEAVE/ETA											
PHASE REL TO ETA AT X=0 - DEG											
GEN BY RESULTANT ROLL/ETA											
PHASE REL TO ETA AT X=0 - DEG											
TRANS BY FID BOY/ETA											
PHASE REL TO ETA AT X=0 - DEG											
TOTAL TRANSMITTED/ETA											
PHASE REL TO ETA AT X=0 - DEG											
MOTION RESPONSE											
SWAY AMPLITUDE/ETA											
PHASE REL TO ETA AT X=0 - DEG											
HEAVE AMPLITUDE/ETA											
PHASE REL TO ETA AT X=0 - DEG											
ROLL AMPLITUDE/RAD/ETA											
PHASE REL TO ETA AT X=0 - DEG											
WAVE FIELD - AMPLITUDE RATIOS											
POSITION - X/NAVELENGTH											
DIMENSIONAL POSITION - X											
GEN BY RESULTANT SWAY/ETA											
PHASE REL TO ETA AT X=0 - DEG											
GEN BY RESULTANT HEAVE/ETA											
PHASE REL TO ETA AT X=0 - DEG											
GEN BY RESULTANT ROLL/ETA											
PHASE REL TO ETA AT X=0 - DEG											
TRANS BY FID BOY/ETA											
PHASE REL TO ETA AT X=0 - DEG											
TOTAL TRANSMITTED/ETA											
PHASE REL TO ETA AT X=0 - DEG											

Table D-3. Continued



PHASE REL TO ETA AT X=0 - DEG -112.4946 -50.2947 -103.0379 -117.8941 -117.3149 -115.8049 -113.5926 -138.6019 -86.6649 -89.6985  
 REFLECTED BY FXD BODY/ETA .1190 .8163 .9230 .9491 .9529 .9543 .9551 .9546 .9376 .9532  
 PHASE REL TO ETA AT X=0 - DEG 63.7635 140.0773 174.1707 117.3206 118.2930 122.8550 129.8806 162.6836 170.5966 -174.8329  
 TOTAL REFLECTED/ETA .1029 .4451 .7619 .9367 .9745 .8645 .8997 .9261 .9327 .9328  
 PHASE REL TO ETA AT X=0 - DEG -94.0142 -110.3045 -139.0236 177.3225 162.8642 159.3332 154.7122 164.1800 172.2029 179.2602

# MOORING LINE MODEL RESULTS

## SHOREWARD MOORING LINE

CHANGE IN FORCE PER UNIT DISPLACEMENT IN SWAY, HEAVE AND ROLL, RESPECTIVELY = -1376.0000 410.6000 -1637.0000

MOORING LINE RESPONSE  
 FORCE AMPLITUDE/ETA 1.487E+03 1.083E+03 6.345E+02 2.712E+02 4.577E+02 4.481E+02 3.856E+02 2.279E+02 7.544E+01 9.646E+01  
 PHASE REL TO ETA AT X=0 - DEG 22.5037 45.3005 66.8203 -32.2325 -21.5524 -14.6238 -9.9398 -4.8284 -4.2163 -175.6131  
 FORCE AMPLITUDE/ROE\*CGAREA\*ETA 1.841E+00 1.341E+00 8.105E-01 3.358E-01 5.643E-01 5.548E-01 4.775E-01 2.823E-01 9.341E-02 1.194E-01

# MOORING LINE MODEL RESULTS

## SEAWARD MOORING LINE

CHANGE IN FORCE PER UNIT DISPLACEMENT IN SWAY, HEAVE AND ROLL, RESPECTIVELY = 1172.0000 280.9000 1713.0000

MOORING LINE RESPONSE  
 FORCE AMPLITUDE/ETA 1.311E+03 1.397E+03 1.482E+03 1.131E+03 8.384E+02 6.460E+02 5.251E+02 3.135E+02 1.472E+02 2.216E+01  
 PHASE REL TO ETA AT X=0 - DEG 154.4105 151.9442 156.7943 -174.5353 -176.3792 -176.7023 -176.8630 -176.8128 -177.4416 19.1138  
 FORCE AMPLITUDE/ROE\*CGAREA\*ETA 1.623E+00 1.674E+00 1.839E+00 1.426E+00 1.038E+00 8.247E-01 6.502E-01 3.962E-01 1.823E-01 2.744E-02

Table D-3. Continued

DYNAMIC MODEL RESULTS

AREA=	12.600	B=	10.000	KG=	.000	YG=	-2.340	MASS=	25.100	INERTIA=	621.000
ADDITIONAL DAMPING ADDED=	IN SWAY=	1.00	LAMDA11	IN HEAVE=	1.00	LAMDA22	IN ROLL=	1.00	LAMDA33		
SPIRING CONSTANTS	K11	K12	K13	K21	K22	K23	K31	K32	K33		
HYDROSTATIC	110.800	-5.240	166.200	.000	.000	.000	.000	.000	.000	1165.000	
MORING										2.063	281.800
BEAM/HAULENGTH											
DIMENSIONAL FREQUENCY - HZ											
	.1000	.1493	.1800	.2168	.2500	.2800	.3122	.3710	.4290	.4478	
	.2284	.2857	.3037	.3333	.3579	.3788	.4000	.4360	.4589	.5000	
MOTION RESPONSE											
SWAY AMPLITUDE/ETA											
PHASE REL TO ETA AT X=0 - DEG	.5857	.4323	.4106	.3716	.3400	.3057	.2587	.1387	.0019	.1119	
	-94.6025	-96.3710	-97.5115	-99.6797	-62.4719	-66.2493	-71.6435	-84.5311	-78.6415	61.0374	
HEAVE AMPLITUDE/ETA											
PHASE REL TO ETA AT X=0 - DEG	1.5994	1.1794	1.3829	1.2531	.7680	.4916	.3222	.1671	.0954	.0361	
	11.0451	-12.5409	-35.9320	-83.3707	-103.0333	-110.5530	-111.5952	-107.8820	-99.6718	-89.2259	
ROLL AMPLITUDE/RAD/ETA											
PHASE REL TO ETA AT X=0 - DEG	2.4528	1.3478	1.1093	.6054	.6258	.5281	.4912	.5468	.6908	.6226	
	-61.0343	-109.1399	-112.0653	-113.1534	-109.1716	-102.3773	-92.2317	-31.7304	-90.7043	-98.3733	
WAVE FIELD - AMPLITUDE RATIOS											
POSITION - X/HAULENGTH											
DIMENSIONAL POSITION - X											
GEN BY RESULTANT SWAY/ETA											
PHASE REL TO ETA AT X=0 - DEG	2048	.7930	.3157	.3315	.3304	.3132	.2728	.1303	.0288	.2112	
	78.2636	94.4038	91.2472	89.2055	86.7731	85.4107	83.4260	77.7315	-254.0727	-114.8790	
GEN BY RESULTANT HEAVE/ETA											
PHASE REL TO ETA AT X=0 - DEG	1436	.4528	.4506	.3131	.1629	.0927	.0544	.0234	.0110	.0032	
	90.3359	-12.9391	-55.5251	-110.1407	-133.2364	-136.5365	-136.6626	-124.3738	-106.9463	-86.5152	
GEN BY RESULTANT ROLL/ETA											
PHASE REL TO ETA AT X=0 - DEG	1439	.1664	.1541	.1374	.1148	.1050	.1053	.1364	.0083	.1342	
	101.9318	41.5183	34.6955	34.7319	39.5775	49.2759	62.8379	80.5261	-266.1463	-274.7131	
TRANS BY FWD BODY/ETA											
PHASE REL TO ETA AT X=0 - DEG	26.3043	.4342	.1626	.0349	.0426	.0448	.0429	.6386	.1027	.0399	
	.9870	.4342	-124.4512	-63.8678	-22.2265	-16.4142	-17.2571	-31.5947	53.4327	-4.8132	
TOTAL TRANSMITTED/ETA											
PHASE REL TO ETA AT X=0 - DEG	.8970	.3933	.2964	.0847	.2709	.3248	.3248	.2336	.1044	.0771	
	3.0729	-15.3732	-19.2820	71.7761	82.5810	78.0874	75.6150	72.2741	54.1883	-120.7664	
WAVE FIELD - AMPLITUDE RATIOS											
POSITION - X/HAULENGTH											
DIMENSIONAL POSITION - X											
GEN BY RESULTANT SWAY/ETA											
PHASE REL TO ETA AT X=0 - DEG	2048	.7930	.3157	.3315	.3304	.3132	.2728	.1308	.0288	.2112	
	-101.7434	-85.5092	-66.7597	-91.6014	-93.2339	-94.5963	-96.5920	-102.2755	-74.0657	65.1280	
GEN BY RESULTANT HEAVE/ETA											
PHASE REL TO ETA AT X=0 - DEG	1436	.4528	.4506	.3131	.1629	.0927	.0544	.0234	.0110	.0032	
	90.3359	-12.9391	-55.5251	-110.1407	-133.2364	-136.5365	-136.6626	-124.3738	-106.9463	-86.5152	
GEN BY RESULTANT ROLL/ETA											
PHASE REL TO ETA AT X=0 - DEG	1439	.1664	.1541	.1374	.1148	.1050	.1053	.1364	.0083	.1342	
	101.9318	41.5183	34.6955	34.7319	39.5775	49.2759	62.8379	80.5261	-266.1463	-274.7131	

Table D-3. Continued



PHASE REL TO ETA AT X=0 - DEG -78.1752 -139.3989 -143.3115 -145.2759 -140.4794 -136.7280 -117.1690 -99.4609 -86.1399 -94.0012  
 REFLECTED BY FWD ROV/ETA .1190 .0163 .9230 .9491 .9529 .9543 .9551 .9546 .9576 .9582  
 PHASE REL TO ETA AT X=0 - DEG 63.7635 149.0773 124.1707 117.3206 114.2930 122.8550 129.8806 145.6856 170.5966 -174.4339  
 TOTAL REFLECTED/ETA .0946 .3707 .4353 .6777 .7417 .7647 .8026 .8897 .9538 .9752  
 PHASE REL TO ETA AT X=0 - DEG -65.9434 -166.6858 -172.9573 167.8642 154.6875 152.8944 159.6557 163.2463 172.2152 -177.7925

# MOORING LINE MODEL RESULTS

## SHOREWARD MOORING LINE

CHANGE IN FORCE PER UNIT DISPLACEMENT IN SWAY, HEAVE AND ROLL, RESPECTIVELY --1376.0000 410.6000 -1607.0000

## MOORING LINE RESPONSE

FORCE AMPLITUDE/ETA 1.328E+03 6.340E+02 3.409E+02 1.724E+02 3.242E+02 4.559E+02 3.342E+02 2.179E+02 7.924E+01 8.660E+01  
 PHASE REL TO ETA AT X=0 - DEG 16.5361 10.4163 95.8873 -66.3177 -51.4041 -38.4782 -28.3381 -13.7787 -4.3807 -135.5998  
 FORCE AMPLITUDE/ROEG\*G\*AREA\*ETA 1.644E+00 7.859E-01 4.716E-01 1.639E-01 4.015E-01 4.407E-01 4.139E-01 2.698E-01 9.317E-02 1.072E-01

# MOORING LINE MODEL RESULTS

## SEAWARD MOORING LINE

CHANGE IN FORCE PER UNIT DISPLACEMENT IN SWAY, HEAVE AND ROLL, RESPECTIVELY - 1172.0000 286.9000 1713.0000

## MOORING LINE RESPONSE

FORCE AMPLITUDE/ETA 1.197E+03 8.884E+02 9.474E+02 8.708E+02 6.718E+02 5.511E+02 4.595E+02 2.905E+02 1.471E+02 4.829E+01  
 PHASE REL TO ETA AT X=0 - DEG 143.6852 143.5624 146.2269 155.1982 171.4939 172.9785 172.7651 177.2141 177.8580 93.7362  
 FORCE AMPLITUDE/ROEG\*G\*AREA\*ETA 1.483E+00 1.100E+00 1.187E+00 1.098E+00 8.319E-01 6.824E-01 5.690E-01 3.799E-01 1.421E-01 6.103E-02

Table D-3. Continued

## APPENDIX E

### DERIVATION OF PRESSURE TO SECOND ORDER FOR TWO PROGRESSIVE WAVES AT DIFFERENT FREQUENCIES

Consider the problem of the nonlinear interactions of waves at two distinct frequencies traveling in the same direction. The complete boundary value problem is well known.

The Laplace equation,

$$\nabla^2 \phi = 0, \quad (\text{E-1})$$

applies throughout the fluid below the free surface.

The boundary condition,

$$\frac{\partial^2 \phi}{\partial t^2} + g \frac{\partial \phi}{\partial y} + 2 \nabla \phi \cdot \nabla \frac{\partial \phi}{\partial t} + \frac{1}{2} \nabla \phi \cdot \nabla (\nabla \phi \cdot \nabla \phi) = 0, \quad (\text{E-2})$$

must be satisfied on the free surface,  $y = \eta$ . The boundary condition on the bottom is:

$$\lim_{y \rightarrow -\infty} \frac{\partial \phi}{\partial y} = 0 \quad (\text{E-3})$$

for an infinitely deep fluid. In addition a radiation condition requiring the generated waves to travel away from the body is needed to ensure uniqueness of the solution.

In this formulation the  $x$  axis lies in the direction of incident wave propagation.

The difficulty in solving this boundary value problem stems from the nonlinearity of the free-surface boundary condition.

In order to "linearize" the free-surface boundary condition, expand the velocity potential,  $\phi$ , in a Taylor series about the undisturbed free surface:

$$\begin{aligned} \phi(x, \eta, t) &= \phi(x, 0, t) \\ &+ \eta \left[ \frac{\partial \phi(x, y, t)}{\partial y} \right]_{y=0} + \frac{1}{2} \eta^2 \left[ \frac{\partial^2 \phi(x, y, t)}{\partial y^2} \right]_{y=0} + O(\eta^3). \end{aligned} \quad (\text{E-4})$$

Also expand  $\eta$  and  $\phi$  in power series:

$$\begin{aligned} \eta(x, t) &= \epsilon \eta^{(1)}(x, t) + \epsilon^2 \eta^{(2)}(x, t) + O(\epsilon^3), \\ \phi(x, y, t) &= \epsilon \phi^{(1)}(x, y, t) + \epsilon^2 \phi^{(2)}(x, y, t) + O(\epsilon^3). \end{aligned} \quad (\text{E-5})$$



Substituting the expansion for  $\phi$  into the free-surface boundary condition:

$$\begin{aligned}
 & \epsilon \frac{\partial^2 \phi^{(1)}(x, y, t)}{\partial t^2} + \epsilon^2 \frac{\partial^2 \phi^{(2)}}{\partial t^2} + g\epsilon \frac{\partial \phi^{(1)}}{\partial y} + g\epsilon^2 \frac{\partial \phi^{(2)}}{\partial y} \\
 & + 2\left[\epsilon \left\{ \frac{\partial \phi^{(1)}}{\partial x} \hat{i} + \frac{\partial \phi^{(1)}}{\partial y} \hat{j} \right\} + \epsilon^2 \left\{ \frac{\partial \phi^{(2)}}{\partial x} \hat{i} + \frac{\partial \phi^{(2)}}{\partial y} \hat{j} \right\}\right] \cdot \\
 & \left[ \hat{i} \frac{\partial}{\partial x} + \hat{j} \frac{\partial}{\partial y} \right] \left[ \epsilon \frac{\partial \phi^{(1)}}{\partial t} + \epsilon^2 \frac{\partial \phi^{(2)}}{\partial t} \right] \\
 & + \frac{1}{2} \left[ \epsilon \frac{\partial \phi^{(1)}}{\partial x} \hat{i} + \frac{\partial \phi^{(1)}}{\partial y} \hat{j} \right] + \epsilon^2 \left\{ \frac{\partial \phi^{(2)}}{\partial x} \hat{i} + \frac{\partial \phi^{(2)}}{\partial y} \hat{j} \right\} \cdot \\
 & \left[ \hat{i} \frac{\partial}{\partial x} + \hat{j} \frac{\partial}{\partial y} \right] \left[ \epsilon \left\{ \frac{\partial \phi^{(1)}}{\partial x} \hat{i} + \frac{\partial \phi^{(1)}}{\partial y} \hat{j} \right\} + \epsilon^2 \left\{ \frac{\partial \phi^{(2)}}{\partial x} \hat{i} + \frac{\partial \phi^{(2)}}{\partial y} \hat{j} \right\} \right] \cdot \\
 & \left[ \epsilon \left\{ \frac{\partial \phi^{(1)}}{\partial x} \hat{i} + \frac{\partial \phi^{(1)}}{\partial y} \hat{j} \right\} + \epsilon^2 \left\{ \frac{\partial \phi^{(2)}}{\partial x} \hat{i} + \frac{\partial \phi^{(2)}}{\partial y} \hat{j} \right\} \right] + O(\epsilon^3) = 0 \quad (E-6)
 \end{aligned}$$

on  $y = \eta$ .

Now use the Taylor expansion for  $\phi(x, \eta, t)$  and neglect terms of order  $\epsilon^3$  in the boundary condition:

$$\begin{aligned}
 & \epsilon \left\{ \frac{\partial^2 \phi^{(1)}(x, 0, t)}{\partial t^2} + \epsilon \eta^{(1)}(x, t) \frac{\partial^3 \phi^{(1)}}{\partial y \partial t^2} \right\} + \epsilon^2 \frac{\partial^2 \phi^{(2)}}{\partial t^2} \\
 & + g\epsilon \left\{ \frac{\partial \phi^{(1)}}{\partial y} + \epsilon \eta^{(1)}(x, t) \frac{\partial^2 \phi^{(1)}}{\partial y^2} \right\} + g\epsilon^2 \frac{\partial \phi^{(2)}}{\partial y} \\
 & + 2\epsilon^2 \left[ \frac{\partial \phi^{(1)}}{\partial x} \frac{\partial^2 \phi^{(1)}}{\partial t \partial x} + \frac{\partial \phi^{(1)}}{\partial y} \frac{\partial^2 \phi^{(1)}}{\partial t \partial y} \right] + O(\epsilon^3) = 0. \quad (E-7)
 \end{aligned}$$

Grouping terms by order:

First Order  $\epsilon$ :

$$\frac{\partial^2 \phi^{(1)}}{\partial t^2} + g \frac{\partial \phi^{(1)}}{\partial y} = 0 \quad \text{on } y = 0. \quad (E-8)$$

Second Order  $\epsilon^2$ :

$$\begin{aligned}
 & \frac{\partial^2 \phi^{(2)}}{\partial t^2} + g \frac{\partial \phi^{(2)}}{\partial y} + \eta^{(1)} \frac{\partial}{\partial y} \left\{ \frac{\partial^2 \phi^{(1)}}{\partial t^2} + g \frac{\partial \phi^{(1)}}{\partial y} \right\} + 2 \frac{\partial \phi^{(1)}}{\partial x} \frac{\partial^2 \phi^{(1)}}{\partial x \partial t} \\
 & + 2 \frac{\partial \phi^{(1)}}{\partial y} \frac{\partial \phi^{(1)}}{\partial y \partial t} = 0 \quad \text{on } y = 0. \quad (E-9)
 \end{aligned}$$

Using the dynamic boundary condition on the free surface, one finds:

$$\eta(x,t) = -\frac{1}{g} \left\{ \frac{\partial \phi}{\partial t} + \frac{1}{2} \nabla \phi \cdot \nabla \phi \right\} \text{ on } y = \eta. \quad (\text{E-10})$$

Substituting the expansions into this equation yields:

$$\begin{aligned} \epsilon \eta^{(1)}(x,t) + \epsilon^2 \eta^{(2)} + O(\epsilon^3) &= -\frac{1}{g} \left\{ \frac{\partial \phi}{\partial t} + \frac{1}{2} \nabla \phi \cdot \nabla \phi \right\}_{y=0} \\ &- \frac{\eta}{g} \frac{\partial}{\partial y} \left\{ \frac{\partial \phi}{\partial t} + \frac{1}{2} \nabla \phi \cdot \nabla \phi \right\}_{y=0} + O(\eta^2). \end{aligned} \quad (\text{E-11})$$

Substituting for  $\phi$ , the right-hand side becomes:

$$\begin{aligned} &= -\frac{1}{g} \left\{ \epsilon \frac{\partial \phi^{(1)}}{\partial t} + \epsilon^2 \frac{\partial \phi^{(2)}}{\partial t} + \frac{\epsilon^2}{2} \left[ \left( \frac{\partial \phi^{(1)}}{\partial x} \right)^2 + \left( \frac{\partial \phi^{(1)}}{\partial y} \right)^2 \right] \right\} \\ &- \frac{\epsilon^2 \eta^{(1)}}{g} \left\{ \frac{\partial^2 \phi^{(1)}}{\partial y \partial t} \right\} + O(\epsilon^3), \text{ on } y = 0. \end{aligned}$$

First Order  $\epsilon$ :

$$\eta^{(1)}(x,t) = -\frac{1}{g} \frac{\partial \phi^{(1)}(x,0,t)}{\partial t}. \quad (\text{E-12})$$

Second Order  $\epsilon^2$ :

$$\begin{aligned} \eta^{(2)}(x,t) &= -\frac{1}{g} \left\{ \eta^{(1)} \frac{\partial^2 \phi^{(1)}}{\partial y \partial t} + \frac{\partial \phi^{(1)}}{\partial t} \right\} - \frac{1}{2g} \left\{ \left( \frac{\partial \phi^{(1)}}{\partial x} \right)^2 + \left( \frac{\partial \phi^{(1)}}{\partial y} \right)^2 \right\} \\ &\text{on } y = 0 \end{aligned}$$

or

$$\begin{aligned} \eta^{(2)}(x,t) &= -\frac{1}{g} \left\{ -\frac{1}{g} \frac{\partial \phi^{(1)}}{\partial t} \frac{\partial^2 \phi^{(1)}}{\partial y \partial t} + \frac{\partial \phi^{(2)}}{\partial t} \right\} - \frac{1}{2g} \left\{ \left( \frac{\partial \phi^{(1)}}{\partial x} \right)^2 \right. \\ &\left. + \left( \frac{\partial \phi^{(1)}}{\partial y} \right)^2 \right\} \text{ on } y = 0. \end{aligned} \quad (\text{E-13})$$

Using the first-order relationship above in the second-order boundary condition on the free surface (E-9), one finds:

$$\begin{aligned} \frac{\partial^2 \phi^{(2)}}{\partial t^2} + g \frac{\partial \phi^{(2)}}{\partial y} &= +\frac{1}{g} \frac{\partial \phi^{(1)}}{\partial t} \frac{\partial}{\partial y} \left\{ \frac{\partial^2 \phi^{(1)}}{\partial t^2} + g \frac{\partial \phi^{(1)}}{\partial y} \right\} \\ &- 2 \frac{\partial \phi^{(1)}}{\partial x} \frac{\partial^2 \phi^{(1)}}{\partial x \partial t} - 2 \frac{\partial \phi^{(1)}}{\partial y} \frac{\partial^2 \phi^{(1)}}{\partial y \partial t} \end{aligned} \quad (\text{E-14})$$



1. First-Order Solution of the Boundary Value Problem.

This solution results from the superposition of the velocity potentials for individual waves:

$$\begin{aligned}\phi^{(1)}(x,y,t) &= \frac{gA_1}{\omega_1} e^{k_1 y} \cos(k_1 x - \omega_1 t + \delta_1) \\ &+ \frac{gA_2}{\omega_2} e^{k_2 y} \cos(k_2 x - \omega_2 t + \delta_2).\end{aligned}\quad (E-15)$$

Check the solution:

$$\begin{aligned}\nabla^2 \phi^{(1)} &= 0. \\ \lim_{y \rightarrow -\infty} \frac{\partial \phi^{(1)}}{\partial y} &\rightarrow 0 \text{ because of exponential function.} \\ \frac{\partial^2 \phi^{(1)}}{\partial t^2} + g \frac{\partial \phi^{(1)}}{\partial y} &= -g\omega_1 A_1 e^{k_1 y} \cos(k_1 x - \omega_1 t + \delta_1) \\ &- g\omega_2 A_2 e^{k_2 y} \cos(k_2 x - \omega_2 t + \delta_2) \\ &+ g\{\omega_1 A_1 e^{k_1 t} \cos(k_1 x - \omega_1 t + \delta_1) \\ &+ \omega_2 A_2 e^{k_2 y} \cos(k_2 x - \omega_2 t + \delta_2)\} = 0.\end{aligned}$$

Therefore, this is a solution.

Surface elevation then becomes:

$$\begin{aligned}\eta^{(1)}(x,t) &= -\frac{1}{g} \frac{\partial \phi^{(1)}(x,0,t)}{\partial t} = -A_1 \sin(k_1 x - \omega_1 t + \delta_1) \\ &- A_2 \sin(k_2 x - \omega_2 t + \delta_2).\end{aligned}\quad (E-16)$$

To prepare for the second-order solution, construct the right-hand side of the free-surface boundary condition (E-14):

$$\begin{aligned}&\left[ \frac{1}{2} \frac{\partial \phi^{(1)}}{\partial t} \frac{\partial}{\partial y} \left\{ \frac{\partial^2 \phi^{(1)}}{\partial t^2} + g \frac{\partial \phi^{(1)}}{\partial y} \right\} - 2 \frac{\partial \phi^{(1)}}{\partial x} \frac{\partial^2 \phi^{(1)}}{\partial x \partial t} \right. \\ &\left. - 2 \frac{\partial \phi^{(1)}}{\partial y} \frac{\partial^2 \phi^{(1)}}{\partial y \partial t} \right]_{y=0} = \frac{1}{g} \{ gA_1 \sin(k_1 x - \omega_1 t + \delta_1) \\ &+ gA_2 \sin(k_2 x - \omega_2 t + \delta_2) \} \{0\} - 2 \{ -\omega_1 A_1 \sin(k_1 x - \omega_1 t + \delta_1) \} \quad (E-17)\end{aligned}$$

$$\begin{aligned}
& - \omega_2 A_2 \sin(k_2 x - \omega_2 t + \delta_2) \} \times \{ \omega_1^2 A_1 \cos(k_1 x - \omega_1 t + \delta_1) \\
& + \omega_2^2 A_2 \cos(k_2 x - \omega_2 t + \delta_2) \} - 2 \{ \omega_1 A_1 \cos(k_1 x - \omega_1 t + \delta_1) \\
& + \omega_2 A_2 \cos(k_2 x - \omega_2 t + \delta_2) \} \times \{ \omega_1^2 A_1 \sin(k_1 x - \omega_1 t + \delta_1) \\
& + \omega_2^2 A_2 \sin(k_2 x - \omega_2 t + \delta_2) \} = 0.
\end{aligned}$$

Since this condition is homogeneous, the first-order potential is the solution to the second-order problem.

## 2. Second-Order Results.

The free-surface elevation will be modified when terms of second order are included:

$$\begin{aligned}
\eta^{(2)}(x, t) &= \frac{1}{g} \left\{ \frac{\partial \phi^{(1)}}{\partial t} \frac{\partial^2 \phi^{(1)}}{\partial y \partial t} \right\} - \frac{1}{2g} \left\{ \left( \frac{\partial \phi^{(1)}}{\partial x} \right)^2 + \left( \frac{\partial \phi^{(1)}}{\partial y} \right)^2 \right\} \Big|_{y=0} \\
&= + \frac{1}{g} \{ g A_1 \sin(k_1 x - \omega_1 t + \delta_1) + g A_2 \sin(k_2 x - \omega_2 t + \delta_2) \} \times \\
&\quad \{ A_1 \omega_1^2 \sin(k_1 x - \omega_1 t + \delta_1) + A_2 \omega_2^2 \sin(k_2 x - \omega_2 t + \delta_2) \} \\
&\quad - \frac{1}{2g} \{ [- \omega_1 A_1 \sin(k_1 x - \omega_1 t + \delta_1) - \omega_2 A_2 \sin(k_2 x - \omega_2 t + \delta_2)]^2 \\
&\quad + [\omega_1 A_1 \cos(k_1 x - \omega_1 t + \delta_1) + \omega_2 A_2 \cos(k_2 x - \omega_2 t + \delta_2)]^2 \}
\end{aligned}$$

or

$$\begin{aligned}
g \eta^{(2)}(x, t) &= \omega_1^2 A_1^2 \sin^2(k_1 x - \omega_1 t + \delta_1) \\
&\quad + \omega_1^2 A_1 A_2 \sin(k_2 x - \omega_2 t + \delta_2) \sin(k_1 x - \omega_1 t + \delta_1) \\
&\quad + \omega_2^2 A_1 A_2 \sin(k_1 x - \omega_1 t + \delta_1) \sin(k_2 x - \omega_2 t + \delta_2) \\
&\quad + \omega_2^2 A_2^2 \sin^2(k_2 x - \omega_2 t + \delta_2) \\
&\quad + \frac{1}{2} \{ \omega_1^2 A_1^2 \sin^2(k_1 x - \omega_1 t + \delta_1) \\
&\quad + 2 \omega_1 \omega_2 A_1 A_2 \sin(k_1 x - \omega_1 t + \delta_1) \sin(k_2 x - \omega_2 t + \delta_2)
\end{aligned}$$



$$\begin{aligned}
& + \omega_2^2 A_2^2 \sin^2(k_2 x - \omega_2 t + \delta_2) \\
& + \omega_1^2 A_1^2 \cos^2(k_1 x_1 - \omega_1 t + \delta_1) \\
& + 2\omega_1 \omega_2 A_1 A_2 \cos(k_1 x - \omega_1 t + \delta_1) \cos(k_2 x - \omega_2 t + \delta_2) \\
& + \omega_2^2 A_2^2 \cos^2(k_2 x - \omega_2 t + \delta_2).
\end{aligned}$$

Using the trigonometric relationships:

$$\begin{aligned}
g\eta^2(x, t) &= \omega_1^2 A_1^2 \sin^2(k_1 x - \omega_1 t + \delta_1) + \omega_2^2 A_2^2 \sin^2(k_2 x - \omega_2 t + \delta_2) \\
&+ \frac{1}{2} \omega_1^2 A_1 A_2 \{ \cos[(k_1 - k_2)x - (\omega_1 - \omega_2)t + \delta_1 - \delta_2] \\
&- \cos[(k_1 + k_2)x - (\omega_1 + \omega_2)t + \delta_1 + \delta_2] \} \\
&+ \frac{1}{2} \omega_2^2 A_1 A_2 \{ \cos[(k_1 - k_2)x - (\omega_1 - \omega_2)t + \delta_1 - \delta_2] \\
&- \cos[(k_1 + k_2)x - (\omega_1 + \omega_2)t + \delta_1 + \delta_2] \} \\
&- \frac{1}{2} \{ \omega_1^2 A_1^2 + \omega_2^2 A_2^2 \} - \omega_1 \omega_2 A_1 A_2 \cos[(k_1 - k_2)x \\
&- (\omega_1 - \omega_2)t + \delta_1 - \delta_2].
\end{aligned}$$

Combining further:

$$\begin{aligned}
g\eta^{(2)}(x, t) &= -\frac{1}{2} \omega_1^2 A_1^2 \cos[2\{k_1 x - \omega_1 t + \delta_1\}] \\
&- \frac{1}{2} \omega_2^2 A_2^2 \cos[2\{k_2 x - \omega_2 t + \delta_2\}] \quad (E-18) \\
&- \frac{1}{2} (\omega_1^2 + \omega_2^2) A_1 A_2 \cos[(k_1 + k_2)x - (\omega_1 + \omega_2)t + \delta_1 + \delta_2] \\
&+ \frac{1}{2} (\omega_1^2 - 2\omega_1 \omega_2 + \omega_2^2) A_1 A_2 \cos[(k_1 - k_2)x - (\omega_1 - \omega_2)t + \delta_1 - \delta_2],
\end{aligned}$$

which is the final form for the second-order term for free-surface elevation.

Now, turn to the equation for pressure which is necessary to compute the force on the body.

Take the pressure to be zero at the free surface. Then Bernoulli's equation may be written:

$$P = -\rho \frac{\partial \phi}{\partial t} - \frac{1}{2} \rho \nabla \phi \cdot \nabla \phi - \rho g y. \quad (E-19)$$

Substituting the expansion for  $\phi$ :

$$P = -\rho \left\{ \epsilon \frac{\partial \phi^{(1)}}{\partial t} + \epsilon^2 \frac{\partial \phi^{(2)}}{\partial t} + \frac{1}{2} \left[ \epsilon^2 \left( \frac{\partial \phi^{(1)}}{\partial x} \right)^2 + \epsilon^2 \left( \frac{\partial \phi^{(1)}}{\partial y} \right)^2 \right] + g y \right\} + O(\epsilon^3).$$

Since  $\phi^{(2)} = 0$ , we can drop this term and proceed to separate the equation by order:

$$P^{(1)} = -\rho \frac{\partial \phi^{(1)}}{\partial t} - \rho g y \quad (E-20)$$

and

$$P^{(2)} = -\frac{\rho}{2} \left[ \left( \frac{\partial \phi^{(1)}}{\partial x} \right)^2 + \left( \frac{\partial \phi^{(1)}}{\partial y} \right)^2 \right]. \quad (E-21)$$

Substituting the velocity potential into the equation, one finds:

$$P^{(1)} = -\rho g \{ A_1 e^{k_1 y} \sin(k_1 x - \omega_1 t + \delta_1) + A_2 e^{k_2 y} \sin(k_2 x - \omega_2 t + \delta_2) + y \} \quad (E-22)$$

for the first order, and

$$P^{(2)} = -\frac{\rho}{2} \{ [-\omega_1 A_1 e^{k_1 y} \sin(k_1 x - \omega_1 t + \delta_1) - \omega_2 A_2 e^{k_2 y} \sin(k_2 x - \omega_2 t + \delta_2)]^2 + [\omega_1 A_1 e^{k_1 y} \cos(k_1 x - \omega_1 t + \delta_1) + \omega_2 A_2 e^{k_2 y} \cos(k_2 x - \omega_2 t + \delta_2)]^2 \}$$

for the second order. Note that this is identical to part of the



equation for surface elevation. The second-order pressure may be reduced to:

$$p^{(2)} = -\frac{\rho}{2} \{ \omega_1^2 A_1^2 e^{2k_1 y} + \omega_2^2 A_2^2 e^{2k_2 y} - 2\omega_1 \omega_2 A_1 A_2 e^{(k_1 + k_2)y} \cos[(k_1 - k_2)x - (\omega_1 - \omega_2)t + \delta_1 - \delta_2] \} \quad (E-23)$$

which indicates that the second-order pressure is composed of a component independent of time and at the "difference frequency".

This is surprising since the equation for the free-surface elevation (eq. 18) includes terms at twice the incident wave frequencies and at the sum of these two frequencies. Using trigonometric relationships the first two terms in equation (E-23) could be expanded to yield terms at twice the incident wave frequency. A term at the sum of the two incident wave frequencies may appear in the pressure computed using the velocity potentials representing wave diffraction or forced oscillation. It might also appear if the present analysis were carried to the third order. The derivation included here was intended to reveal the presence of a low-frequency component in the exciting force and has not been used to determine the other velocity potentials or carried beyond the second order.

### 3. List of Special Symbols for Appendix E.

$A_1, A_2$	= Wave amplitudes
$g$	= Acceleration of gravity
$k_1, k_2$	= Wave numbers, $\frac{\omega_1}{g}$ , $\frac{\omega_2}{g}$ , respectively
$x, y$	= Cartesian coordinates (x-directed parallel to the direction of wave propagation, y-directed vertically upward)
$\delta_1, \delta_2$	= Wave phase angles
$\eta(x, t)$	= Free-surface elevation
$\phi(x, y, t)$	= Velocity potential
$\omega_1, \omega_2$	= Wave circular frequencies

## APPENDIX F

### PHYSICAL PROPERTIES OF SEVERAL FLOATING BREAKWATERS

1. Proposed Oak Harbor Floating Breakwater (Davidson, 1971).

a. Physical Properties.

$$m = \text{mass per unit length} = 25.1 \text{ slug/ft}$$

$$I = \text{mass moment of inertia} = 621 \text{ slug-ft}^2/\text{ft}$$

$$x_g = \text{x-coordinate of center of gravity} = 0.0 \text{ ft.} \\ (\text{on centerline})$$

$$y_g = \text{y-coordinate of center of gravity} = -2.34 \text{ ft (below WL)}$$

$$KH_{22} = 64.5 \text{ lb/ft/ft}$$

$$KH_{33} = 1,165 \text{ ft-lb/ft}$$

$$\text{All other } KH_{ij} = 0$$

b. Mooring Line Tension Response (change per unit displacement).

$$\frac{\Delta T}{\Delta x} = 1,170 \text{ lb/ft}$$

$$\frac{\Delta T}{\Delta y} = 281 \text{ lb/ft}$$

$$\frac{\Delta T}{\Delta \theta} = 1,710 \text{ lb}$$

c. Computed Mooring Spring Constants (depth = 29.5 feet)

$$KM_{11} = 119 \text{ lb/ft/ft}$$

$$KM_{12} = -5.24 \text{ lb/ft/ft}$$

$$KM_{13} = 166 \text{ lb/ft}$$

$$KM_{21} = -5.73 \text{ lb/ft/ft}$$

$$KM_{22} = 10.2 \text{ lb/ft/ft}$$

$$KM_{23} = -3.37 \text{ lb/ft}$$

$$KM_{31} = 160 \text{ lb/ft}$$

$$KM_{32} = 2.06 \text{ lb/ft}$$



$$KM_{33} = 282. \text{ ft-lb/ft}$$

Rectangular Breakwater Tested by Nece and Richey (1972).

Physical Properties (at prototype scale). The cross section is a rectangle of beam 10 feet and draft 5 feet.

$$m = .100 \text{ slugs/ft}$$

$$I = 2,740 \text{ slug-ft}^2/\text{ft}$$

$$x_g = 0.0 \text{ ft (on centerline)}$$

$$y_g = -1.0 \text{ ft (below WL)}$$

$$KH_{22} = 640 \text{ lb/ft/ft}$$

$$KH_{33} = 5,340 \text{ ft-lb/ft}$$

$$\text{All other } KH_{ij} = 0$$

$$\text{All } KM_{ij} = 0.$$

Rectangular Breakwater Tested by Sutko and Haden (1974).

Physical Properties of Model. The cross section is a rectangle of beam 0.333 feet and draft 0.222 feet.

$$m = 0.143 \text{ slug/ft}$$

$$I = 0.023 \text{ slug-ft}^2/\text{ft}$$

$$x_g = 0.0 \text{ ft (on centerline)}$$

$$y_g = -0.123 \text{ ft (below WL)}$$

$$KH_{22} = 20.7 \text{ lb/ft/ft}$$

$$KH_{33} = 0.244 \text{ ft-lb/ft}$$

$$\text{All other } KH_{ij} = 0$$

$$\text{All } KM_{ij} = 0$$

Alaska-Type Breakwater.

a. Physical Properties.

$$m = 62.3 \text{ slug/ft}$$

$$\begin{aligned}
 I &= 4,234 \text{ slug-ft/ft} \\
 x_g &= 0.0 \text{ ft} \\
 y_g &= -1.3 \text{ ft (below WL)} \\
 KH_{22} &= 528 \text{ lb/ft/ft} \\
 KH_{33} &= 32,885 \text{ ft-lb/ft} \\
 \text{All other } KH_{ij} &= 0
 \end{aligned}$$

b. Mooring Line Tension Response (change per unit displacement).

$$\frac{\Delta T}{\Delta x} = 97.0 \text{ lb/ft}$$

$$\frac{\Delta T}{\Delta y} = 90.5 \text{ lb/ft}$$

$$\frac{\Delta T}{\Delta \theta} = -572 \text{ lb}$$

c. Computed Mooring Spring Constants (tide = +7.0 feet).

$$KM_{11} = 3.0 \text{ lb/ft/ft}$$

$$KM_{12} = 0.245 \text{ lb/ft/ft}$$

$$KM_{13} = -9.23 \text{ lb/ft}$$

$$KM_{21} = 0.302 \text{ lb/ft/ft}$$

$$KM_{22} = 1.91 \text{ lb/ft/ft}$$

$$KM_{23} = -2.68 \text{ lb/ft}$$

$$KM_{31} = -9.52 \text{ lb/ft}$$

$$KM_{32} = -2.82 \text{ lb/ft}$$

$$KM_{33} = 88.9 \text{ ft-lb/ft}$$

5. Friday Harbor Breakwater.

a. Physical Properties.

$$m = 61.02 \text{ slugs/ft}$$

$$I = 4,160 \text{ slugs-ft}^3/\text{ft}$$



$$x_g = 0.0 \text{ ft (on centerline)}$$

$$y_g = -0.49 \text{ ft (below WL)}$$

$$KH_{22} = 884 \text{ lb/ft/ft}$$

$$KH_{33} = 55,610 \text{ ft-lb/ft}$$

$$\text{All other } KH_{ij} = 0$$

b. Mooring Line Tension Response.

$$\frac{\Delta T}{\Delta x} = 222 \text{ lb/ft}$$

$$\frac{\Delta T}{\Delta y} = 25.0 \text{ lb/ft}$$

$$\frac{\Delta T}{\Delta \theta} = 657 \text{ lb}$$

c. Computed Mooring Spring Constants (tide = +5.33 feet).

$$KM_{11} = 6.46 \text{ lb/ft/ft}$$

$$KM_{12} = 0.510 \text{ lb/ft/ft}$$

$$KM_{13} = 18.5 \text{ ft-lb/ft/ft}$$

$$KM_{21} = 0.510 \text{ lb/ft/ft}$$

$$KM_{22} = 0.390 \text{ lb/ft/ft}$$

$$KM_{23} = 1.71 \text{ ft-lb/ft/ft}$$

$$KM_{31} = 18.6 \text{ lb/ft}$$

$$KM_{32} = 1.71 \text{ lb/ft}$$

$$KM_{33} = 64.6 \text{ ft-lb/ft}$$

## APPENDIX G

### DATA SUMMARY SHEETS FOR FRIDAY HARBOR FLOATING BREAKWATER (WINTER 1975)

Appendix G contains a summary of all the data recorded at the Friday Harbor breakwater during the winter season of 1975. Seven tapes were recorded during this period, with a total of 95 records. The tapes are numbered in sequence from FH7-1 through FH13-8. The date of each tape is given along with the pertinent statistical data for each record in the tapes. The number of days and hours given for each record begins with the day and hour given for that particular tape.

All minimum and maximum values are measured from zero mean. The transmitted wave data were digitally high-pass filtered (cutoff frequency was 0.05 hertz) before these calculations to remove tidal draft.



SUMMARY OF STATISTICAL DATA FOR FRIDAY HARBOR FLOATING BREAKWATER (FH7 - 1330 - 12/30/74)  
 (MAX. AND MIN. VALUES MEASURED FROM ZERO MEAN)  
 SAMPLING PERIOD = 500 MS  
 NUMBER OF SAMPLES = 2047

REC. TIME NO. IN DAYS AND HOURS	TRANS. COEF.	WIND		LOAD CELLS		SE TRAN		WAVE GAGES		ACCELEROMETERS	
		SP.	DIR.	NW	SW	NE	SE	TRAN 1	TRAN 2	INC.	REF. M. VER.
		MPH	DEG.	LBS	LBS	LBS	LBS	FT.	FT.	FT.	FT.
1	0	MAX.	2.8	58.1	39.10	30.90	31.92	17.55	.113	.110	.297
		MIN.	-2.1	-57.4	-20.90	-33.10	-16.08	-18.79	-.137	-.133	-.317
		MEAN	2.1	109.9	.00	981.12	896.26	959.38	6.938	7.226	4.118
		STDEV	1.06	27.87	9.155	9.611	7.016	6.077	.0385	.0367	.0848
2	20	MAX.	8.1	60.7	57.90	161.55	42.34	96.34	.167	.181	.742
		MIN.	-11.2	-65.3	-78.10	-110.45	-37.66	-60.62	-.176	-.296	-.487
		MEAN	14.1	180.3	.00	1181.83	930.07	11370.02	7.630	7.509	4.058
		STDEV	3.62	14.27	24.055	51.877	14.026	30.339	.0534	.0553	.1519
3	21	MAX.	13.2	93.2	75.58	325.98	66.36	193.09	.135	.128	.766
		MIN.	-7.7	-95.8	-12.42	-174.02	-53.64	-84.99	-.153	-.162	-.540
		MEAN	17.6	178.5	55.01	1161.24	887.82	1025.22	5.990	5.834	4.034
		STDEV	3.27	19.83	16.689	65.078	13.839	38.005	.0444	.0469	.1626
4	3	MAX.	11.8	51.7	75.58	445.25	43.05	278.10	.205	.205	.823
		MIN.	-9.7	-116.3	-12.42	-182.75	-40.95	-112.16	-.156	-.176	-.559
		MEAN	21.6	178.7	1.63	1075.80	799.38	1027.13	5.174	4.994	4.080
		STDEV	3.93	24.09	.000	89.072	14.051	55.777	.0683	.0673	.1715
5	3	MAX.	14.1	61.9	15.65	333.14	47.80	221.94	.183	.204	.778
		MIN.	-9.6	-95.6	-3.35	-228.86	-60.20	-128.83	-.172	-.156	-.502
		MEAN	20.5	189.5	3.08	1069.49	719.23	952.61	5.093	4.908	4.150
		STDEV	3.91	19.78	2.037	97.282	16.930	61.033	.0567	.0598	.1687
6	5	MAX.	8.2	57.2	40.51	156.49	23.37	90.27	.093	.137	.802
		MIN.	-5.6	-68.8	-35.49	-95.51	-36.63	-47.19	-.113	-.107	-.452
		MEAN	16.2	172.9	120.45	990.62	874.81	904.88	5.526	5.300	4.024
		STDEV	2.89	14.72	18.688	50.922	11.194	27.538	.0328	.0334	.1743

# SUMMARY OF STATISTICAL DATA FOR FRIDAY HARBOR FLOATING BREAKWATER (FHT - 1330 - 12/30/74)

(MAX. AND MIN. VALUES MEASURED FROM ZERO MEAN)

SAMPLING PERIOD = 200 MS

NUMBER OF SAMPLES = 2047

REC. TIME NO. IN DAYS AND HOURS	TRANS. COEF.	WIND SP. MPH	WIND DIR. DEG.	LOAD CELLS		NE LBS	SE TRAN 1		WAVE GAGES		ACCELEROMETERS	
				NW LBS	SW LBS		LBS	FT.	TRAN 2 FT.	INC. FT.	REF. N. VER. FT.	HOR. S. VER. (FT/SEC/SEC)
7	5	MAX.	12.7	70.3	259.79	50.95	162.78	.134	.181	1.047	1.182	.768
		MIN.	-8.1	-150.2	-212.21	-49.05	-112.14	-.138	-.140	-.643	-.917	-.828
		MEAN	22.9	150.2	1181.21	810.04	1104.56	5.670	5.452	4.035	4.668	13.223
		STDEV	3.50	37.11	82.997	14.872	46.791	.0395	.0422	.2216	.2427	.2034
8	11	MAX.	6.8	27.0	291.23	37.67	173.79	.137	.137	1.188	1.457	.769
		MIN.	-6.1	-67.5	-204.77	-42.33	-116.93	-.186	-.199	-.732	-.847	-.667
		MEAN	22.8	160.9	1143.02	733.83	1147.23	5.440	5.220	4.047	4.874	13.387
		STDEV	2.89	14.06	86.332	13.652	46.214	.0411	.0446	.2521	.2939	.1984
9	12	MAX.	12.4	47.8	362.35	34.46	197.82	.161	.142	.961	1.043	.498
		MIN.	-8.1	-109.7	-177.65	-33.54	-107.12	-.139	-.170	-.550	-.596	-.636
		MEAN	22.3	161.4	1094.26	804.04	1087.69	5.279	5.062	4.044	4.855	13.274
		STDEV	3.27	23.39	80.256	12.471	47.411	.0428	.0433	.2111	.2186	.1412
10	13	MAX.	11.5	62.5	397.52	48.77	283.36	.248	.221	.962	1.086	.474
		MIN.	-8.4	-126.5	-238.48	-47.23	-127.44	-.167	-.170	-.626	-.604	-.471
		MEAN	22.5	167.7	1196.93	732.67	1176.63	5.514	5.305	4.094	4.687	13.221
		STDEV	4.83	24.85	131.584	19.011	82.184	.0481	.0510	.2037	.2414	.1262
11	14	MAX.	13.4	58.3	305.94	43.06	195.54	.163	.148	.904	.931	.322
		MIN.	-11.0	-88.7	-214.06	-44.94	-110.98	-.183	-.152	-.504	-.529	-.308
		MEAN	20.3	171.6	1143.02	804.64	1102.61	3.196	6.015	4.102	4.689	13.257
		STDEV	4.24	17.36	86.769	15.340	52.033	.0483	.0486	.1891	.2138	.1000
12	15	MAX.	13.1	54.1	306.05	41.58	191.57	.189	.186	.636	.603	.280
		MIN.	-7.1	-82.4	-117.95	-86.42	-70.71	-.169	-.159	-.439	-.549	-.245
		MEAN	17.7	175.7	1036.93	626.09	1015.94	7.264	7.108	4.062	4.683	13.227
		STDEV	3.84	16.70	62.609	19.570	38.895	.0639	.0638	.1440	.1499	.0708



SUMMARY OF STATISTICAL DATA FOR FRIDAY HARBOR FLOATING BREAKWATER (FHT - 1330 - 12/30/74)  
 (MAX. AND MIN. VALUES MEASURED FROM ZERO MEAN)  
 SAMPLING PERIOD - 500 MS  
 NUMBER OF SAMPLES - 2047

REC. TIME MO. IN DAYS AND HOURS	TRANS. COEF.	WIND		LOAD CELLS		SE TRAN 1		WAVE GAGES		ACCELEROMETERS	
		SP.	DIR.	NW	SW	NE	LBS	TRAN 2	INC.	REF. N.VER.	HOR. S.VER.
		MPH	DEG.	LBS	LBS	LBS	LBS	FT.	FT.	FT.	(FT/SEC/SEC)
13	7	MAX, 8.5	43.2	46.32	199.03	39.26	130.43	.111	.117	.663	.733
	21	MIN. -6.3	-61.8	-101.68	-104.97	-60.74	-127.11	-.122	-.128	-.437	-.496
		MEAN 17.5	156.1	287.74	1299.86	983.14	1305.05	7.195	9.069	4.060	4.656
14	7	MAX, 6.7	41.6	66.11	173.65	37.35	116.29	.150	.151	.768	.864
	22	MIN. -5.5	-84.4	-77.89	-86.35	-50.65	-55.93	-.378	-.434	-.512	-.544
		MEAN 18.3	147.0	200.76	1209.88	844.27	1185.52	8.776	8.632	4.160	4.730
15	8	MAX, 8.1	54.2	108.73	195.61	57.30	109.47	.183	.231	.747	.669
	0	MIN. -4.4	-103.3	-67.27	-148.39	-38.70	-78.55	-.205	-.223	-.456	-.457
		MEAN 18.9	124.3	.00	1182.50	822.80	1022.38	7.214	7.056	7.027	4.643
16	8	MAX, 12.6	39.2	33.70	328.02	44.49	193.38	.213	.233	.845	.877
	1	MIN. -7.0	-86.8	-2.30	-187.98	-47.51	-106.82	-.233	-.233	-.461	-.454
		MEAN 20.5	149.1	.00	1084.30	801.94	1070.00	5.437	5.227	4.057	4.640
17	8	MAX, 9.2	34.8	33.70	224.20	38.81	118.01	.197	.171	.666	.659
	3	MIN. -6.8	-59.7	-2.30	-147.80	-25.19	-74.75	-.206	-.208	-.435	-.419
		MEAN 20.0	164.1	.00	1082.30	748.74	918.50	3.663	3.397	4.006	4.602
18	8	MAX, 8.3	56.8	33.70	162.23	20.87	93.13	.177	.139	.634	.612
	4	MIN. -7.2	-79.7	-2.30	-117.77	-27.13	-44.33	-.123	-.115	-.390	-.412
		MEAN 14.5	183.5	.00	913.56	721.19	697.64	2.339	2.040	4.013	4.547
		MAX, 3.26	15.83	.000	47.441	7.594	21.849	.0429	.0434	.1401	.1333
		MIN.									
		MEAN									

SUMMARY OF STATISTICAL DATA FOR FAJDAY HARBOR FLOATING BREAKWATER (FHT - 1330 - 12/30/74)  
 (MAX. AND MIN. VALUES MEASURED FROM ZERO MEAN)  
 SAMPLING PERIOD - 500 MS  
 NUMBER OF SAMPLES - 2047

REC. TIME NO. IN DAYS AND HOURS	TRANS. COEF.	WIND		LOAD CELLS		SE TRAN		WAVE GAGES		ACCELEROMETERS	
		SP.	DIR.	NW	SW	NE	LBS	FT.	FT.	REF. N. VER.	HOR. S. VER.
		MPH	DEG.	LBS	LBS	LBS	LBS	FT.	FT.	FT.	(FT/SEC/SEC)
19	8	MAX. 9.1	51.0	54.07	197.81	35.50	78.93	.262	.234	.660	.283 .241 .488
		.55 MIN. -6.7	-64.5	-49.93	-182.19	-68.50	-66.43	-176	-179	-440	-305 -209 -527
	8	MEAN 14.7	179.4	117.10	956.60	848.57	789.76	5.050	4.829	4.677	13.361 13.744 12.879
		STDEV 3.01	13.88	21.840	41.586	14.847	20.752	.0937	.0845	.1669	.0908 .0640 .1067
20	0	MAX. 1.4	38.4	23.66	216.09	98.24	69.67	.083	.380	.179	.184 .111 .177
		.46 MIN. -1.8	-245.1	-.34	-15.91	-17.76	-36.19	-.070	-.140	-.171	-.988 -.081 -.246
	0	MEAN 2.9	245.1	.00	799.53	787.14	581.92	1.881	1.619	4.511	13.546 13.820 12.939
		STDEV .64	57.29	2.534	16.865	20.600	11.112	.0170	.0303	.0475	.1192 .0143 .0511



SUMMARY OF STATISTICAL DATA FOR FRIDAY HARBOUR FLOATING BREAKWATER (FH8 - 2400 - 1/8/75)  
 (MAX. AND MIN. VALUES MEASURED FROM ZERO MEAN)  
 SAMPLING PERIOD = 900 MS  
 NUMBER OF SAMPLES = 2047

REC. TIME NO. IN DAYS AND HOURS	TRANS. COEF.	WIND		LOAD CELLS		SE TRAN		WAVE GAGES		ACCELEROMETERS	
		SP.	DIR.	NW	SW	NE	LB	TRAN 1	TRAN 2	REF. N.VER.	HDR. S.VER.
		MPH	DEG.	LB	LB	LB	LB	FT.	FT.	FT.	(FT/SEC/SEC)
1	0	MAX.	1.8	32.9	24.96	80.24	8.72	.113	.109	.146	.078
	0	MIN.	-2.1	-325.1	-107.04	-15.76	-49.74	-.109	-.099	-.110	-.076
	0	MEAN	2.4	325.1	5099.04	794.73	4646.24	4.054	4.194	4.116	4.492
	0	STDEV	.79	65.65	23.966	10.425	10.748	.0075	.0073	.0407	.0235
2	2	MAX.	8.9	37.3	55.20	24.71	154.79	.102	.086	.607	.751
	18	MIN.	-6.8	-66.7	-76.80	-119.48	-27.29	-.199	-.183	-.366	-.520
	18	MEAN	18.0	157.3	676.80	911.50	920.16	2.412	2.611	4.091	4.536
	18	STDEV	3.12	15.47	24.306	66.479	31.996	.0236	.0235	.1381	.1536
3	2	MAX.	10.6	38.1	50.88	322.56	172.25	.097	.106	.701	.879
	19	MIN.	-6.4	-70.8	-57.12	-201.44	-94.77	-.093	-.097	-.451	-.606
	19	MEAN	20.2	165.3	625.12	917.44	987.93	.579	.826	4.049	4.433
	19	STDEV	3.17	13.98	19.813	99.539	53.237	.0266	.0269	.1607	.2025
4	2	MAX.	13.6	43.1	48.64	660.25	382.88	.130	.094	.634	.903
	20	MIN.	-10.5	-72.3	-71.36	-199.75	-94.28	-.090	-.092	-.416	-.556
	20	MEAN	20.1	177.5	607.36	859.75	910.68	-.555	-.552	3.936	4.394
	20	STDEV	4.75	14.76	22.521	141.836	76.751	.0277	.0256	.1428	.1856
5	2	MAX.	8.9	35.9	44.31	223.88	119.70	.078	.061	.576	.548
	22	MIN.	-6.5	-77.9	-55.69	-124.12	-55.68	-.062	-.060	-.448	-.476
	22	MEAN	17.1	171.8	623.69	808.12	812.97	-.073	.219	3.942	4.405
	22	STDEV	2.95	15.10	17.970	67.053	32.891	.0196	.0188	.1237	.1343
6	2	MAX.	11.7	103.1	67.31	231.71	121.87	.174	.159	.618	.733
	23	MIN.	-8.2	-94.0	-56.69	-104.29	-42.45	-.245	-.239	-.534	-.650
	23	MEAN	15.6	191.5	704.69	804.29	779.40	2.223	2.427	4.105	4.426
	23	STDEV	3.08	20.09	22.001	53.054	24.474	.0400	.0367	.1676	.1853

SUMMARY OF STATISTICAL DATA FOR FRIDAY HARBOR FLOATING BREAKWATER (FHW - 2400 - 1/8/75)  
 (MAX. AND MIN. VALUES MEASURED FROM ZERO MEAN)  
 SAMPLING PERIOD = 500 MS  
 NUMBER OF SAMPLES = 2047

REC. TIME NO. IN DAYS AND HOURS	TRANS. COEF.	WIND SP. MPH	WIND DIR. DEG.	LOAD CELLS		NE	SE TRAN 1		WAVE GAGES		ACCELEROMETERS	
				NW LBS	SW LBS		LBS	FT.	TRAN 2 FT.	INC. FT.	REF. N. VER. FT.	HOR. S. VER. (FT/SEC/SEC)
1 13 23	.18	MAX.	9.0	55.8	51.01	187.16	28.92	99.72	.136	.134	.637	.427
		MIN.	-7.7	-71.2	-72.99	-104.84	-31.08	-53.54	-0.134	-0.142	-0.361	-0.246
		MEAN	16.7	191.3	832.60	935.54	758.91	820.28	5.236	5.378	4.034	13.174
2 21 7	.15	STDEV	3.49	14.92	18.110	50.773	9.177	27.526	.0245	.0246	.1348	.1455
		MAX.	7.1	52.9	36.08	72.69	35.36	47.05	.069	.062	.622	.471
		MIN.	-5.7	-148.4	-39.92	-63.31	-28.64	-41.43	-0.080	-0.071	-0.376	-0.371
3 21 10	.15	MEAN	16.3	148.4	1031.91	1215.33	896.63	1292.40	9.180	9.141	4.204	5.152
		STDEV	2.37	40.81	13.179	23.756	10.432	15.784	.0207	.0197	.1364	.1301
		MAX.	6.1	148.8	36.96	132.15	25.85	81.35	.073	.063	.632	.311
4 21 11	.12	MIN.	-5.7	-44.2	-51.04	-83.85	-30.15	-40.31	-0.059	-0.075	-0.366	-0.194
		MEAN	15.7	44.2	855.13	1027.85	782.20	10180.04	5.147	6.223	4.040	5.023
		STDEV	2.64	44.14	14.533	36.725	8.396	19.000	.0202	.0192	.1358	.1077
5 21 14	.10	MAX.	6.9	194.1	46.88	159.88	21.54	79.51	.058	.057	.642	.312
		MIN.	-8.5	-36.9	-59.12	-112.12	-22.96	-51.63	-0.064	-0.063	-0.383	-0.362
		MEAN	17.8	36.9	767.12	1012.12	730.96	958.72	4.499	4.634	4.108	5.005
6 21 15	.15	STDEV	2.94	45.71	19.735	50.283	7.926	23.144	.0176	.0174	.1429	.1036
		MAX.	6.7	167.7	55.14	142.96	18.76	70.82	.084	.085	1.054	.641
		MIN.	-5.9	-23.7	-56.86	-141.04	-21.24	-46.10	-0.071	-0.063	-0.533	-0.211
7 21 15	.15	MEAN	17.7	23.7	788.86	1004.04	737.24	964.70	4.703	4.841	4.207	4.979
		STDEV	2.57	34.64	17.808	45.376	7.724	22.556	.0205	.0190	.2137	.1405
		MAX.	7.5	172.1	54.69	173.78	28.03	91.16	.080	.064	.735	.604
8 21 15	.15	MIN.	-6.7	-24.2	-69.31	-118.22	-27.97	-58.94	-0.095	-0.085	-0.468	-0.297
		MEAN	19.5	24.2	813.31	1082.22	747.97	1045.21	5.461	5.553	4.091	5.015
		STDEV	3.13	38.42	21.681	51.506	10.536	27.655	.0225	.0225	.1540	.1166



SUMMARY OF STATISTICAL DATA FOR FRIDAY HARBOR FLOATING BREAKWATER (FH9 - 2400 - 1/8/75)  
(MAX. AND MIN. VALUES MEASURED FROM ZERO MEAN)  
SAMPLING PERIOD = 500 MS  
NUMBER OF SAMPLES = 2047

REC. TIME NO. IN DAYS AND HOURS	TRANS. COEF.	WIND		LOAD CELLS		SE TRAN 1		WAVE GAGES		ACCELEROMETERS	
		SP.	DIR.	NW	SW	NE	SE	TRAN 1	TRAN 2	REF.	N. VER.
		MPH	DEG.	LBS	LBS	LBS	LBS	FT.	FT.	FT.	(FT/SEC/SEC)
7	21	MAX.	7.9	165.3	45.00	29.56	52.12	.087	.106	.769	.781
	16	MIN.	-5.3	-31.1	-51.00	-30.44	-49.00	-.077	-.078	-.511	-.499
		MEAN	17.2	31.1	895.00	798.44	1028.05	6.728	6.784	4.083	5.068
		STDEV	2.65	41.20	19.174	38.806	20.378	.0242	.0236	.1680	.1849
8	21	MAX.	10.0	169.6	45.43	34.55	92.04	.112	.099	.944	.866
	17	MIN.	-6.7	-23.4	-62.57	-82.64	-43.45	-.097	-.133	-.592	-.618
		MEAN	18.6	23.4	938.57	1164.64	827.45	7.614	7.642	4.291	5.182
		STDEV	3.08	35.43	19.020	40.774	25.726	.0303	.0301	.1949	.2155
9	21	MAX.	6.5	163.9	38.76	111.78	73.25	.087	.096	.805	.726
	18	MIN.	-5.4	-20.9	-41.24	-68.22	-38.93	-.098	-.084	-.450	-.554
		MEAN	17.3	20.9	929.24	1168.22	817.64	7.364	7.408	4.098	5.072
		STDEV	2.48	33.17	13.796	30.255	17.901	.0262	.0242	.1631	.1744
10	21	MAX.	5.9	162.8	57.93	142.37	82.58	.104	.094	.695	.914
	19	MIN.	-6.0	-25.3	-50.07	-113.63	-53.30	-.096	-.105	-.508	-.571
		MEAN	18.2	25.3	870.87	1073.65	782.28	6.436	6.510	4.054	5.039
		STDEV	2.29	37.61	16.768	42.001	24.075	.0293	.0305	.1716	.2082
11	21	MAX.	6.9	143.6	55.25	198.81	105.90	.111	.138	.909	1.104
	21	MIN.	-5.7	-16.5	-64.45	-141.19	-71.06	-.120	-.107	-.474	-.688
		MEAN	21.7	17.2	772.45	1093.19	724.72	4.855	4.993	4.096	5.032
		STDEV	2.69	28.57	21.662	56.483	32.725	.0349	.0358	.1829	.2278
12	21	MAX.	8.2	111.7	61.49	242.35	129.85	.115	.098	.926	.863
	22	MIN.	-10.7	-12.1	-62.51	-193.65	-31.24	-.118	-.099	-.585	-.750
		MEAN	22.3	13.9	714.51	1017.65	699.24	3.187	3.383	4.131	4.987
		STDEV	3.37	20.24	18.393	73.711	36.399	.0309	.0306	.1899	.2173

SUMMARY OF STATISTICAL DATA FOR FRIDAY HARBOR FLOATING BREAKWATER (FM9 - 2400 - 1/8/75)  
 (MAX. AND MIN. VALUES MEASURED FROM ZERO MEAN)  
 SAMPLING PERIOD - 900 MS  
 NUMBER OF SAMPLES - 2047

REC. TIME NO. IN DAYS AND HOURS	TRANS. IN COEF.	WIND		LOAD CELLS		SE TRAN 1		WAVE GAGES		ACCELEROMETERS					
		SP.	DIR.	NW	SW	NE	TRAN 1	TRAN 2	INC.	REF. M.VER.	HOW. S.VER.				
		MPH	DEG.	LBS	LBS	LBS	LB.	FT.	FT.	FT.	FT.	(FT/SEC/SEC)			
13	21 23	MAX.	9.0	110.6	41.47	222.02	16.95	119.11	.090	.101	.725	.949	.474	.359	.627
		MIN.	-6.7	-11.5	-54.53	-113.98	-27.05	-54.69	-1.100	-1.00	-4.78	-.536	-.536	-.320	-.473
		MEAN	20.2	13.0	702.53	929.98	687.05	898.45	2.111	2.348	4.024	4.952	13.319	13.904	12.909
		STDEV	2.77	20.10	16.287	62.127	7.077	29.598	.0269	.0254	.1707	.1959	.1262	.1071	.1322
14	21 24	MAX.	10.6	198.9	41.79	292.93	23.93	142.02	.116	.095	.900	.746	.475	.356	.539
		MIN.	-6.4	-19.3	-66.21	-163.07	-28.07	-90.24	-.089	-.092	-.610	-.687	-.367	-.323	-.561
		MEAN	21.2	19.3	698.21	967.07	686.07	952.44	2.240	2.473	4.054	4.951	13.319	13.907	12.912
		STDEV	3.59	33.11	17.753	76.333	8.323	38.727	.0281	.0282	.1822	.1940	.1358	.1112	.1399
15	22 1	MAX.	7.9	47.9	65.96	212.45	22.99	114.64	.073	.102	.756	.697	.473	.271	.370
		MIN.	-7.5	-4.9	-58.04	-134.55	-25.01	-62.32	-.113	-.03	-.447	-.455	-.369	-.238	-.391
		MEAN	20.1	6.6	742.04	947.55	709.01	921.77	3.034	3.242	4.054	4.973	13.320	13.907	12.912
		STDEV	3.27	8.58	26.975	68.463	11.023	33.782	.0258	.0260	.1379	.1685	.1125	.0824	.0997
16	22 7	MAX.	8.6	170.7	38.09	98.72	35.68	64.33	.074	.064	.456	.559	.306	.280	.432
		MIN.	-8.2	-25.6	-57.91	-65.28	-46.32	-43.11	-.081	-.056	-.363	-.388	-.368	-.314	-.394
		MEAN	14.2	25.6	1105.91	1241.28	936.32	1305.14	9.807	9.745	4.113	5.060	13.319	13.898	12.915
		STDEV	3.12	47.24	18.338	31.378	16.039	21.074	.0182	.0181	.1228	.1336	.1086	.0791	.1032
17	22 8	MAX.	8.3	189.4	49.89	121.44	43.84	76.55	.080	.062	.629	.703	.302	.264	.279
		MIN.	-8.4	-18.5	-62.11	-78.56	-52.16	-53.01	-.079	-.076	-.369	-.500	-.372	-.245	-.313
		MEAN	17.4	18.5	1074.11	1266.56	904.16	1358.19	9.711	9.656	4.095	5.044	13.321	13.914	12.918
		STDEV	3.14	38.72	20.233	36.920	16.823	23.271	.0213	.0206	.1298	.1511	.1143	.0757	.0920
18	22 10	MAX.	10.5	187.0	47.56	240.43	27.45	148.56	.064	.069	.631	.644	.472	.257	.370
		MIN.	-8.1	-25.8	-88.44	-99.57	-36.55	-53.68	-.083	-.090	-.393	-.431	-.202	-.338	-.307
		MEAN	18.4	25.8	880.44	1067.57	756.55	1047.89	6.175	6.272	4.095	5.027	13.320	13.922	12.912
		STDEV	3.32	43.71	21.148	55.706	11.080	32.035	.0206	.0209	.1412	.1585	.1090	.0785	.0927



SUMMARY OF STATISTICAL DATA FOR FRIDAY HARBOR FLOATING BREAKWATER (FH9 - 2400 - 1/8/75)  
 (MAX. AND MIN. VALUES MEASURED FROM ZERO MEAN)  
 SAMPLING PERIOD - 500 MS  
 NUMBER OF SAMPLES - 2047

REC. TIME NO. IN DAYS AND HOURS	TRANS. COEF.	WIND SP. DIR.	WIND NMPH DEG.	LOAD CELLS		NE LBS	SE TAAN 1 TRAN 2 INC.		WAVE GAGES		ACCELEROMETERS	
				NW LBS	SW LBS		LBS	FT.	FT.	FT.	REF. N.VER.	HOR. S.VER.
19	.14	MAX.	7.8 148.8	62.45	164.06	26.25	94.19	.077	.075	.779	.693	.488
		MIN.	-6.3 -14.6	-57.55	-123.94	-21.75	-62.23	-.074	-.083	-.398	-.485	-.354
		MEAN	18.8 15.7	813.55	999.94	799.75	953.55	4.658	4.816	4.072	5.003	13.312
20	.14	MAX.	7.3 173.6	40.32	130.44	14.50	61.50	.048	.053	.553	.524	.315
		MIN.	-7.4 -16.1	-59.68	-69.56	-21.50	-26.98	-.053	-.058	-.318	-.346	-.170
		MEAN	15.5 16.3	819.68	921.56	733.50	856.29	4.129	4.298	4.017	4.967	13.315
21	.15	MAX.	6.2 170.3	39.14	92.39	21.00	37.50	.070	.067	.434	.583	.400
		MIN.	-5.4 -26.0	-44.86	-83.61	-19.00	-32.02	-.057	-.059	-.334	-.339	-.205
		MEAN	16.3 26.0	860.86	971.61	755.00	921.06	5.022	5.165	4.033	4.960	13.322
22	.15	MAX.	6.8 171.5	43.29	109.51	22.46	57.98	.096	.080	.690	.743	.634
		MIN.	-6.1 -23.2	-44.71	-110.49	-25.54	-52.62	-.094	-.069	-.411	-.614	-.376
		MEAN	17.9 23.2	904.71	1058.49	785.54	1049.22	6.298	6.388	4.058	5.055	13.323
23	.15	MAX.	11.5 139.6	59.44	237.32	45.55	150.06	.093	.106	.861	1.029	.632
		MIN.	-8.7 -81.5	-88.56	-146.68	-46.45	-80.62	-.104	-.092	-.444	-.737	-.426
		MEAN	20.3 81.5	924.56	1130.88	790.45	1144.09	7.105	7.168	4.143	5.102	13.324
24	.15	MAX.	9.7 57.9	56.46	222.09	32.20	136.19	.103	.123	.904	1.126	.629
		MIN.	-7.0 -159.9	-87.54	-133.91	-43.80	-64.47	-.118	-.128	-.606	-.922	-.718
		MEAN	18.9 159.9	939.54	1125.91	795.80	1151.21	7.261	7.309	4.101	5.108	13.326
		MAX.	3.46 41.48	21.917	54.967	13.017	32.035	.0341	.0360	.2233	.2373	.1563
		MIN.										
		MEAN										

SUMMARY OF STATISTICAL DATA FOR FRIDAY HARBOR FLOATING BREAKWATER (FH9 - 2400 - 1/8/75)  
 (MAX. AND MIN. VALUES MEASURED FROM ZERO MEAN)  
 SAMPLING PERIOD = 500 MS  
 NUMBER OF SAMPLES = 2047

REC. TIME NO. IN DAYS AND HOURS	TRANS. COEF.	WIND SP. MPH	WIND DIR. DEG.	LOAD CELLS		NE LBS	SE TRAN 1		WAVE GAGES		ACCELEROMETERS	
				NW LBS	SW LBS		LBS	FT.	TRAN 2 FT.	INC. FT.	REF. N. VER. FT.	HOR. S. VER. (FT/SEC/SEC)
25	22	7.6	31.9	61.65	135.64	36.11	80.27	.078	.101	.733	.947	.795
		MAX.										
	.11	MIN.	-6.8-103.4	-46.35	-132.36	-27.89	-71.41	-.060	-.088	-.598	-.589	-.552
	20	MEAN	20.0 100.3	918.35	1140.36	783.89	1140.79	6.934	6.990	4.093	5.082	13.327
		STDEV	2.41 20.23	16.545	46.342	10.659	27.186	.0215	.0234	.1992	.2218	.2070
												.1904
												.2828



SUMMARY OF STATISTICAL DATA FOR FRIDAY HARBOR FLOATING BREAKWATER (FH10 - 1345 - 2/9/75)  
 (MAX. AND MIN. VALUES MEASURED FROM ZERO MEAN)  
 SAMPLING PERIOD = 500 MS  
 NUMBER OF SAMPLES = 2047

REC. TIME NO. IN DAYS AND HOURS	TRANS. COEF.	WIND		LOAD CELLS		SE TRAN		WAVE GAGES		ACCELEROMETERS	
		SP.	DIR.	NW	SW	NE	LBS	FT.	INC.	REF. N.VER.	HOR. S.VER.
		MPH	DEG.	LBS	LBS	LBS	LBS	FT.	FT.	FT.	(FT/SEC/SEC)
1	0	MAX.	3.9	54.4	10.24	10.75	9.29	9.15	.072	.075	.155
		MIN.	-2.2	-176.6	-23.93	-19.79	-15.51	-17.71	-.157	-.154	-.130
		MEAN	3.5	184.9	1132.65	1104.29	930.21	1035.99	8.611	8.653	13.310
		STDEV	.86	37.62	3.957	5.271	3.182	3.632	.0174	.0148	.0333
2	2	MAX.	9.1	63.6	94.83	168.74	67.48	73.97	.497	.558	.835
		MIN.	-13.7	-99.7	-91.17	-111.26	-48.08	-50.85	-.301	-.213	-.547
		MEAN	15.0	188.0	995.47	921.26	816.33	848.72	5.722	5.834	4.425
		STDEV	3.72	19.53	24.742	50.725	15.561	22.265	.0485	.0460	.1912
3	5	MAX.	8.9	47.9	52.32	197.75	54.14	129.15	.137	.128	.799
		MIN.	-6.5	-61.0	-67.68	-206.25	-33.82	-150.51	-.380	-.329	-.379
		MEAN	14.8	181.0	892.12	1102.25	789.82	1161.04	6.747	6.819	4.078
		STDEV	2.54	12.26	21.037	61.374	11.987	36.717	.0386	.0398	.1621
4	5	MAX.	11.8	45.3	93.12	389.26	43.28	208.18	.124	.113	.717
		MIN.	-7.4	-63.6	-106.88	-170.74	-40.72	-84.12	-.112	-.113	-.358
		MEAN	16.4	178.2	739.13	1039.06	791.55	973.00	4.355	4.606	3.981
		STDEV	3.30	12.02	27.303	78.380	11.272	42.955	.0350	.0363	.1519

SUMMARY OF STATISTICAL DATA FOR FRIDAY HARBOR FLOATING BREAKWATER (FH11 - 0900 - 3/1/75)  
 (MAX. AND MIN. VALUES MEASURED FROM ZERO MEAN)  
 SAMPLING PERIOD = 500 MS  
 NUMBER OF SAMPLES = 2047

REC. TIME NO. IN DAYS AND HOURS	TRANS. COEF.	WIND		LOAD CELLS		NE		SE		WAVE GAGES		REF.		ACCELEROMETERS	
		SP.	DIR.	NW	SW	LBS	LBS	LBS	LBS	TRAN 1	TRAN 2	INC.	FT.	N. VER.	HOR. S. VER.
		MPH	DEG.							FT.	FT.				(FT/SEC/SEC)
1	0	MAX.	2.4	128.3	4325.99	8340.80	120.04	19.86	1.604	7.637	.274	.309	.135	.087	.166
		MIN.	-3.1	-53.2	-36.01	-71.09	-22.68	-26.34	-5.417	-25.254	-.213	-.213	-.314	-.339	-.292
		MEAN	3.1	139.2	1669.47	2456.21	962.04	1082.58	7.584	4.338	3.993	5.063	5.066	5.259	5.069
		STDEV	1.30	28.78	187.585	361.436	8.115	7.520	.2352	1.0975	.0462	.0441	.0283	.0269	.0306
2	0	MAX.	8.9	55.4	56.11	202.38	37.07	123.87	.055	.064	.831	1.049	.611	.459	.853
		MIN.	-5.8	-150.8	-67.89	-157.62	-36.93	-88.13	-.125	-.146	-.296	-.615	-.598	-.490	-.736
		MEAN	19.0	150.8	903.89	1129.62	808.93	1124.13	8.992	7.209	3.868	4.980	5.201	5.405	5.198
		STDEV	3.36	42.43	22.494	65.805	13.598	37.841	.0169	.0177	.1680	.2166	.1235	.1094	.1707
3	4	MAX.	8.9	98.0	48.01	189.99	17.95	109.74	.068	.091	.563	.628	.230	.365	.343
		MIN.	-7.8	-105.0	-59.99	-114.01	-24.05	-50.26	-.084	-.079	-.308	-.293	-.274	-.279	-.364
		MEAN	19.6	105.0	721.99	1002.01	716.05	1046.26	4.111	4.540	4.135	5.119	5.247	5.364	5.230
		STDEV	2.90	62.24	22.328	56.817	7.509	28.550	.0227	.0236	.1399	.1339	.0677	.0831	.0874
4	7	MAX.	12.3	103.8	63.31	182.54	40.74	122.53	.148	.147	.770	.759	.422	.420	.629
		MIN.	-8.6	-115.7	-78.69	-111.46	-45.26	-87.47	-.150	-.128	-.254	-.368	-.452	-.427	-.757
		MEAN	18.2	115.7	920.69	1125.46	827.26	1137.47	7.847	8.100	4.107	5.219	5.290	5.377	5.252
		STDEV	3.98	55.66	24.406	53.350	14.372	33.448	.0400	.0406	.1620	.1781	.1137	.1113	.1605
5	7	MAX.	8.9	148.9	56.27	271.12	28.51	134.52	.119	.118	.593	.862	.425	.516	.634
		MIN.	-7.5	-52.4	-91.73	-132.88	-31.49	-87.48	-.176	-.155	-.250	-.393	-.482	-.331	-.549
		MEAN	20.3	52.4	797.73	1032.88	755.49	1087.48	5.684	6.041	4.043	5.168	5.287	5.382	5.248
		STDEV	3.12	48.10	22.882	59.094	10.775	32.883	.0354	.0366	.1364	.1793	.1217	.1047	.1496
6	7	MAX.	12.6	151.0	54.02	246.45	27.25	117.61	.123	.121	.594	.694	.435	.309	.407
		MIN.	-7.3	-38.8	-67.98	-139.55	-28.75	-68.39	-.169	-.149	-.251	-.330	-.471	-.267	-.471
		MEAN	21.1	38.8	727.98	965.55	724.75	1054.39	4.167	4.596	4.002	5.106	5.277	5.386	5.237
		STDEV	3.61	41.15	24.034	63.906	8.467	30.352	.0343	.0332	.1395	.1549	.0988	.0937	.1172



SUMMARY OF STATISTICAL DATA FOR FRIDAY HARBOR FLOATING BREAKWATER (FH11 - 0900 - 3/1/75)  
 (MAX. AND MIN. VALUES MEASURED FROM ZERO MEAN)  
 SAMPLING PERIOD - 500 MS  
 NUMBER OF SAMPLES - 2047

REC. TIME NO.	IN DAYS AND HOURS	TRANS. COEF.	WIND		LOAD CELLS		NE		SE		WAVE GAGES		ACCELEROMETERS	
			SP. MPH	DIR. DEG.	NW LBS	SW LBS	LBS	LBS	LBS	FT.	TRAN 1 FT.	TRAN 2 FT.	REF. N. VER. FT.	HOR. S. VER. (FT/SEC/SEC)
7	7 16	.23	MAX.	12.0	103.7	69.54	204.55	21.21	82.84	.118	.084	.643	.734	.333
			MIN.	-9.2	-13.4	-64.46	-164.45	-22.79	-63.16	-.116	-.101	-.202	-.341	-.376
			MEAN	19.4	15.4	688.46	898.45	710.79	1029.16	2.907	3.413	3.953	5.065	5.396
			STDEV	3.58	18.97	23.151	66.432	8.436	29.896	.0311	.0279	.1338	.1495	.0888
8	9 5	.23	MAX.	10.6	198.4	64.00	254.24	33.13	124.01	.118	.116	.728	.728	.375
			MIN.	-10.9	-47.4	-100.00	-141.76	-40.87	-71.99	-.119	-.122	-.270	-.398	-.543
			MEAN	18.9	47.4	803.59	1023.79	762.86	1076.01	5.602	5.977	4.020	5.123	5.388
			STDEV	4.14	48.68	28.009	68.262	13.612	37.728	.0347	.0341	.1539	.1648	.1153
9	9 7	.22	MAX.	11.5	172.1	75.33	333.18	40.17	205.59	.127	.192	.906	.781	.362
			MIN.	-8.7	-50.7	-100.47	-192.82	-45.83	-98.41	-.153	-.143	-.323	-.396	-.407
			MEAN	22.8	50.7	786.47	1088.82	749.83	1122.41	5.745	6.118	4.101	5.120	5.312
			STDEV	4.16	48.49	34.270	93.910	16.206	53.863	.0401	.0409	.1823	.1583	.1316
10	9 8	.25	MAX.	10.0	173.3	76.09	254.25	45.26	156.35	.195	.184	.852	.857	.361
			MIN.	-8.0	-46.1	-85.91	-175.75	-38.74	-105.85	-.148	-.172	-.325	-.371	-.472
			MEAN	23.4	46.1	868.75	1145.72	774.24	1147.39	6.072	6.385	4.101	5.171	5.311
			STDEV	3.59	44.60	28.525	77.068	14.429	46.228	.0432	.0442	.1709	.1821	.1212
11	9 9	.36	MAX.	10.9	112.1	79.21	236.06	53.39	147.27	.645	.598	.824	.948	.528
			MIN.	-7.4	-90.8	-88.79	-187.94	-42.61	-114.73	-.259	-.233	-.328	-.435	-.543
			MEAN	23.8	90.8	912.49	1206.49	800.65	1217.61	7.101	7.388	4.079	5.158	5.314
			STDEV	3.19	59.15	30.270	77.342	17.305	48.061	.0630	.0625	.1744	.1911	.1464
12	9 10	.40	MAX.	10.7	112.9	114.20	290.57	72.66	187.48	.640	.632	1.006	1.195	.835
			MIN.	-8.6	-91.7	-113.80	-199.43	-63.34	-122.52	-.364	-.266	-.350	-.495	-.912
			MEAN	22.0	91.7	930.52	1234.76	827.45	1206.81	8.011	8.351	4.050	5.193	5.314
			STDEV	4.32	55.19	35.451	87.205	20.977	53.710	.0857	.0812	.2137	.2437	.2267

SUMMARY OF STATISTICAL DATA FOR FRIDAY HARBOR FLOATING BREAKWATER (FH11 - 0900 - 3/1/75)

(MAX. AND MIN. VALUES MEASURED FROM ZERO MEAN)

SAMPLING PERIOD - 500 HS

NUMBER OF SAMPLES - 2047

REC. TIME NO. IN DAYS AND HOURS	TRANS. COEF.	WIND		LOAD CELLS		NE		SE TRAN 1		WAVE GAGES		ACCELEROMETERS	
		SP.	DIR.	NW	SW	LBS	LBS	LBS	FT.	TRAN 2	INC.	REF. N.VER.	HOR. S.VER.
		MPH	DEG.	LBS	LBS	LBS	LBS	LBS	FT.	FT.	FT.	FT.	(FT/SEC/SEC)
13		MAX,	13.1	128.1	109.04	235.47	80.71	163.28	.451	.364	.985	1.191	.700
	9	MIN.	-7.5	-79.8	-104.96	-194.53	-67.29	-118.72	-.389	-.393	-.398	-.525	-.812
	11	MEAN	21.9	79.8	981.86	1241.07	903.97	1182.33	3.837	8.995	4.122	5.240	5.314
		STDEV	4.03	54.05	34.954	68.446	22.771	44.982	.1015	.1081	.2449	.2493	.2242
14		MAX,	14.4	177.1	110.99	309.13	59.98	153.69	.307	.272	1.097	1.172	.806
	9	MIN.	-11.9	-57.2	-121.01	-212.87	-58.02	-120.31	-.317	-.349	-.388	-.544	-.840
	12	MEAN	21.6	57.2	970.40	1215.72	862.61	1214.26	3.609	8.708	4.113	5.241	5.309
		STDEV	4.70	51.46	39.062	84.688	22.362	50.437	.0892	.0926	.2244	.2564	.2097



SUMMARY OF STATISTICAL DATA FOR FRIDAY HARBOR FLOATING BREAKWATER (FM12 - 2230 - 3/20/75)  
 (MAX. AND MIN. VALUES MEASURED FROM ZERO MEAN)  
 SAMPLING PERIOD = 500 MS  
 NUMBER OF SAMPLES = 2047

REC. TIME NO. IN DAYS AND HOURS	TRANS. COEF.	WIND		LOAD CELLS		NE		SE		WAVE GAGES		ACCELEROMETERS			
		SP.	DIR.	NW	SW	LBS	LBS	LBS	LBS	TRAN 1	TRAN 2	INC.	REF. N. VER. HOR. S. VER.		
		MPH	DEG.	LBS	LBS	LBS	LBS	LBS	LBS	FT.	FT.	FT.	FT.	(FT/SEC/SEC)	
1	0	MAX.	8.4	140.0	62.20	99.15	44.33	48.56	.074	.069	.496	.501	.215	.193	.208
		MIN.	-5.7	-99.2	-39.80	-48.85	-15.67	-23.44	-.083	-.076	-.272	-.241	-.222	-.146	-.197
		MEAN	12.8	99.2	871.85	937.28	832.65	1007.27	5.990	5.305	4.201	5.220	5.329	5.333	5.234
		STDEV	2.62	69.47	13.971	21.354	9.562	11.443	.0179	.0194	.1084	.1173	.0585	.0503	.0653
2	0	MAX.	9.1	135.4	21.49	64.59	14.20	34.85	.057	.046	.545	.488	.189	.183	.261
		MIN.	-7.3	-115.4	-24.51	-43.41	-15.80	-21.15	-.051	-.056	-.275	-.229	-.214	-.156	-.314
		MEAN	11.8	115.4	884.51	949.42	827.80	1013.15	6.513	6.799	4.179	5.183	5.321	5.343	5.215
		STDEV	2.76	65.96	9.098	19.909	5.368	11.137	.0159	.0156	.1130	.1069	.0545	.0508	.0681
3	0	MAX.	8.6	94.7	40.25	138.96	34.40	85.85	.112	.144	.636	.780	.483	.462	.782
		MIN.	-6.2	-104.9	-65.75	-69.04	-39.60	-42.15	-.093	-.114	-.260	-.321	-.525	-.352	-.874
		MEAN	18.1	104.9	923.75	1111.04	843.60	1114.15	7.924	8.157	4.036	5.172	5.330	5.369	5.234
		STDEV	2.73	60.15	18.660	35.685	10.805	22.129	.0301	.0327	.1449	.1649	.1431	.1226	.1788
4	0	MAX.	13.1	95.2	58.23	178.02	45.47	103.88	.156	.163	.827	.955	.615	.631	1.360
		MIN.	-7.1	-104.5	-83.77	-117.98	-48.53	-66.12	-.147	-.194	-.350	-.401	-.661	-.691	-1.175
		MEAN	21.3	104.5	941.77	1179.99	850.53	1158.12	8.542	8.746	4.152	5.227	5.332	5.369	5.231
		STDEV	5.26	58.38	22.653	43.195	14.695	26.162	.0460	.0484	.1957	.2147	.1900	.1698	.2938
5	0	MAX.	7.6	151.9	50.92	153.14	31.67	87.41	.093	.122	.738	.796	.484	.364	.748
		MIN.	-6.5	-34.6	-75.08	-94.86	-36.33	-58.59	-.102	-.094	-.286	-.330	-.491	-.517	-.705
		MEAN	20.6	34.6	935.08	1174.86	846.33	1156.59	8.516	8.718	4.087	5.207	5.329	5.365	5.235
		STDEV	2.93	41.42	19.137	39.018	11.795	25.009	.0288	.0280	.1513	.1705	.1370	.1097	.1568
6	0	MAX.	7.2	115.9	46.85	107.50	27.83	55.02	.086	.114	.668	.813	.319	.272	.549
		MIN.	-4.7	-14.4	-53.15	-72.50	-22.17	-44.98	-.080	-.094	-.279	-.339	-.353	-.270	-.431
		MEAN	18.8	16.2	911.15	1116.50	836.17	1120.98	7.988	8.207	4.107	5.216	5.326	5.355	5.231
		STDEV	2.13	22.37	14.011	26.324	7.753	15.326	.0264	.0270	.1363	.1646	.1143	.0971	.1315

SUMMARY OF STATISTICAL DATA FOR FRIDAY HARBOR FLOATING BREAKWATER (FH12 - 2230 - 3/20/75)  
 (MAX. AND MIN. VALUES MEASURED FROM ZERO MEAN)  
 SAMPLING PERIOD - 500 MS  
 NUMBER OF SAMPLES - 2047

REC. TIME NO. IN DAYS AND HOURS	TRANS. COEF.	WIND		LOAD CELLS		SE		WAVE GAGES		ACCELEROMETERS	
		SP.	DIR.	NW	SW	NE	SE	TRAN 1	TRAN 2	REF. N. VER.	HOR. S. VER.
		MPH	DEG.	LBS	LBS	LBS	LBS	FT.	FT.	FT.	(FT/SEC/SEC)
7	0	MAX.	10.2	138.0	50.55	150.86	35.35	98.39	.073	.532	.703
	9	MIN.	-6.9	-17.1	-77.45	-85.14	-46.65	-59.61	-.069	-.236	-.270
		MEAN	18.4	18.2	931.45	1107.14	840.65	1117.61	8.087	4.115	5.223
		STDEV	3.20	27.26	19.667	36.519	11.697	22.201	.0221	.1285	.1431
8	0	MAX.	10.4	114.0	72.43	196.27	40.01	129.16	.125	.703	.833
	10	MIN.	-7.6	-16.3	-83.57	-129.73	-53.99	-74.84	-.098	-.270	-.319
		MEAN	22.1	16.8	907.57	1159.72	823.99	1152.84	8.224	4.148	5.248
		STDEV	3.33	22.59	26.255	53.094	14.696	32.687	.0288	.1447	.1750
9	0	MAX.	9.0	108.0	49.65	143.41	32.26	100.63	.105	.671	.741
	11	MIN.	-0.1	-88.3	-72.35	-82.59	-39.74	-53.37	-.103	-.221	-.309
		MEAN	19.2	88.3	936.35	1138.59	842.74	1133.37	8.376	4.105	5.237
		STDEV	3.48	61.75	23.462	44.187	13.576	29.269	.0282	.1395	.1522
10	0	MAX.	11.1	140.5	100.80	296.82	54.69	170.49	.129	.844	.993
	13	MIN.	-9.5	-17.9	-123.20	-175.18	-59.31	-91.51	-.127	-.142	-.283
		MEAN	24.5	18.8	893.20	1187.18	809.31	1177.51	8.147	4.085	5.216
		STDEV	3.94	28.18	36.376	77.993	19.146	45.590	.0376	.1709	.2003
11	0	MAX.	11.5	146.0	95.24	256.21	57.20	145.45	.204	.909	.922
	14	MIN.	-12.9	-53.6	-100.76	-247.79	-46.80	-132.55	-.178	-.320	-.409
		MEAN	27.7	53.6	810.76	1205.79	772.80	1192.55	7.398	4.097	5.158
		STDEV	4.37	52.33	29.763	83.770	17.150	48.104	.0569	.2077	.2283
12	0	MAX.	10.8	103.5	67.14	250.15	38.58	168.48	.171	.860	.960
	15	MIN.	-8.5	-13.6	-82.86	-189.85	-39.42	-107.52	-.150	-.318	-.397
		MEAN	25.2	14.9	770.86	1121.85	751.42	1141.52	6.172	4.088	5.146
		STDEV	3.95	10.45	25.076	69.811	12.488	41.639	.0492	.1874	.2182



# SUMMARY OF STATISTICAL DATA FOR FRIDAY HARBOR FLOATING BREAKWATER (FH12 - 2230 - 3/20/75)

(MAX. AND MIN. VALUES MEASURED FROM ZERO MEAN)  
 SAMPLING PERIOD - 300 MS  
 NUMBER OF SAMPLES - 2047

REC. TIME MO. IN DAYS AND HOURS	TRANS. COEF.	WIND		LOAD CELLS		SE TRAN		WAVE GAGES		ACCELEROMETERS					
		SP.	DIR.	N#	SW	NE	LBS	TRAN 1	TRAN 2	INC.	REF.	N.VER.	HOR. S.VER.		
		MPH	DEG.	LBS	LBS	LBS	LBS	FT.	FT.	FT.	FT.	(FT/SEC/SEC)			
13	0	MAX.	12.0	63.8	55.36	183.38	20.98	102.28	.136	.122	.638	.843	.466	.467	.603
	16	MIN.	-7.3	-8.0	-64.64	-124.62	-29.02	-63.42	-.109	-.118	-.233	-.309	-.475	-.448	-.711
		MEAN	20.8	9.5	726.64	960.62	727.02	1045.42	4.630	5.046	3.958	5.085	5.280	5.364	5.180
		STDEV	4.36	11.27	24.012	66.572	9.373	36.446	.0328	.0364	.1416	.1707	.1370	.1225	.1779
14	0	MAX.	10.4	64.4	58.40	184.95	21.44	88.24	.095	.094	.625	.622	.404	.339	.604
	17	MIN.	-8.5	-8.2	-65.60	-104.05	-22.56	-51.76	-.085	-.102	-.194	-.300	-.402	-.305	-.545
		MEAN	20.1	9.3	693.60	867.05	704.56	1007.76	3.202	3.672	3.945	5.050	5.274	5.356	5.176
		STDEV	3.75	12.01	21.781	54.227	7.195	24.182	.0264	.0291	.1316	.1453	.1061	.0896	.1237
15	6	MAX.	13.9	80.8	136.21	110.20	139.25	49.16	.135	.131	.367	.397	.278	.169	.190
	14	MIN.	-11.5	-318.5	-79.79	-157.80	-66.75	-58.84	-.116	-.126	-.273	-.243	-.260	-.170	-.216
		MEAN	20.2	318.5	1011.89	851.69	964.82	960.82	7.768	7.985	4.254	5.274	5.401	5.357	5.218
		STDEV	5.06	103.60	40.126	51.751	39.679	20.837	.0371	.0357	.1018	.0852	.0579	.0486	.0585
16	6	MAX.	13.5	110.9	233.84	218.92	109.24	80.79	.504	.468	.293	.286	.177	.182	.183
	18	MIN.	-20.8	-290.0	-112.16	-137.08	-56.76	-43.21	-.181	-.155	-.142	-.149	-.192	-.157	-.188
		MEAN	20.8	290.0	833.51	642.61	795.57	919.64	2.661	3.097	3.922	5.054	5.328	5.338	5.152
		STDEV	4.62	107.69	51.112	54.756	26.527	16.088	.0389	.0338	.0613	.0657	.0539	.0444	.0550
17	10	MAX.	8.7	109.1	49.20	161.30	24.34	83.70	.114	.092	.529	.615	.239	.186	.284
	6	MIN.	-7.7	-143.4	-60.50	-96.70	-36.66	-52.30	-.093	-.077	-.214	-.235	-.265	-.187	-.257
		MEAN	15.7	143.4	782.50	1040.70	788.66	1078.31	6.362	6.644	4.143	5.185	5.406	5.408	5.226
		STDEV	3.35	59.27	22.067	52.260	11.290	26.120	.0232	.0245	.1189	.1312	.0678	.0557	.0783
18	10	MAX.	8.1	120.5	43.59	166.82	25.81	82.68	.089	.089	.349	.525	.171	.153	.183
	3	MIN.	-5.1	-143.5	-68.41	-94.18	-30.19	-49.32	-.081	-.075	-.163	-.217	-.198	-.152	-.256
		MEAN	15.7	143.5	778.41	1027.18	784.19	1071.32	6.106	6.399	4.094	5.145	5.406	5.407	5.225
		STDEV	2.64	53.90	19.434	47.133	9.794	23.689	.0208	.0242	.0894	.1136	.0441	.0467	.0545

SUMMARY OF STATISTICAL DATA FOR FRIDAY HARBOR FLOATING BREAKWATER (FH13 - 2230 - 3/20/75)  
 (MAX. AND MIN. VALUES MEASURED FROM ZERO MEAN)  
 SAMPLING PERIOD = 500 MS  
 NUMBER OF SAMPLES = 2047

REC. TIME NO.	DAYS AND HOURS	TRANS. IN COEF.	WIND		LOAD CELLS		SE TRAN		WAVE GAGES		ACCELEROMETERS				
			SP.	DIR.	SW	NE	LBS	FT.	TRAN 1	TRAN 2	REF. N.AVER.	MOR. S.AVER.			
			MPH	DEG.	LBS	LBS	LBS	FT.	FT.	FT.	(FT/SEC/SEC)				
1	23	MAX,	9.7	59.3	107.60	340.36	31.81	133.56	.170	.209	.675	.812	.429	.578	.799
		.57 MIN.	-12.4	-130.4	-101.34	-133.64	-38.19	-66.44	-.377	-.255	-.272	-.366	-.479	-.507	-.790
		MEAN	20.8	171.0	705.89	1141.38	794.16	1147.37	3.519	4.586	4.177	5.243	5.516	5.490	5.015
		STDEV	3.36	26.69	28.223	74.717	9.644	29.630	.0497	.0491	.1359	.1803	.1346	.1251	.1997
2	24	MAX,	12.8	76.4	57.60	307.88	24.96	132.10	.124	.118	.500	.651	.386	.353	.441
		.35 MIN.	-9.0	-136.5	-76.40	-136.12	-37.04	-49.90	-.113	-.113	-.166	-.322	-.387	-.291	-.404
		MEAN	20.6	136.5	476.40	888.12	727.04	985.90	2.434	3.055	4.122	5.173	5.494	5.477	5.001
		STDEV	4.10	49.30	25.606	75.594	10.994	30.246	.0389	.0346	.1088	.1428	.1093	.0916	.1298
3	24	MAX,	9.2	76.1	79.26	289.34	36.66	134.10	.191	.176	.745	.936	.624	.880	.912
		.32 MIN.	-7.2	-136.8	-90.74	-160.66	-39.34	-77.90	-.178	-.147	-.279	-.446	-.620	-.951	-.642
		MEAN	20.7	136.8	520.74	1042.66	743.34	1063.90	4.157	4.686	4.236	5.246	5.492	5.493	5.003
		STDEV	3.69	46.94	30.135	76.112	13.818	37.252	.0549	.0515	.1707	.2079	.1816	.1923	.1914
4	24	MAX,	11.3	86.0	71.05	306.84	41.42	199.86	.250	.250	.932	1.105	.793	1.001	1.119
		.30 MIN.	-8.3	-121.9	-94.95	-171.11	-50.58	-86.14	-.228	-.211	-.348	-.559	-.820	-.999	-.808
		MEAN	22.4	121.9	578.95	1157.11	770.58	1124.14	5.926	6.361	4.303	5.360	5.490	5.506	5.000
		STDEV	3.83	49.11	35.103	96.943	17.090	53.806	.0645	.0641	.2117	.2435	.2229	.2187	.2349
5	24	MAX,	9.0	127.2	76.65	186.45	36.81	107.21	.183	.173	.694	.923	.525	.684	.570
		.32 MIN.	-8.1	-80.7	-81.35	-123.55	-41.19	-68.79	-.159	-.192	-.293	-.433	-.483	-.672	-.512
		MEAN	19.9	80.7	685.35	1171.55	823.19	1160.79	7.735	8.070	4.260	5.361	5.490	5.485	5.007
		STDEV	3.03	48.88	24.136	47.125	12.540	27.668	.0504	.0457	.1575	.1972	.1405	.1432	.1374
6	24	MAX,	6.7	56.5	56.83	142.38	36.66	77.08	.171	.165	.754	.972	.595	.919	.577
		.32 MIN.	-5.5	-151.4	-67.17	-97.62	-35.34	-62.94	-.165	-.165	-.244	-.462	-.715	-.912	-.640
		MEAN	19.6	151.4	787.17	1245.62	873.34	1204.92	9.161	9.407	4.200	5.338	5.487	5.486	5.000
		STDEV	2.67	36.45	24.240	40.460	13.459	24.938	.0507	.0476	.1600	.2124	.1767	.1960	.1822



SUMMARY OF STATISTICAL DATA FOR FRIDAY HARBOR FLOATING BREAKWATER (FH13 - 2230 - 3/20/75)  
 (MAX. AND MIN. VALUES MEASURED FROM ZERO MEAN)  
 SAMPLING PERIOD - 500 MS  
 NUMBER OF SAMPLES - 2047

REC. TIME NO. IN DAYS AND HOURS	TRANS. COEF.	WIND		LOAD CELLS		NE		SE		WAVE GAGES		ACCELEROMETERS	
		SP.	DIR.	NW	SW	LBS	LBS	LBS	FT.	TRAN 1	TRAN 2	INC.	REF. N.VER. HOR. S.VER.
		MPH	DEG.	LBS	LBS	LBS	LBS	LBS	FT.	FT.	FT.	FT.	(FT/SEC/SEC)
7	24	MAX, 13.8	125.5	91.92	346.20	48.48	198.64	.198	.218	.811	.636	.386	.446
	17	MIN, -10.3	-123.6	-118.08	-231.80	-49.52	-117.36	-.167	-.183	-.264	-.394	-.454	-.571
		MEAN 22.8	123.6	596.09	1135.77	767.51	1137.36	6.385	6.800	4.271	5.272	5.494	5.486
		STDEV 4.74	49.67	40.252	111.057	17.216	58.518	.0551	.0572	.1696	.1708	.1153	.1147
8	24	MAX, 10.4	111.9	83.84	460.62	42.06	207.33	.089	.082	.765	.891	.863	1.370
	18	MIN, -10.1	-125.7	-114.16	-223.38	-43.94	-130.67	-.073	-.079	-.259	-.415	-.918	-1.308
		MEAN 24.9	125.7	548.16	1193.38	741.94	1108.67	5.945	6.388	4.240	5.267	5.486	5.512
		STDEV 4.00	48.06	38.769	114.883	16.219	61.259	.0235	.0234	.1644	.2069	.2075	.2559

## APPENDIX H

### INCIDENT AND TRANSMITTED WAVE SPECTRAL PLOTS

Appendix H contains the incident and transmitted wave spectral plots along with the corresponding transmission response curve for 11 representative records. The data for the first nine were recorded at Friday Harbor, Washington, during the winter of 1975. Figures H-11 and H-12 were computed from similar data collected in Alaska during the winters of 1974 and 1975.

The original time series were high-pass filtered at a cutoff frequency of 0.05 hertz to remove tidal drift. Each series consisted of 2,048 data samples and were sampled at a period of 0.5 second for the Friday Harbor data and 0.44 second for the Alaska data.

The standard deviations and corresponding overall transmission coefficients for each of the Friday Harbor plots are given in Appendix G.



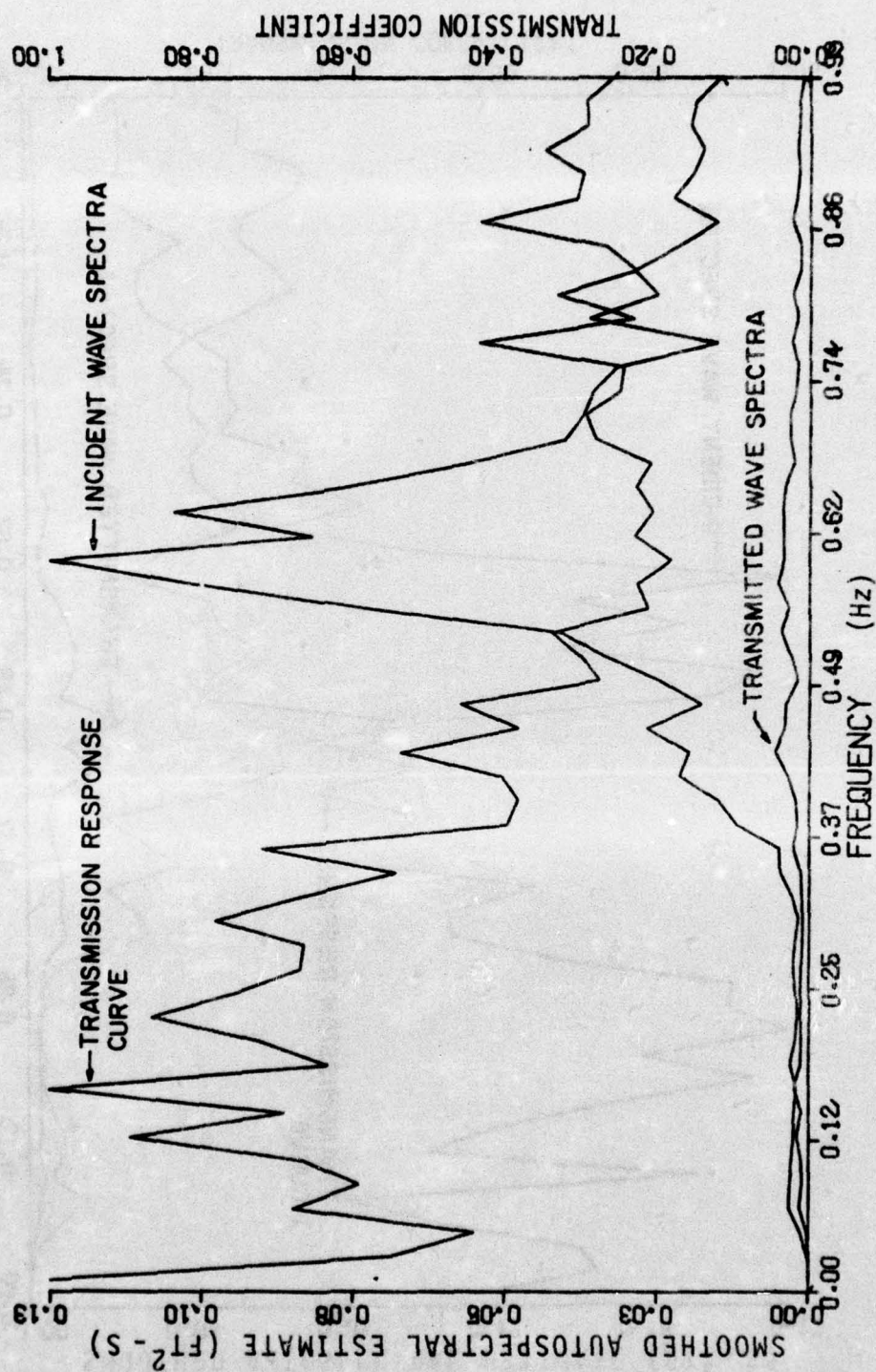


Figure H-1. Incident and transmitted wave spectral data (FH7-6)

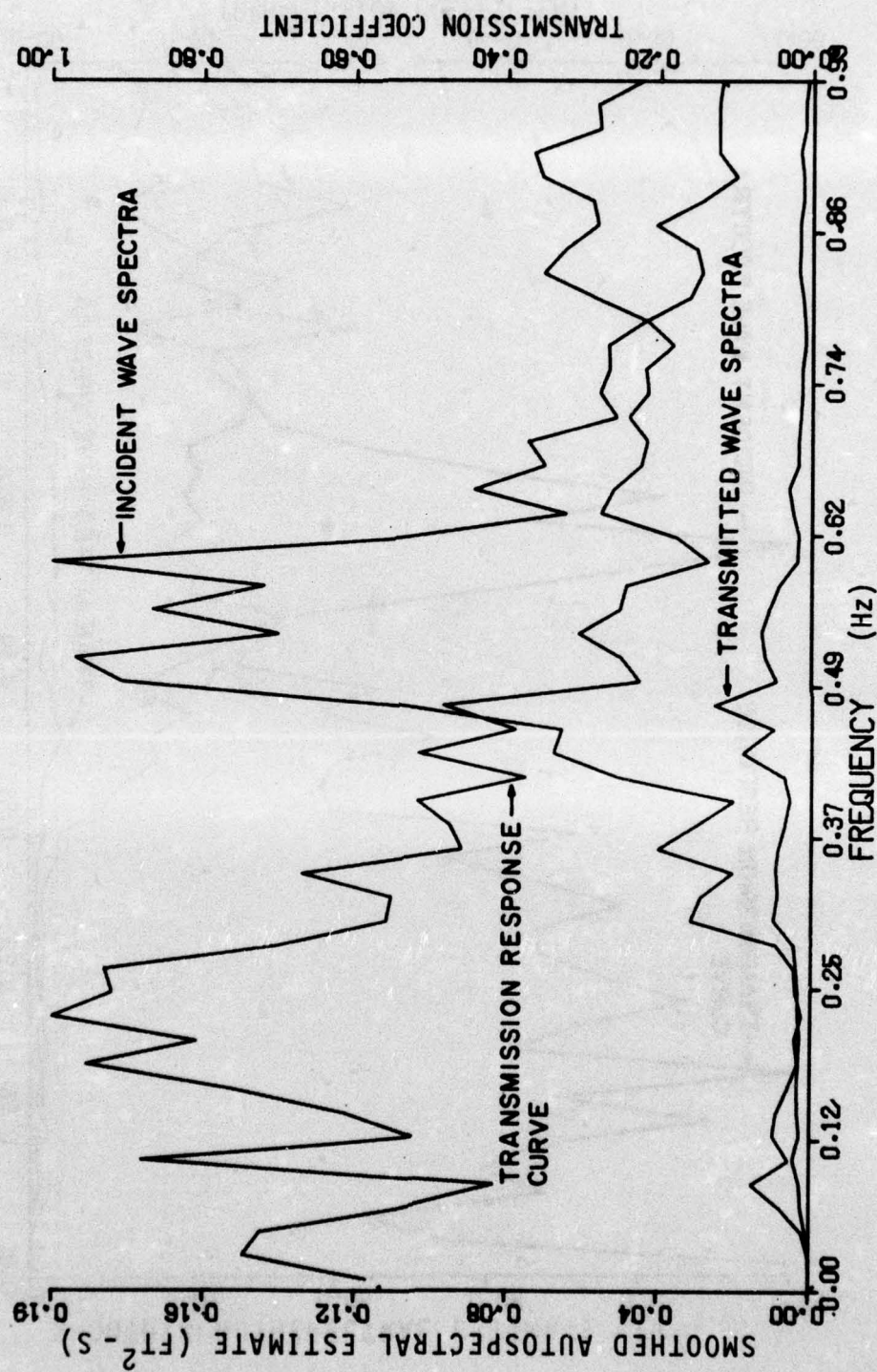


Figure H-2. Incident and transmitted wave spectral data (FH7-7)



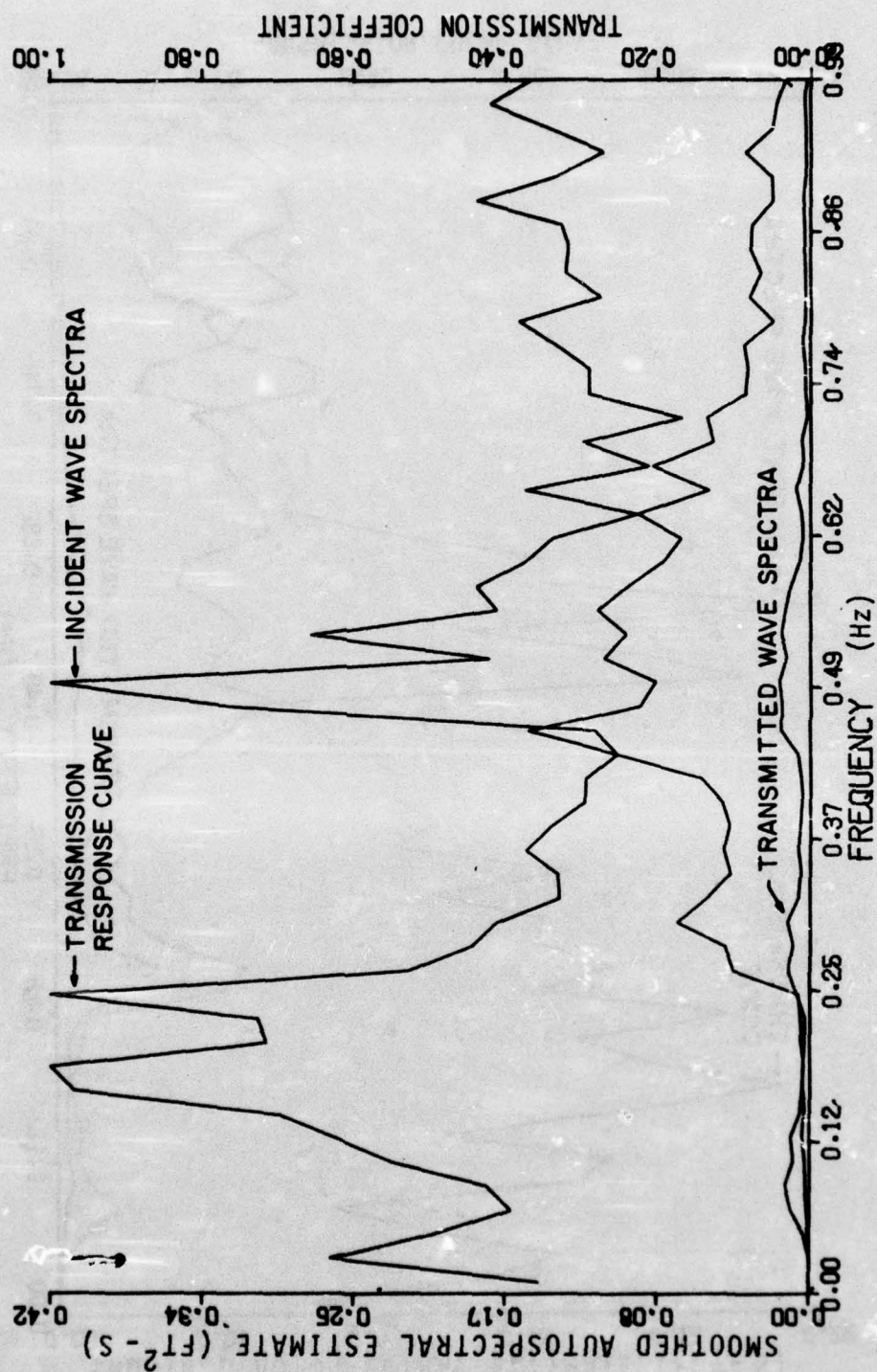


Figure H-3. Incident and transmitted wave spectral data (FH7-8).

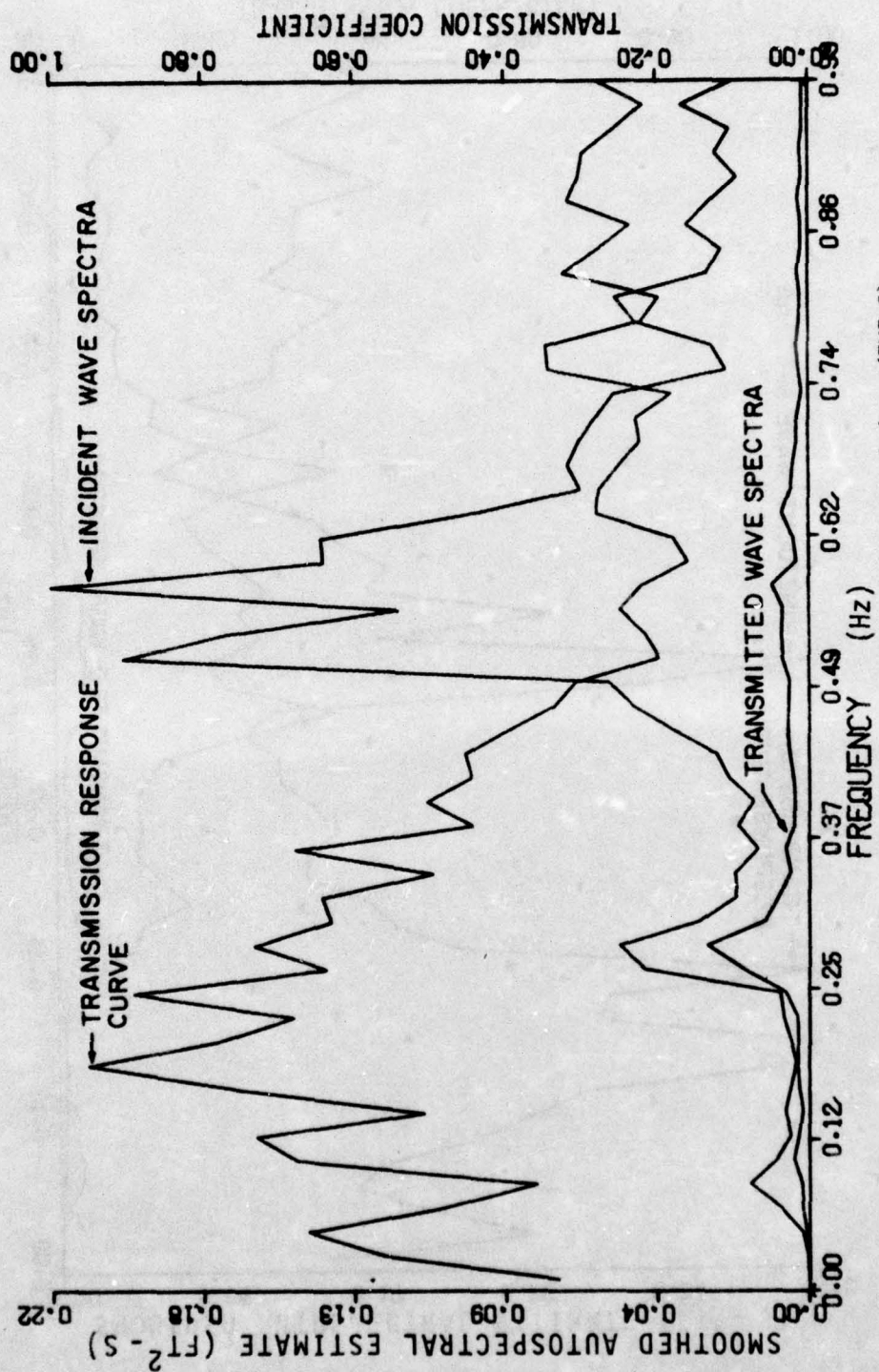


Figure H-4. Incident and transmitted wave spectral data (FH7-9).



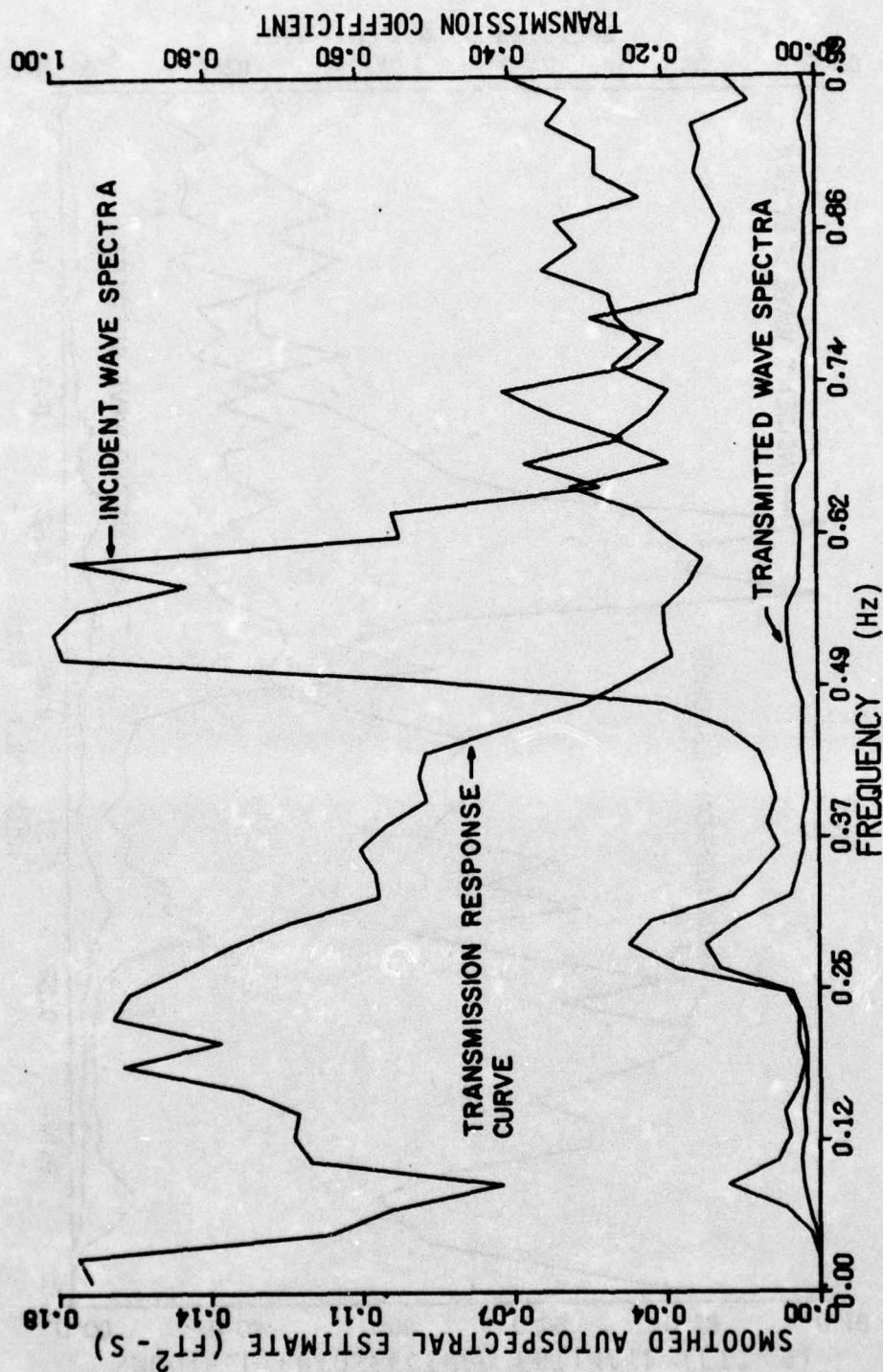


Figure H-5. Incident and transmitted wave spectral data (FH7-10).

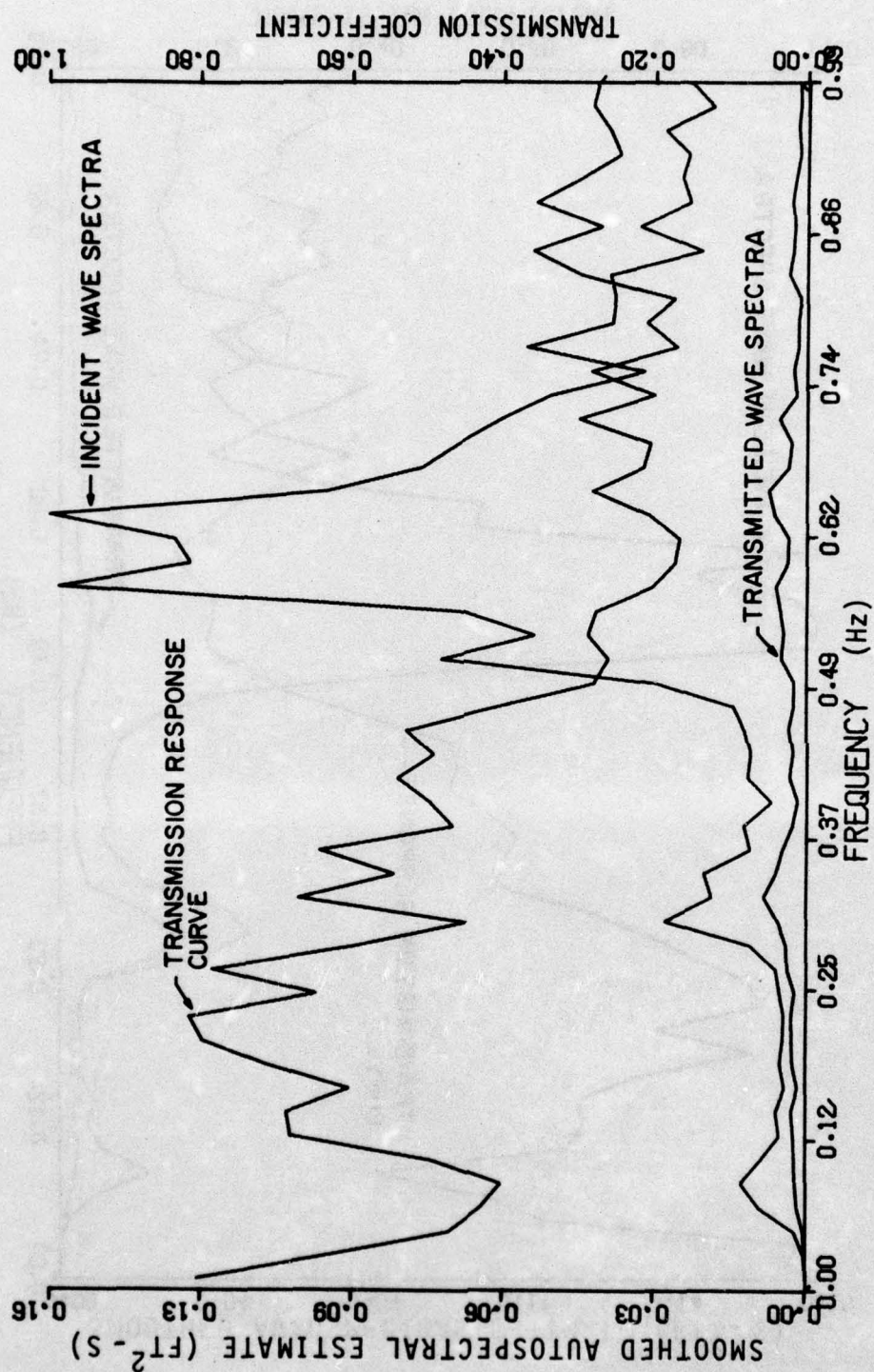


Figure H-6. Incident and transmitted wave spectral data (FH7-11).



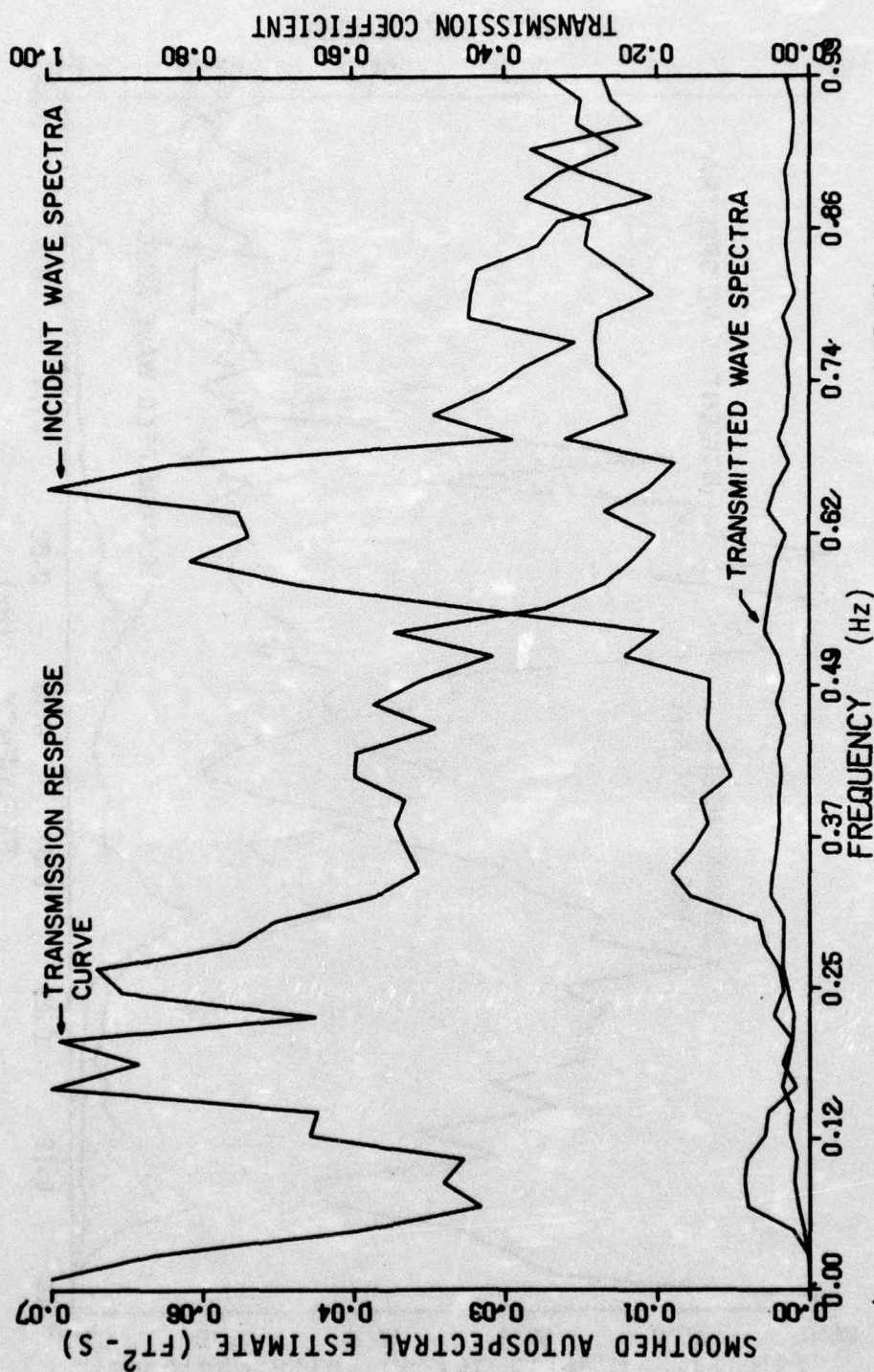


Figure H-7. Incident and transmitted wave spectral data (FH7-12).

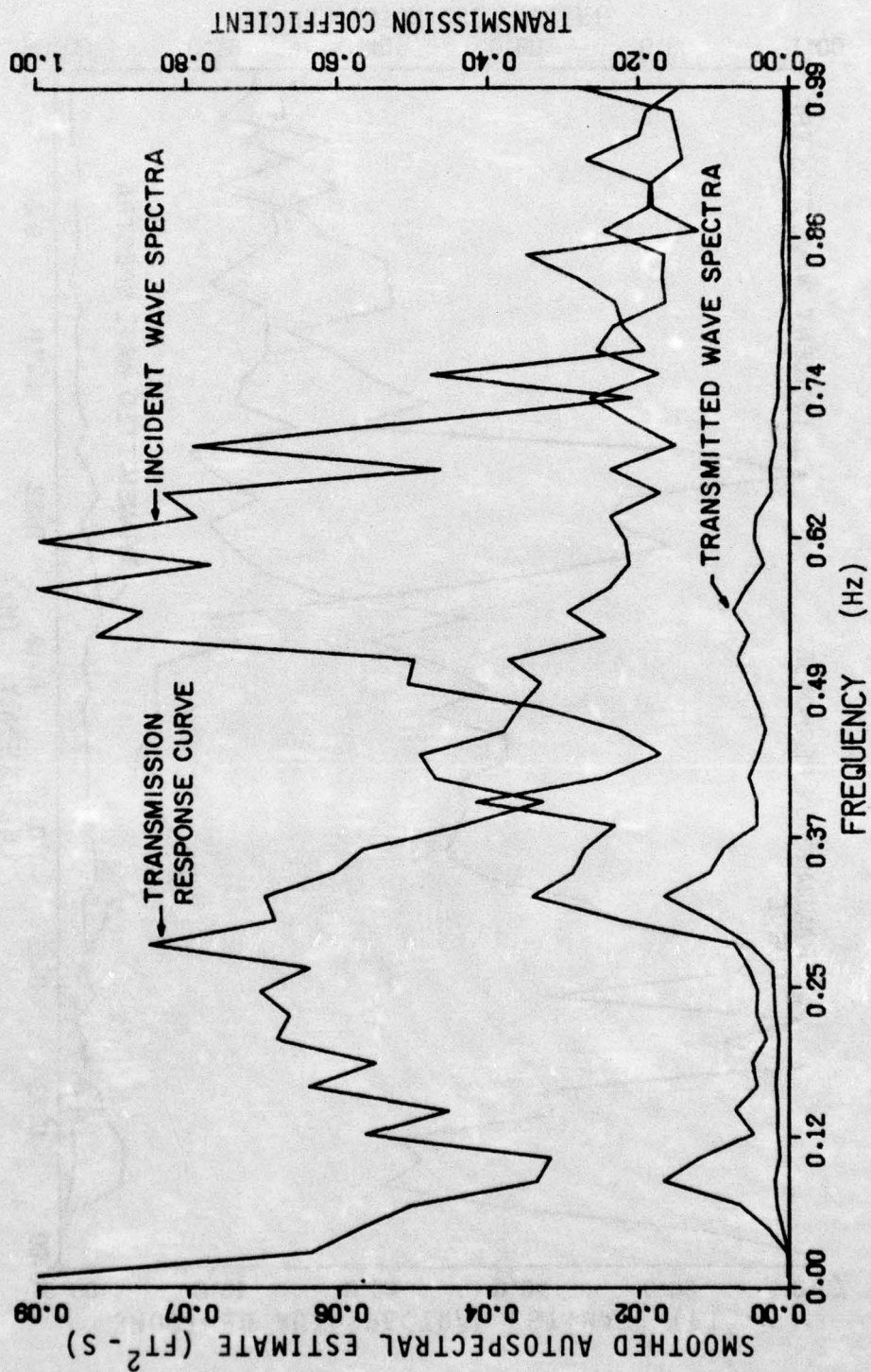


Figure H-8. Incident and transmitted wave spectral data (FH11-11).



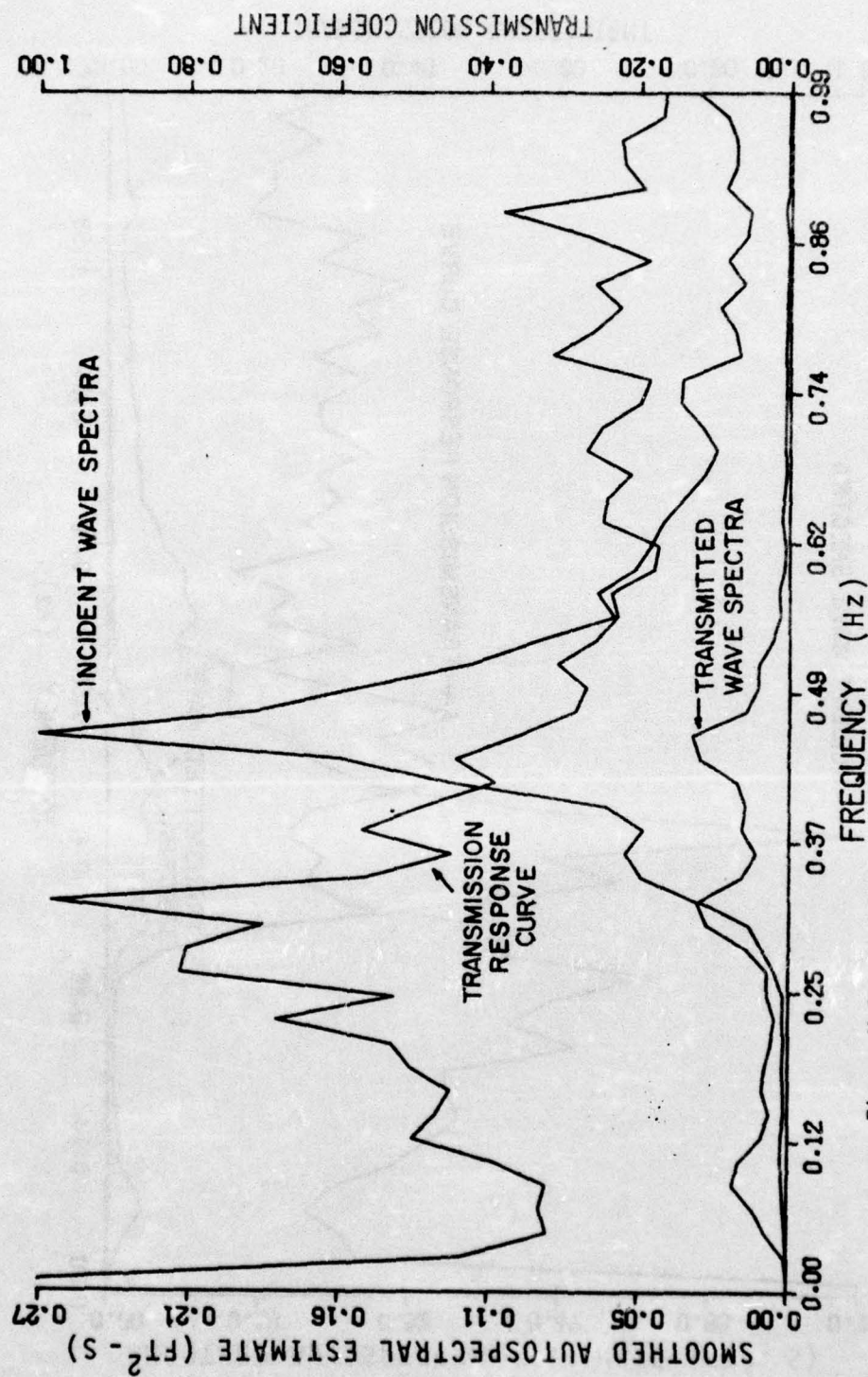


Figure H-9. Incident and transmitted wave spectral data (FH11-12).

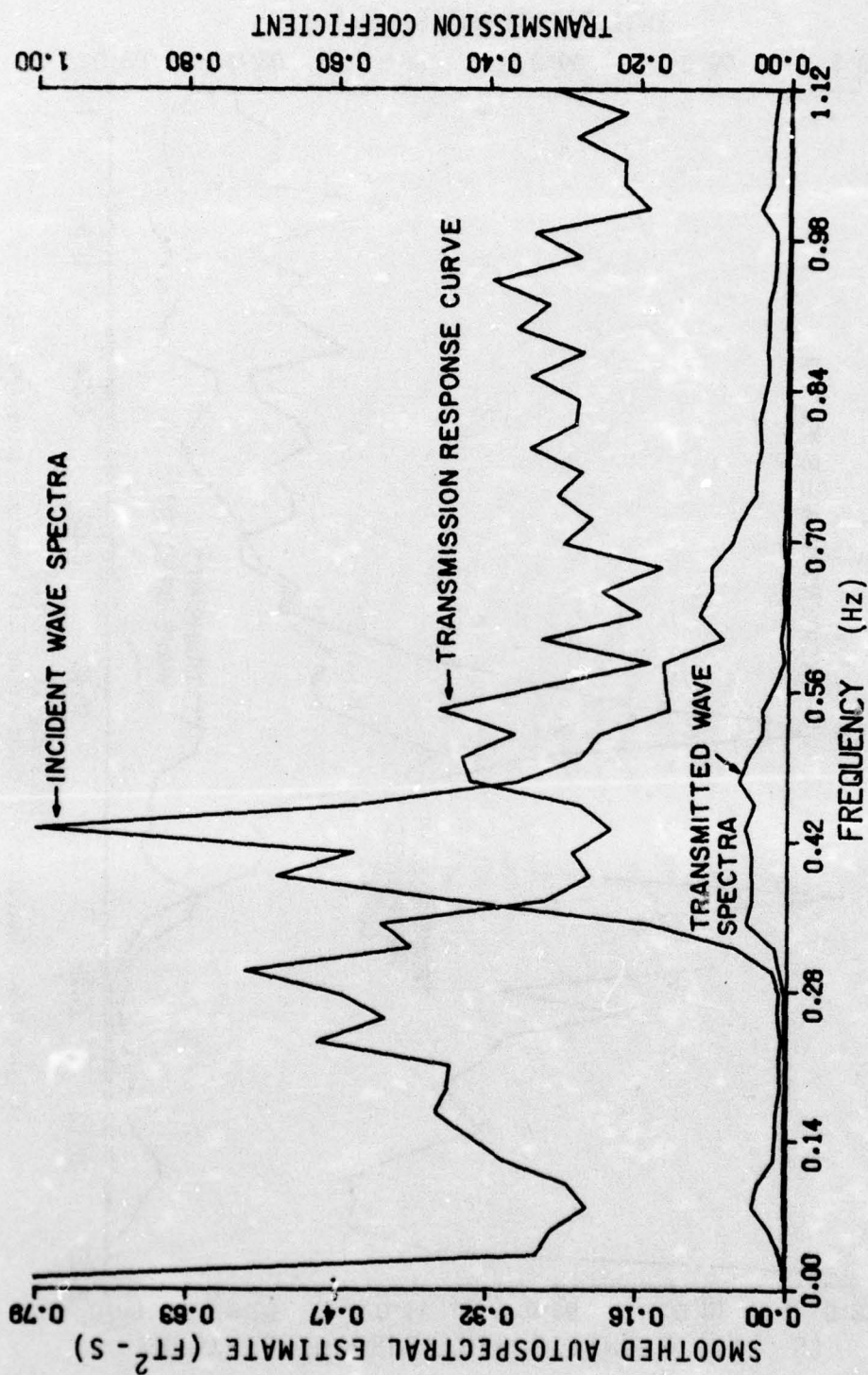


Figure H-10. Incident and transmitted wave spectral data (TK7-1), Tenakee Springs, Alaska.



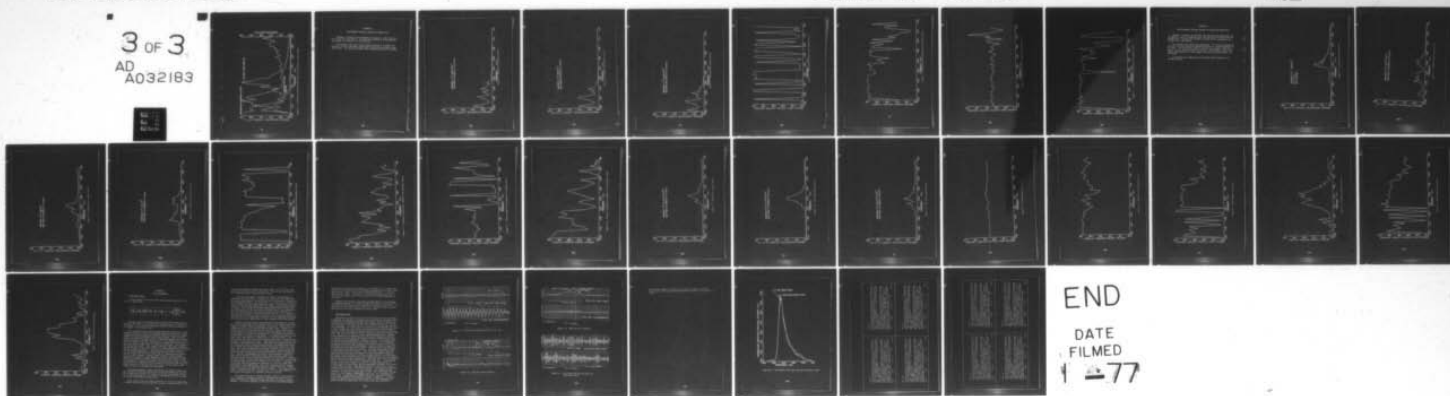
AD-A032 183

WASHINGTON UNIV SEATTLE OCEAN ENGINEERING RESEARCH LAB F/G 13/2  
FLOATING BREAKWATER FIELD ASSESSMENT PROGRAM, FRIDAY HARBOR, WA--ETC(U)  
SEP 76 B H ADEE, E P RICHEY, D R CHRISTENSEN DACW72-74-C-0012  
CERC-TP-76-17 NL

UNCLASSIFIED

3 OF 3

AD  
A032183



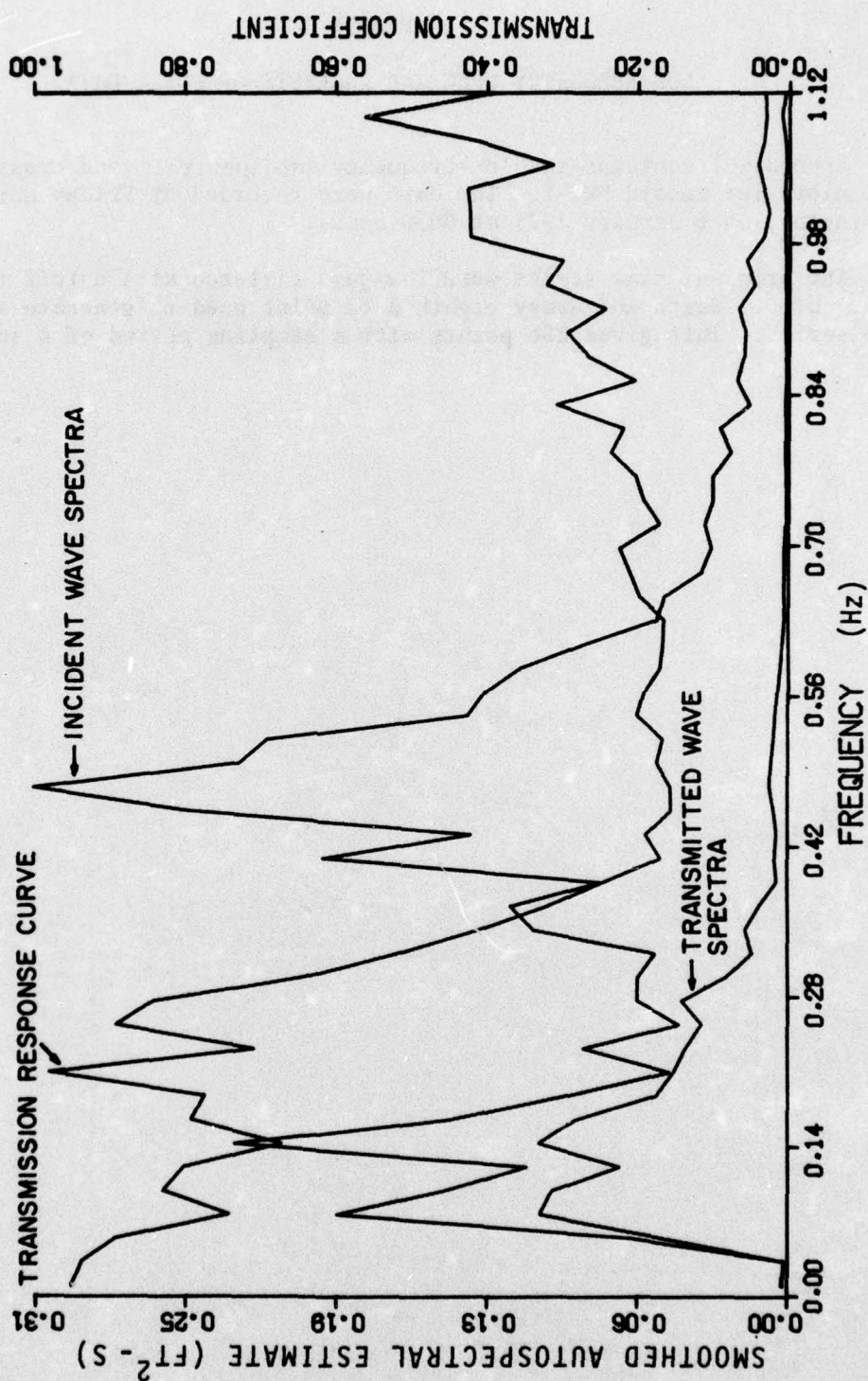


Figure H-11. Incident and transmitted wave spectral data (SK4-10), Sitka, Alaska.



## APPENDIX I

### LOW-FREQUENCY SPECTRAL ANALYSIS OF FORCE DATA

Appendix I contains the low-frequency autospectral and cross-spectral plots for record FH7-8. The data were recorded at Friday Harbor, Washington, on 6 January 1975 at 0030 hours.

The original time series were low-pass filtered at a cutoff frequency of 0.2 hertz and every eighth data point used to generate a new time series. This gives 256 points with a sampling period of 4 seconds.

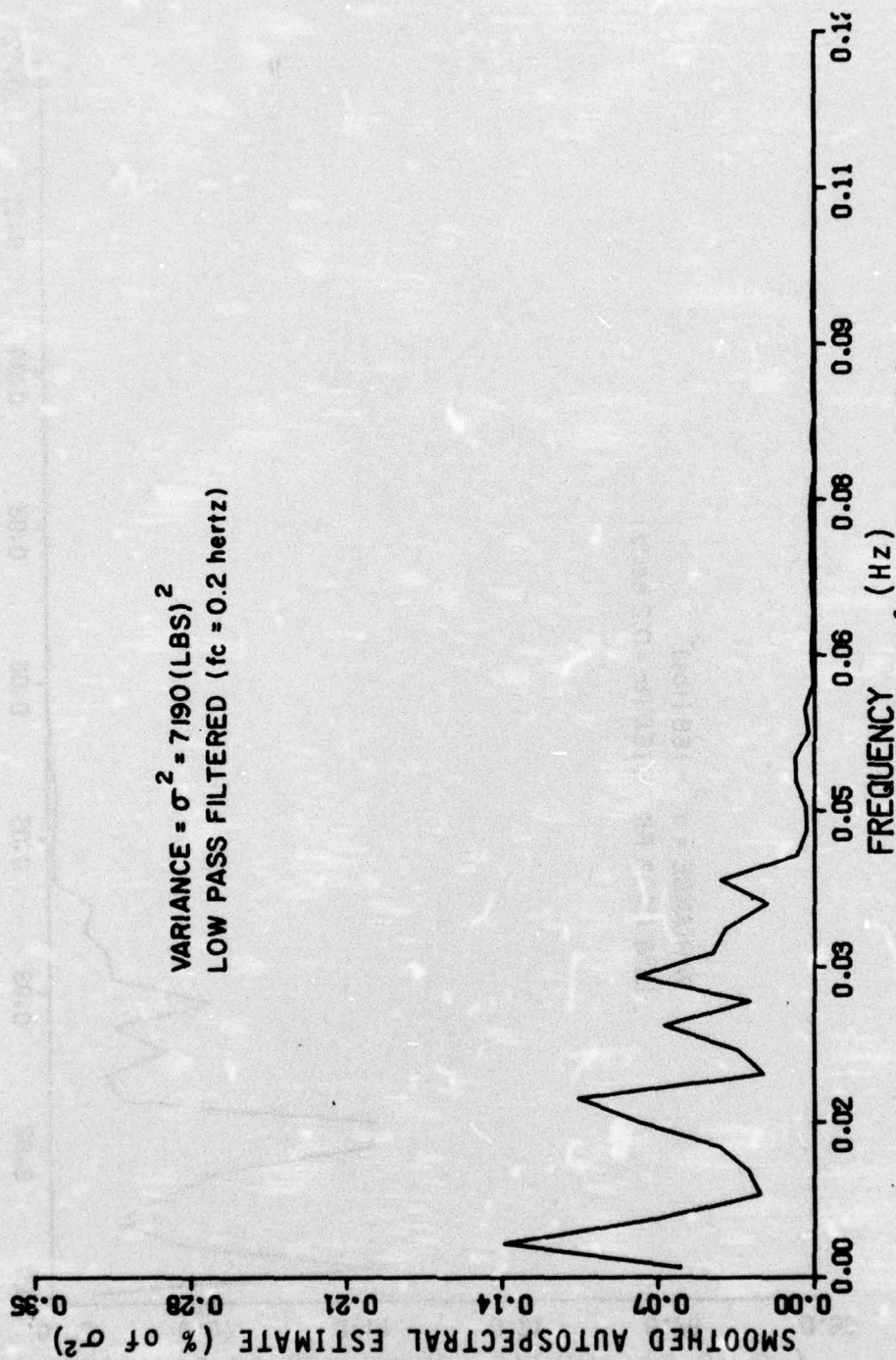


Figure I-1. Southwest force spectra (FH7-8).



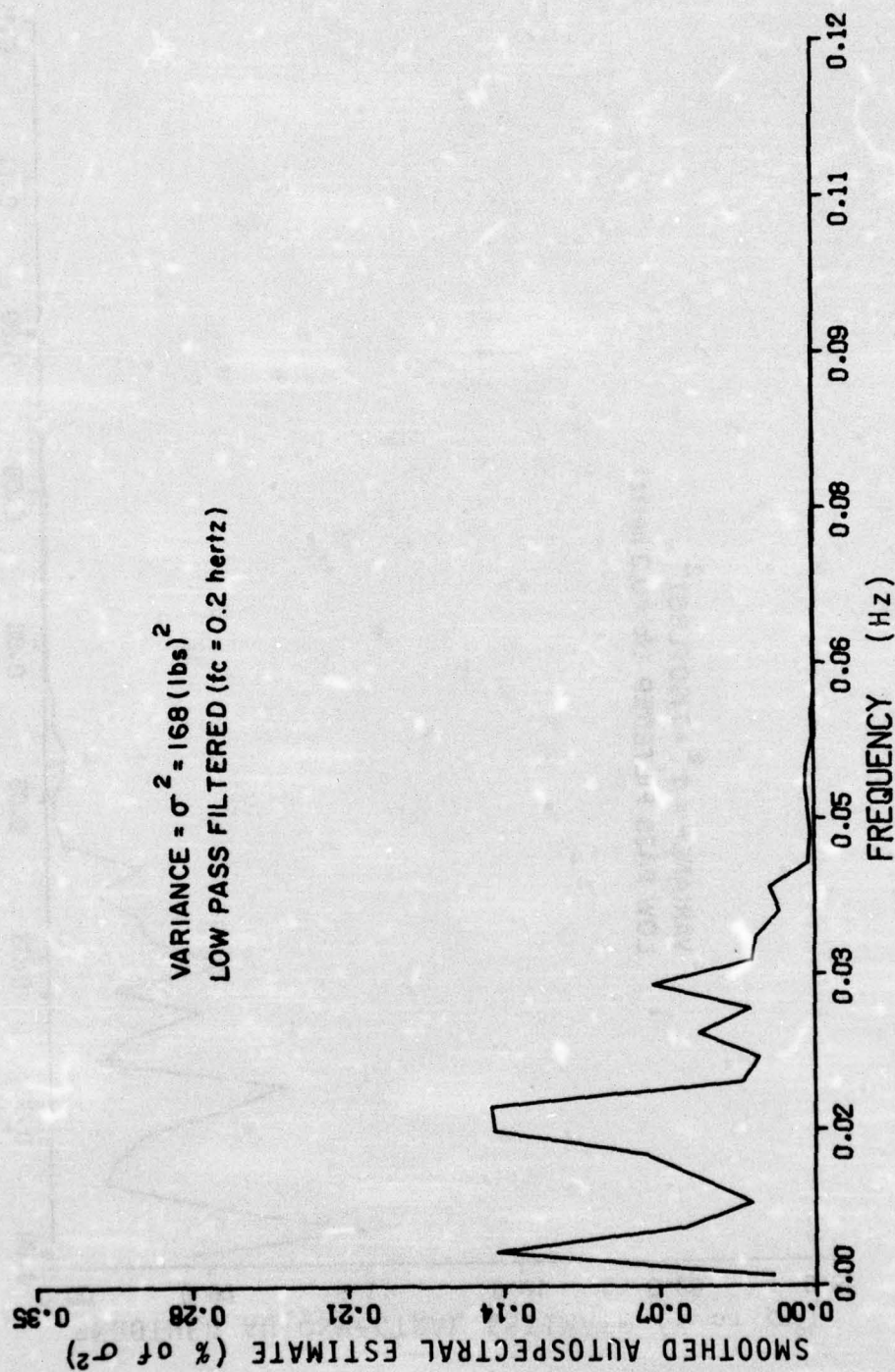


Figure I-2. Northeast force spectra (FH7-8).

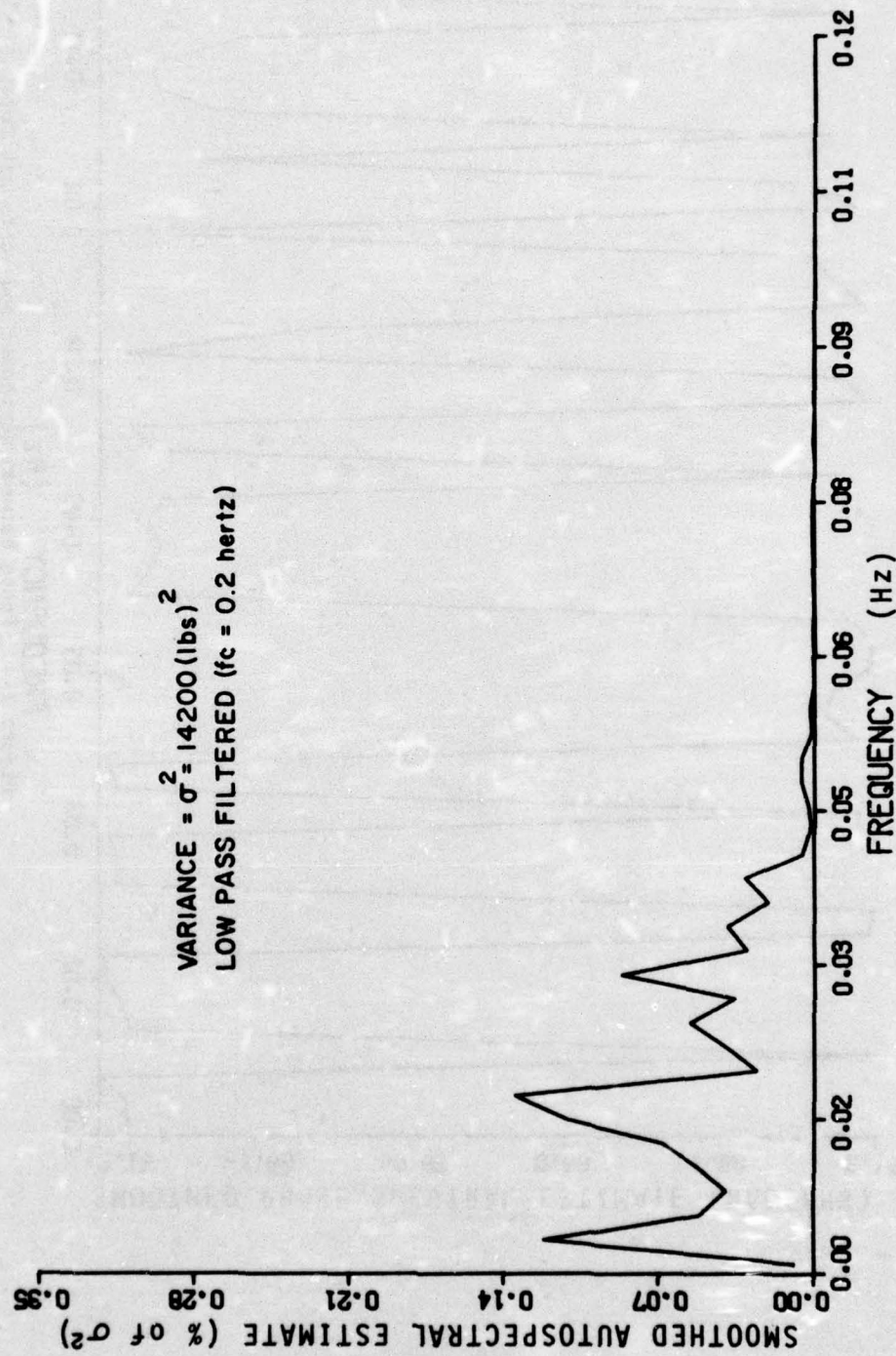


Figure 1-3. Southeast force spectra (FH7-8).



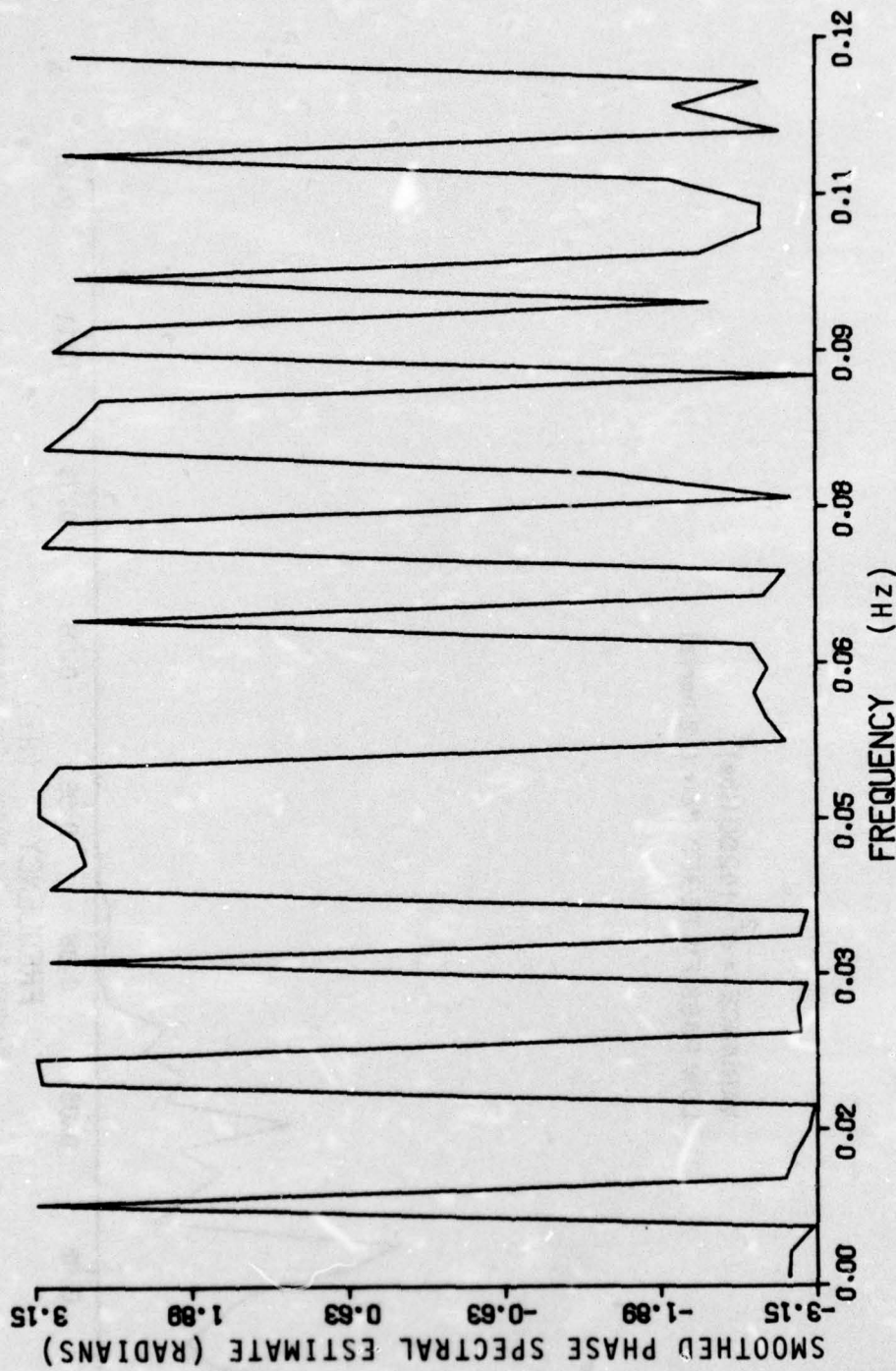


Figure I-4. Phase between northeast and southeast forces.

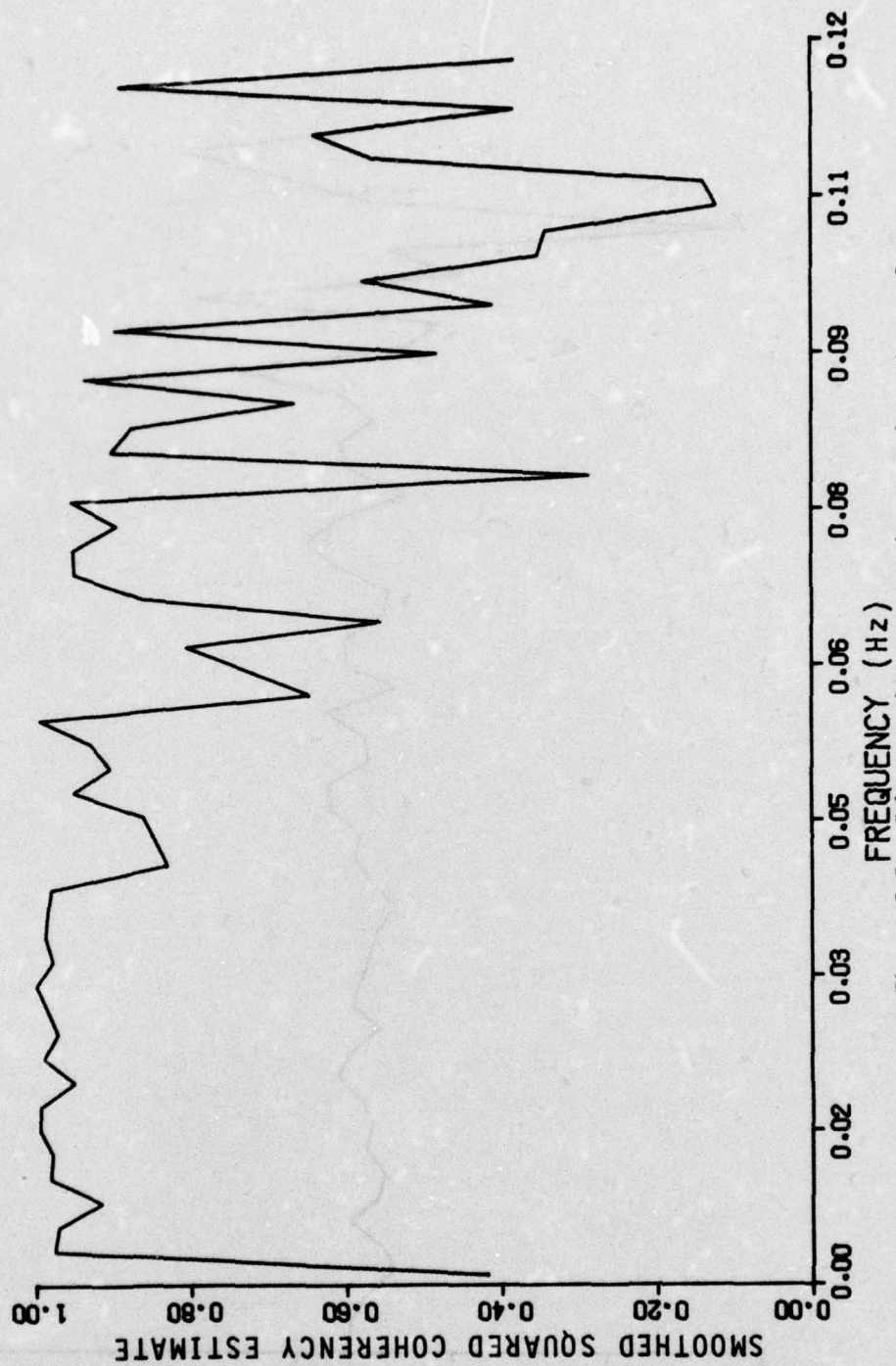


Figure I-5. Coherency between northeast and southeast forces.



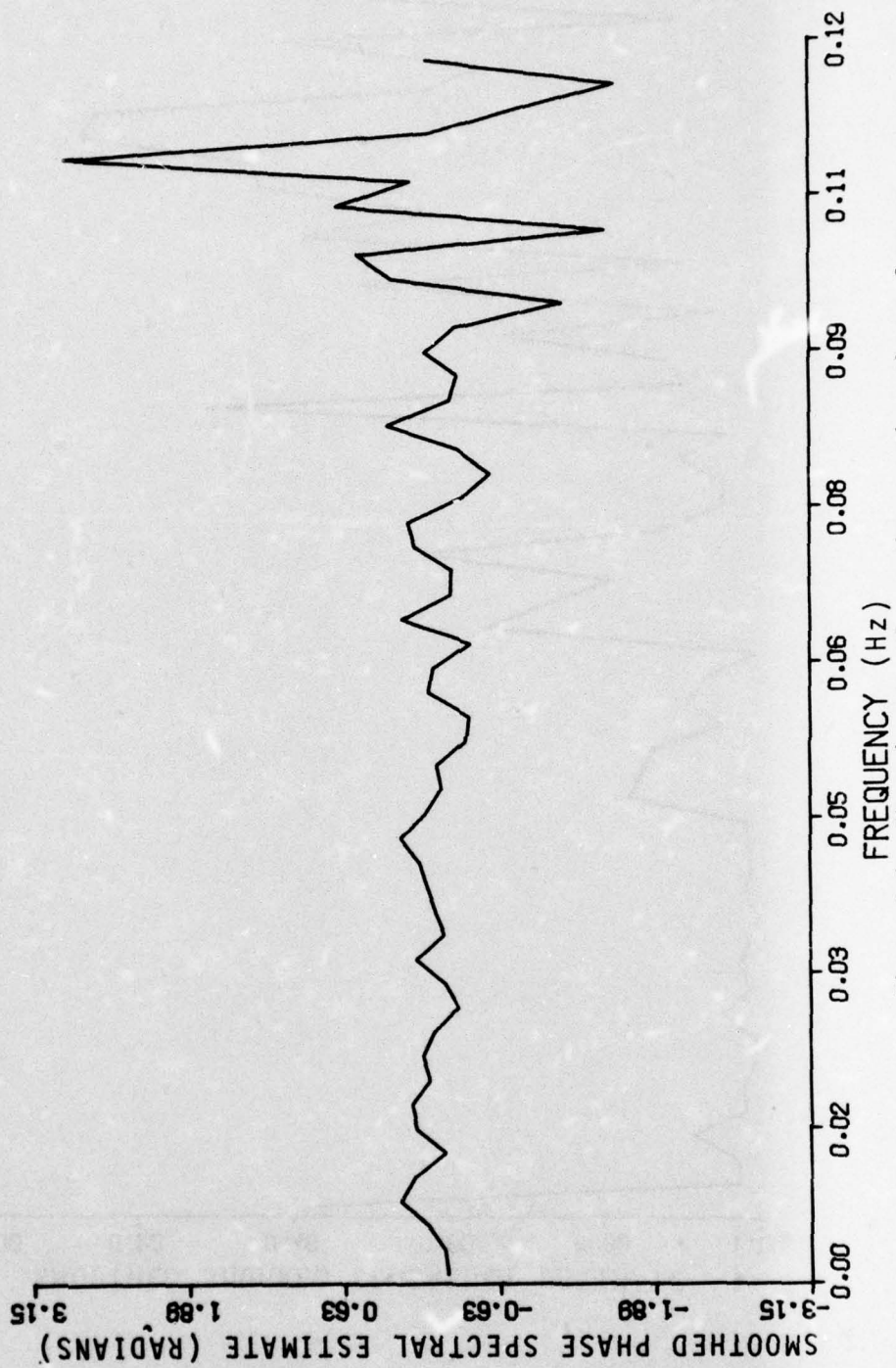


Figure I-6. Phase between the southeast and southwest forces.

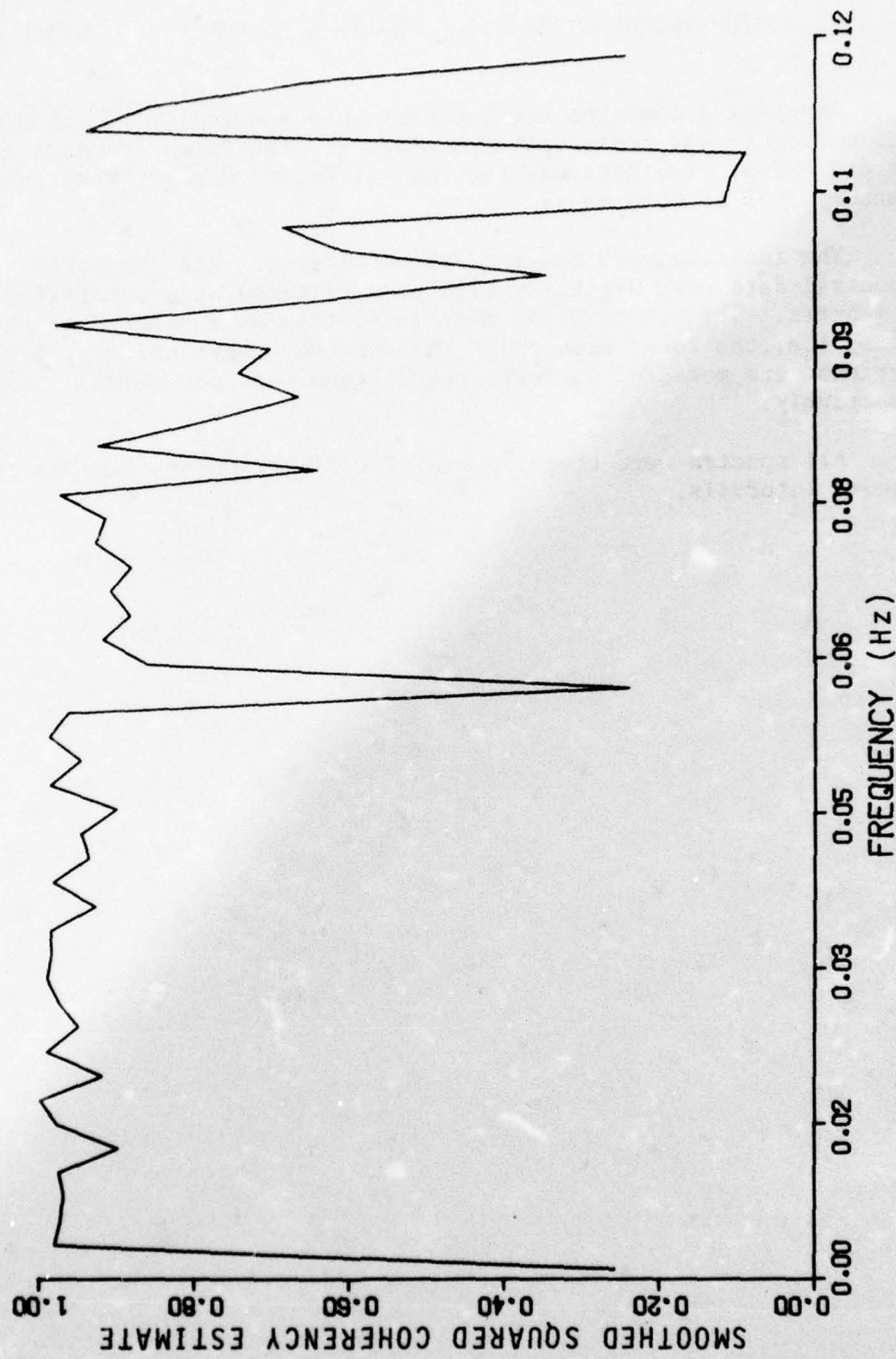


Figure I-7. Coherency between the southeast and southwest forces.



## APPENDIX J

### HIGH-FREQUENCY SPECTRAL ANALYSIS OF FORCE AND MOTION DATA

Appendix J contains the incident wave spectral plot along with the autospectral and cross-spectral plots for the force and motion data for record FH7-8. The data was recorded at Friday Harbor, Washington, on 6 January 1975 at 0030 hours.

The incident wave spectra was unfiltered. All the force and motion spectral data were digitally high-pass filtered at a cutoff frequency of 0.1 hertz. The autospectral data is plotted as a percent of the variance, i.e., the total area under the spectra. Wave heights, forces, and motions were measured in feet, pounds, and feet per second square, respectively.

All spectra were computed from 2,048 data points sampled at 0.5-second intervals.

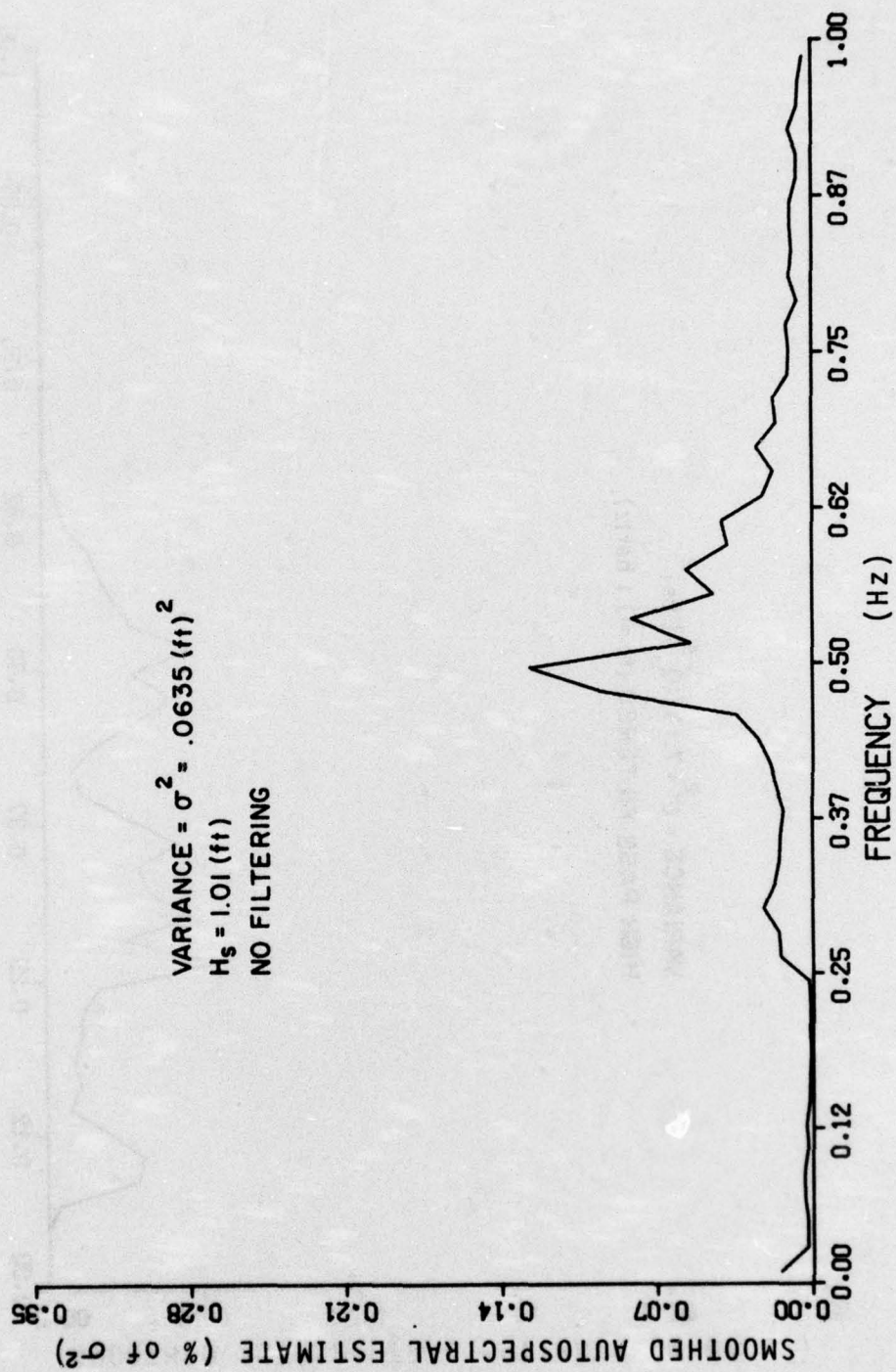


Figure J-1. Incident wave spectra (FH7-8).



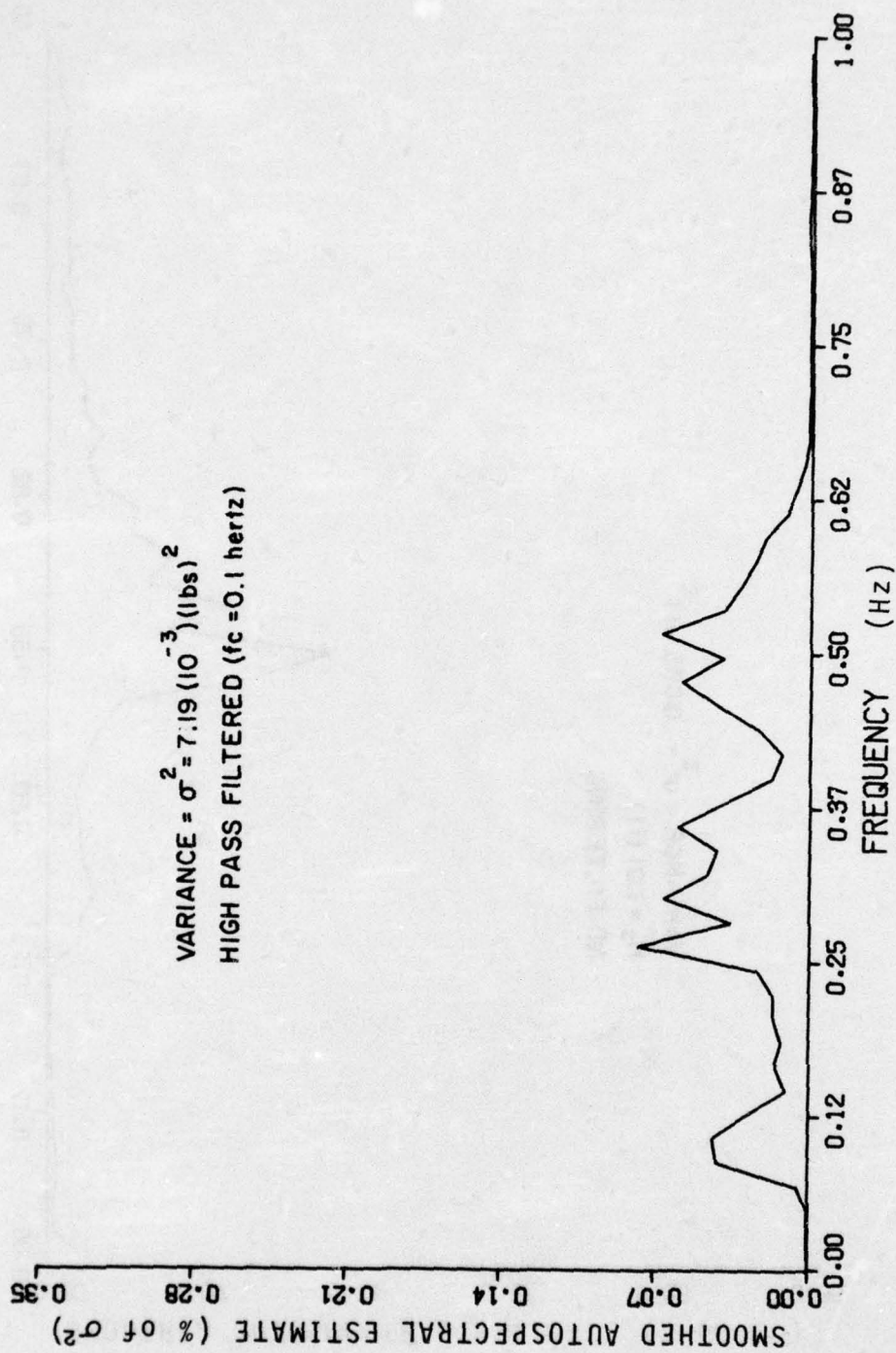


Figure J-2. Southeast force spectra (FH7-8).

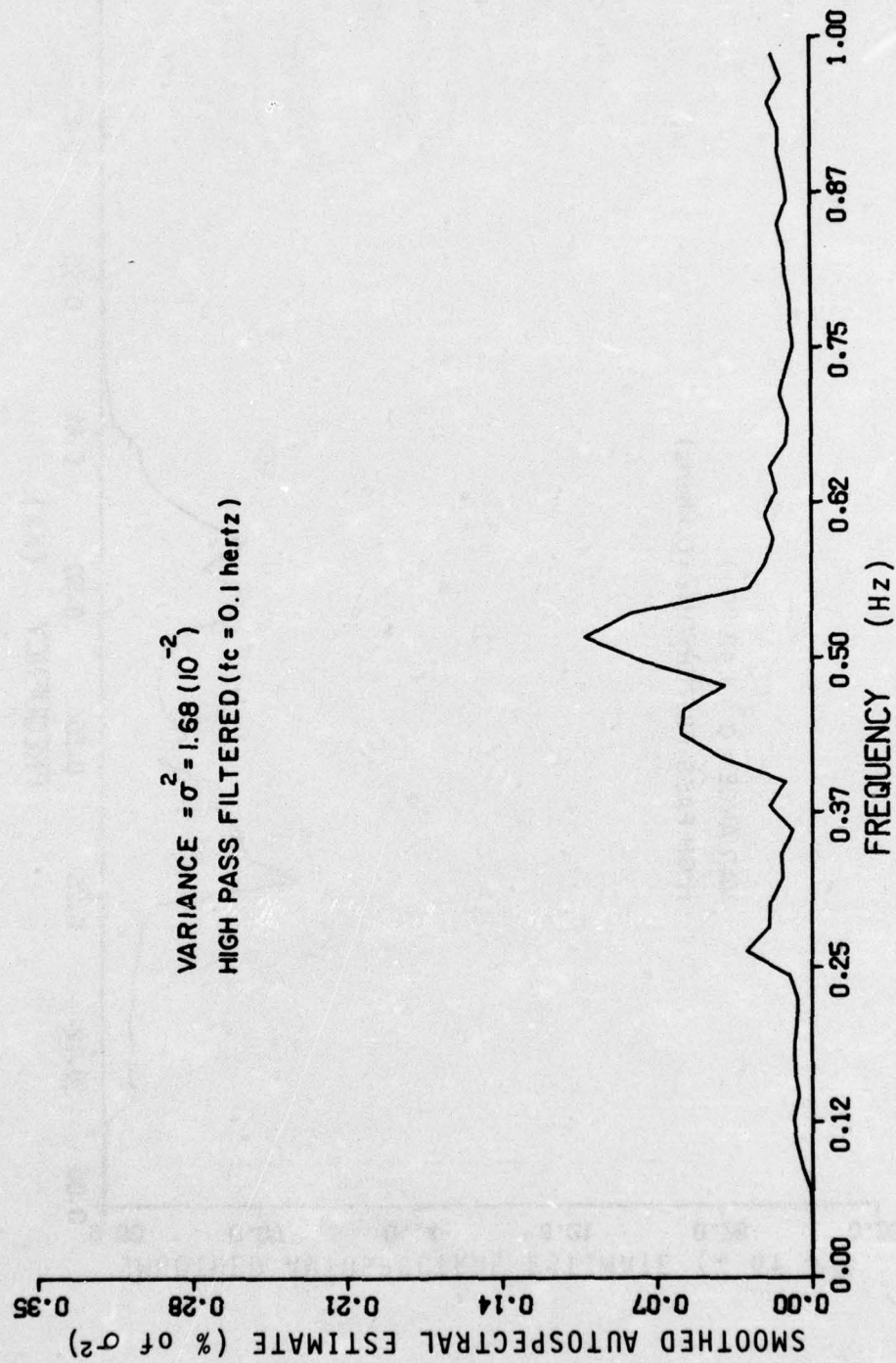


Figure J-3. Northeast force spectra (FH7-8).



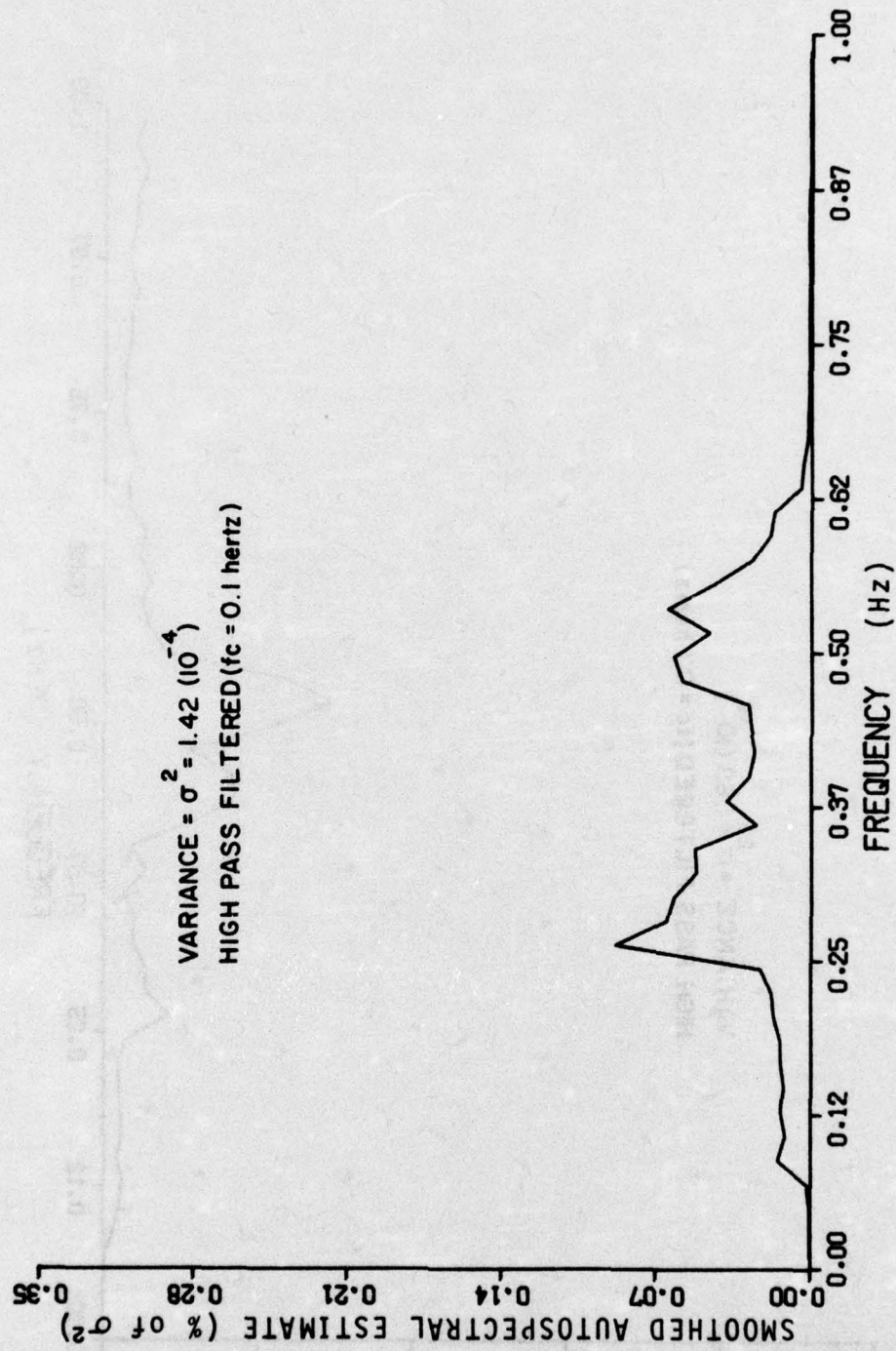


Figure J-4. Southeast force spectra (FH7-8)

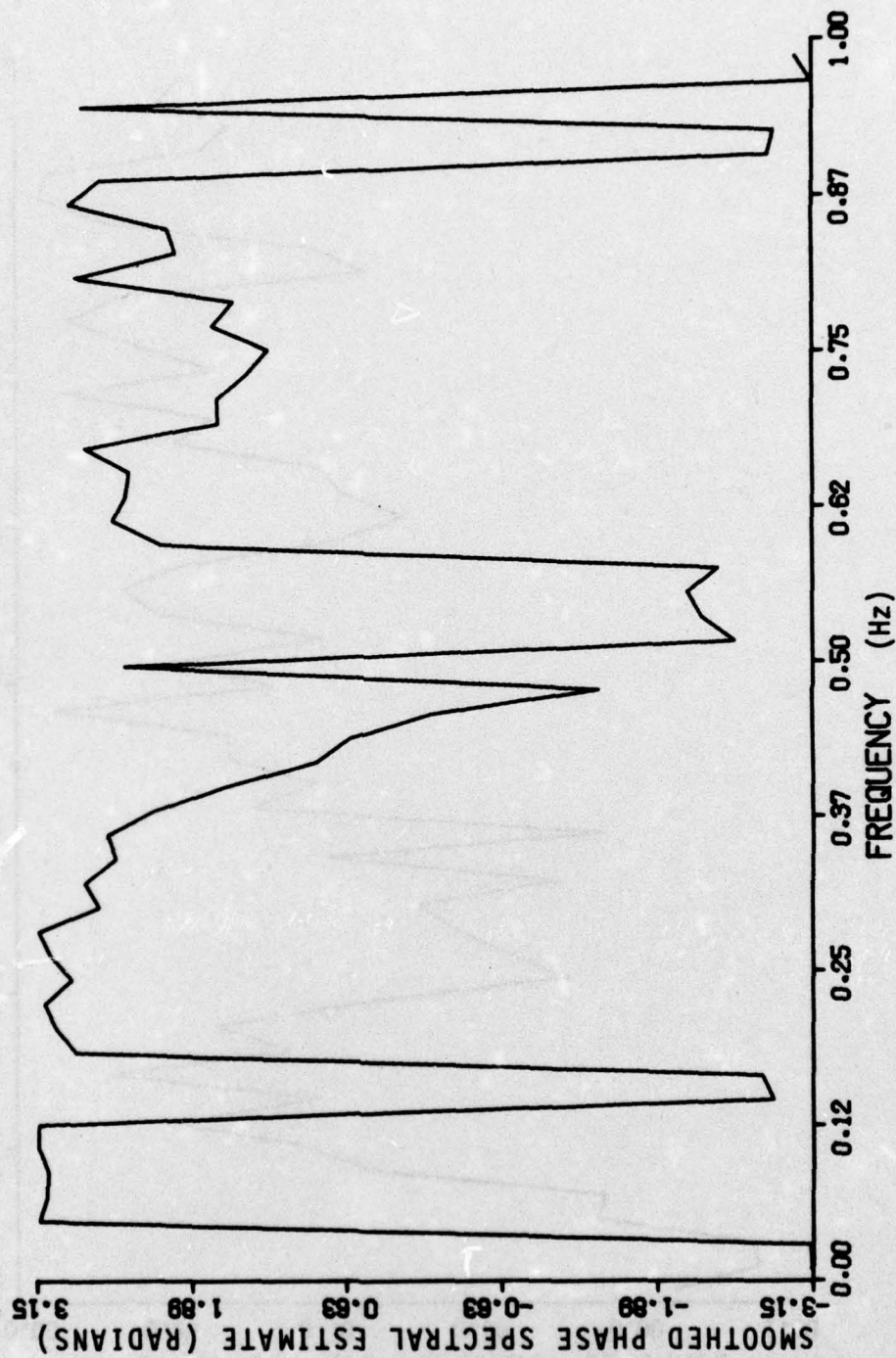


Figure J-5. Phase between the northeast and southeast forces.



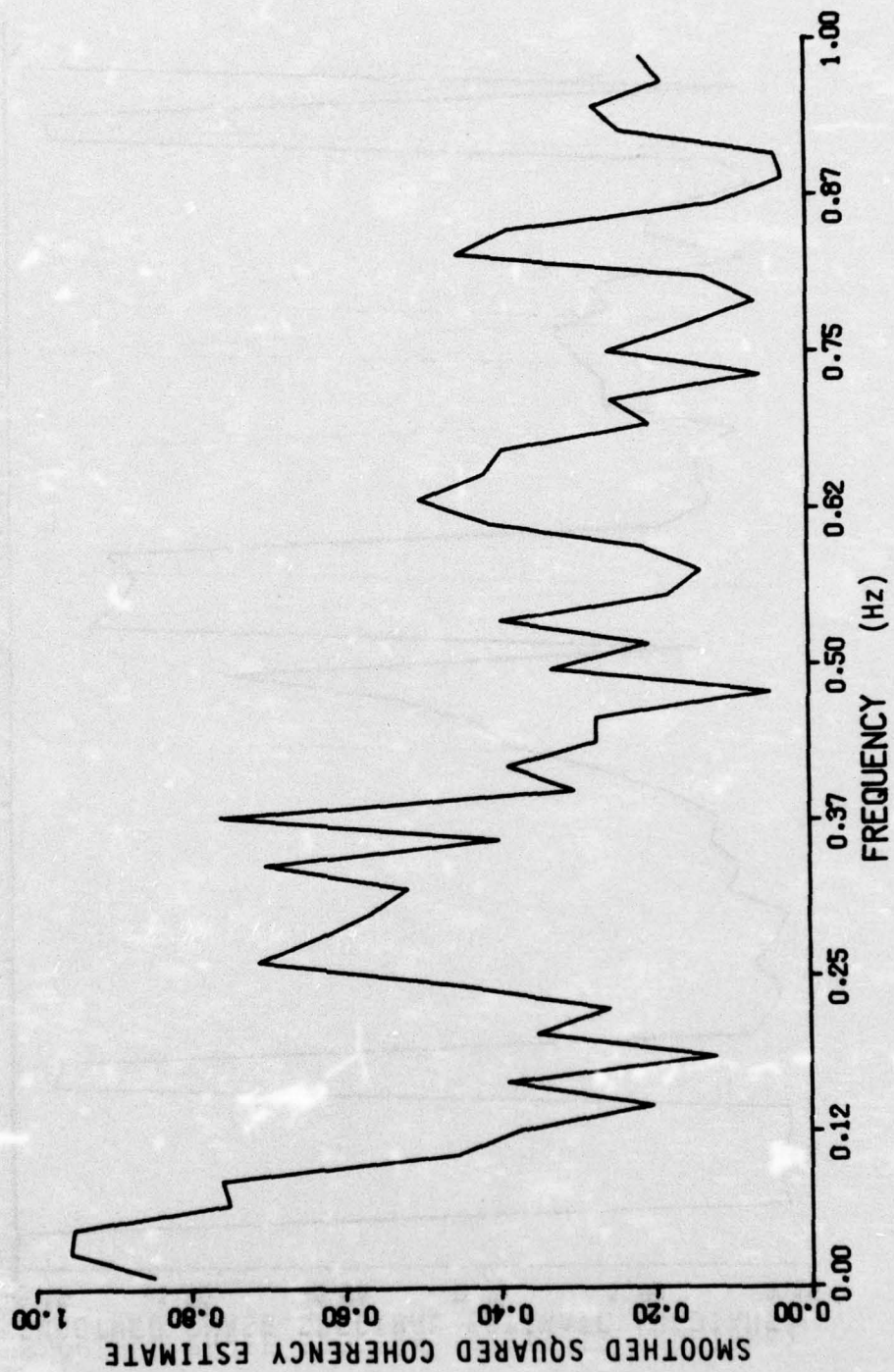


Figure J-6. Coherency between the northeast and southeast forces.

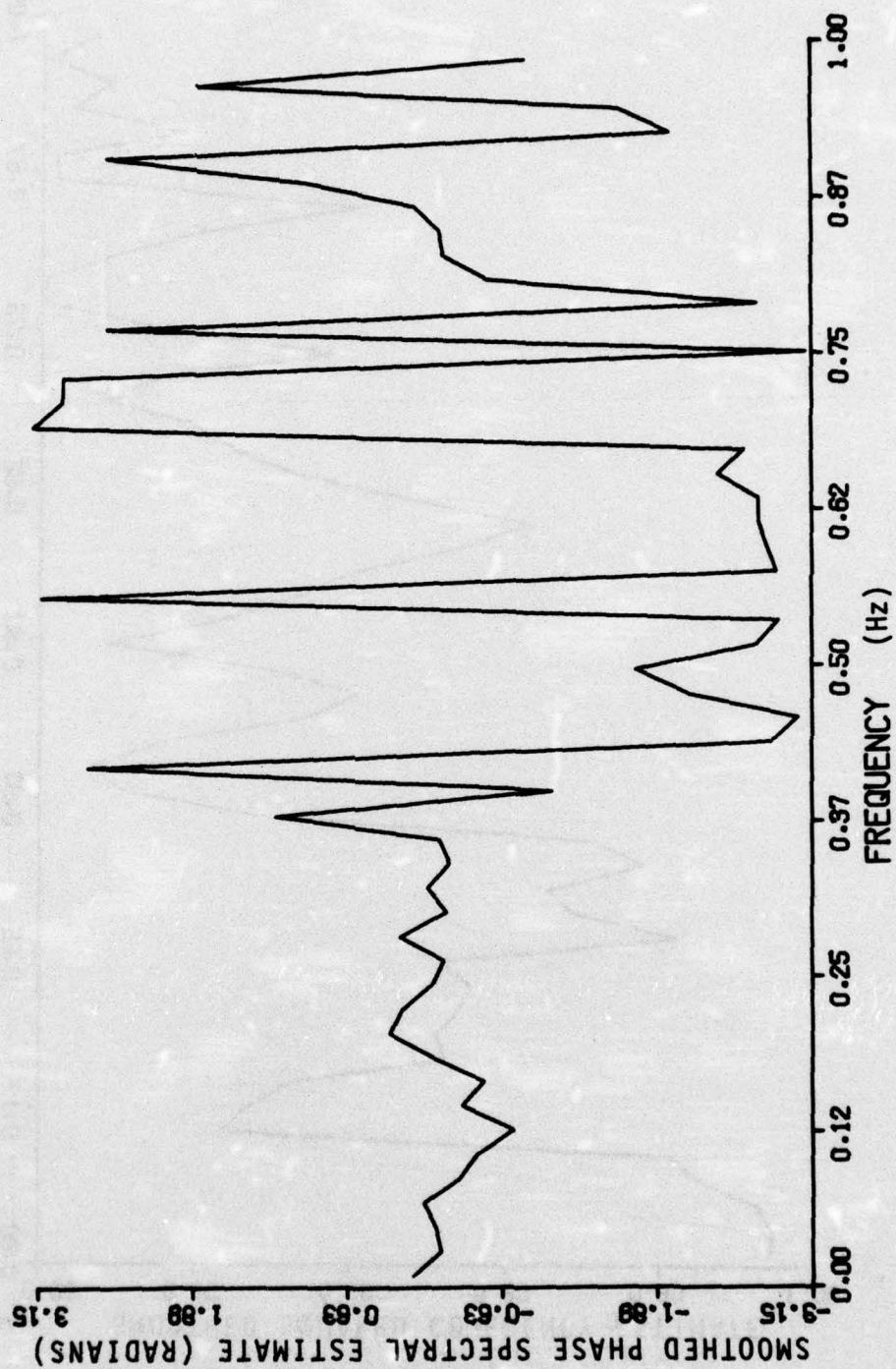


Figure J-7. Phase between the southeast and southwest forces.



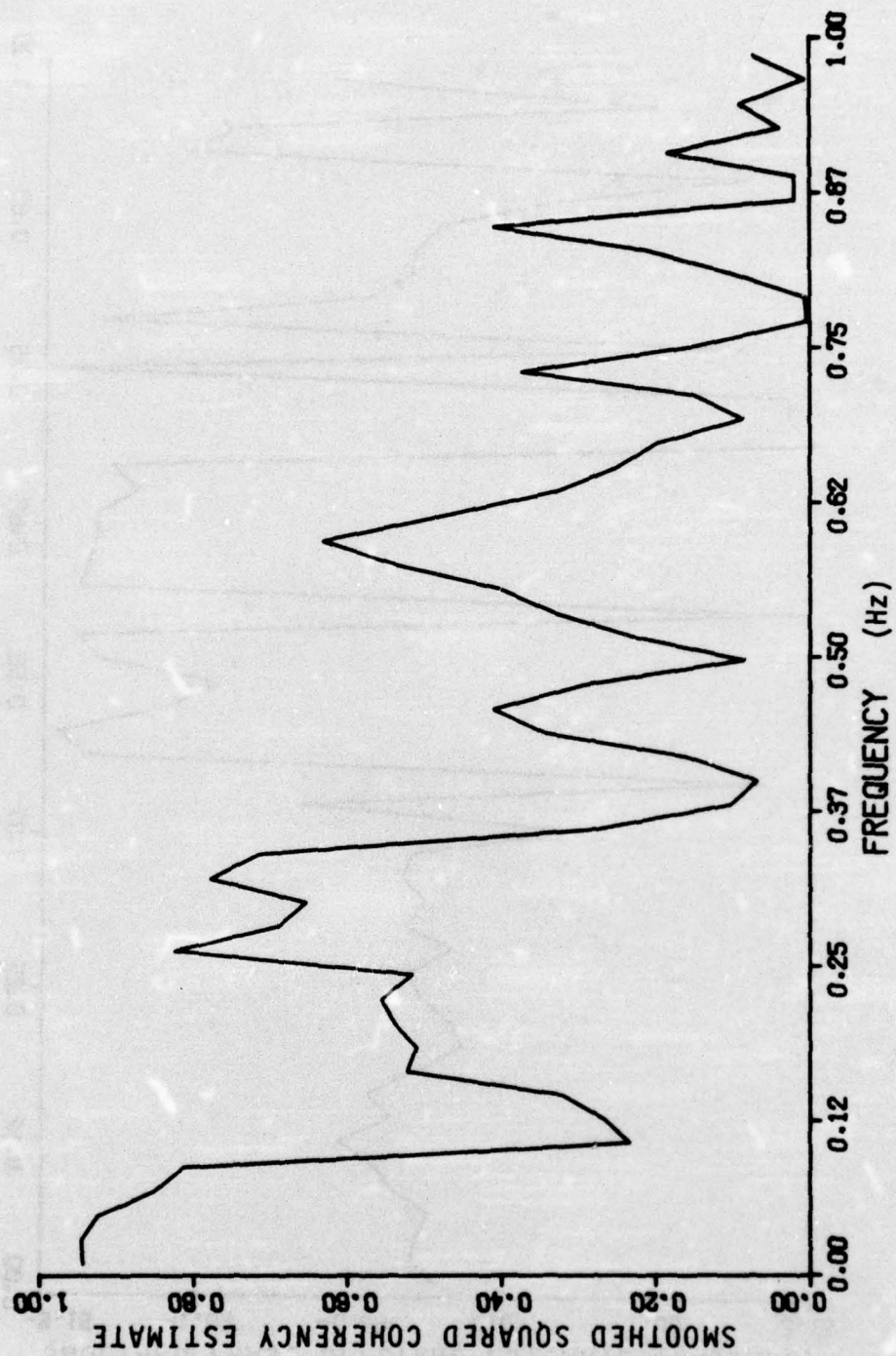


Figure J-8. Coherency between the southeast and southwest forces.

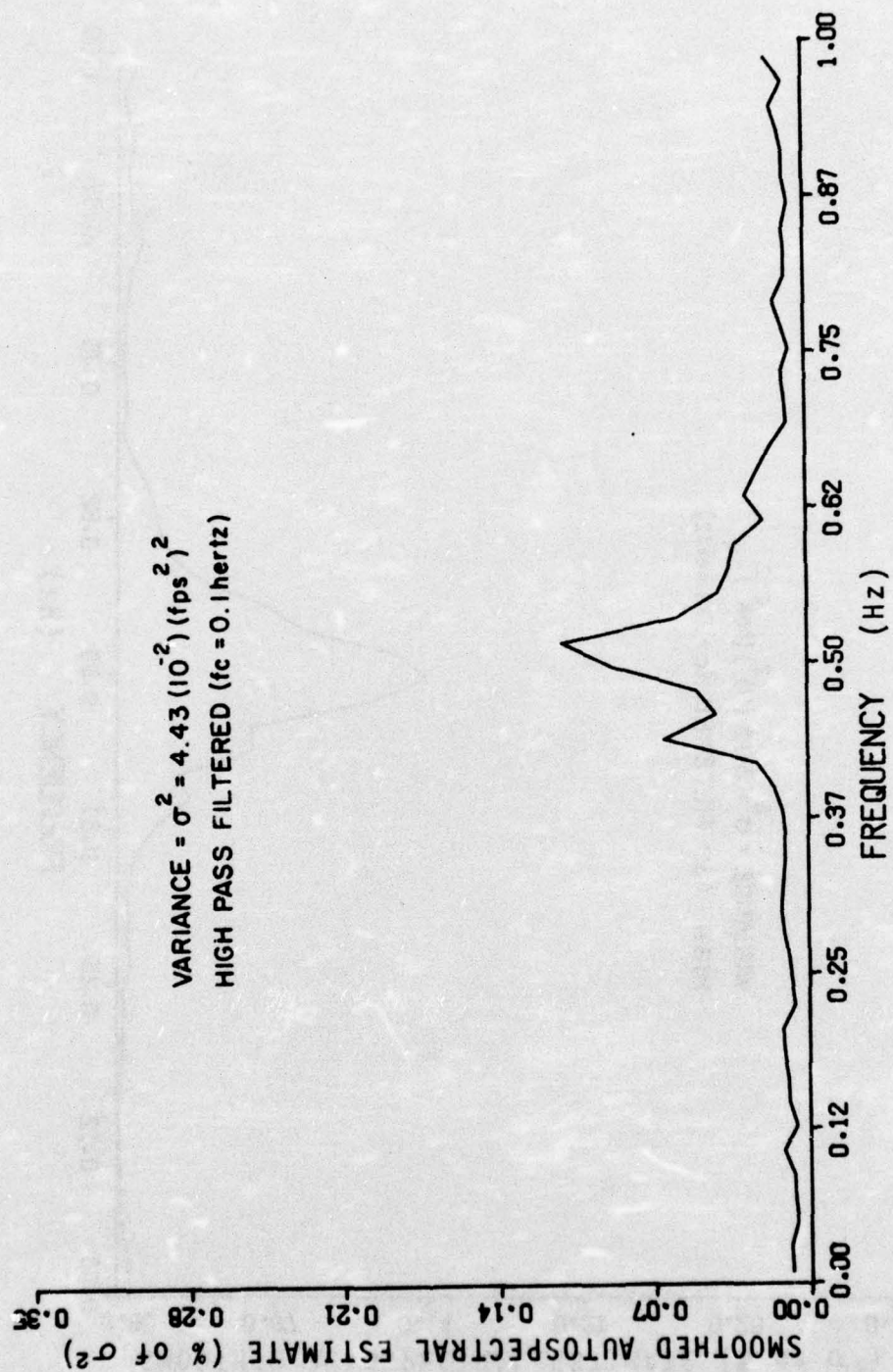


Figure J-9. Heave motion spectra (FH7-8).



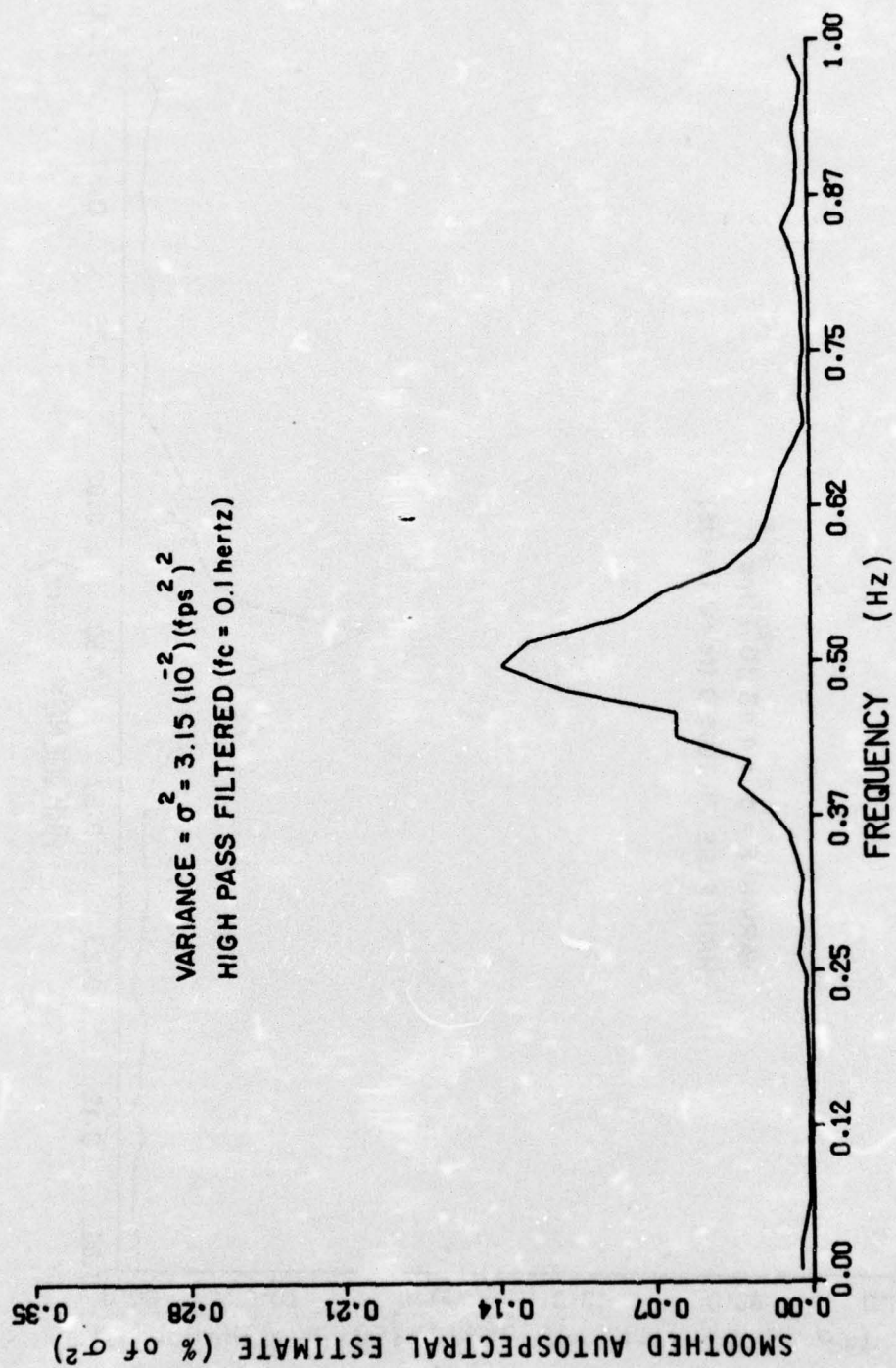


Figure J-10. Sway motion spectra (FH7-8).

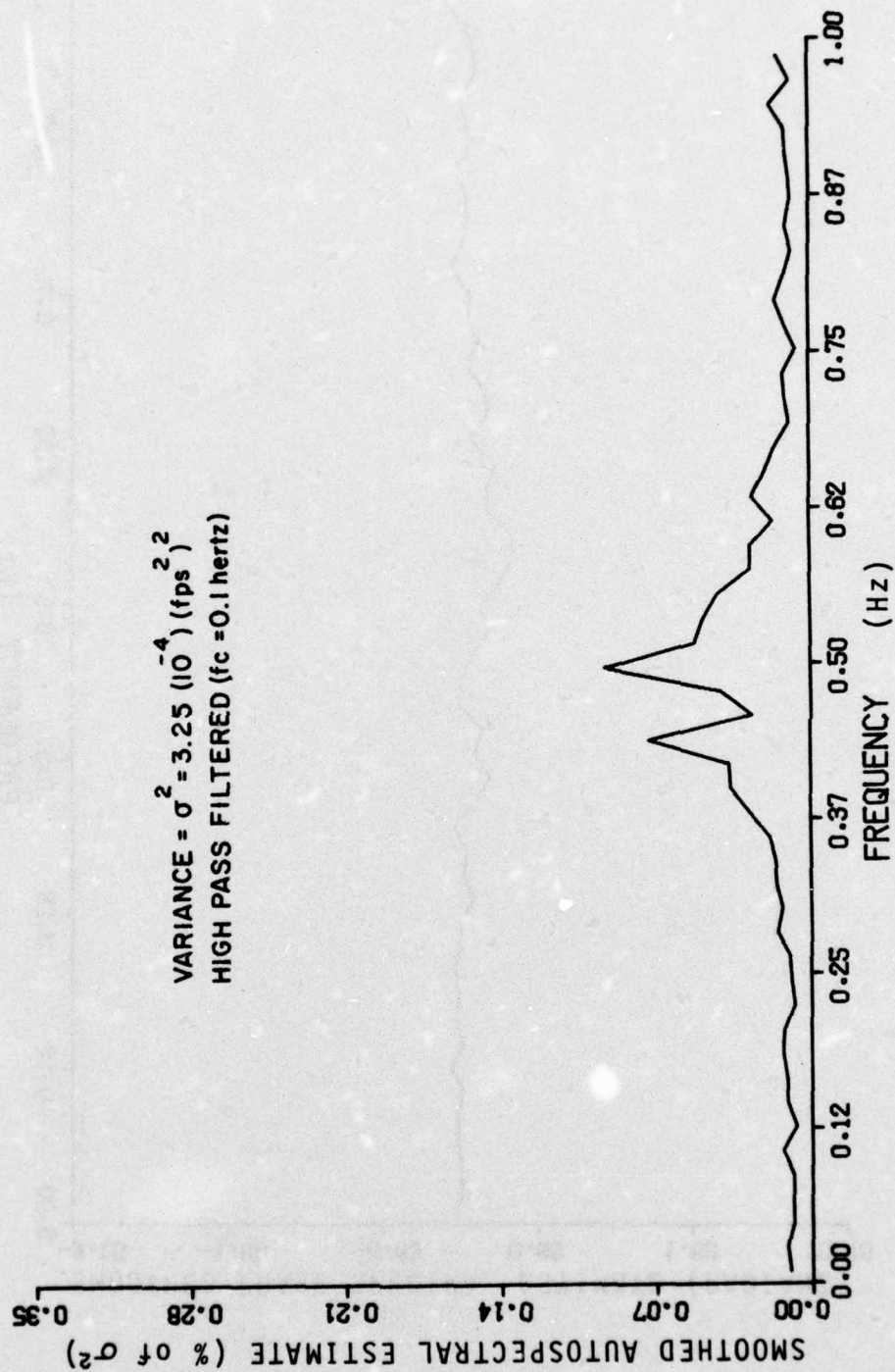


Figure J-11. Roll motion spectra (FH7-8).



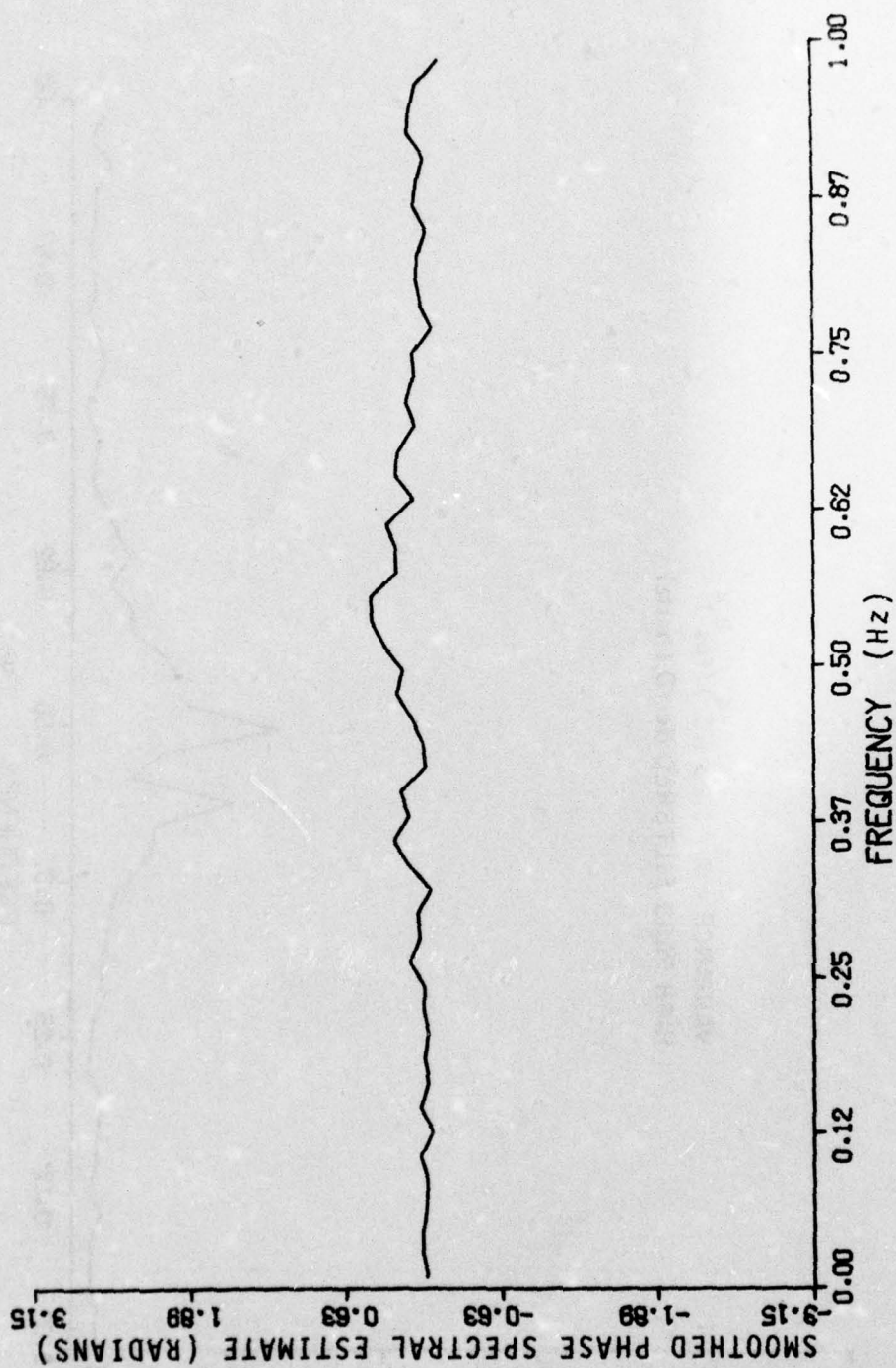


Figure J-12. Phase between heave and roll.

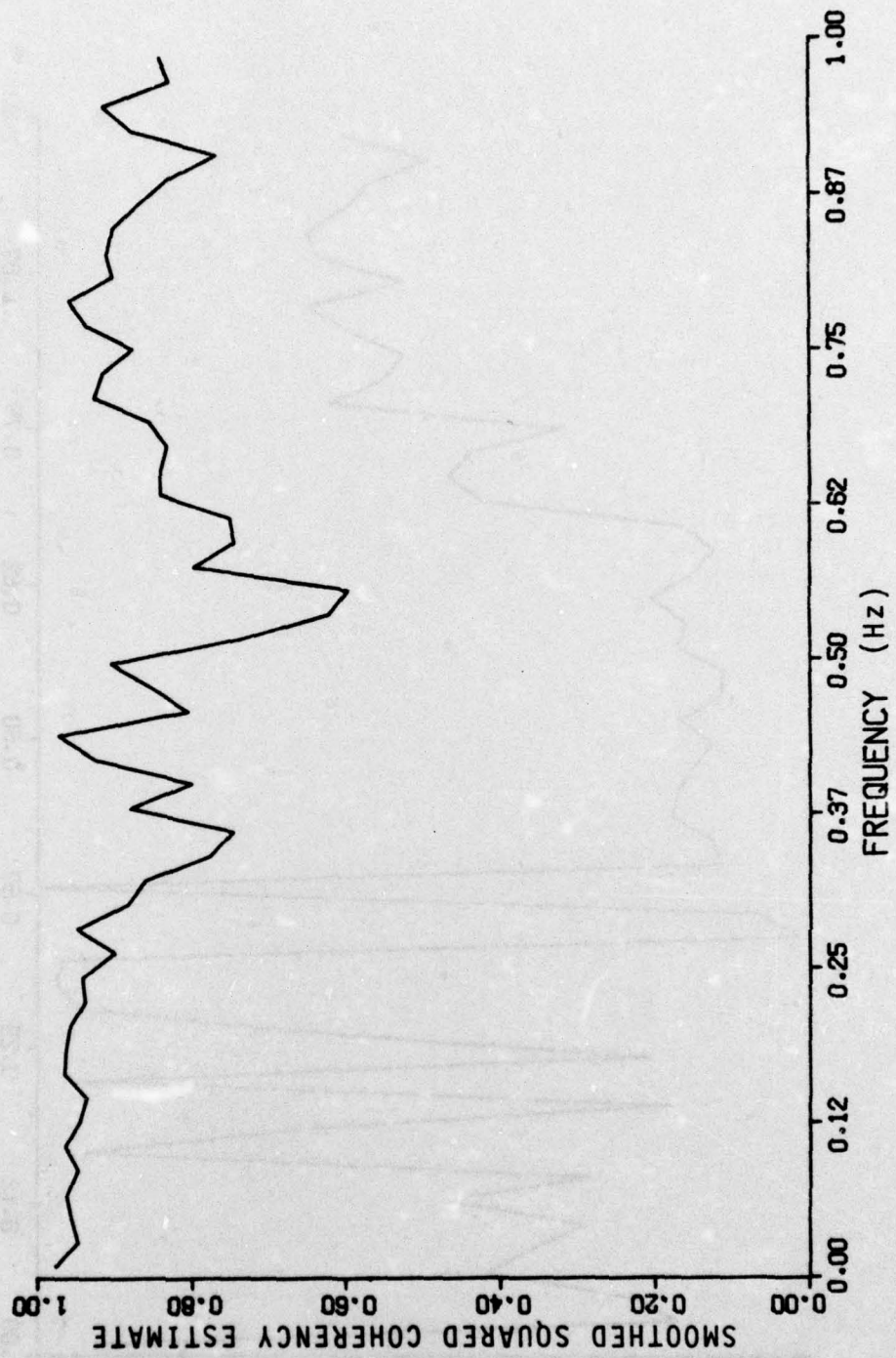


Figure J-13. Coherency between heave and roll.



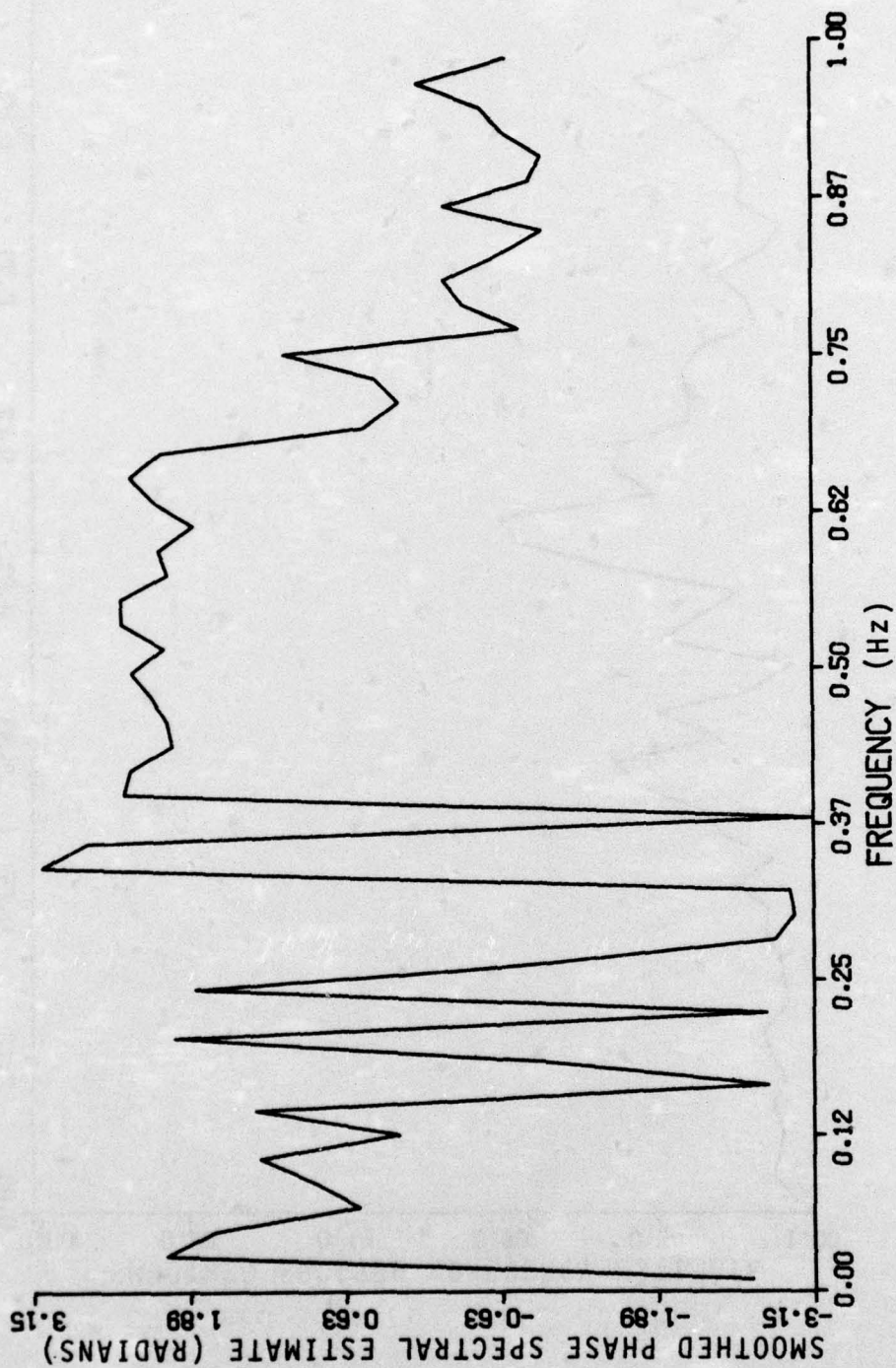


Figure J-14. Phase between sway and roll.

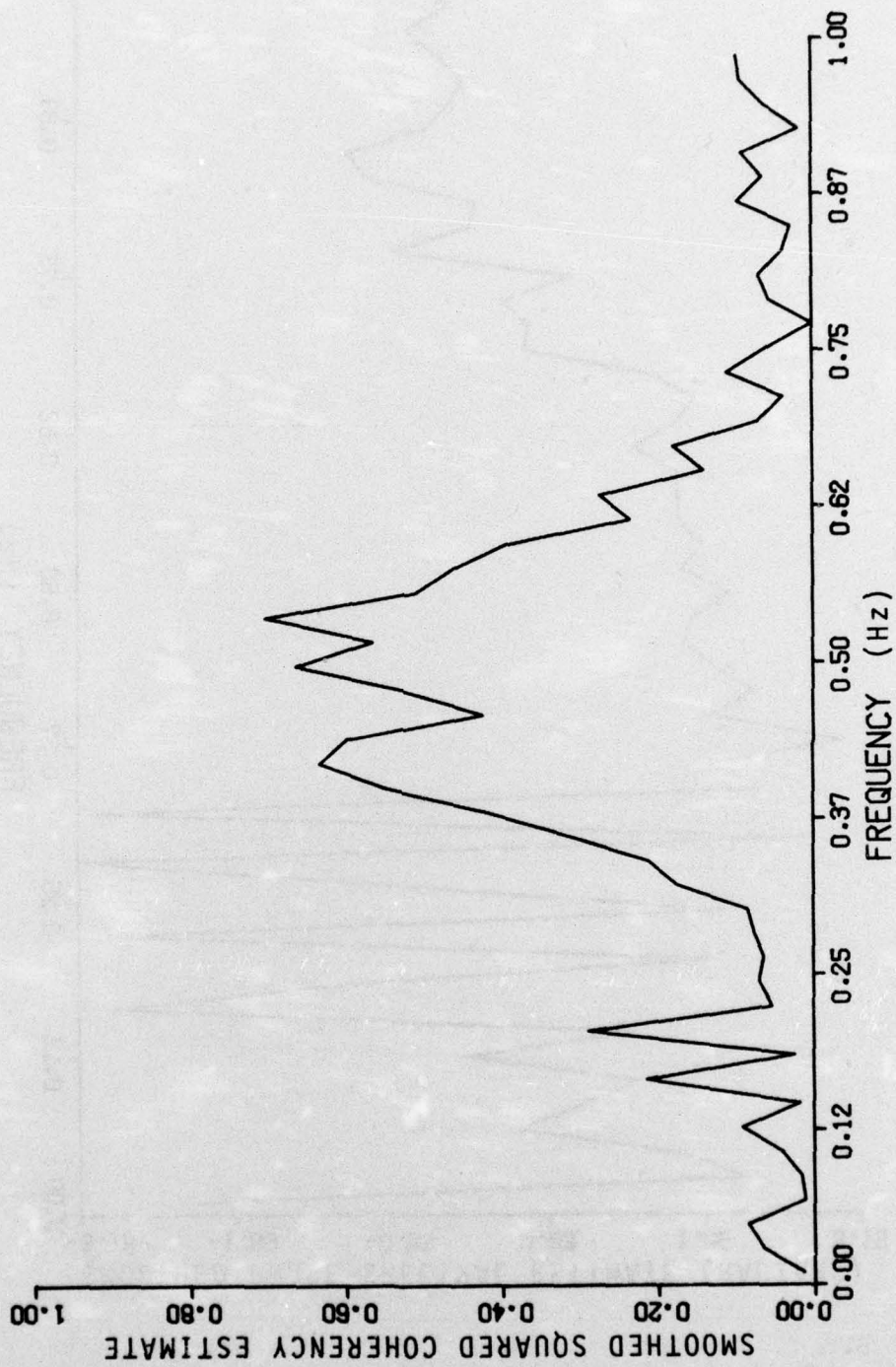


Figure J-15. Coherency between sway and roll.



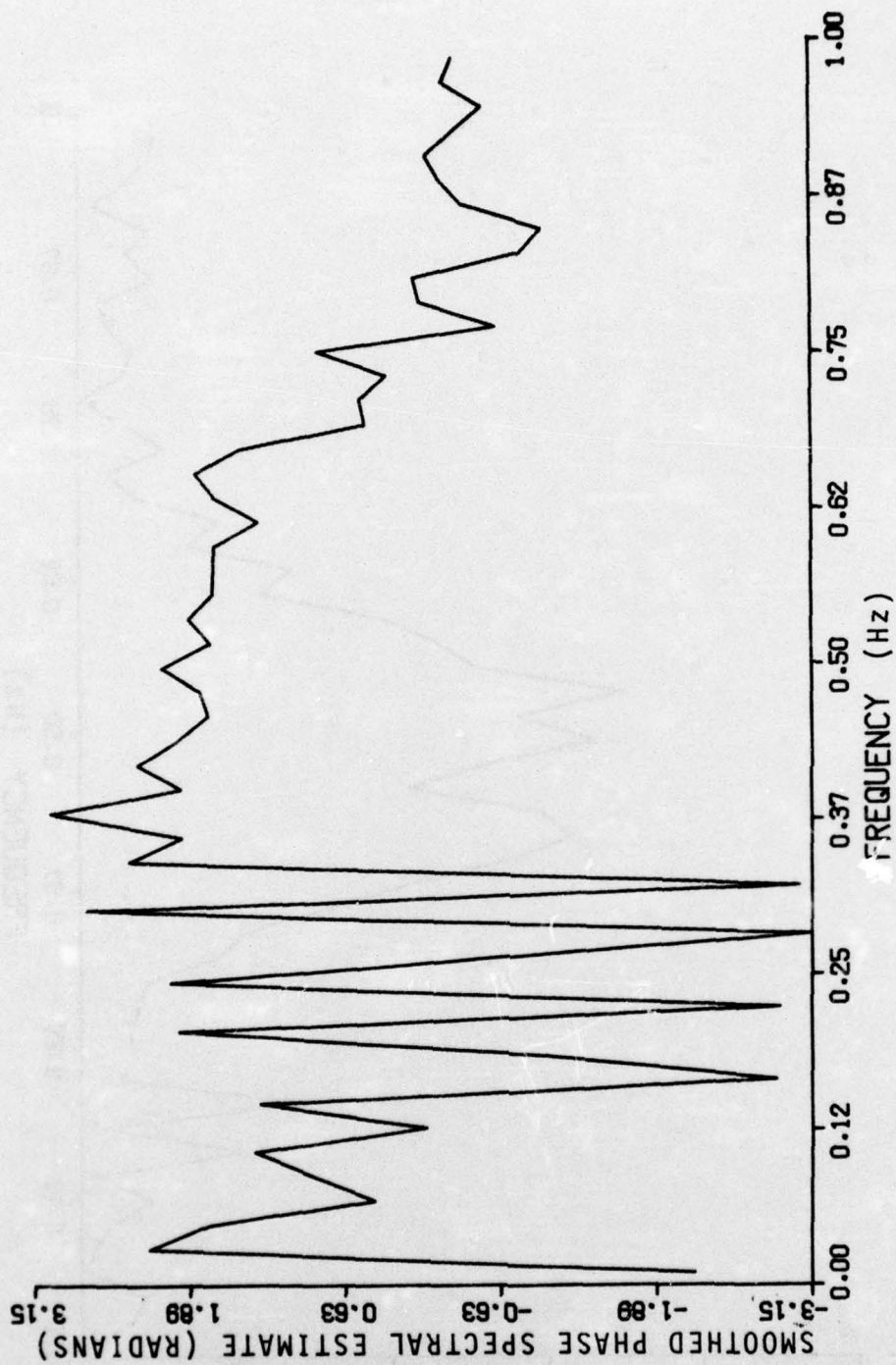


Figure J-16. Phase between sway and heave.

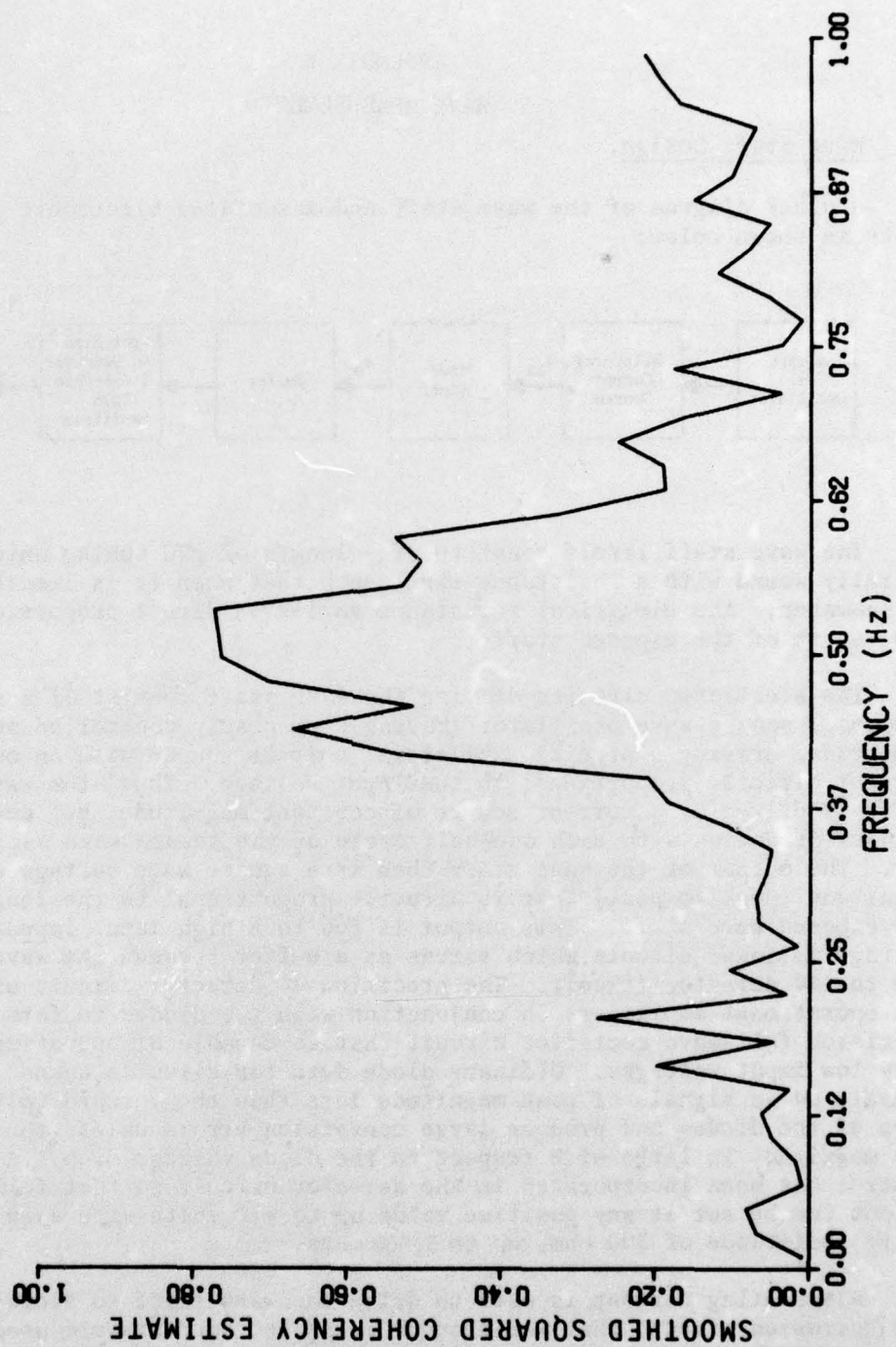


Figure J-17. Coherency between sway and heave.

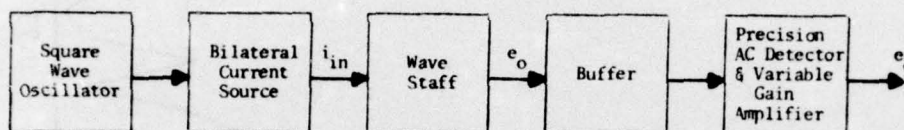


## APPENDIX K

### WAVE MEASUREMENT

#### 1. Wave Staff Design.

A block diagram of the wave staff and associated electronic circuits is shown below:



The wave staff itself consists of a length of PVC tubing which is spirally wound with a resistance wire, such that when it is immersed in seawater, the electrical resistance varies in direct proportion to the length of the exposed staff.

The electronic circuits driving the wave staff consist of a fixed frequency square wave oscillator (having a precisely controlled output amplitude) driving a precision bilateral current source with an output current directly proportional to the input voltage. Thus, the wave staff is driven by a current source of constant magnitude, but one which changes direction with each one-half cycle of the square wave oscillator. The output of the wave staff then is a square wave voltage with a magnitude (peak to peak) that is directly proportional to the length of the exposed wave staff. This output is fed to a high input impedance voltage follower circuit which serves as a buffer between the wave staff and the ac detector circuit. The precision ac detector circuit uses two operational amplifiers in conjunction with two diodes to form a precision full-wave rectifier circuit that is capable of operating at very low input voltages. Ordinary diode detector circuits cannot operate on ac signals of peak magnitude less than the forward voltage drop of the diodes and produce large conversion errors unless the signal magnitude is large with respect to the diode voltage drop. A gain control has been incorporated in the detector circuit so that full-scale output can be set at any positive value up to +10 volts with a wave staff resistance of 300 ohms up to 3,000 ohms.

Alternating current is used to drive the wave staff to avoid both the corrosion effects that would occur if direct current were used and the dc offset which occurs as a result of the use of dissimilar metals in a conducting solution. The latter is eliminated by use of ac coupling in the output from the wave staff.

Bench tests of the wave staff electronic circuits were made using a 1,000-ohm variable precision resistor in place of the wave staff. The

circuit was adjusted to produce an output range of 0 to 10 volts with the resistor varied from 0 to 1,000 ohms. Linearity was determined to be 0.1 percent of full scale over this range.

Tests were also made to determine the effect of temperature on sensitivity and zero drift. A decrease in sensitivity was noted with decreasing temperature of about 0.03 percent of reading per °Celsius over the temperature range of 0 to 24°Celsius. A zero drift of 2 millivolts was also noted over the same temperature range. A  $\pm 10$  percent change in supply voltage from the nominal  $\pm 15$  volts produced no observable change in output. If we assume an operating temperature range of  $\pm 5^\circ$ Celsius, the maximum error in the wave staff electronics due to the combined effects of nonlinearity and sensitivity variations with temperature is  $\pm 0.2$  percent of reading. Since the primary interest is in a dynamic measurement of waves, the zero drift noted will have negligible effect on the experiment since temperature variations of any appreciable magnitude will only occur over long periods of time compared to the wave periods.

Further calibration tests were conducted using actual wave staffs of 1-inch diameter and 20-foot lengths, and 3.5-inch diameter and 8-foot lengths at various depths of immersion in saltwater. These tests were conducted from a dock at Shilshole Bay on Puget Sound. Because of ripples and waves on the water of the order of 1 inch (peak-to-valley) it was difficult to obtain a highly precise measurement. The output was recorded on a strip chart recorder and it was therefore possible to average these variations to some degree. The readout resolution of the strip chart (and accuracy) is about  $\pm 1/4$  of a minor division. Full scale across the chart is 50 minor divisions and, thus, the resolution is about 0.5 percent of full scale. Some nonlinearity is noted near full immersion (see calibration curve). Some offset was expected because of the finite resistance of the saltwater path in the ground return which is not taken into account during initial calibration of the wave staff unit. The initial calibration is made with the wave staff on the dock where full scale and zero are set by making actual contact between the ground wire and the wave staff resistance element at the corresponding ends. However, measurements were made of the resistance of the saltwater path to ground in the same location where the wave staffs were immersed and the value of resistance measured (on the order of 10 ohms) does not account for the offset observed at full immersion. In addition, the offset should occur at all readings and it does not. Therefore, it is believed that the nonlinearity observed is a result of some other phenomenon as yet undetermined. Both units produced highest accuracy near center scale with decreasing accuracy toward either end. Overall accuracy including end points is about  $\pm 3$  percent. If the range of operation is reduced so as not to use the last 1 foot on each end of the wave staff, the accuracy is improved to about  $\pm 1$  percent.

The output from the wave staff electronic circuit is fed directly into a voltage to frequency converter; the frequency output is then counted and stored on separate storage registers, once every 50 milliseconds. If an 8-bit register is used for the wave staff measurement,



the maximum count that can be stored is 255; therefore, the sample time must be on the order of 25.5 milliseconds (maximum count divided by maximum frequency output from voltage to frequency converter). The wave buoys use an 8-bit register with a 32.5-millisecond sample time while the wave staffs use a 16-bit register with a 250-millisecond sample time.

The error due to gain instability and nonlinearity of the voltage to frequency converter is of such low magnitude that it can be neglected and the overall accuracy of the recording is essentially the same as given for the wave staff unit by itself (i.e., between  $\pm 1$  and  $\pm 3$  percent depending on the range of operation on wave staff).

## 2. Spar Buoy Design.

Spar buoys were used at two of the sites because of their advantage in handling and transport and because they minimized the placement difficulties due to navigational hazards, water depth, and tidal conditions. The spar buoys were made of two PVC pipes coupled together near the center of the buoy. The lower section is a 15 foot by 6 inch pipe filled with styrofoam. The top section is 12 feet by 3 inches wherein the upper 8 feet is wound with a resistance wire which measures wave elevation. The wave staff electronics are mounted inside the top section, above the waterline, with the remainder being filled with a wood core to add stiffness. The buoys also have a 2.5-foot diameter damping plate mounted on the bottom and are anchored using a dual point mooring system with the anchor lines attached at the center of drag on the buoy to prevent it from being pulled underwater in strong currents. One of these buoys was tested in the Puget Sound just north of Seattle. Its performance exceeded expectations both in terms of minimized response to the waves and accuracy of wave height measurement. Figure K-1 gives a sample of the output from the buoy's wave staff in saltwater for a plus and minus 1 foot excitation of the buoy in heave. This was accomplished by pushing the buoy up and down by hand. Some distortion results from this approach which shows up in the output of the accelerometer mounted at the center of the response of the buoy in heave and roll in calm water. The natural periods for heave and roll taken from these plots are approximately 18 and 14 seconds, respectively. These are well out of the range of the 3-to-4-second wave periods expected at the site. Visual observations of the buoy in waves in excess of 1.5 feet indicated no observable heave or roll motion, but some yaw about the anchor line caused by the current and wind. This motion resulted in less than a 1 foot variation from the buoy's horizontal position in calm water and appeared to have periods in excess of 30 to 60 seconds. For comparative measurements, the buoy was located about 30 feet from an existing four-gage array of 1-inch diameter Oceanographic Services, Inc. resistance wire wave staffs. A comparison of simultaneous output from the two wave staffs (buoy mounted and stationary) is shown in Figure K-4. The autospectras computed from data obtained from one of the stationary wave staffs and from the spar buoy, in a 25-miles per hour storm with

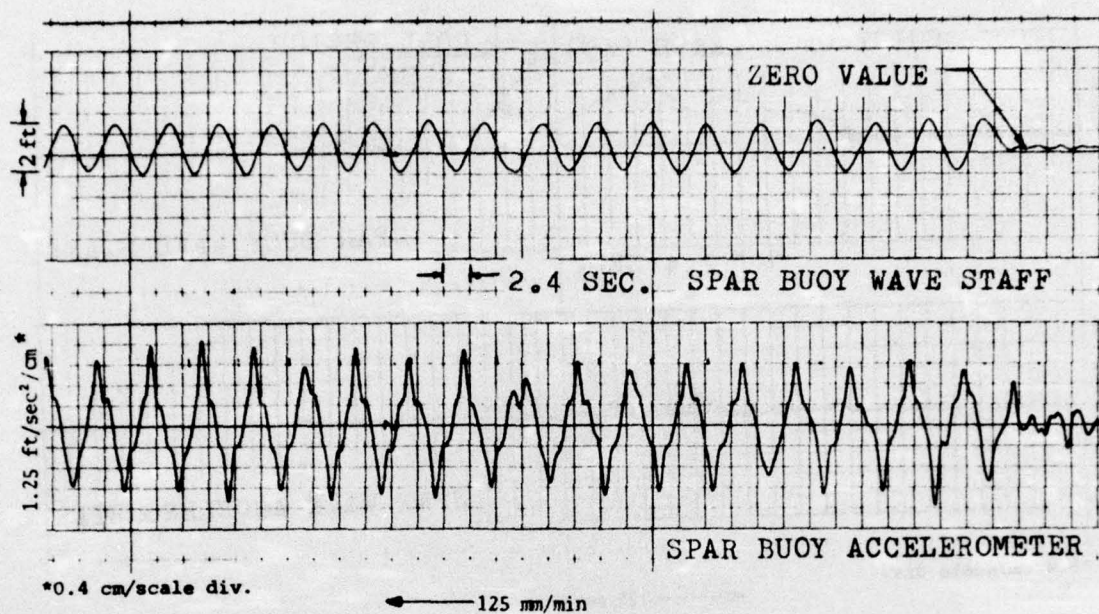


Figure K-1. Wave and acceleration data for spar buoy.

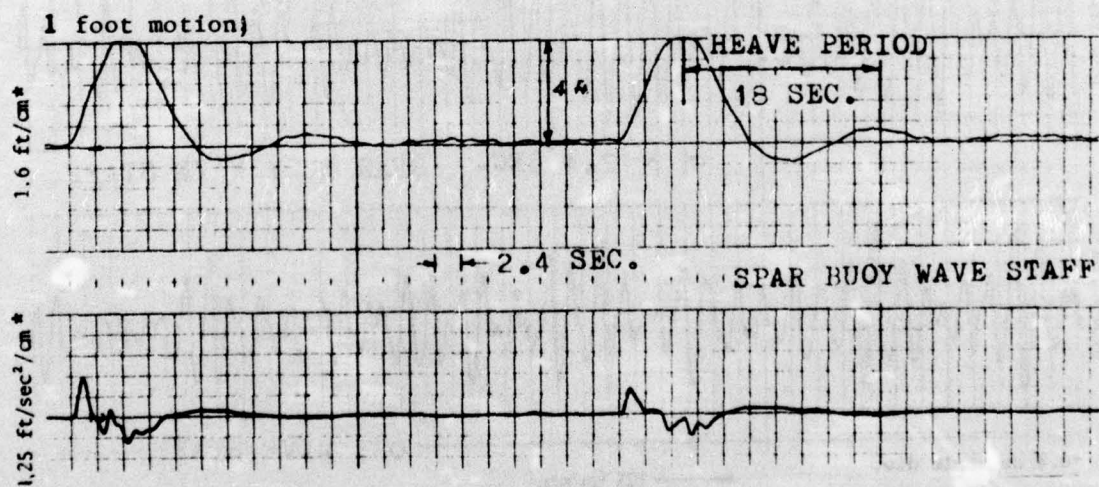


Figure K-2. Spar buoy heave response.



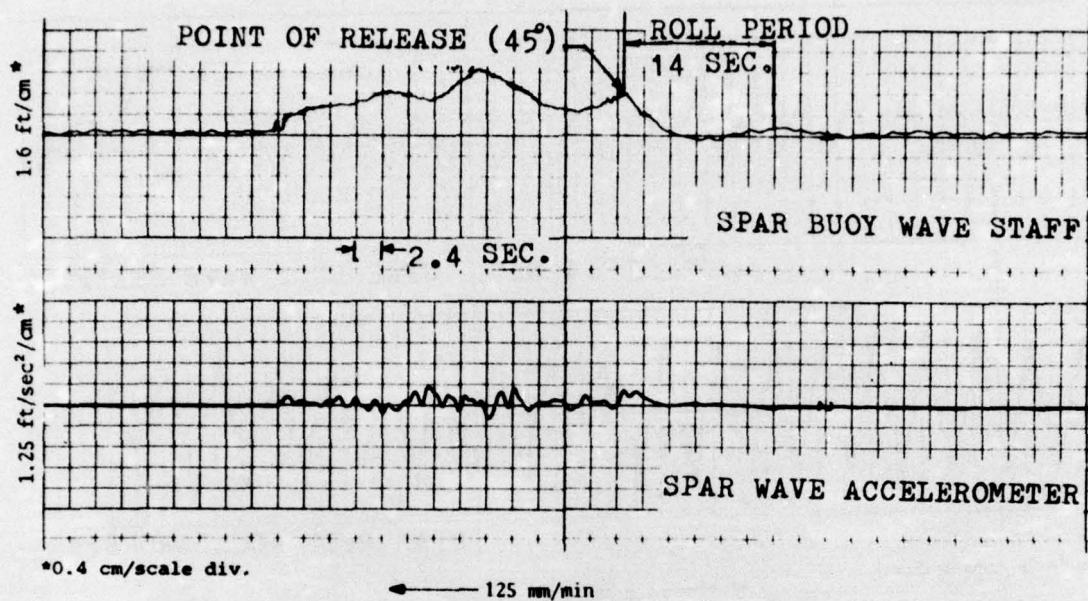


Figure K-3. Spar buoy roll response.

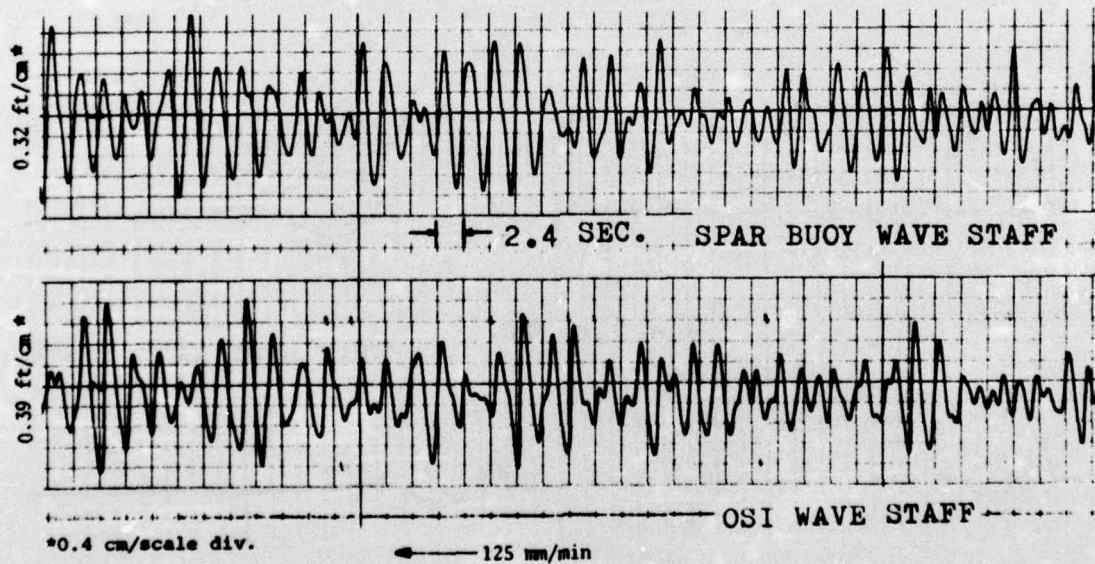


Figure K-4. Wind wave data for spar buoy and stationary staff.

maximum wave heights in excess of 1.5 feet are shown in Figure K-5. These spectra were computed from simultaneous records of 20 minutes in length.





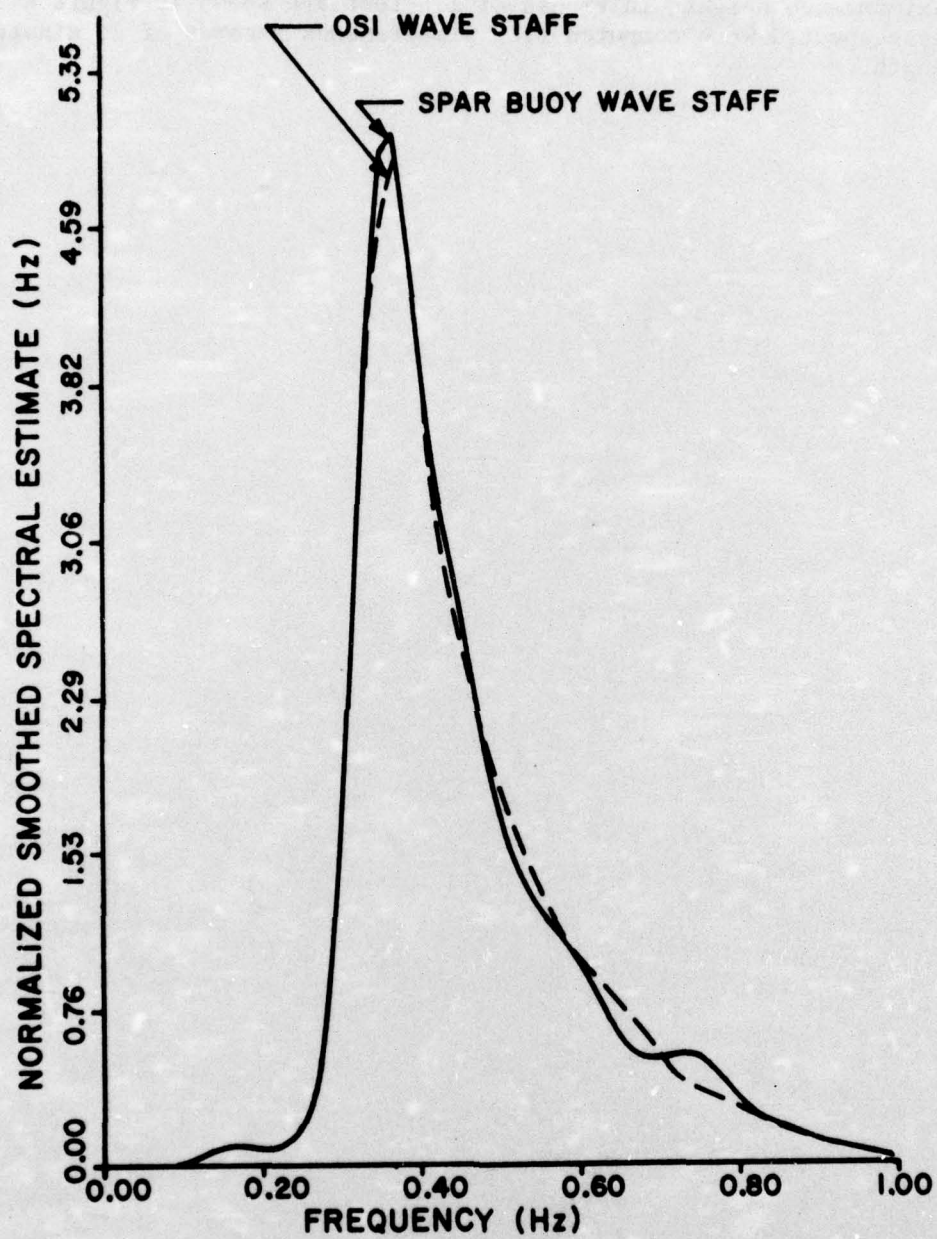


Figure K-5. Wave spectra from spar buoy and stationary staff.

<p>Adee, B. H.</p> <p>Floating breakwater field assessment program, Friday Harbor, Washington / by B. H. Adee, E. P. Richey...[et al.]. -- Fort Belvoir, Va. : U.S. Coastal Engineering Research Center, 1976.</p> <p>224 p. : ill. (Technical paper - U.S. Coastal Engineering Research Center ; no. 76-17) Also (Contract - U.S. Coastal Engineering Research Center ; DACW72-74-C-0012)</p> <p>Bibliography : p. 72.</p> <p>This study presents a theoretical model for predicting the dynamic behavior of a floating breakwater, and a report on a field experiment designed to provide basic data for verifying the model.</p> <p>1. Floating breakwaters. 2. Friday Harbor, Wash. 3. Wave attenuation. 4. Wave reflection. 5. Wave transmission. I. Title. II. Richey, E. P., Joint author. III. Series : U.S. Coastal Engineering Research Center. Technical paper no. 76-17. IV. U.S. Coastal Engineering Research Center. Contract DACW72-74-C-0012.</p> <p>TC203 .U581tp no. 76-17 627 .U581tp</p>	<p>Adee, B. H.</p> <p>Floating breakwater field assessment program, Friday Harbor, Washington / by B. H. Adee, E. P. Richey...[et al.]. -- Fort Belvoir, Va. : U.S. Coastal Engineering Research Center, 1976.</p> <p>224 p. : ill. (Technical paper - U.S. Coastal Engineering Research Center ; no. 76-17) Also (Contract - U.S. Coastal Engineering Research Center ; DACW72-74-C-0012)</p> <p>Bibliography : p. 72.</p> <p>This study presents a theoretical model for predicting the dynamic behavior of a floating breakwater, and a report on a field experiment designed to provide basic data for verifying the model.</p> <p>1. Floating breakwaters. 2. Friday Harbor, Wash. 3. Wave attenuation. 4. Wave reflection. 5. Wave transmission. I. Title. II. Richey, E. P., Joint author. III. Series : U.S. Coastal Engineering Research Center. Technical paper no. 76-17. IV. U.S. Coastal Engineering Research Center. Contract DACW72-74-C-0012.</p> <p>TC203 .U581tp no. 76-17 627 .U581tp</p>
<p>Adee, B. H.</p> <p>Floating breakwater field assessment program, Friday Harbor, Washington / by B. H. Adee, E. P. Richey...[et al.]. -- Fort Belvoir, Va. : U.S. Coastal Engineering Research Center, 1976.</p> <p>224 p. : ill. (Technical paper - U.S. Coastal Engineering Research Center ; no. 76-17) Also (Contract - U.S. Coastal Engineering Research Center ; DACW72-74-C-0012)</p> <p>Bibliography : p. 72.</p> <p>This study presents a theoretical model for predicting the dynamic behavior of a floating breakwater, and a report on a field experiment designed to provide basic data for verifying the model.</p> <p>1. Floating breakwaters. 2. Friday Harbor, Wash. 3. Wave attenuation. 4. Wave reflection. 5. Wave transmission. I. Title. II. Richey, E. P., Joint author. III. Series : U.S. Coastal Engineering Research Center. Technical paper no. 76-17. IV. U.S. Coastal Engineering Research Center. Contract DACW72-74-C-0012.</p> <p>TC203 .U581tp no. 76-17 627 .U581tp</p>	<p>Adee, B. H.</p> <p>Floating breakwater field assessment program, Friday Harbor, Washington / by B. H. Adee, E. P. Richey...[et al.]. -- Fort Belvoir, Va. : U.S. Coastal Engineering Research Center, 1976.</p> <p>224 p. : ill. (Technical paper - U.S. Coastal Engineering Research Center ; no. 76-17) Also (Contract - U.S. Coastal Engineering Research Center ; DACW72-74-C-0012)</p> <p>Bibliography : p. 72.</p> <p>This study presents a theoretical model for predicting the dynamic behavior of a floating breakwater, and a report on a field experiment designed to provide basic data for verifying the model.</p> <p>1. Floating breakwaters. 2. Friday Harbor, Wash. 3. Wave attenuation. 4. Wave reflection. 5. Wave transmission. I. Title. II. Richey, E. P., Joint author. III. Series : U.S. Coastal Engineering Research Center. Technical paper no. 76-17. IV. U.S. Coastal Engineering Research Center. Contract DACW72-74-C-0012.</p> <p>TC203 .U581tp no. 76-17 627 .U581tp</p>



<p>Adee, B. H.</p> <p>Floating breakwater field assessment program, Friday Harbor, Washington / by B. H. Adee, E. P. Richey...[et al.]. -- Fort Belvoir, Va. : U.S. Coastal Engineering Research Center, 1976.</p> <p>224 p. : ill. (Technical paper - U.S. Coastal Engineering Research Center ; no. 76-17) Also (Contract - U.S. Coastal Engineering Research Center ; DACN72-74-C-0012)</p> <p>Bibliography : p. 72.</p> <p>This study presents a theoretical model for predicting the dynamic behavior of a floating breakwater, and a report on a field experiment designed to provide basic data for verifying the model.</p> <p>1. Floating breakwaters. 2. Friday Harbor, Wash. 3. Wave attenuation. 4. Wave reflection. 5. Wave transmission. I. Title. II. Richey, E. P., Joint author. III. Series : U.S. Coastal Engineering Research Center. Technical paper no. 76-17. IV. U.S. Coastal Engineering Research Center. Contract DACN72-74-C-0012.</p> <p>TC203 .U581tp no. 76-17 627 .U581tp</p>	<p>Adee, B. H.</p> <p>Floating breakwater field assessment program, Friday Harbor, Washington / by B. H. Adee, E. P. Richey...[et al.]. -- Fort Belvoir, Va. : U.S. Coastal Engineering Research Center, 1976.</p> <p>224 p. : ill. (Technical paper - U.S. Coastal Engineering Research Center ; no. 76-17) Also (Contract - U.S. Coastal Engineering Research Center ; DACN72-74-C-0012)</p> <p>Bibliography : p. 72.</p> <p>This study presents a theoretical model for predicting the dynamic behavior of a floating breakwater, and a report on a field experiment designed to provide basic data for verifying the model.</p> <p>1. Floating breakwaters. 2. Friday Harbor, Wash. 3. Wave attenuation. 4. Wave reflection. 5. Wave transmission. I. Title. II. Richey, E. P., Joint author. III. Series : U.S. Coastal Engineering Research Center. Technical paper no. 76-17. IV. U.S. Coastal Engineering Research Center. Contract DACN72-74-C-0012.</p> <p>TC203 .U581tp no. 76-17 627 .U581tp</p>
<p>Adee, B. H.</p> <p>Floating breakwater field assessment program, Friday Harbor, Washington / by B. H. Adee, E. P. Richey...[et al.]. -- Fort Belvoir, Va. : U.S. Coastal Engineering Research Center, 1976.</p> <p>224 p. : ill. (Technical paper - U.S. Coastal Engineering Research Center ; no. 76-17) Also (Contract - U.S. Coastal Engineering Research Center ; DACN72-74-C-0012)</p> <p>Bibliography : p. 72.</p> <p>This study presents a theoretical model for predicting the dynamic behavior of a floating breakwater, and a report on a field experiment designed to provide basic data for verifying the model.</p> <p>1. Floating breakwaters. 2. Friday Harbor, Wash. 3. Wave attenuation. 4. Wave reflection. 5. Wave transmission. I. Title. II. Richey, E. P., Joint author. III. Series : U.S. Coastal Engineering Research Center. Technical paper no. 76-17. IV. U.S. Coastal Engineering Research Center. Contract DACN72-74-C-0012.</p> <p>TC203 .U581tp no. 76-17 627 .U581tp</p>	<p>Adee, B. H.</p> <p>Floating breakwater field assessment program, Friday Harbor, Washington / by B. H. Adee, E. P. Richey...[et al.]. -- Fort Belvoir, Va. : U.S. Coastal Engineering Research Center, 1976.</p> <p>224 p. : ill. (Technical paper - U.S. Coastal Engineering Research Center ; no. 76-17) Also (Contract - U.S. Coastal Engineering Research Center ; DACN72-74-C-0012)</p> <p>Bibliography : p. 72.</p> <p>This study presents a theoretical model for predicting the dynamic behavior of a floating breakwater, and a report on a field experiment designed to provide basic data for verifying the model.</p> <p>1. Floating breakwaters. 2. Friday Harbor, Wash. 3. Wave attenuation. 4. Wave reflection. 5. Wave transmission. I. Title. II. Richey, E. P., Joint author. III. Series : U.S. Coastal Engineering Research Center. Technical paper no. 76-17. IV. U.S. Coastal Engineering Research Center. Contract DACN72-74-C-0012.</p> <p>TC203 .U581tp no. 76-17 627 .U581tp</p>